GE Energy Nuclear

26A6642AL
Revision 3
February 2007

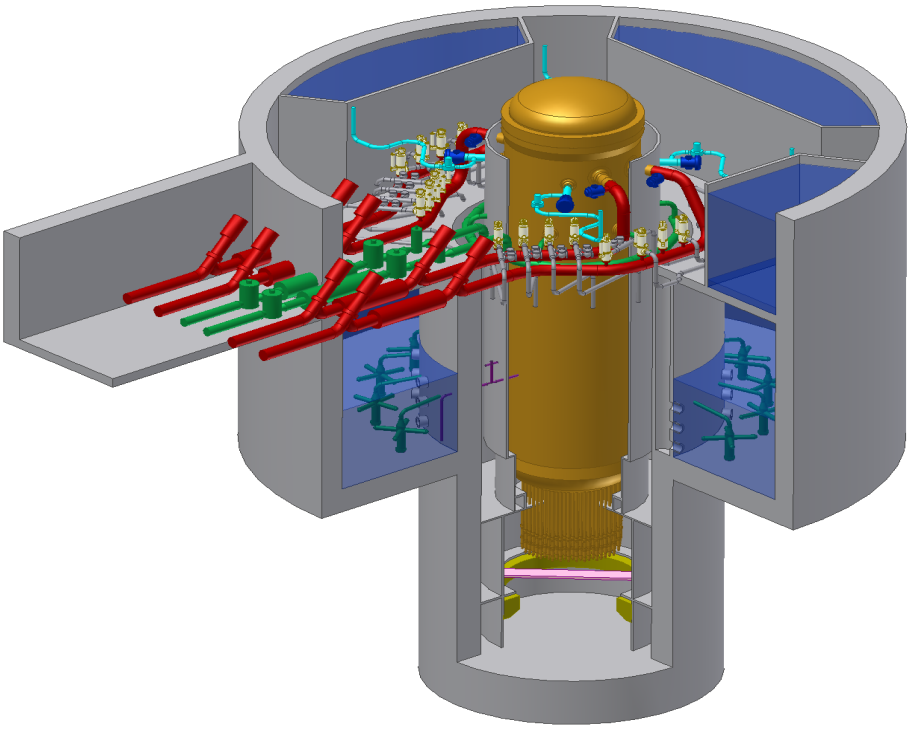

ESBWR Design Control Document

Tier 2

Chapter 3

Design of Structures, Components, Equipment, and Systems

Appendices 3A-3F

Contents

List of Tables

List of Illustrations

Global Abbreviations And Acronyms List

Term	Definition
10 CFR	Title 10, Code of Federal Regulations
A/D	Analog-to-Digital
AASHTO	American Association of Highway and Transportation Officials
AB	Auxiliary Boiler
ABS	Auxiliary Boiler System or Absolute Sum
ABWR	Advanced Boiling Water Reactor
ac / AC	Alternating Current
AC	Air Conditioning
ACF	Automatic Control Function
ACI	American Concrete Institute
ACS	Atmospheric Control System
AD	Administration Building
ADS	Automatic Depressurization System
AEC	Atomic Energy Commission
AFIP	Automated Fixed In-Core Probe
AGMA	American Gear Manufacturer's Association
AHS	Auxiliary Heat Sink
AISC	American Institute of Steel Construction
AISI	American Iron and Steel Institute
AL	Analytical Limit
ALARA	As Low As Reasonably Achievable
ALWR	Advanced Light Water Reactor
ANS	American Nuclear Society
ANSI	American National Standards Institute
AOO	Anticipated Operational Occurrence
AOV	Air Operated Valve
AP	Annulus Pressurization
API	American Petroleum Institute
APLHGR	Average Planar Linear Heat Generation Rate
APRM	Average Power Range Monitor
APR	Automatic Power Regulator
APRS	Automatic Power Regulator System
ARI	Alternate Rod Insertion
ARMS	Area Radiation Monitoring System
ARS	Amplified Response Spectrum
ASA	American Standards Association
ASCE	American Society of Civil Engineers
ASD	Adjustable Speed Drive
ASHRAE	American Society of Heating, Refrigerating, and Air Conditioning Engineers

Term	Definition
ASME	American Society of Mechanical Engineers
AST	Alternate Source Term
ASTM	American Society of Testing Methods
AT	Unit Auxiliary Transformer
ATLM	Automated Thermal Limit Monitor
ATWS	Anticipated Transients Without Scram
AV	Allowable Value
AWS	American Welding Society
AWWA	American Water Works Association
B&PV	Boiler and Pressure Vessel
BAF	Bottom of Active Fuel
BE	Best Estimate
BHP	Brake Horse Power
BOP	Balance of Plant
BPU	Bypass Unit
BPWS	Banked Position Withdrawal Sequence
BRE	Battery Room Exhaust
BRL	Background Radiation Level
BTP	NRC Branch Technical Position
BTU	British Thermal Unit
BWR	Boiling Water Reactor
BWROG	Boiling Water Reactor Owners Group
CAV	Cumulative absolute velocity
C&FS	Condensate and Feedwater System
C&I	Control and Instrumentation
C/C	Cooling and Cleanup
C-I	Class one (I)
C-II	Class two (II)
CB	Control Building
CBGAVS	Control Building General Area HVAC Subsystem
CBVS	Control Building HVAC System
CCI	Core-Concrete Interaction
CDF	Core Damage Frequency
CFR	Code of Federal Regulations
CH	Pool Chugging
CIRC	Circulating Water System
CIS	Containment Inerting System
CIV	Combined Intermediate Valve
CLAVS	Reactor Building Clean Area HVAC Subsystem
CM	Cold Machine Shop

Term	Definition
CMS	Containment Monitoring System
CMU	Control Room Multiplexing Unit
CO	Condensation Oscillation
COL	Combined Operating License
COLR	Core Operating Limits Report
CONAVS	Reactor Building Contaminated Area HVAC Subsystem
CPR	Critical Power Ratio
CPS	Condensate Purification System
CPU	Central Processing Unit
CR	Control Rod
CRD	Control Rod Drive
CRDA	Control Rod Drop Accident
CRDH	Control Rod Drive Housing
CRDHS	Control Rod Drive Hydraulic System
CRGT	Control Rod Guide Tube
CRHA	Control Room Habitability Area
CRHAVS	Control Room Habitability Area HVAC Subsystem
CRT	Cathode Ray Tube
CS&TS	Condensate Storage and Transfer System
CSDM	Cold Shutdown Margin
CS / CST	Condensate Storage Tank
CT	Compact Tension
CTVCF	Constant Voltage Constant Frequency
CUF	Cumulative usage factor
CWS	Chilled Water System
D-RAP	Design Reliability Assurance Program
DAC	Design Acceptance Criteria
DAW	Dry Active Waste
DBA	Design Basis Accident
dc / DC	Direct Current
DCS	Drywell Cooling System
DCIS	Distributed Control and Information System
DEGB	Double Ended Guillotine Break
DEPSS	Drywell Equipment and Pipe Support Structure
DF	Decontamination Factor
D/F	Diaphragm Floor
DG	Diesel-Generator
DGVS	Electrical Building Diesel Generators HVAC Subsystem
DHR	Decay Heat Removal
DLF	Dynamic Load Factor

Term	Definition
DM&C	Digital Measurement and Control
DOF	Degree of freedom
DOI	Dedicated Operators Interface
DOT	Department of Transportation
dPT	Differential Pressure Transmitter
DPS	Diverse Protection System
DPV	Depressurization Valve
DR&T	Design Review and Testing
DTM	Digital Trip Module
DW	Drywell
EB	Electrical Building
EBVS	Electrical Building HVAC System
ECCS	Emergency Core Cooling System
EDO	Environmental Qualification Document
EER	Electrical Building Electric and Electronic Rooms
EERVS	Electrical Building Electric and Electronic Rooms HVAC Subsystem
EFDS	Equipment and Floor Drainage System
EFPY	Effective full power years
EHC	Electrohydraulic Control (Pressure Regulator)
ENS	Emergency Notification System
EOC	Emergency Operations Center
EOC	End of Cycle
EOF	Emergency Operations Facility
EOP	Emergency Operating Procedures
EPDS	Electric Power Distribution System
EPFM	Elastic Plastic Fracture Mechanics
EPG	Emergency Procedure Guidelines
EPRI	Electric Power Research Institute
EQ	Environmental Qualification
ERICP	Emergency Rod Insertion Control Panel
ERIP	Emergency Rod Insertion Panel
ESF	Engineered Safety Feature
ESP	Early Site Permit
ETS	Emergency Trip System
FAC	Flow-Accelerated Corrosion
FAPCS	Fuel and Auxiliary Pools Cooling System
FATT	Fracture Appearance Transition Temperature
FB	Fuel Building
FBFPVS	Fuel Building Fuel Pool Area HVAC Subsystem
FBGAVS	Fuel Building General Area HVAC Subsystem

Term	Definition
FBVS	Fuel Building HVAC System
FCI	Fuel-Coolant Interaction
FCM	File Control Module
FCS	Flammability Control System
FCU	Fan Cooling Unit
FDDI	Fiber Distributed Data Interface
FFT	Fast Fourier Transform
FFWTR	Final Feedwater Temperature Reduction
FHA	Fire Hazards Analysis
FIV	Flow-Induced Vibration
FMCRD	Fine Motion Control Rod Drive
FMEA	Failure Modes and Effects Analysis
FO	Diesel Fuel Oil Storage Tank
FOAKE	First-of-a-Kind Engineering
FPE	Fire Pump Enclosure
FRS	Floor Response Spectra
FPS	Fire Protection System
FTDC	Fault-Tolerant Digital Controller
FTS	Fuel Transfer System
FW	Feedwater
FWCS	Feedwater Control System
FWS	Fire Water Storage Tank
GDC	General Design Criteria
GDCS	Gravity-Driven Cooling System
GE	General Electric Company
GE-NE	GE Nuclear Energy
GEN	Main Generator System
GETAB	General Electric Thermal Analysis Basis
GL	Generic Letter
GLSOS	Generator Lube and Seal Oil System
GM	Geiger-Mueller Counter
GM-B	Beta-Sensitive GM Detector
GMAW	Gas Metal Arc Welding
GSIC	Gamma-Sensitive Ion Chamber
GTAW	Gas Tungsten Arc Welding
GWSR	Ganged Withdrawal Sequence Restriction
HAZ	Heat-Affected Zone
HCU	Hydraulic Control Unit
HCW	High Conductivity Waste
HDVS	Heater Drain and Vent System

Term	Definition
HEI	Heat Exchange Institute
HELB	High Energy Line Break
HEP	Human error probability
HEPA	High Efficiency Particulate Air/Absolute
HFE	Human Factors Engineering
HFF	Hollow Fiber Filter
HGCS	Hydrogen Gas Control System
HIC	High Integrity Container
HID	High Intensity Discharge
HIS	Hydraulic Institute Standards
HM	Hot Machine Shop & Storage
HP	High Pressure
HPNSS	High Pressure Nitrogen Supply System
HPT	High-pressure turbine
HRA	Human Reliability Assessment
HSI	Human-System Interface
HSSS	Hardware/Software System Specification
HVAC	Heating, Ventilation and Air Conditioning
HVL	Horizontal Vent Chugging
HVS	High Velocity Separator
HWCS	Hydrogen Water Chemistry System
HWS	Hot Water System
HX	Heat Exchanger
I&C	Instrumentation and Control
I/O	Input/Output
IAS	Instrument Air System
IASCC	Irradiation Assisted Stress Corrosion Cracking
IBC	International Building Code
IC	Isolation Condenser
ICD	Interface Control Diagram
ICS	Isolation Condenser System
IE	Inspection and Enforcement
IEB	Inspection and Enforcement Bulletin
IED	Instrument and Electrical Diagram
IEEE	Institute of Electrical and Electronic Engineers
IGSCC	Intergranular Stress Corrosion Cracking
IIS	Iron Injection System
ILRT	Integrated Leak Rate Test
IOP	Integrated Operating Procedure
IMC	Induction Motor Controller

Term	Definition
IMCC	Induction Motor Controller Cabinet
IRM	Intermediate Range Monitor
ISA	Instrument Society of America
ISI	In-Service Inspection
ISLT	In-Service Leak Test
ISM	Independent Support Motion
ISMA	Independent Support Motion Response Spectrum Analysis
ISO	International Standards Organization
ITA	Inspections, Tests or Analyses
ITAAC	Inspections, Tests, Analyses and Acceptance Criteria
ITA	Initial Test Program
J-R	Curve representing J-integral Resistance
LAPP	Loss of Alternate Preferred Power
LB	Lower Bound
LBB	Leak Before Break
LCO	Local Condensation Oscillation
LCW	Low Conductivity Waste
LD	Logic Diagram
LDA	Lay down Area
LD&IS	Leak Detection and Isolation System
LERF	Large early release frequency
LEFM	Linear Elastic Fracture Mechanics
LFCV	Low Flow Control Valve
LHGR	Linear Heat Generation Rate
LLRT	Local Leak Rate Test
LMU	Local Multiplexer Unit
LO	Dirty/Clean Lube Oil Storage Tank
LOCA	Loss-of-Coolant-Accident
LOFW	Loss-of-feedwater
LOOP	Loss of Offsite Power
LOPP	Loss of Preferred Power
LP	Low Pressure
LPCI	Low Pressure Coolant Injection
LPCRD	Locking Piston Control Rod Drive
LPRM	Local Power Range Monitor
LPSP	Low Power Setpoint
LWMS	Liquid Waste Management System
MAAP	Modular Accident Analysis Program
MAPLHGR	Maximum Average Planar Linear Head Generation Rate
MAPRAT	Maximum Average Planar Ratio

Term	Definition
MBB	Motor Built-In Brake
MCC	Motor Control Center
MCES	Main Condenser Evacuation System
MCPR	Minimum Critical Power Ratio
MCR	Main Control Room
MCRP	Main Control Room Panel
MELB	Moderate Energy Line Break
MLHGR	Maximum Linear Heat Generation Rate
MMI	Man-Machine Interface
MMIS	Man-Machine Interface Systems
MOV	Motor-Operated Valve
MPC	Maximum Permissible Concentration
MPL	Master Parts List
MS	Main Steam
MSIV	Main Steam Isolation Valve
MSL	Main Steamline
MSLB	Main Steamline Break
MSLBA	Main Steamline Break Accident
MSR	Moisture Separator Reheater
MSV	Mean Square Voltage
MT	Main Transformer
MTTR	Mean Time To Repair
MWS	Makeup Water System
N-DCIS	NonSafety-Related Distributed Control and Information System
NBR	Nuclear Boiler Rated
NBS	Nuclear Boiler System
NCIG	Nuclear Construction Issues Group
NDE	Nondestructive Examination
NDRC	National Defense Research Committee
NDT	Nil Ductility Temperature
NFPA	National Fire Protection Association
NIST	National Institute of Standard Technology
NMS	Neutron Monitoring System
NOV	Nitrogen Operated Valve
NPHS	Normal Power Heat Sink
NPSH	Net Positive Suction Head
NRC	Nuclear Regulatory Commission
NRHX	Non-Regenerative Heat Exchanger
NS	Non-seismic
NSSS	Nuclear Steam Supply System

Term	Definition
NT	Nitrogen Storage Tank
NTSP	Nominal Trip Setpoint
O&M	Operation and Maintenance
O-RAP	Operational Reliability Assurance Program
OBCV	Overboard Control Valve
OBE	Operating Basis Earthquake
OGS	Offgas System
OHLHS	Overhead Heavy Load Handling System
OIS	Oxygen Injection System
OLMCPR	Operating Limit Minimum Critical Power Ratio
OLU	Output Logic Unit
OOS	Out-of-Service
ORNL	Oak Ridge National Laboratory
OSC	Operational Support Center
OSHA	Occupational Safety and Health Administration
OSI	Open Systems Interconnect
P&ID	Piping and Instrumentation Diagram
PA/PL	Page/Party-Line
PABX	Private Automatic Branch (Telephone) Exchange
PAM	Post Accident Monitoring
PAR	Passive Autocatalytic Recombiner
PAS	Plant Automation System
PAW	Platinum Arc welding
PCC	Passive Containment Cooling
PCCS	Passive Containment Cooling System
PCT	Peak cladding temperature
PCV	Primary Containment Vessel
PFD	Process Flow Diagram
PGA	Peak Ground Acceleration
PGCS	Power Generation and Control Subsystem of Plant Automation System
PH	Pump House
PL	Parking Lot
PM	Preventive Maintenance
PMCS	Performance Monitoring and Control Subsystem of NE-DCIS
PMF	Probable Maximum Flood
PMP	Probable Maximum Precipitation
PQCL	Product Quality Check List
PRA	Probabilistic Risk Assessment
PRMS	Process Radiation Monitoring System
PRNM	Power Range Neutron Monitoring

Term	Definition
PS	Pool Swell
PSD	Power Spectra Density
PSS	Process Sampling System
PSWS	Plant Service Water System
PT	Pressure Transmitter
PWR	Pressurized Water Reactor
Q-DCIS	Safety-Related Distributed Control and Information System
QA	Quality Assurance
RACS	Rod Action Control Subsystem
RAM	Reliability, Availability and Maintainability
RAPI	Rod Action and Position Information
RAT	Reserve Auxiliary Transformer
RB	Reactor Building
RBC	Rod Brake Controller
RBCC	Rod Brake Controller Cabinet
RBCWS	Reactor Building Chilled Water Subsystem
RBFB	Reactor Building/Fuel Building
RBS	Rod Block Setpoint
RBV	Reactor Building Vibration
RBVS	Reactor Building HVAC System
RC&IS	Rod Control and Information System
RCC	Remote Communication Cabinet
RCCV	Reinforced Concrete Containment Vessel
RCCWS	Reactor Component Cooling Water System
RCPB	Reactor Coolant Pressure Boundary
RCS	Reactor Coolant System
RDA	Rod Drop Accident
RDC	Resolver-to-Digital Converter
REPAVS	Reactor Building Refueling and Pool Area HVAC Subsystem
RFP	Reactor Feed Pump
RG	Regulatory Guide
RHR	Residual Heat Removal (function)
RHX	Regenerative Heat Exchanger
RMS	Root Mean Square
RMS	Radiation Monitoring Subsystem
RMU	Remote Multiplexer Unit
RO	Reverse Osmosis
ROM	Read-only Memory
RPS	Reactor Protection System
RPV	Reactor Pressure Vessel

Term	Definition
RRPS	Reference Rod Pull Sequence
RSM	Rod Server Module
RSPC	Rod Server Processing Channel
RSS	Remote Shutdown System
RSSM	Reed Switch Sensor Module
RSW	Reactor Shield Wall
RTIF	Reactor Trip and Isolation Function(s)
RT_{NDT}	Reference Temperature of Nil-Ductility Transition
TRNSS	Regulatory Treatment of Non-Safety Systems
RTP	Reactor Thermal Power
RW	Radwaste Building
RWCR	Radwaste Building Control Room
RWCRVS	Radwaste Building Control Room HVAC Subsystem
RWGA	Radwaste Building General Area
RWGAVS	Radwaste Building General Area HVAC Subsystem
RWVS	Radwaste Building HVAC System
RWCU	Reactor Water Cleanup
RWE	Rod Withdrawal Error
RWM	Rod Worth Minimizer
SA	Severe Accident
SAM	Seismic Anchor Movement
SAR	Safety Analysis Report
SB	Service Building
S/C	Digital Gamma-Sensitive GM Detector
S/D	Scintillation Detector
S/DRSRO	Single/Dual Rod Sequence Restriction Override
S/N	Signal-to-Noise
S/P	Suppression Pool
SAS	Service Air System
SAW	Submerged Arc Welding
SB&PC	Steam Bypass and Pressure Control System
SBO	Station Blackout
SBWR	Simplified Boiling Water Reactor
SCEW	System Component Evaluation Work
SCRRI	Selected Control Rod Run-in
SCWS	Stator Cooling Water System
SDC	Shutdown Cooling
SDM	Shutdown Margin
SDS	System Design Specification
SER	Safety Evaluation Report

Term	Definition
SF	Service Water Building
SFP	Spent Fuel Pool
SIL	Service Information Letter
SIT	Structural Integrity Test
SIU	Signal Interface Unit
SJAE	Steam Jet Air Ejector
SLC	Standby Liquid Control
SLCS	Standby Liquid Control system
SLMCPR	Safety Limit Minimum Critical Power Ratio
SMAW	Shielded Metal Arc Welding
SMU	SSLC Multiplexing Unit
SOV	Solenoid Operated Valve
SP	Suppression Pool
SPC	Suppression Pool Cooling
SPDS	Safety Parameter Display System
SPTMS	Suppression Pool Temperature Monitoring Subsystem of Containment Monitoring System
SR	Surveillance Requirement
SRM	Source Range Monitor
SRNM	Startup Range Neutron Monitor
SRO	Senior Reactor Operator
SRP	Standard Review Plan
SRS	Software Requirements Specification
SRSRO	Single Rod Sequence Restriction Override
SRSS	Square Root of the Sum of the Squares
SRV	Safety Relief Valve Discharge
SRVDL	Safety relief valve discharge line
SSAR	Standard Safety Analysis Report
SSC(s)	Structure, System and Component(s)
SSE	Safe Shutdown Earthquake
SSLC	Safety System Logic and Control
SSI	Soil-Structure Interaction
SSPC	Steel Structures Painting Council
ST	Spare Transformer
STP	Sewage Treatment Plant
STRAP	Scram Time Recording and Analysis Panel
STRP	Scram Time Recording Panel
SV	Safety Valve
SWH	Static water head
SWMS	Solid Waste Management System
SY	Switch Yard

Term	Definition
TAF	Top of Active Fuel
TASS	Turbine Auxiliary Steam System
TB	Turbine Building
TBCE	Turbine Building Compartment Exhaust
TBE	Turbine Building Exhaust
TBLOE	Turbine Building Lube Oil Area Exhaust
TBS	Turbine Bypass System
TBV	Turbine Bypass Valve
TBVS	Turbine Building HVAC System
TC	Training Center
TCCWS	Turbine Component Cooling Water System
TCV	Turbine Control Valve
TDH	Total Developed Head
TEMA	Tubular Exchanger Manufacturers' Association
TFSP	Turbine first stage pressure
TG	Turbine Generator
TGCS	Turbine generator Control System
TGSS	Turbine Gland Seal System
THA	Time-history Accelerograph
TLOS	Turbine Lubricating Oil System
TLU	Trip Logic Unit
TMI	Three Mile Island
TMSS	Turbine Main Steam System
TRM	Technical Requirements Manual
TS	Technical Specification(s)
TSC	Technical Support Center
TSCVS	Electrical Building Technical Support Center HVAC Subsystem
TSI	Turbine Supervisory Instrument
TSV	Turbine Stop Valve
UB	Upper Bound
UBC	Uniform Building Code
UHS	Ultimate Heat Sink
UL	Underwriter's Laboratories Inc.
UPS	Uninterruptible Power Supply
USE	Upper Shelf Energy
USM	Uniform Support Motion
USMA	Uniform Support Motion response spectrum analysis
USNRC	United States Nuclear Regulatory Commission
USS	United States Standard
UV	Ultraviolet

Term	Definition
V&V	Verification and Validation
Vac / VAC	Volts Alternating Current
Vdc / VDC	Volts Direct Current
VDU	Video Display Unit
VW	Vent Wall
VWO	Valves Wide Open
WD	Wash Down Bays
WH	Warehouse
WS	Water Storage
WT	Water Treatment
WW	Wetwell
XMFR	Transformer
ZPA	Zero Period Acceleration

3A. SEISMIC SOIL-STRUCTURE INTERACTION ANALYSIS

3A.1 INTRODUCTION

This appendix presents Soil-Structure Interaction (SSI) analysis performed for two site conditions, generic site and North Anna ESP site-specific, adopted to establish seismic design loads for the Reactor Building (RB), Fuel Building (FB) and Control Building (CB) of the ESBWR standard plant under safe shutdown earthquake (SSE) excitation. The RB and FB are integrated and founded on a common basemat. They are termed RBFB hereafter. The SSE design ground motion at the foundation level for both site conditions is described in Subsection 3.7.1. The SSI analysis results are presented here in the form of site-enveloped seismic responses at key locations in the RBFB and CB. The structural adequacy calculations for the RB, FB and CB are shown in Appendix 3G.

For a standard plant design, the analysis must be performed over a range of site parameters. The site parameters considered and their ranges together form the generic site conditions. The generic site conditions are selected to provide an adequate seismic design margin for the standard plant located at any site with site parameters within the range of parameters considered in this study. In addition, the North Anna ESP site-specific condition is also considered in this study. When actual sites for these facilities are selected, site-specific geotechnical data will be developed and submitted to the NRC demonstrating compatibility with the site enveloping parameters considered in the standard design.

This appendix details the basis for selecting the site conditions and analysis cases, and the method of the seismic soil-structure interaction analysis. Descriptions of the input motion and damping values, the structural model, and the soil model are included. The parametric study SSI results as well as the enveloping seismic responses are also presented.

To demonstrate the seismic adequacy of the standard ESBWR design, 27 RBFB cases and 11 CB cases are analyzed for the uniform site cases using the sway-rocking stick model for the SSE condition. In addition, 11 RBFB cases and 6 CB cases are analyzed for the layered site cases using the SASSI SSI model. The enveloped results reported in this appendix form the design SSE loads.

3A.2 ESBWR STANDARD PLANT SITE PLAN

The typical site plan of the ESBWR standard plant is shown in Figure 1.1-1. The plan orientations are identified by 0°–180° (NS) and 90°–270° (EW) directions. The RBFB complex and the CB are rectangular in plan with dimensions and embedment depths shown in Table 3A.2-1.

In modeling the building, the 0°–180° (NS) and 90°–270° (EW) directions are designated as X- and Y-axes, respectively. The Z-axis is in the vertical direction.

Table 3A.2-1

Standard ESBWR Building Dimensions

	RBFB Complex Dimensions (m)	CB Dimension (m)
0°–180° (NS) width	70.0	30.3
90°–270° (EW) width	49.0	23.8
Embedment depth	20	14.9

3A.3 SITE CONDITIONS

This section describes the generic site conditions and the North Anna ESP site-specific conditions used in the SSI analysis.

3A.3.1 Generic Site Conditions

The design philosophy of the standard plant stipulates that the design should be applicable to as many practical sites as possible, which are suitable for nuclear plant construction. To implement this philosophy, the effects of a wide range of subsurface conditions are considered in the seismic design. To evaluate these effects, a series of seismic soil-structure interaction (SSI) analyses in various subsurface conditions are performed. However, performing SSI analysis for combinations of all possible site properties and conditions where a nuclear power plant may be sited would be a formidable task. The purpose of this section is to define a limited number of bounding subsurface conditions selected according to experience gained from previous generic SSI studies. Three subsurface conditions are finally selected to encompass a wide range of applicable site properties and conditions. They are classified as soft, medium and hard sites. The soft site is intended to cover a spectrum of soft soil conditions. The medium site is for medium stiff soil and soft rock conditions, and the hard site for competent rock conditions. For hard sites a fixed-base case is also considered to account for very stiff sites. These sites are considered to be uniform half-space with final enveloping properties provided in Table 3A.3-1 for SSI analysis. These values are considered to be compatible with the strain level expected during SSE. They were used directly in computing soil spring and damper properties.

In addition to these uniform sites, four layered sites are also considered. They are composed of soft, medium and hard soil layers of varying depths as shown in Table 3A.3-3, taking into account variation of shear wave velocity with depth so that the effect of impedance mismatches between layers can be captured.

3A.3.2 North Anna ESP Site Conditions

As described in Subsection 3.7.1, the North Anna ESP site-specific conditions are also considered for the ESBWR design. North Anna is a rock site. The foundation properties considered in the SSI analysis are presented in Table 3A.3-2.

Table 3A.3-1

Generic Site Properties for SSI Analysis

(1), (2)	Soft	Medium	Hard	Fixed Base
Shear wave velocity (m/s)	300	800	1700	>1700
Mass density (kg/m^3)	2000	2200	2500	NA
Poisson's ratio	0.478	0.40	0.35	NA
Material damping (%)	5	4	3	NA

(1) The shear wave velocity and material damping specified above are used as strain compatible values.

(2) The maximum ground water table is 0.61m (2 ft) below grade. The effect of ground water on SSI analysis is considered in the selected values for the Poisson's ratio, resulting in the P-wave velocity no less than the minimum P-wave velocity of water (1460 m/sec).

Table 3A.3-2

North Anna Site-specific Properties for SSI Analysis

	RBFB Complex			Control Building		
	(BE)	(UB)	(LB)	(BE)	(UB)	(LB)
Low strain shear modulus (kg/m^2)	G 6.70E+08	1.5G 1.00E+09	G/1.5 4.47E+08	G 4.97E+08	1.5G 7.46E+08	G/1.5 3.31E+08
Shear wave velocity (m/s)	1589	1946	1297	1369	1677	1118
Mass density (kg/m^3)	2606	2606	2606	2606	2606	2606
Poisson's ratio	0.33	0.33	0.33	0.33	0.33	0.33
Material damping (%)	2	2	2	2	2	2

Note: The rock properties are provided for three conditions, G, 1.5G, & G/1.5, which are considered as best-estimate (BE), upper bound (UB) and lower bound (LB) cases.

Table 3A.3-3

Layered Site Cases

(1), (2) Layer	Shear Wave Velocity (m/s)/Depth (m)			
	CASE 1	CASE 2	CASE 3	CASE 4
Top	300/20	300/20	300/20	300/20
Middle	300/20	800/20	300/40	800/40
Bedrock	1700	1700	1700	1700

(1) The 20 m depth of the middle layer corresponds to the embedded depth of the RBFB and the 40 m depth corresponds to about one-half the largest plan dimension of the RBFB foundation.

(2) Properties of the three layers of soils are the same as the generic site properties for soft, medium, and hard soils in Table 3A.3-1.

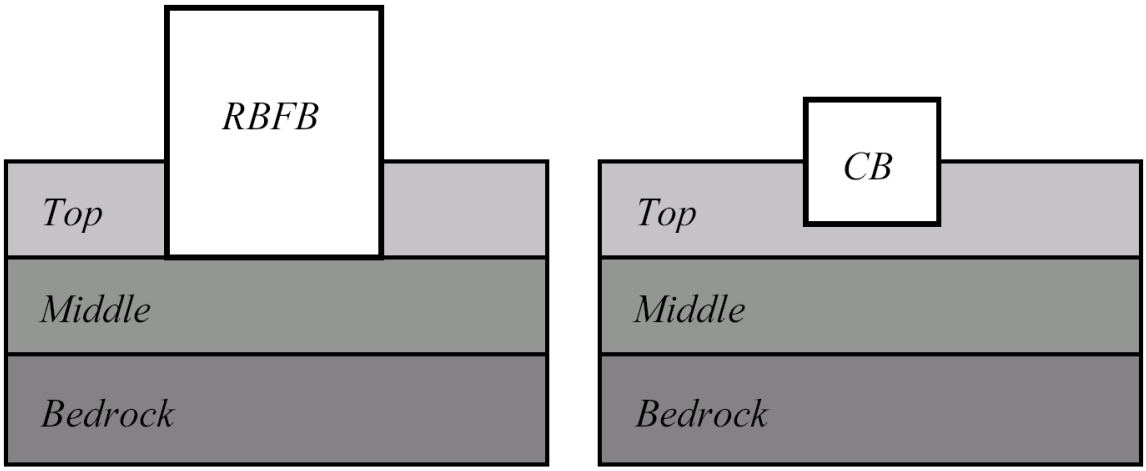

3A.4 INPUT MOTION AND DAMPING VALUES

3A.4.1 Input Motion

The time-history method is used in performing the seismic soil-structure interaction analysis. Earthquake input motions in the form of synthetic acceleration time histories are generated as described in Subsection 3.7.1 for three orthogonal components designated as H_1, H_2, and V. The H_1 and H_2 are the two horizontal components mutually perpendicular to each other. In the SSI analyses, H_1 and H_2 components are used in the horizontal X-(0°) and Y-(90°) directions, respectively. The V component is used in the vertical Z-direction.

Depending on the soil characteristics at the site and subject to availability of appropriate recorded ground-motion data, the control motion is defined on the soil surface at the top of finished grade or on an outcrop or a hypothetical outcrop at a location on the top of the competent material in accordance with the NRC Standard Review Plan (SRP) 3.7.1. For the generic sites defined in Section 3A.3.1, the design response spectra are conservatively applied at the level of foundation in the free field. The input motion for North Anna ESP site is also defined at the foundation level.

For the layered site cases, the input ground motion is defined as an outcrop motion at the RBFB foundation level for all the buildings. The corresponding surface motion is generated for use as input to the SASSI calculation for each site.

Vertically propagating plane seismic shear waves for the horizontal components and compression waves for the vertical component are assumed to generate the input motion.

3A.4.2 Damping Values

The structural components damping values used in the seismic analysis are in accordance with those specified in Regulatory Guide 1.61. These values for the SSE are summarized in Table 3.7-1.

3A.5 SOIL-STRUCTURE INTERACTION ANALYSIS METHOD

The seismic analysis for uniform sites is performed using the program DAC3N with the sway-rocking soil-structure interaction model. The seismic analysis for layered sites is performed using the program SASSI with the finite elements for modeling the soil-structure interaction.

3A.5.1 DAC3N Analysis Method

The analysis model is a lumped mass-beam model with soil springs. The structural models are described in Subsection 3.7.2, and in Subsection 3A.7 in more detail.

To account for soil-structure interaction effect, sway-rocking base soil springs are attached to the structural model. The base spring is evaluated from vibration admittance theory, based on three-dimensional wave propagation theory for uniform half space soil. For this evaluation, soil material damping values are conservatively neglected. Though the spring values consist of frequency dependent real and imaginary parts, they are simplified and replaced with frequency independent soil spring K_c, and damping coefficient C_c, respectively, for the time history analysis solved in time domain. The method used to obtain the equivalent frequency-independent soil stiffness and damping is illustrated in Figure 3A.5-1. The calculated K_c and C_c values are tabulated in Tables 3A.5-1 and 3A.5-2 for the RBFB complex and the CB, respectively.

The effect of lateral soil/backfill on embedded foundations is conservatively accounted for by applying the control motion directly at the foundation level. Dynamic lateral soil pressures are calculated separately and considered in the design of external walls, using the elastic solution procedures in Section 3.5.3.2 of ASCE 4-98.

Because the three component ground motion time histories are statistically independent as described in Subsections 3.7.1.1.2 and 3.7.1.1.3, they are input simultaneously in the response analysis using the time history method of analysis solved by direct integration. The numerical integration time step is 0.002 sec. for the RG 1.60 input motion and 0.001 sec. for the North Anna site input motion and the single envelope input motion. Structural responses in terms of accelerations, forces, and moments are computed directly. Floor response spectra are obtained from the calculated response acceleration time histories (Subsection 3.7.2.5).

3A.5.2 SASSI Analysis Method

For the seismic analysis of layered sites, the linear finite element computer program SASSI2000 is used. The program uses finite elements with complex moduli for modeling the structure and foundation properties and is based on the subtraction method and the frequency domain complex response method. The lumped mass-beam model described in Subsection 3A.5.1 is coupled with finite element soil model. The model details are described in Subsection 3A.7. Structural responses in terms of accelerations, forces and moments are computed directly. Floor response spectra are obtained from the calculated response acceleration time histories.

The SSI analyses for the three directional earthquake components are performed separately. The maximum co-directional responses to each of the three earthquake components are combined using algebraic sum in the time domain.

Table 3A.5-1

Soil Spring and Damping Coefficient for RBFB complex

			Generic Site			North Anna Site		
			Soft 300 m/s	Medium 800 m/s	Hard 1700 m/s	BE 1589 m/s	UB 1946 m/s	LB 1297 m/s
Soil Spring Kc	X-dir	MN/m	2.910E+04	2.178E+05	1.087E+06	9.676E+05	1.451E+06	6.447E+05
	Y-dir	MN/m	3.085E+04	2.281E+05	1.131E+06	1.001E+06	1.501E+06	6.670E+05
	Z-dir	MN/m	4.366E+04	2.972E+05	1.408E+06	1.245E+06	1.868E+06	8.297E+05
	X-X Rot.	MN•m/rad	2.466E+07	1.678E+08	7.950E+08	6.871E+08	1.030E+09	4.578E+08
	Y-Y Rot.	MN•m/rad	4.280E+07	2.913E+08	1.379E+09	1.145E+09	1.717E+09	7.627E+08
	Z-Z Rot.	MN•m/rad	9.804E+15	9.804E+15	9.804E+15	9.804E+15	9.804E+15	9.804E+15
Damping coefficient Cc	X-dir	MN•sec/m	1.708E+03	4.837E+03	1.143E+04	1.083E+04	1.324E+04	8.870E+03
	Y-dir	MN•sec/m	1.910E+03	5.294E+03	1.236E+04	1.159E+04	1.416E+04	9.484E+03
	Z-dir	MN•sec/m	3.852E+03	9.740E+03	2.114E+04	2.011E+04	2.437E+04	1.663E+04
	X-X Rot.	MN•m•sec/rad	2.512E+05	4.378E+05	4.626E+05	4.631E+05	4.235E+05	4.877E+05
	Y-Y Rot.	MN•m•sec/rad	8.432E+05	1.590E+06	1.694E+06	1.567E+06	1.444E+06	1.643E+06
	Z-Z Rot.	MN•m•sec/rad	0.0	0.0	0.0	0.0	0.0	0.0

Table 3A.5-2

Soil Spring and Damping Coefficient for CB

			Generic Site			North Anna Site		
			Soft	Medium	Hard	BE	UB	LB
			300 m/s	800 m/s	1700 m/s	1369 m/s	1677 m/s	1118 m/s
Soil Spring Kc	X-dir	MN/m	1.322E+04	9.876E+04	4.925E+05	3.297E+05	4.948E+05	2.199E+05
	Y-dir	MN/m	1.372E+04	1.017E+05	5.049E+05	3.375E+05	5.064E+05	2.250E+05
	Z-dir	MN/m	1.963E+04	1.336E+05	6.329E+05	4.157E+05	6.237E+05	2.773E+05
	X-X Rot.	MN•m/rad	2.508E+06	1.707E+07	8.085E+07	5.311E+07	7.969E+07	3.542E+07
	Y-Y Rot.	MN•m/rad	3.543E+06	2.411E+07	1.142E+08	7.501E+07	1.125E+08	5.003E+07
	Z-Z Rot.	MN•m/rad	9.804E+15	9.804E+15	9.804E+15	9.804E+15	9.804E+15	9.804E+15
Damping coefficient Cc	X-dir	MN•sec/m	3.515E+02	9.961E+02	2.349E+03	1.975E+03	2.412E+03	1.620E+03
	Y-dir	MN•sec/m	3.796E+02	1.058E+03	2.470E+03	2.071E+03	2.527E+03	1.698E+03
	Z-dir	MN•sec/m	7.794E+02	1.986E+03	4.307E+03	3.561E+03	4.314E+03	2.940E+03
	X-X Rot.	MN•m•sec/rad	1.421E+04	2.775E+04	3.073E+04	3.330E+04	3.163E+04	3.364E+04
	Y-Y Rot.	MN•m•sec/rad	2.720E+04	5.542E+04	6.489E+04	6.916E+04	6.670E+04	6.872E+04
	Z-Z Rot.	MN•m•sec/rad	0.0	0.0	0.0	0.0	0.0	0.0

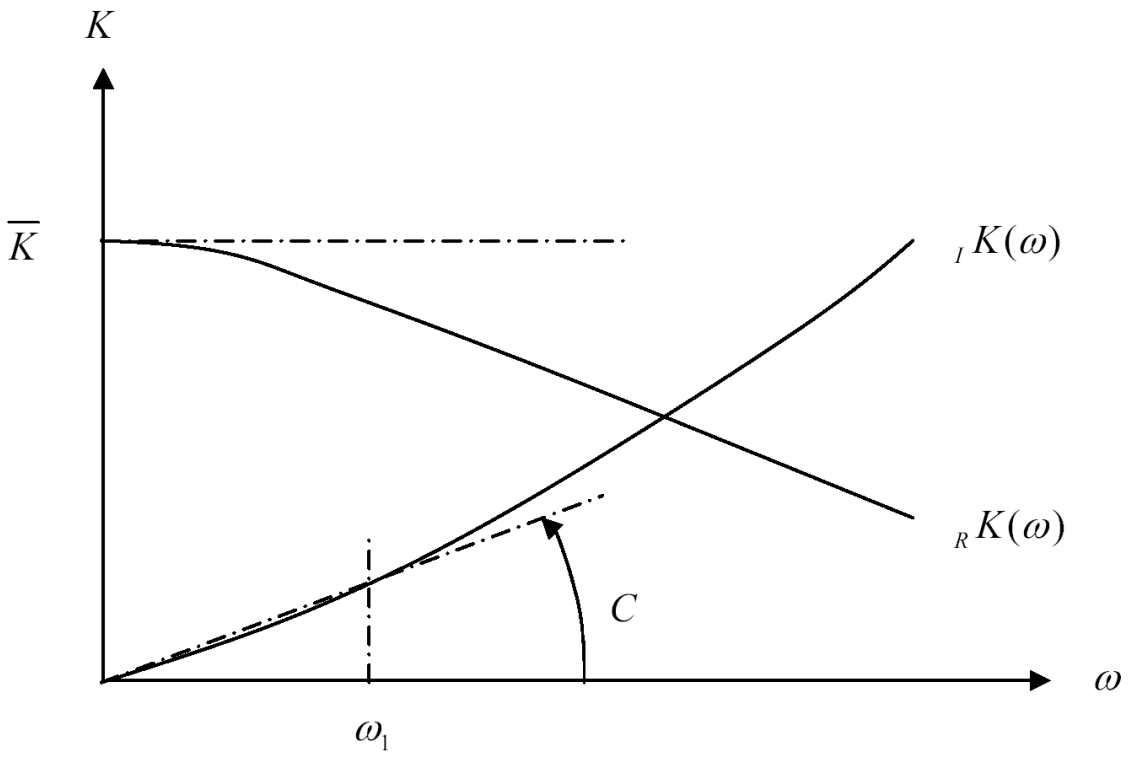

Note:

(1) The translational and rotational components of the soil springs $(\overline{K}_S, \overline{K}_R)$ are represented by the static theoretical solutions of the elastic wave theory with frequency $(\omega = 0)$.

(2) The damping constants (h_{S1}, h_{R1}) of the translational and rotational components of the soil springs corresponding to the fundamental frequency (ω_1) of the soil/building coupled system are calculated as follows:

$$h_{S1} = \frac{{}_I K_S(\omega_1)}{2_R K_S(\omega_1)}, \qquad h_{R1} = \frac{{}_I K_R(\omega_1)}{2_R K_R(\omega_1)}$$

(3) The damping constants (h_S, h_R) of the soil spring is approximated linearly as follows:

$$h_S(\omega) = \frac{h_{S1}}{\omega_1}\omega, \qquad h_R(\omega) = \frac{h_{R1}}{\omega_1}\omega$$

(4) The viscous damping coefficient is derived as follows:

$$C_S = \frac{2h_{S1}}{\omega_1}\overline{K}_S \qquad C_R = \frac{2h_{R1}}{\omega_1}\overline{K}_R$$

Figure 3A.5-1. Method for Frequency-Independent Soil Properties

3A.6 SOIL-STRUCTURE INTERACTION ANALYSIS CASES

To establish design envelopes of seismic responses of the RBFB complex, SSI analyses are performed for 27 cases of uniform sites and 6 cases of layered sites, as summarized in Table 3A.6-1. Similarly for the CB, SSI analyses are performed for 11 cases of uniform sites and 6 cases of layered sites.

The enveloping results are obtained from the responses of all SSI cases to cover a wide range of conditions.

Table 3A.6-1

Seismic SSI Analysis Cases

Building	No.	Model	Input Motion	Uniform Soil Condition						
				Generic Site				North Anna ESP Site		
				Soft	Medium	Hard	Fixed	NA-BE	NA-UB	NA-LB
RBFB	RU-1	Base	RG 1.60 (0.3g)	*	*	*	*			
	RU-2	Base	NA site spectra					*	*	*
	RU-3	Base	Single envelope spectra	*	*	*	*			
	RU-4	Updated(1)	Single envelope spectra	*	*	*	*			
	RU-5	In-fill Concret(2)	Single envelope spectra	*	*	*	*			
	RU-6	LOCA flooding(3)	Single envelope spectra	*	*	*	*			
	RU-7	Wall Out-of-plane(4)	Single envelope spectra	*	*	*	*			
CB	CU-1	Base	RG 1.60 (0.3g)	*	*	*	*			
	CU-2	Base	NA site spectra					*	*	*
	CU-3	Base	Single envelope spectra	*	*	*	*			

(1) Updated model for RSW, VW and DF properties

(2) Updated model + VW DF in-fill concrete 50% stiffness

(3) Updated model + LOCA flooding condition

(4) Wall out-of-plane oscillator model

Building	No.	Model	Input Motion	Layered Soil Conditions			
				case1	case2	case3	case4
RBFB	RL-1	Base	Single envelope spectra	*			
	RL-2	Base	Single envelope spectra		*		
	RL-3	Base	Single envelope spectra			*	
	RL-4	Base	Single envelope spectra				*
	RL-5	Cracked(1)	Single envelope spectra	(critical case from RL-1 to RL-4)			
	RL-6	Cracked wall out-of-plane(2)	Single envelope spectra	(critical case from RL-1 to RL-4)			
CB	CL-1	Base	Single envelope spectra	*			
	CL-2	Base	Single envelope spectra		*		
	CL-3	Base	Single envelope spectra			*	
	CL-4	Base	Single envelope spectra				*
	CL-5	Cracked(1)	Single envelope spectra	(critical case from CL-1 to CL-4)			
	CL-6	SSI effect(3)	Single envelope spectra	(critical case from CL-1 to CL-4)			

(1) Concrete stiffness 50% reduced model considering crack effect

(2) Wall out-of-plane oscillator model considering crack effect

(3) Soil response obtained from the RBFB analysis is used as input motion for CB model

3A.7 ANALYSIS MODELS

The analysis model is a three-dimensional lumped mass-beam model that considers shear, bending, torsion and axial deformations. The structural elements of the reactor building outside containment and the fuel building are reduced to one set of stick models. The containment and the containment internal structures including the reactor pressure vessel are modelled as separate interconnected sticks. The control building is modelled with a single stick.

3A.7.1 Method of Dynamic Structural Model Development

Evaluation of stiffness for the seismic model is done according to the following assumptions.

- Exterior walls and those inner walls that are continuous up from the basemat and have 500 mm or more in thickness are treated as seismic walls.
- Those openings that have 2.0 m^2 or larger area are explicitly considered in the stiffness evaluation.

Effective Shear Area (Sx, Sy):

As effective shear area, seismic walls parallel to each of two earthquake directions are considered. When openings exist in a wall, equivalent shear area is calculated so that shear displacements of two walls, with and without openings, are equal.

Moment of Inertia (Iyy, Ixx):

Moment of inertia of seismic walls is calculated according to the following procedures.

- Moment of inertia in each direction is calculated around a horizontal axis that goes through the centroid.
- When openings exist in a wall, equivalent moment of inertia is calculated so that angles of rotation of two walls, with and without openings, are equal.
- The effective flange length is taken to be eight times the flange wall thickness, and it is limited to one-half of the flange wall length.

Torsional Constant (Izz):

Torsional constant of seismic walls is calculated around the vertical axis that goes through the center of rigidity.

Vertical Axial Area (Sa):

Vertical axial area of each element is equal to the summation of effective shear areas that are evaluated in two directions for the horizontal analysis. However, the overlap area at the corner of box walls is subtracted from the summation.

The locations (X_c and Y_c) of centroid of axial area for various sections define the locations of center of rigidity of the equivalent beam stick model in the vertical direction.

Because the stick model has different center-of-rigidity locations in the horizontal and the vertical directions, the lumped mass-beam model comprises two stick models. One stick consists of elements with axial areas located at the centers of rigidity for axial area, and another stick

consists of elements with all other remaining sectional properties (i.e., excluding axial area) located at the centers of rigidity for shear and torsional deformations. Both sticks are connected at common centers of mass at various floor elevations.

As described above, the RBFB complex is represented by several stick models. These stick models are interconnected by horizontal links representing the floor diaphragm at respective elevations. These links are modeled as rigid springs for floor in-plane translational displacement and having no stiffness for all other deformations.

The vertical floor frequencies are obtained at major floor locations by independent modal analysis of the respective floor finite element model. These frequencies are included in the stick model by a series of vertical single degree-of-freedom oscillators at the corresponding floor elevations.

The out-of-plane vibrations frequencies of walls are evaluated by using finite element model in the same manner as the slab frequencies. These frequencies are included in the stick model by a series of horizontal single degree-of-freedom oscillators at the corresponding wall elevations to obtain design loads of these walls and design Floor Response Spectra (FRS) for the components attached to these walls.

To obtain the mass properties for the stick model, the dead load, 25% of the live load, 100% of the roof snow load and an additional 50 psf load for piping and cable trays, etc. were used to compute the lumped mass properties following the steps described below.

(1) Depending on whether the floor has a regular or an irregular layout, hand calculations or floor finite element models are used to obtain the total mass (M_x, $M_{y,}$ M_z), the mass moments of inertia (M_{xx}, M_{yy}, M_{zz}) and the center of mass of each floor. Similar calculations are performed for the tributary areas of the walls above and below the floors.

(2) These properties are subsequently reduced to one center of mass with its associated properties at each floor elevation. The water masses in the pools are also included in this calculation.

(3) The bending mass moment of inertia at various floor elevations are also added to each floor mass.

Based on the methodology described above, the lumped mass-beam stick model for SSI is developed as described in Section 3A.7.2.

3A.7.2 Lumped Mass-Beam Stick Model for SSI Analysis

The lumped mass-beam stick models for the RBFB complex in the XZ- and YZ-planes are shown in Figures 3A.7-1. Similarly, the stick models corresponding to the RCCV and pedestal wall are shown in Figures 3A.7-2 and 3A.7-3. The overall integrated building model is shown in Figure 3A.7-4. As shown in the figure, the building model is also coupled to the vent wall (VW), the reactor shield wall (RSW) and the reactor pressure vessel (RPV). They are symmetric in both horizontal directions.

The stick models are interconnected at floor elevations by horizontal links. These links are rigid for floor in-plane displacements and have no stiffness for out-of-plane displacement and rotations.

The lumped mass-beam stick models for the CB in the XZ- and YZ-planes are shown in Figures 3A.7-5. The overall CB seismic model is shown in Figure 3A.7-6.

To account for soil-structure interaction effect, sway-rocking base soil springs are attached to this structural model, as described in Section 3A.5. Natural frequencies of the seismic model at all site conditions are shown in Tables 3A.7-1 through 3A.7-7 for the RBFB model and Tables 3A.7-8 through 3A.7-14 for the CB model.

3A.7.3 SSI Model for SASSI Analysis

In the SASSI SSI model, the exterior walls below grade and the foundation basemat along with the supporting soil medium are modeled. For this reason, the sectional properties of the stick model below grade are modified to subtract the stiffness properties corresponding to subgrade outer walls. In this model, the basemat and the exterior walls are modeled by plate elements.

For the RBFB complex, the basemat plate elements are shown in Figure 3A.7-7. The thickness of basemat is 4.0 m. The side wall plate elements are shown in Figures 3A.7-8. The thickness of the modeled side wall is 2.0 m between EL –11.5 m to 4.5 m and set as a quarter of basemat width between EL –11.5 m to –15.5m.

The RBFB stick model is connected to the basemat and side walls at floor EL –11.5 m, 6.4m, -1.0 m and 4.5 m by a set of rigid links. At the base of the model at EL –11.5 m, a rigid link is used to connect all the stick models to the middle of the basemat. The overall RBFB SASSI model is shown in Figure 3A.7-9.

For the CB, the basemat plate elements are shown in Figure 3A.7-10. The thickness of basemat is 3.0 m. The side wall plate elements are shown in Figures 3A.7-11. The thickness of the modeled side wall is 0.9 m between EL –7.4 m to 4.5 m and set as a quarter of basemat width between EL –7.4 m to –10.4 m.

The CB stick model is connected to the basemat and side walls at floor EL –10.4 m, 6.4 m, -2.0 m and 4.5 m by a set of rigid links. At the base of the model at EL –7.4 m, a rigid link is used to connect all the stick models to the middle of the basemat. The overall CB SASSI model is shown in Figure 3A.7-12.

Table 3A.7-1

Eigenvalue Analysis Results for RBFB model at Soft Site

Mode No.	Frequency (Hz)	Period (sec)	Participation Factor					
			X dir.	Y dir.	Z dir.	X rot	Y rot	Z rot
1	1.19	0.84	-0.02	1.56	-0.01	-1032	-19	-38
2	1.43	0.70	1.43	0.02	0.10	-8	738	3
3	2.09	0.48	-0.21	0.02	2.34	3	204	0
4	2.78	0.36	-0.20	-0.10	-1.40	-193	604	0
5	2.90	0.34	0.00	0.63	-0.01	1321	16	16
6	3.20	0.31	-0.45	0.00	-0.10	-7	1887	7
7	3.81	0.26	0.00	-0.18	0.00	243	21	-256
8	3.81	0.26	-0.14	-0.01	0.02	10	-498	-8
9	5.23	0.19	0.11	0.00	-0.05	16	-1055	-74
10	5.26	0.19	-0.06	0.01	-0.23	15	615	90
11	5.94	0.17	0.00	-0.05	0.00	1359	189	-13034
12	5.99	0.17	-0.11	0.01	-0.01	31	700	-72
13	5.99	0.17	-0.01	-0.08	0.00	-1899	-164	12881
14	6.76	0.15	-0.05	0.00	-0.13	41	411	-158
15	8.73	0.11	0.00	-0.11	0.01	-564	-64	298
16	9.77	0.10	0.02	0.00	-0.05	-227	7713	139
17	10.11	0.10	-0.19	0.00	0.07	528	-5566	-48
18	10.27	0.10	-0.03	0.02	0.01	-5566	-1230	-2631
19	10.57	0.09	0.00	0.00	-0.02	151	-4336	17
20	10.86	0.09	-0.10	0.00	-0.01	-63	27	-130

Notes: (1) The participation factors are calculated for mode vectors normalized by the maximum mode displacement.

(2) Modal information shown is not used in the response analysis performed by the direct integration method.

Table 3A.7-2

Eigenvalue Analysis Results for RBFB model at Medium Site

Mode No.	Frequency (Hz)	Period (sec)	Participation Factor					
			X dir.	Y dir.	Z dir.	X rot	Y rot	Z rot
1	2.58	0.39	-0.02	1.68	0.01	-1170	-13	-251
2	2.73	0.37	0.99	-0.11	1.49	58	875	34
3	2.95	0.34	1.95	0.02	0.08	-15	1336	29
4	3.81	0.26	0.00	-0.29	-0.04	1023	-2	-46
5	3.81	0.26	-0.86	0.00	-0.20	0	-1337	-34
6	4.93	0.20	-0.56	-0.17	5.93	-201	700	98
7	5.22	0.19	-0.90	0.00	0.04	4	1374	-76
8	5.47	0.18	1.07	0.19	-5.09	270	-1835	-101
9	5.96	0.17	-0.13	4.00	0.64	9794	788	-26998
10	5.98	0.17	1.54	-0.15	1.17	212	-3545	-3213
11	6.00	0.17	-0.09	0.87	-0.08	-2801	-388	29807
12	6.22	0.16	0.25	-4.53	-0.36	-6638	-489	-2842
13	6.58	0.15	4.40	0.23	1.53	360	-10263	52
14	6.79	0.15	-4.00	-0.15	-2.77	-213	9480	-140
15	9.79	0.10	0.00	-0.74	0.04	-690	-25	696
16	10.30	0.10	-0.91	0.01	-0.25	20	6097	103
17	10.30	0.10	0.04	-0.37	-0.08	-4311	336	-1353
18	10.53	0.09	1.39	-0.05	-0.80	-128	5121	311
19	10.92	0.09	-1.16	-0.01	0.36	222	-7359	-216
20	11.21	0.09	0.12	0.01	0.18	317	-4118	29

Notes: (1) The participation factors are calculated for mode vectors normalized by the maximum mode displacement.

(2) Modal information shown is not used in the response analysis performed by the direct integration method.

Table 3A.7-3

Eigenvalue Analysis Results for RBFB model at Hard Site

Mode No.	Frequency (Hz)	Period (sec)	Participation Factor					
			X dir.	Y dir.	Z dir.	X rot	Y rot	Z rot
1	2.74	0.37	0.12	0.03	1.16	-38	197	-3
2	3.52	0.28	-0.11	3.75	0.07	-2594	-77	-1458
3	3.81	0.26	8.25	0.23	0.38	-142	4886	231
4	3.81	0.26	0.07	-2.65	-0.08	2560	70	1185
5	3.95	0.25	-7.16	-0.20	-0.39	137	-4812	-242
6	5.20	0.19	0.07	-0.11	1.87	-72	-19	238
7	5.22	0.19	-0.68	0.00	-0.14	15	297	-128
8	5.98	0.17	0.09	0.62	-0.16	2664	131	-12494
9	5.99	0.17	0.56	-0.03	-0.16	9	-1021	-301
10	6.05	0.17	-0.08	0.29	0.09	-1693	-166	12891
11	6.75	0.15	0.17	-0.26	2.37	-211	-228	-659
12	7.64	0.13	0.12	1.25	-0.48	1676	-276	911
13	8.09	0.12	1.38	-0.33	-2.16	-463	-3023	-214
14	9.09	0.11	1.11	0.14	2.86	169	-1897	-72
15	10.31	0.10	0.00	0.52	-0.29	-2402	-258	-1429
16	10.45	0.10	-1.14	-0.02	-2.10	-83	5436	165
17	10.71	0.09	0.72	0.03	-2.27	80	-1818	1
18	11.22	0.09	0.00	-0.68	0.07	310	57	832
19	11.26	0.09	0.25	-0.01	0.31	6	-1539	-36
20	11.64	0.09	0.00	-2.94	0.07	-2245	24	2090

Notes:

(1) The participation factors are calculated for mode vectors normalized by the maximum mode displacement.

(2) Modal information shown is not used in the response analysis performed by the direct integration method.

Table 3A.7-4

Eigenvalue Analysis Results for RBFB model in Fixed-base Case

Mode No.	Frequency (Hz)	Period (sec)	Participation Factor					
			X dir.	Y dir.	Z dir.	X rot	Y rot	Z rot
1	2.74	0.37	0.07	0.02	1.10	-31	144	-2
2	3.81	0.26	-0.31	6.84	0.15	-3936	-179	-3818
3	3.81	0.26	2.33	0.11	0.06	-45	856	33
4	3.95	0.25	0.25	-5.78	-0.16	3912	172	3528
5	4.40	0.23	1.66	0.07	0.08	-48	1038	70
6	5.21	0.19	0.11	-0.12	1.59	-53	-2	317
7	5.22	0.19	-0.80	0.00	-0.23	24	92	-174
8	5.98	0.17	0.07	0.50	-0.10	1922	100	-8354
9	5.99	0.17	0.45	-0.03	-0.09	11	-794	-212
10	6.09	0.16	-0.06	0.26	0.06	-1204	-118	8782
11	6.75	0.15	0.24	-0.15	1.41	-62	-306	-604
12	8.03	0.12	0.04	1.35	-0.23	1930	-130	1287
13	8.74	0.11	1.55	-0.11	-1.11	-145	-3709	-165
14	10.25	0.10	0.66	0.23	3.65	-582	1260	-368
15	10.32	0.10	-0.12	0.35	-1.18	-1876	-1037	-1037
16	10.65	0.09	1.36	0.06	2.08	7	-4236	-190
17	11.17	0.09	-0.47	-0.09	-2.93	258	-130	206
18	11.23	0.09	0.05	-0.25	0.44	347	234	459
19	11.33	0.09	-0.79	-0.04	-3.61	262	1472	199
20	12.03	0.08	-0.33	-0.06	-1.35	-81	374	22

Notes:

(1) The participation factors are calculated for mode vectors normalized by the maximum mode displacement.

(2) Modal information shown is not used in the response analysis performed by the direct integration method.

Table 3A.7-5

Eigenvalue Analysis Results for RBFB model at Best-estimate North Anna Site

Mode No.	Frequency (Hz)	Period (sec)	Participation Factor					
			X dir.	Y dir.	Z dir.	X rot	Y rot	Z rot
1	2.74	0.37	0.13	0.03	1.17	-39	209	-3
2	3.46	0.29	-0.09	3.26	0.06	-2271	-65	-1201
3	3.81	0.26	14.37	0.38	0.73	-251	9204	418
4	3.81	0.26	0.05	-2.17	-0.07	2237	57	929
5	3.89	0.26	-13.28	-0.35	-0.75	245	-9127	-429
6	5.20	0.19	0.07	-0.11	1.92	-74	-19	230
7	5.22	0.19	-0.68	0.00	-0.13	15	320	-124
8	5.98	0.17	0.10	0.64	-0.17	2802	139	-13290
9	5.99	0.17	0.58	-0.03	-0.17	8	-1063	-306
10	6.05	0.17	-0.08	0.30	0.10	-1789	-176	13684
11	6.75	0.15	0.14	-0.29	2.60	-247	-184	-681
12	7.58	0.13	0.14	1.21	-0.56	1613	-325	854
13	7.98	0.13	-0.95	0.30	1.68	421	2075	182
14	8.93	0.11	1.15	0.14	2.54	179	-2064	-62
15	10.30	0.10	0.01	0.54	-0.26	-2431	-240	-1466
16	10.44	0.10	-1.08	-0.01	-1.86	-83	5493	158
17	10.70	0.09	0.83	0.05	-1.99	80	-1898	-11
18	11.21	0.09	0.00	-0.84	0.07	213	54	943
19	11.25	0.09	0.25	-0.01	0.28	8	-1586	-34
20	11.55	0.09	0.00	-3.07	0.07	-2371	17	2099

Notes:

(1) The participation factors are calculated for mode vectors normalized by the maximum mode displacement.

(2) Modal information shown is not used in the response analysis performed by the direct integration method.

Table 3A.7-6

Eigenvalue Analysis Results for RBFB model at Upper-bound North Anna Site

Mode No.	Frequency (Hz)	Period (sec)	Participation Factor					
			X dir.	Y dir.	Z dir.	X rot	Y rot	Z rot
1	2.74	0.37	0.11	0.03	1.14	-36	185	-2
2	3.61	0.28	-0.16	5.07	0.10	-3503	-115	-2164
3	3.81	0.26	5.29	0.17	0.22	-94	2902	137
4	3.81	0.26	0.11	-3.98	-0.11	3469	107	1888
5	4.04	0.25	-4.21	-0.13	-0.23	89	-2826	-149
6	5.20	0.19	0.08	-0.11	1.78	-67	-17	250
7	5.22	0.19	-0.70	0.00	-0.16	17	250	-136
8	5.98	0.17	0.08	0.58	-0.14	2470	126	-11440
9	5.99	0.17	0.53	-0.03	-0.14	9	-960	-269
10	6.06	0.16	-0.07	0.28	0.08	-1569	-155	11838
11	6.75	0.15	0.20	-0.22	2.02	-158	-278	-627
12	7.74	0.13	0.09	1.30	-0.38	1758	-218	1006
13	8.29	0.12	1.12	-0.18	-1.39	-243	-2491	-136
14	9.45	0.11	1.11	0.15	3.65	131	-1591	-103
15	10.31	0.10	-0.01	0.49	-0.35	-2352	-329	-1365
16	10.48	0.10	-1.31	-0.03	-2.76	-87	5455	185
17	10.73	0.09	0.43	0.00	-3.12	92	-1514	39
18	11.22	0.09	0.00	-0.49	0.08	400	68	697
19	11.26	0.09	0.25	-0.01	0.41	0	-1515	-40
20	11.81	0.08	0.01	-2.69	0.08	-2093	38	2071

Note :

(1) The participation factors are calculated for mode vectors normalized by the maximum mode displacement.

(2) Modal information shown is not used in the response analysis performed by the direct integration method.

Table 3A.7-7

Eigenvalue Analysis Results for RBFB model at Lower-bound North Anna Site

Mode No.	Frequency (Hz)	Period (sec)	Participation Factor					
			X dir.	Y dir.	Z dir.	X rot	Y rot	Z rot
1	2.73	0.37	0.17	0.04	1.21	-47	252	-4
2	3.27	0.31	-0.05	2.35	0.03	-1651	-40	-713
3	3.68	0.27	9.03	0.20	0.52	-137	6322	252
4	3.81	0.26	0.02	-1.25	-0.05	1620	31	446
5	3.81	0.26	-7.93	-0.17	-0.54	130	-6249	-261
6	5.19	0.19	0.04	-0.11	2.21	-88	-11	209
7	5.22	0.19	-0.67	0.00	-0.09	12	426	-112
8	5.98	0.17	0.12	0.74	-0.25	3372	150	-16376
9	5.99	0.17	0.67	-0.04	-0.27	0	-1254	-335
10	6.04	0.17	-0.09	0.32	0.13	-2155	-208	16783
11	6.74	0.15	-0.18	-0.56	4.60	-568	378	-919
12	7.29	0.14	0.52	1.18	-1.87	1547	-1089	785
13	7.50	0.13	-0.40	0.61	1.02	831	831	337
14	8.36	0.12	1.22	0.11	1.47	164	-2418	-39
15	10.30	0.10	0.02	0.66	-0.20	-2465	-150	-1630
16	10.41	0.10	-0.95	0.01	-1.17	-65	5645	142
17	10.67	0.09	1.11	0.12	-1.38	114	-1642	-42
18	11.10	0.09	0.00	-1.80	0.05	-1072	6	1282
19	11.25	0.09	0.27	-0.02	0.19	0	-1694	-26
20	11.27	0.09	0.00	-1.84	0.01	-2250	-10	804

Notes:

(1) The participation factors are calculated for mode vectors normalized by the maximum mode displacement.

(2) Modal information shown is not used in the response analysis performed by the direct integration method.

Table 3A.7-8

Eigenvalue Analysis Results for CB model at Soft Site

Mode No.	Frequency (Hz)	Period (sec)	Participation Factor					
			X dir.	Y dir.	Z dir.	X rot	Y rot	Z rot
1	3.23	0.31	0.01	1.23	0.00	-308	4	-1
2	3.41	0.29	1.19	-0.01	0.00	3	369	1
3	5.19	0.19	0.00	0.00	1.37	-1	0	0
4	7.27	0.14	0.46	0.02	0.00	19	-760	0
5	7.46	0.13	-0.02	0.55	0.00	598	30	0
6	10.32	0.10	0.00	0.00	-0.37	-9	3	0
7	14.92	0.07	0.00	0.00	-0.19	-3	2	-1
8	16.66	0.06	0.00	0.00	0.00	0	0	26
9	20.80	0.05	0.00	0.00	-0.11	20	-3	2
10	22.40	0.04	-0.02	-0.02	0.00	537	-479	11

Notes:

(1) The participation factors are calculated for mode vectors normalized by the maximum mode displacement.

(2) Modal information shown is not used in the response analysis performed by the direct integration method.

Table 3A.7-9

Eigenvalue Analysis Results for CB model at Medium Site

Mode No.	Frequency (Hz)	Period (sec)	Participation Factor					
			X dir.	Y dir.	Z dir.	X rot	Y rot	Z rot
1	6.94	0.14	0.07	1.32	0.01	-308	23	-7
2	7.37	0.14	1.29	-0.07	0.00	15	386	7
3	9.64	0.10	-0.01	-0.01	2.23	-2	3	0
4	13.09	0.08	-0.02	-0.03	3.38	-16	18	0
5	15.42	0.06	0.04	0.05	-2.71	40	-41	-1
6	16.66	0.06	0.00	0.00	0.00	0	-2	46
7	17.10	0.06	0.48	0.09	0.01	70	-610	-57
8	17.62	0.06	-0.09	0.57	0.01	439	122	9
9	20.83	0.05	0.00	-0.01	-1.00	-2	1	1
10	25.58	0.04	-0.12	-0.09	0.01	559	-438	8

Notes:

(1) The participation factors are calculated for mode vectors normalized by the maximum mode displacement.

(2) Modal information shown is not used in the response analysis performed by the direct integration method.

Table 3A.7-10

Eigenvalue Analysis Results for CB model at Hard Site

Mode No.	Frequency (Hz)	Period (sec)	Participation Factor					
			X dir.	Y dir.	Z dir.	X rot	Y rot	Z rot
1	9.28	0.11	0.14	1.33	0.01	-244	39	-16
2	9.85	0.10	1.28	-0.14	0.05	22	313	19
3	9.90	0.10	-0.36	0.00	1.34	-3	-85	-5
4	14.62	0.07	-0.02	-0.02	1.89	-10	13	0
5	16.67	0.06	0.00	0.00	0.00	0	0	-35
6	20.53	0.05	-0.14	-0.15	6.93	-183	246	0
7	22.42	0.04	0.28	0.26	-6.01	330	-522	-2
8	24.11	0.04	0.26	0.10	0.08	119	-494	-6
9	25.18	0.04	-0.12	0.38	0.04	409	232	10
10	27.53	0.04	-0.06	-0.15	-2.73	-49	82	1

Notes:

(1) The participation factors are calculated for mode vectors normalized by the maximum mode displacement.

(2) Modal information shown is not used in the response analysis performed by the direct integration method.

Table 3A.7-11

Eigenvalue Analysis Results for CB model in Fixed-base Case

Mode No.	Frequency (Hz)	Period (sec)	Participation Factor					
			X dir.	Y dir.	Z dir.	X rot	Y rot	Z rot
1	9.94	0.10	0.03	0.07	1.20	-14	11	-1
2	10.28	0.10	0.18	1.29	0.00	-187	43	-23
3	10.89	0.09	1.25	-0.18	0.00	21	248	28
4	14.69	0.07	-0.02	-0.02	1.43	-9	11	0
5	16.67	0.06	0.00	0.00	0.00	0	0	-44
6	20.72	0.05	-0.04	-0.05	2.46	-66	86	0
7	25.62	0.04	-1.04	-0.68	1.68	-1141	2652	21
8	26.16	0.04	1.38	0.49	3.94	798	-3540	-42
9	26.95	0.04	-0.21	0.47	0.03	693	550	20
10	28.80	0.03	-0.14	-0.30	-4.56	-267	315	1

Notes:

(1) The participation factors are calculated for mode vectors normalized by the maximum mode displacement.

(2) Modal information shown is not used in the response analysis performed by the direct integration method.

Table 3A.7-12

Eigenvalue Analysis Results for CB model at Best-estimate North Anna Site

Mode No.	Frequency (Hz)	Period (sec)	Participation Factor					
			X dir.	Y dir.	Z dir.	X rot	Y rot	Z rot
1	8.85	0.11	0.12	1.33	0.01	-264	37	-14
2	9.40	0.11	1.30	-0.12	0.01	22	339	16
3	9.88	0.10	-0.04	-0.02	1.44	0	-6	0
4	14.56	0.07	-0.02	-0.02	2.23	-12	15	0
5	16.67	0.06	0.00	0.00	0.00	0	0	-32
6	19.85	0.05	-0.18	-0.20	9.09	-209	275	-1
7	21.20	0.05	0.29	0.29	-8.33	321	-474	-1
8	23.08	0.04	0.32	0.11	0.05	110	-533	-7
9	24.07	0.04	-0.12	0.44	0.03	413	207	9
10	27.40	0.04	-0.03	-0.09	-1.88	37	20	2

Notes:

(1) The participation factors are calculated for mode vectors normalized by the maximum mode displacement.

(2) Modal information shown is not used in the response analysis performed by the direct integration method.

Table 3A.7-13

Eigenvalue Analysis Results for CB model at Upper-bound North Anna Site

Mode No.	Frequency (Hz)	Period (sec)	Participation Factor					
			X dir.	Y dir.	Z dir.	X rot	Y rot	Z rot
1	9.27	0.11	0.14	1.32	0.01	-245	39	-16
2	9.85	0.10	1.28	-0.14	0.05	22	315	19
3	9.90	0.10	-0.33	0.00	1.34	-2	-77	-4
4	14.62	0.07	-0.02	-0.02	1.89	-10	13	0
5	16.67	0.06	0.00	0.00	0.00	0	0	-35
6	20.53	0.05	-0.15	-0.16	7.08	-186	250	0
7	22.37	0.04	0.28	0.26	-6.17	329	-517	-2
8	24.10	0.04	0.26	0.10	0.07	119	-494	-6
9	25.18	0.04	-0.12	0.38	0.04	410	231	10
10	27.52	0.04	-0.06	-0.15	-2.70	-49	80	1

Notes:

(1) The participation factors are calculated for mode vectors normalized by the maximum mode displacement.

(2) Modal information shown is not used in the response analysis performed by the direct integration method.

Table 3A.7-14

Eigenvalue Analysis Results for CB model at Lower-bound North Anna Site

Mode No.	Frequency (Hz)	Period (sec)	Participation Factor					
			X dir.	Y dir.	Z dir.	X rot	Y rot	Z rot
1	8.29	0.12	0.10	1.33	0.01	-284	33	-12
2	8.82	0.11	1.30	-0.11	0.01	20	363	13
3	9.84	0.10	-0.02	-0.01	1.59	-1	-1	0
4	14.43	0.07	-0.02	-0.03	2.94	-15	19	0
5	16.67	0.06	0.00	0.00	0.00	0	0	-28
6	18.03	0.06	-0.06	-0.07	3.94	-60	73	-1
7	20.92	0.05	0.30	0.23	-3.36	213	-430	-4
8	21.50	0.05	0.38	0.11	0.03	94	-548	-9
9	22.34	0.04	-0.12	0.51	0.02	410	176	8
10	27.32	0.04	-0.02	-0.07	-1.27	147	-26	3

Notes:

(1) The participation factors are calculated for mode vectors normalized by the maximum mode displacement.

(2) Modal information shown is not used in the response analysis performed by the direct integration method.

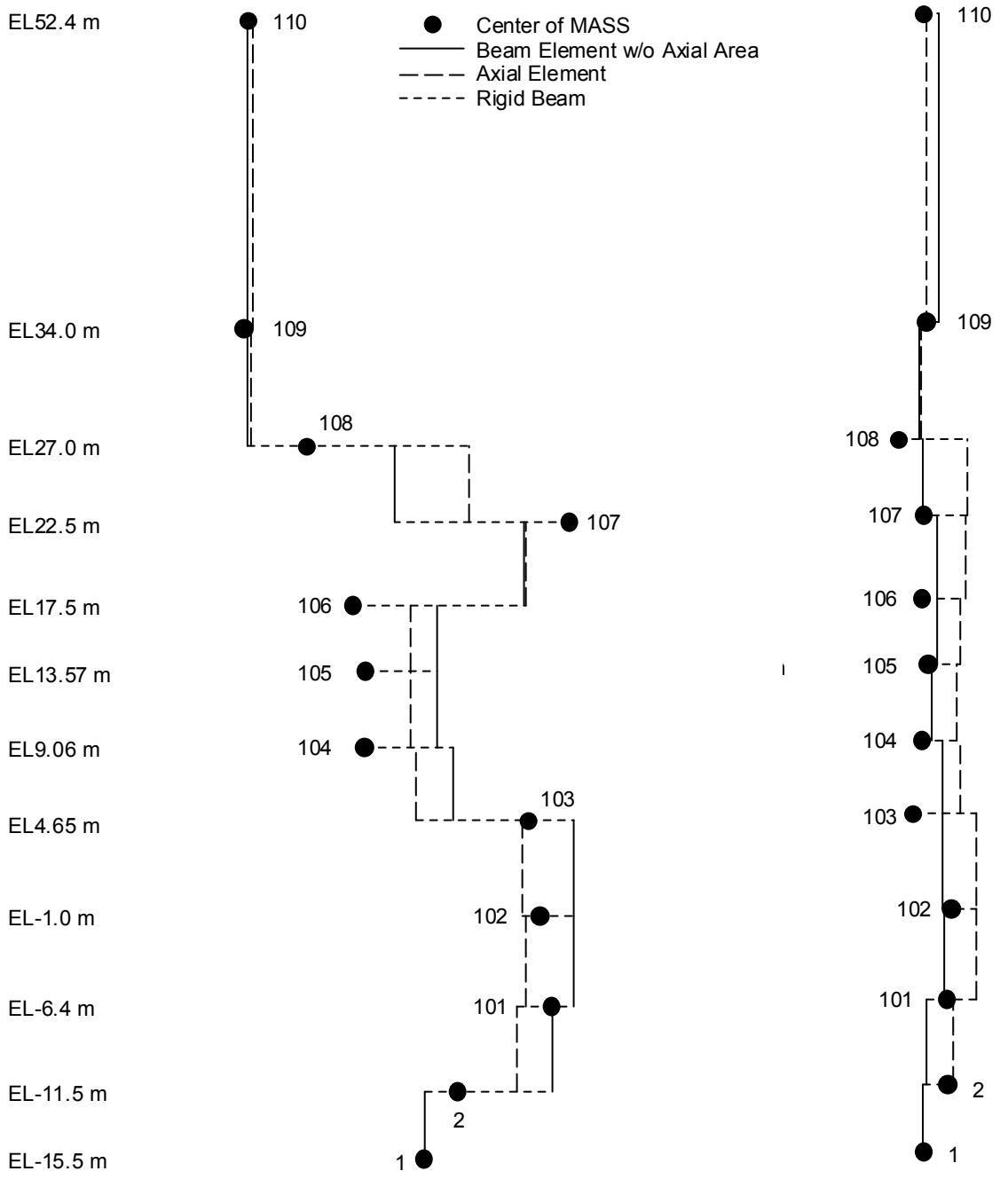

(a) XZ Plane **(b) YZ Plane**

Figure 3A.7-1. RBFB Stick Model

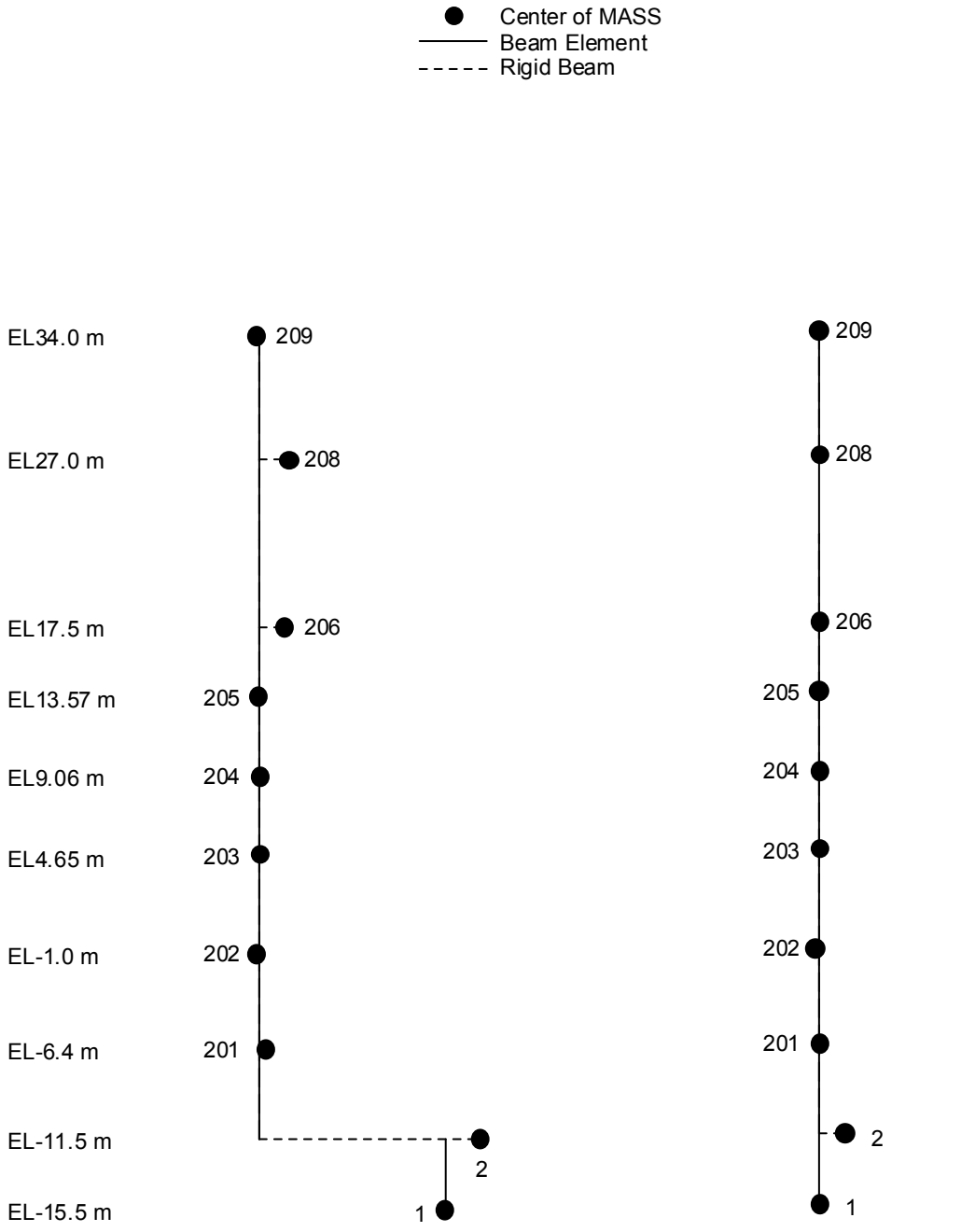

(a) XZ Plane **(b) YZ Plane**

Figure 3A.7-2. RCCV Stick Model

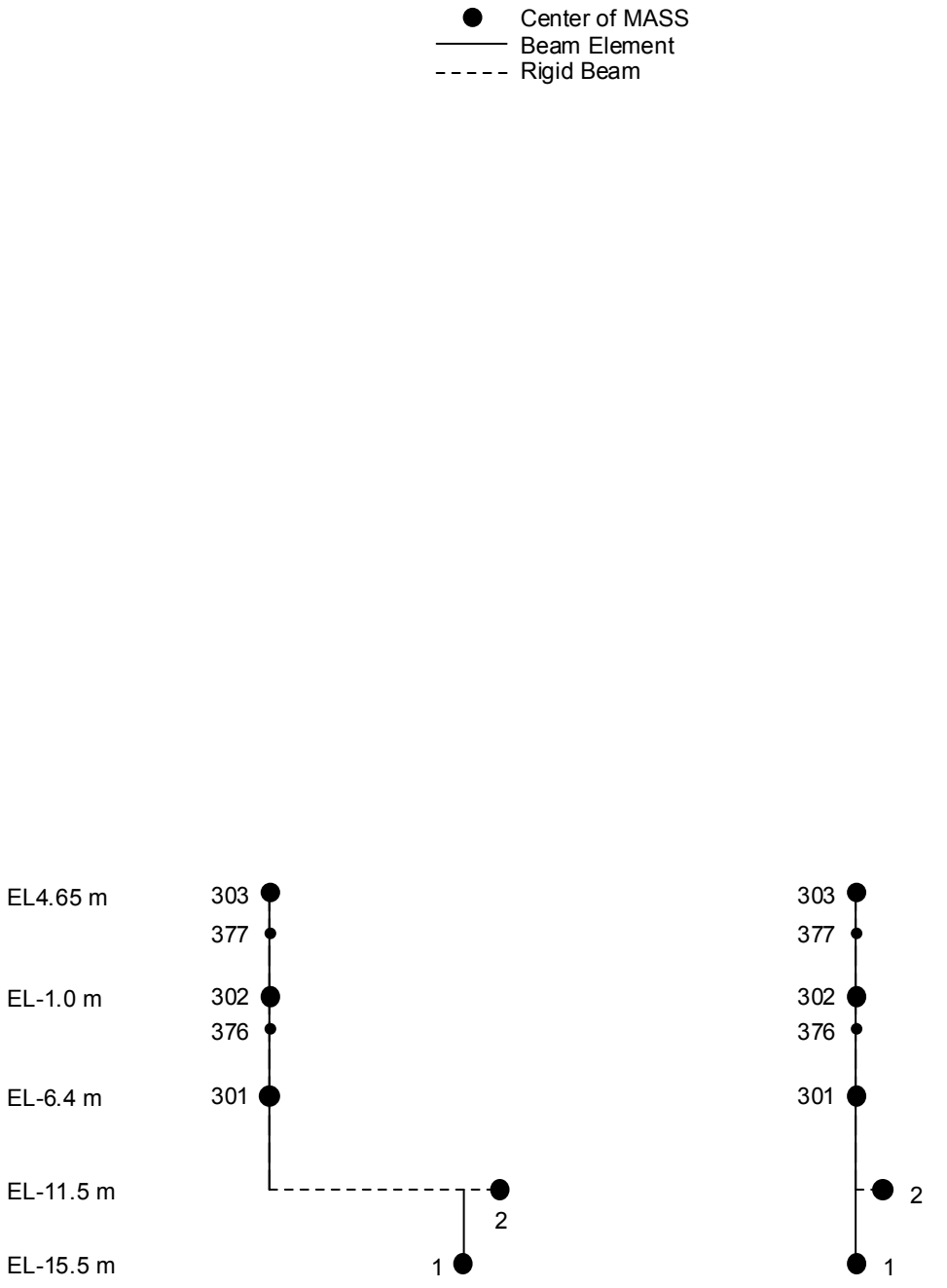

(a) XZ Plane **(b) YZ Plane**

Figure 3A.7-3. Pedestal Stick Model

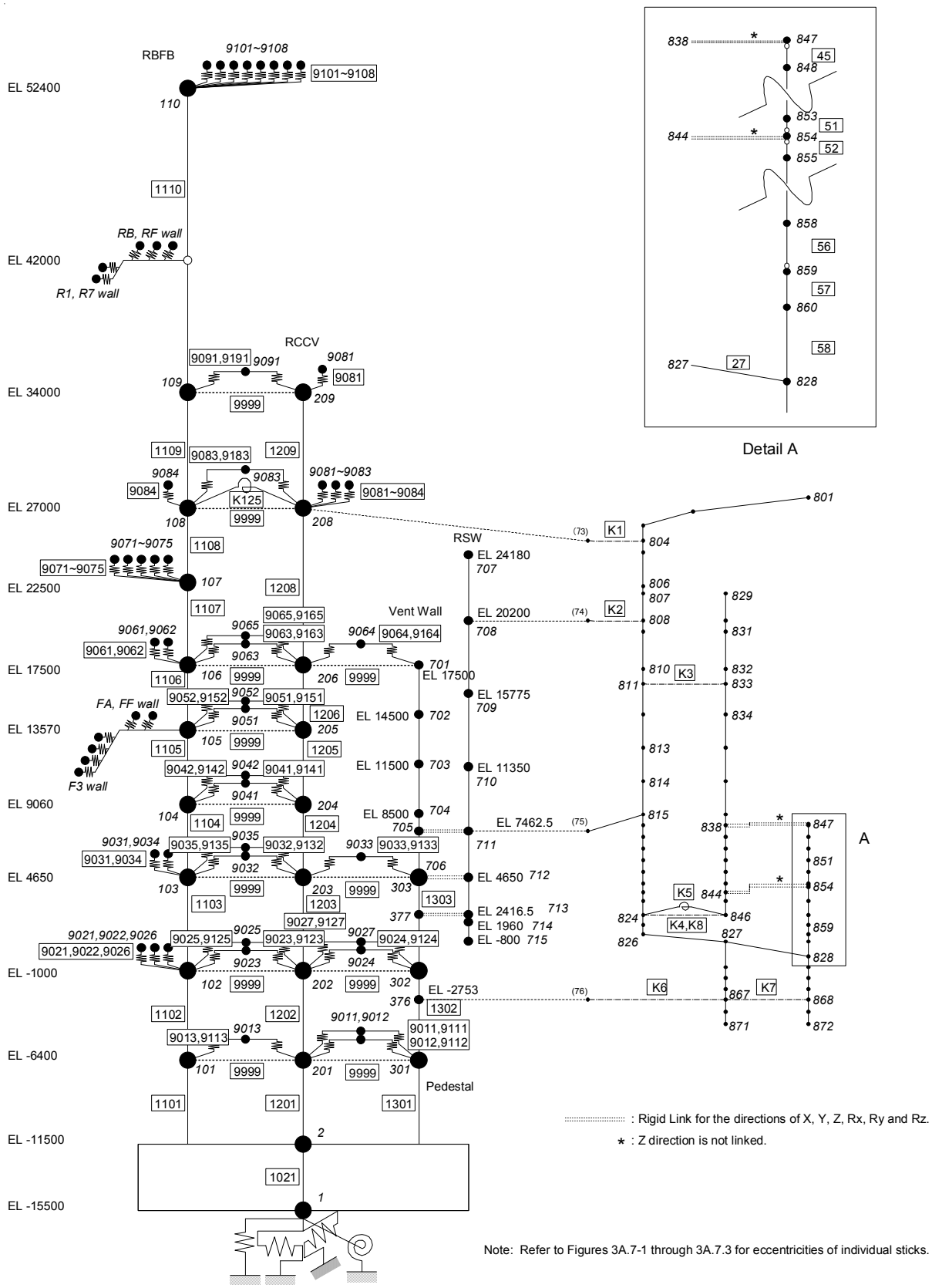

Figure 3A.7-4. ESBWR RBFB Complex Seismic Model

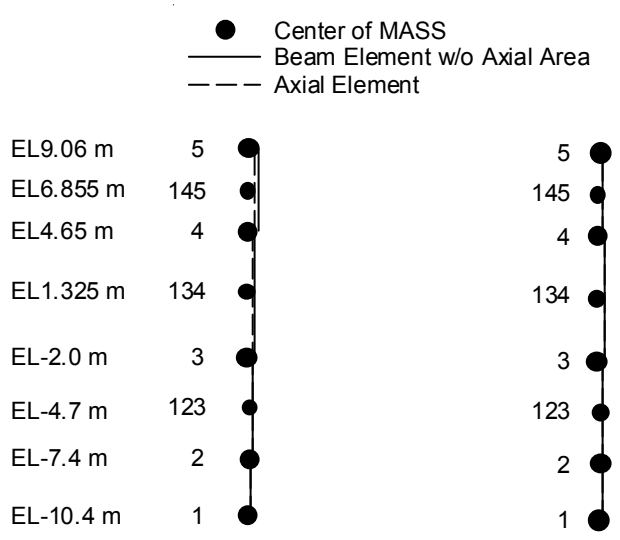

(a) XZ Plane **(b) YZ Plane**

Figure 3A.7-5. Control Building Stick Model

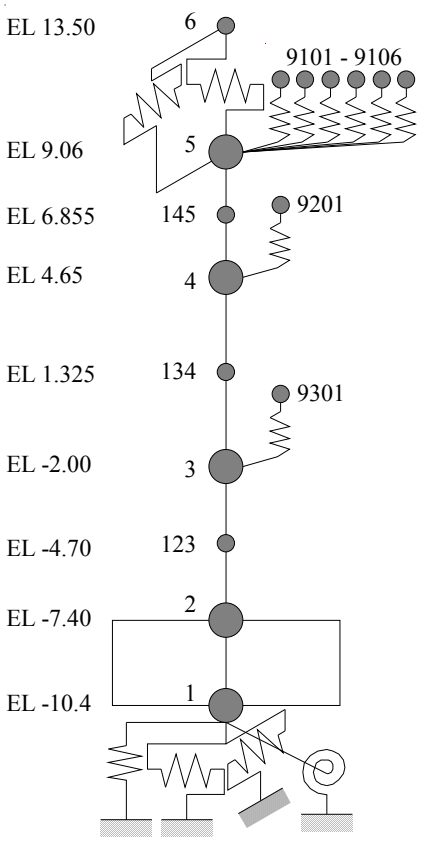

Figure 3A.7-6. ESBWR Control Building Seismic Model

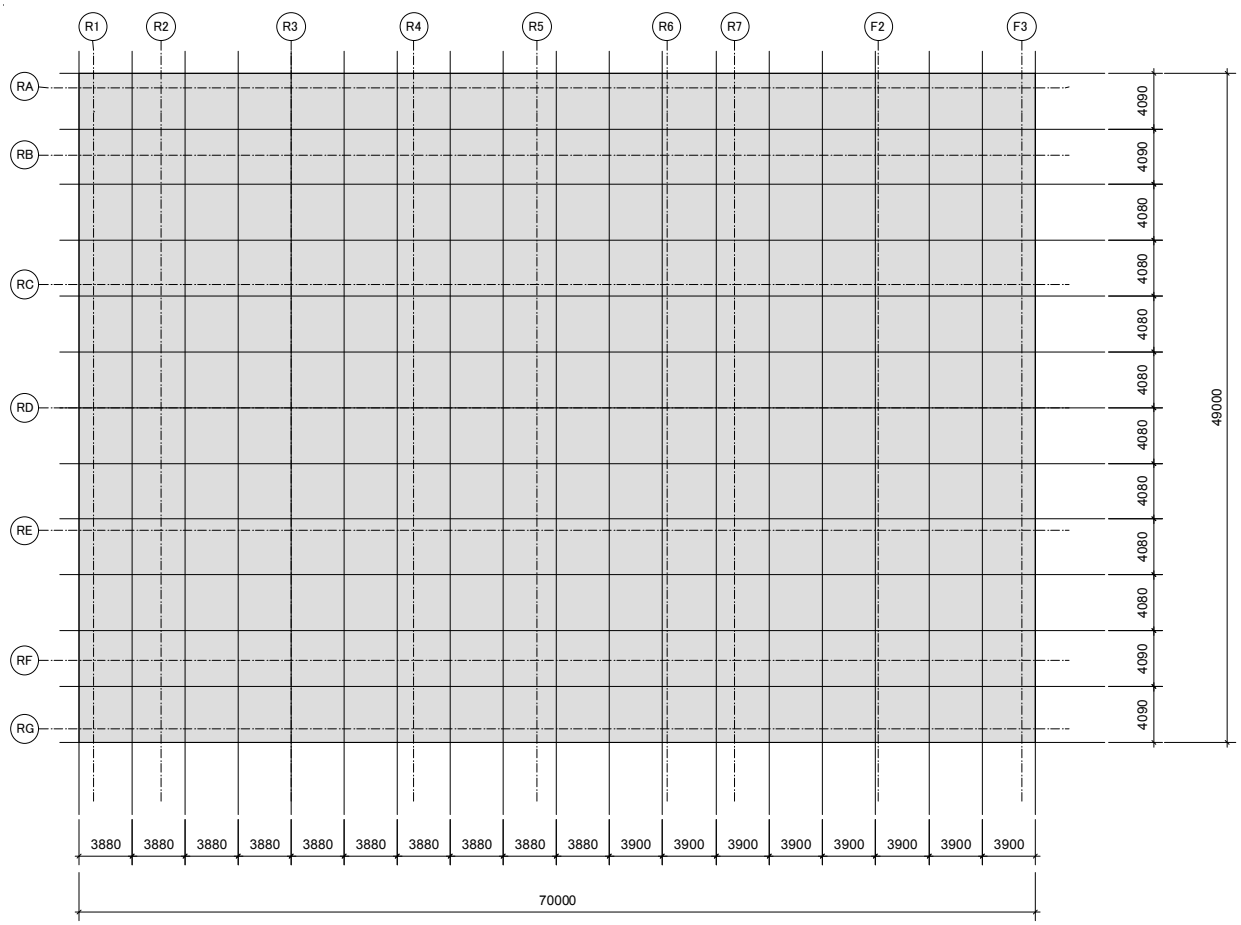

Figure 3A.7-7. SASSI Plate Elements for RBFB Basemat

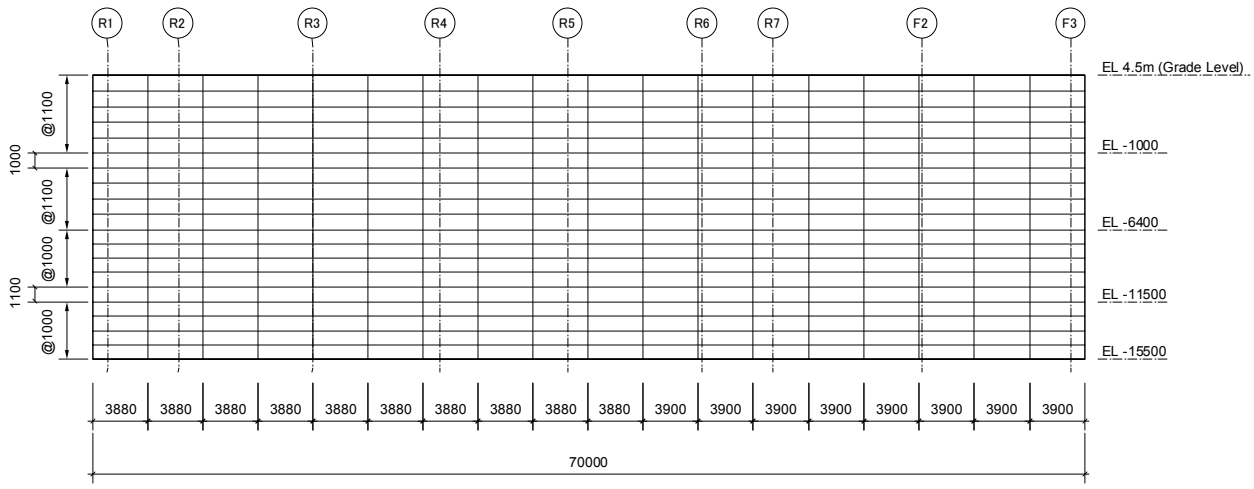

(a) Walls on Column Rows RA and RG

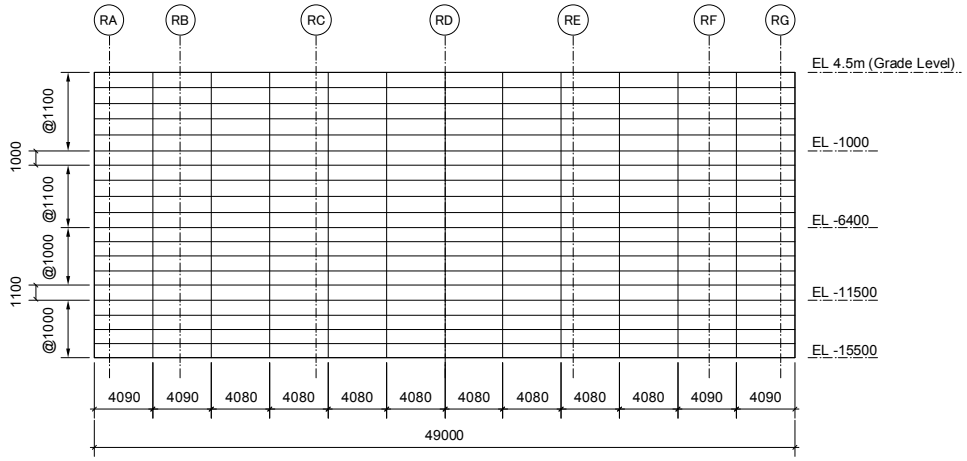

(b) Walls on Column Rows R1 and F3

Figure 3A.7-8. SASSI Plate Elements for RBFB Exterior Walls

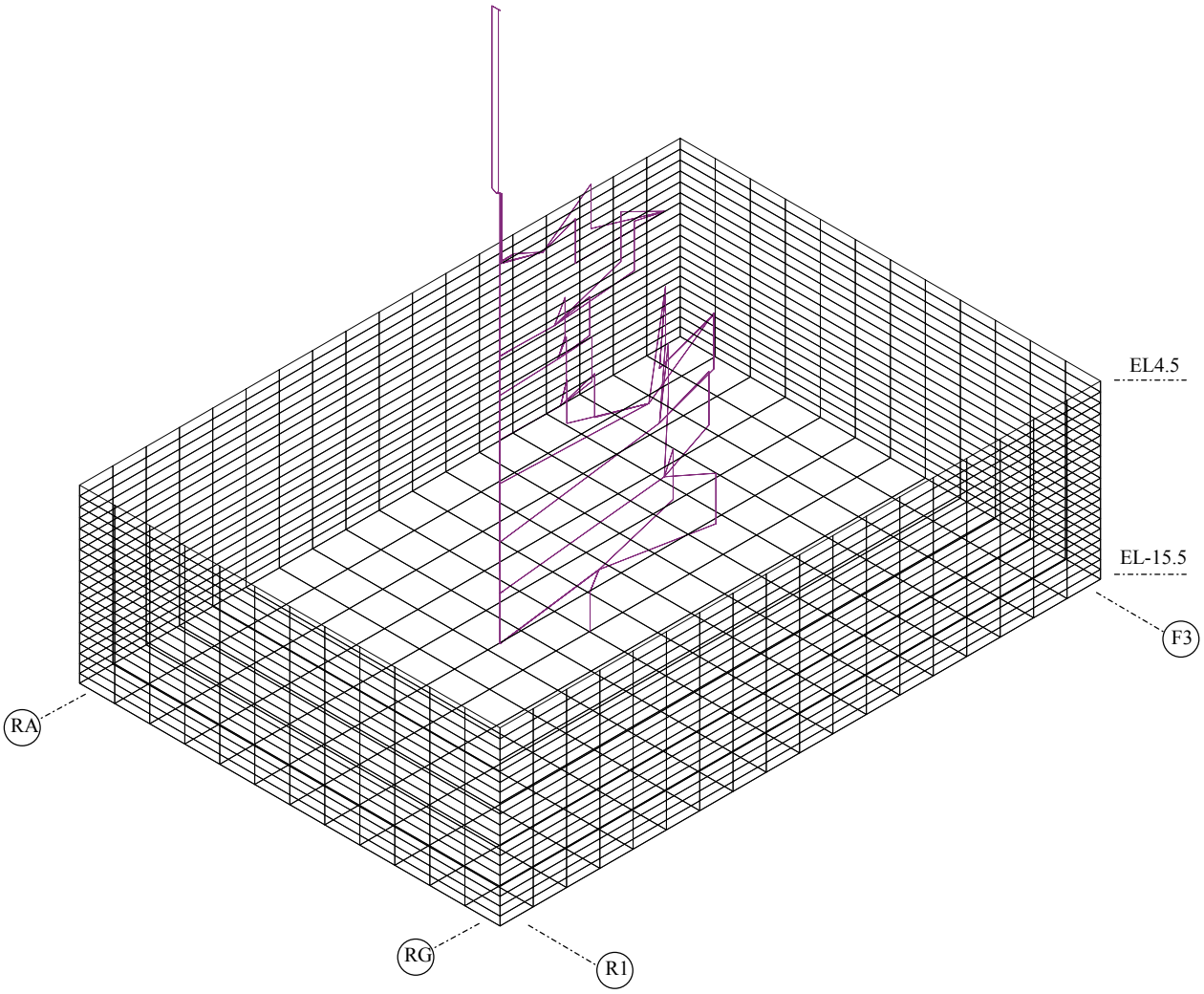

Figure 3A.7-9. Overview of RBFB SASSI Model

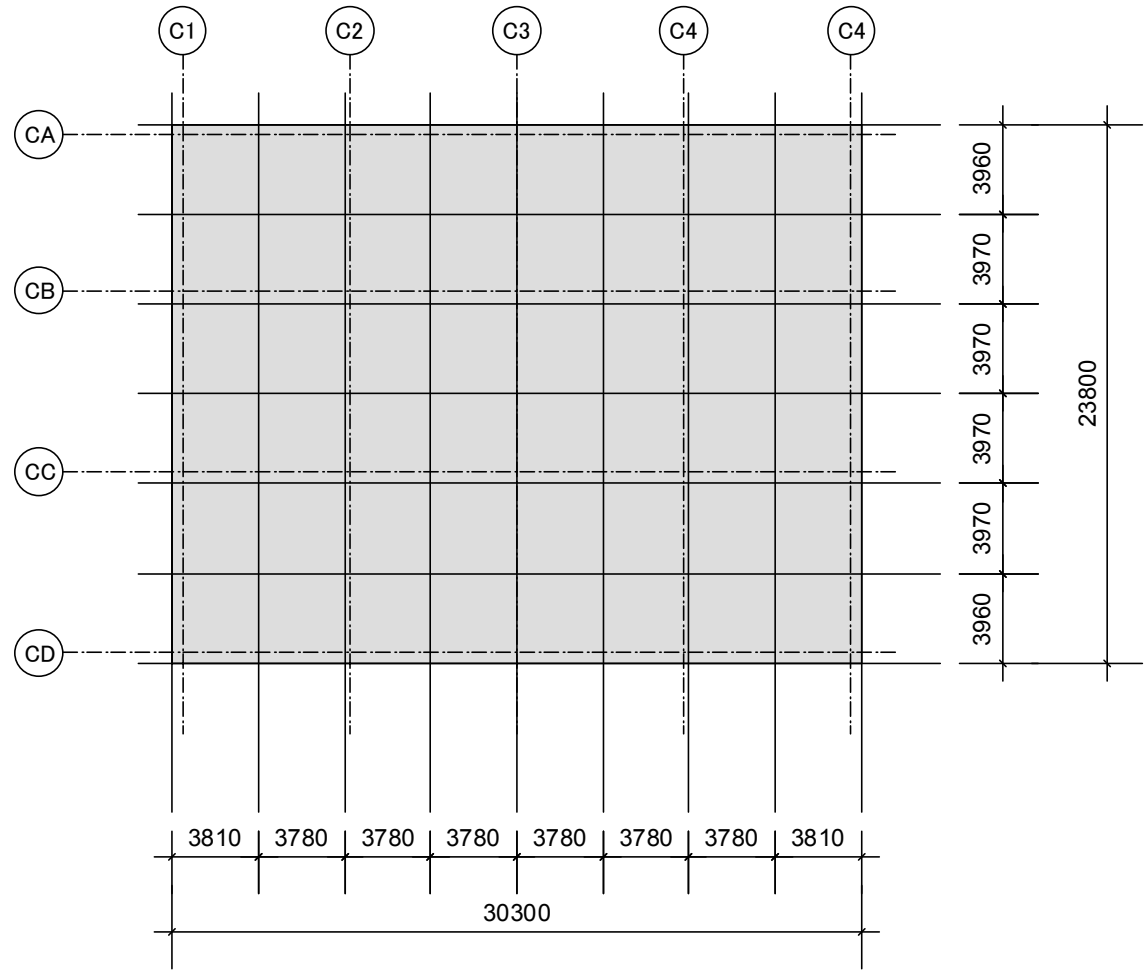

Figure 3A.7-10. SASSI Plate Elements for CB Basemat

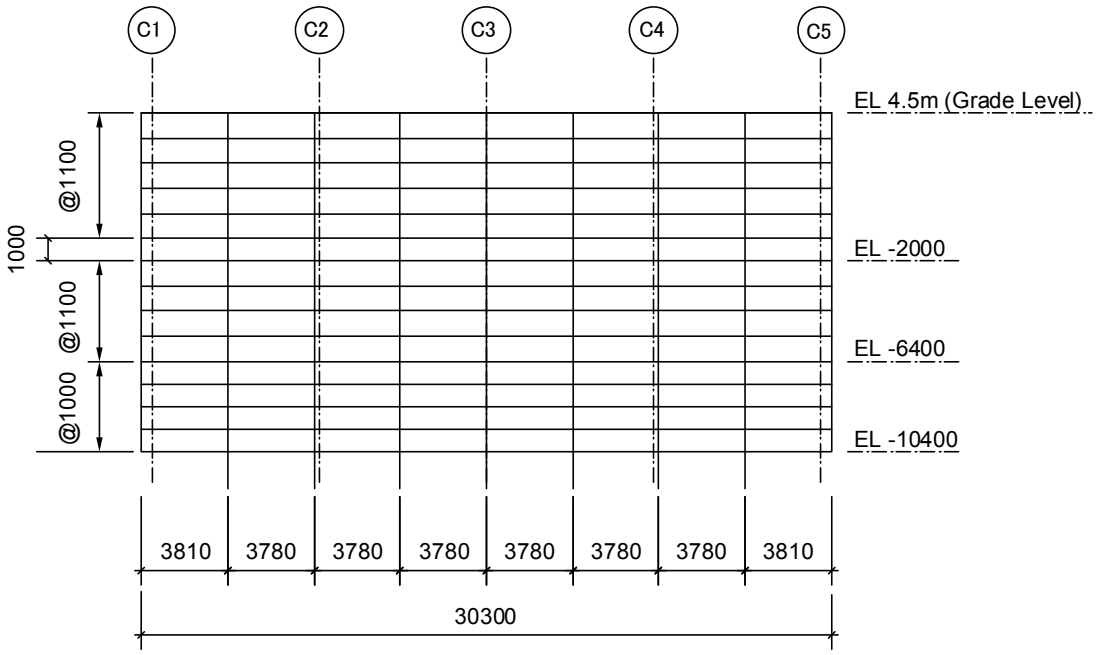

(a) Walls on Column Rows CA and CD

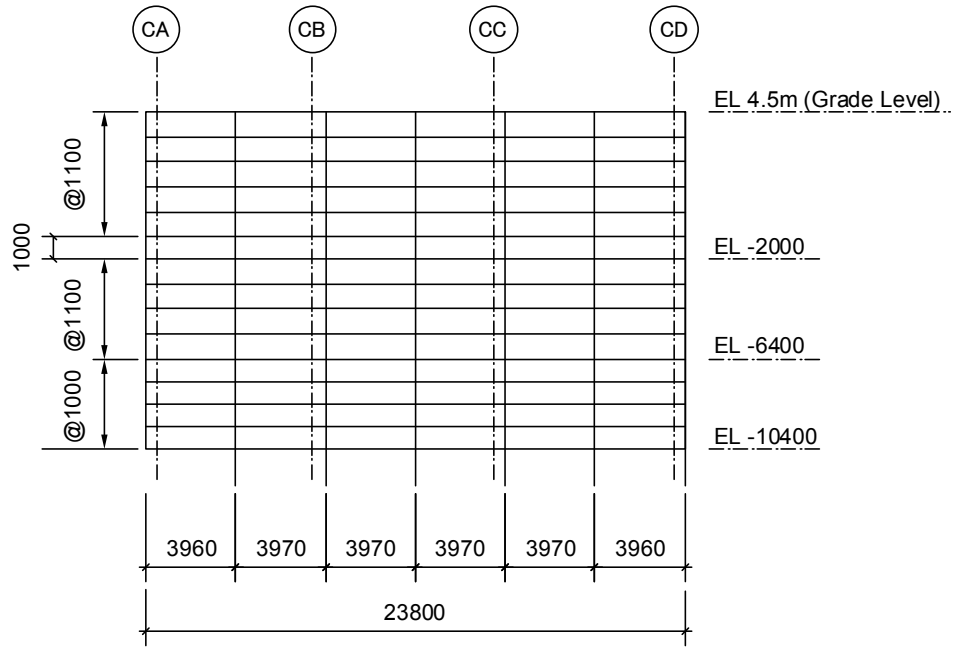

(b) Walls on Column Rows C1 and C5

Figure 3A.7-11. SASSI Plate Elements for CB Exterior Walls

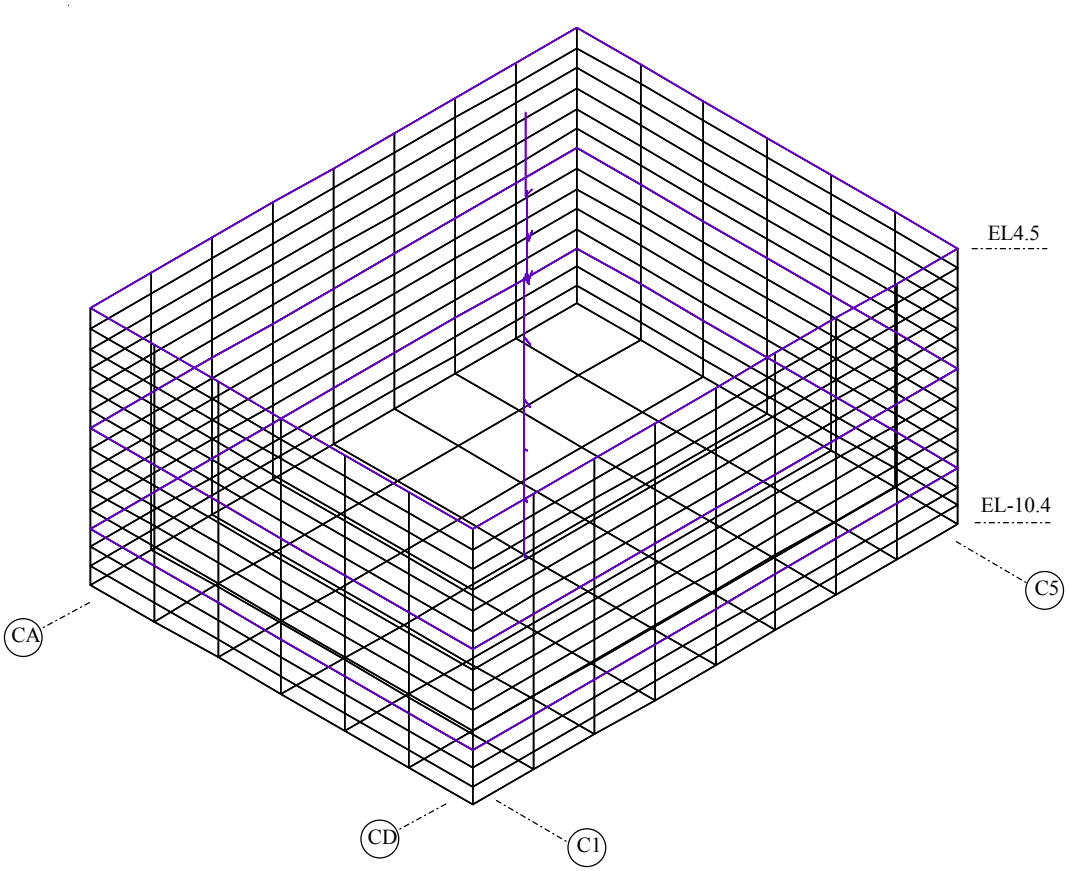

Figure 3A.7-12. Overview of CB SASSI Model

3A.8 ANALYSIS RESULTS

In this section, typical SSI results are presented to show the effect of different soil properties on seismic responses at selected locations in terms of acceleration response spectra and seismic forces. The site-envelope seismic responses are presented in Section 3A.9.

For comparison study, the acceleration response spectra at 5% damping are shown for the following locations:

Location	Node Number
RBFB Refueling Floor	109
RCCV Top Slab	208
Vent Wall Top	701
RSW Top	707
RPV Top	801
RBFB Basemat	2
CB Top	5

For each soil case analyzed, the calculated co-directional floor response spectra in X, Y and Z directions are combined by the SRSS method to obtain floor response spectra at the building edges considering the coupling effects between vertical and rocking and between lateral and torsion motions.

The seismic forces are presented at the following locations:

Location	Connecting Nodes
RPV Support	815 – 711
RSW Base	710 – 711
Vent Wall Base	704 – 705
Pedestal Base	301 – 2
RCCV Base	201 – 2
RBFB Base	101 – 2
CB Base	3 –2

3A.8.1 Effect of Soil Stiffness

For the RG 1.60 (RU-1) and North Anna site (RU-2) spectra motion cases, the horizontal response spectra in the X-direction are shown in Figures 3A.8.1-1a through 3A.8.1-1g. The response spectra in the Y-direction are shown in Figures 3A.8.1-2a through 3A.8.1-2g. The vertical response spectra (Z-direction) are shown in Figure 3A.8.1-3a through 3A.8.1-3g. The

results of the North Anna cases are the envelopes of the three soil conditions, Best-estimate (BE), Upper-bound (UB), and Lower-bound (LB). Generic site responses are higher at frequencies below 10 Hz, whereas North Anna responses are generally more dominant in the higher frequency range above 10 Hz.

The results in terms of seismic forces are compared in Tables 3A.8.1-1 and 3A.8.1-2, respectively for X direction and Y direction. As shown in these tables, the results of generic medium or stiffer sites govern the seismic responses of the RBFB complex structure, except for relatively stiff structures such as the RPV support for which the moment response is controlled by the North Anna site, due to the high-frequency content in its input ground motion. The results of generic hard rock or North Anna sites govern the seismic responses of the CB structure. The results of all soil cases shown are used to obtain the enveloping results (Section 3A.9).

3A.8.2 Effect of Single Envelope Ground Motion

The effect of single envelope ground motion is evaluated by comparing the results of single envelope input motion (RU-3/CU-3) with the envelope results of two separate input motions described in Subsection 3A.8.1 (RU-1and RU-2/ CU-1and CU-2) for the RBFB/CB.

Comparisons of floor response spectra at the selected locations are shown in Figures 3A.8.2-1a through 3A.8.2-1g, Figures 3A.8.2-2a through 3A.9.2-2g, and Figures 3A.8.2-3a through 3A.9.2-3g, respectively for X direction, Y direction, and Z direction.

It is found from the results that the responses due to the single envelope input motion are generally bounded by the envelope responses of RG 1.60 input motion and NA site input motion. However, when analyzed separately, in the lower frequency range the fixed case and hard site case exceed the envelope responses of RG 1.60 input motion and NA site input motion in the higher frequency range. This is because the effect of the high-frequency component of the ground motion is more pronounced for stiffer sites. The fixed case was analyzed only for 0.3g RG 1.60 input motion but not for NA site input motion.

The results in terms of seismic forces are compared in Tables 3A.8.2-1 and 3A.8.2-2, respectively for X direction and Y direction. As shown in these tables, there are some locations where the seismic forces are governed by the results of single envelop input motion. Thus, the results of single envelope spectra input motion are used with the RG1.60 spectra motion and North Anna site spectra motion to obtain the enveloping results (Section 3A.9).

3A.8.3 Effect of Updated Design of RSW and VW

In the design process, the section of the RSW and VW was slightly changed from the originally assumed section. To evaluate the effect of this updated design on the seismic responses, seismic analysis of the updated model for the RSW and VW (RU-4) were performed compared with those of the original model (RU-3) in the case of single envelope input motion.

The results of the updated model are shown in Figures 3A.8.3-1a through 3A.8.3-1f, Figures 3A.8.3-2a through 3A.8.3-2f, and Figures 3A.8.2-3a through 3A.8.2-3f, respectively for X direction, Y direction, and Z direction, compared with the broadened envelope results of RU-3. The seismic shear forces and moments are compared in Table 3A.8.3-1 and Table 3A.8.3-2.

The comparison indicates that the effects on the seismic responses of building stick models are insignificant. However, there are some effects on the internal structure, such as RSW and VW. Thus, the responses from this case are included to obtain the enveloping results (Section 3A.9).

3A.8.4 Effect of In-fill Concrete Stiffness of VW and DF

To evaluate the effect of in-fill concrete on the frequency shift for the VW and DF, the stiffness properties of the two structures in the seismic model were adjusted to include contribution of concrete stiffness (RU-5).

The results of the RU-5 are shown in Figures 3A.8.4-1a through 3A.8.4-1f, Figures 3A.8.4-2a through 3A.8.4-2f, and Figures 3A.8.4-3a through 3A.8.4-3f, respectively for X direction, Y direction, and Z direction, compared with the broadened envelope results of RU-3. The seismic shear forces and moments are compared in Table 3A.8.4-1 and Table 3A.8.4-2.

The comparison indicates that the results of the RU-5, which consider in-fill concrete stiffness, are not completely bounded by the broadened envelope results of RU-3, which does not consider the in-fill concrete stiffness. Thus, the responses from this case are included to obtain the enveloping results (Section 3A.9).

3A.8.5 Effect of LOCA Flooding

To account for the plant condition after a LOCA, a LOCA flooding model was constructed and seismic analyses were performed (RU-6).

The LOCA model results are compared with the broadened envelope results of the normal model RU-3 in terms of acceleration spectra as shown in Figures 3A.8.5-1a through 3A.8.5-1f, Figures 3A.8.5-2a through 3A.8.5-2f, and Figures 3A.8.5-3a through 3A.8.5-3f, respectively for X direction, Y direction, and Z direction. The responses from the LOCA model are included to obtain the enveloping response spectra (Section 3A.9).

The seismic shear forces and moments are compared in Table 3A.8.5-1 and Table 3A.8.5-2. The obtained seismic forces are used for the load combinations including the LOCA flooding condition (Section 3A.9).

3A.8.6 Effect of Layered Sites

The effect of layered sites is evaluated by comparing the results of layered site cases (RL-1 through RL-4/ CL-1 through CL-4) with the broadened envelope results of uniform site cases (RU-3/ CU-3) for the RBFB/ CB.

Comparisons of response spectra are shown in Figures 3A.8.6-1a through 3A.8.6-1g, Figures 3A.8.6-2a through 3A.8.6-2g, and Figures 3A.8.6-3a through 3A.8.6-3g, respectively for X direction, Y direction, and Z direction.

It is found from the results that the responses for the layered site cases are bounded by the broadened envelope responses of uniform site cases in the whole frequency range. Thus the effect of layered sites is included to obtain the enveloping design loads (Section 3A.9).

3A.8.7 Effect of Embedment

It was shown in Subsection 3A.8.6 that the responses for the layered site cases are bounded by the broadened envelope responses of uniform site cases in the whole frequency range. One of reasons for this difference is considered to be the effect of embedment.

As explained in Subsection 3A.5.1, for uniform sites, the SSI analysis method follows the lumped soil spring approach using the program DAC3N. This model neglects the effect of embedment. On the other hand, for layer sites, the finite element method using the program SASSI is employed for SSI analysis including the effect of embedment.

Table 3A.8.7-1 shows the comparisons of the RBFB basemat reaction shear forces between Case RU-3 (Soft uniform site) and Case RL-3 (Soft layered site) and between Case RU-3 (Medium uniform site) and Case RL-4 (Medium layered site). Please note that Case RL-3 has a deeper soft soil layer (40m) supporting the basemat and that Case RL-4 has a deeper medium soil layer (40m) supporting the basemat.

It is found from the results that the effect of embedment works to reduce basemat reaction shear forces. It is considered to be because the building shear force is partially transferred to the lateral soil layers. Regarding the lateral soil pressure, the analysis results are shown in Subsection 3A.8.8.

3A.8.8 Effect of Lateral Soil Pressures

The lateral pressure computed from the equivalent static pressure analysis listed in ASCE 4-98 is used for the design soil pressure. To confirm that the ASCE 4-98 method is conservative, the soil pressures calculated from the SASSI analysis for the layered sites described in Subsection 3A.8.6 are compared with the ASCE 4-98 method soil pressures in Figures 3A.8.8-1 through 3A.8.8-4.

It is found from the results that the SASSI soil pressures are generally bounded by the ASCE 4-98 soil pressures; however, at the elevation close to the ground surface and the basemat elevation, the SASSI soil pressure exceeds the ASCE 4-98 soil pressure. The design soil pressure loads for the exterior walls are calculated by averaging soil pressures which each wall is subjected to. The calculated design soil pressures are summarized in Tables 3A.8.8-1 and 3A.8.8-2, comparing the SASSI soil pressures and the ASCE 4-98 soil pressures. The embedded walls are designed for the worst soil pressures resulting from either SASSI analysis or ASCE 4-98 methodology.

3A.8.9 Effect of Concrete Cracking

In order to address the effect of the cracked concrete stiffness, an additional evaluation is performed using SASSI, assuming that the cracked concrete stiffness is 50% of the uncracked value in accordance with ASCE 43-05.

For the comparison, Case RL-2/CL-2 was selected for the RBFB/CB, because they show the largest responses among various layered sites. Case RL-5/CL-5 is the RBFB/CB cracked case, which has the same layered site as Case RL-2/CL-2.

Comparisons of response spectra at the selected locations are shown in Figures 3A.8.9-1a through 3A.8.9-1g and Figures 3A.8.9-2a through 3A.8.9-2g, respectively for X direction and Y

direction. The broadened envelope results of Case RU-3/CU-3 (uniform site, single envelope input motion case) are also shown in the figures for comparison.

It is found from the results that the FRS peaks move to lower frequencies by concrete cracking; however, both FRS of uncracked and cracked cases are bounded by the broadened envelope responses of uniform site cases in the whole frequency range. Thus the effect of concrete cracking is included to obtain the enveloping design loads (Section 3A.9).

3A.8.10 Effect of Wall Out-of-plane Vibration

It was found from the review of the out-of-plane vibration frequencies of walls that the RB walls above the refueling floor at EL 34.0m and the FB walls at EL 4.65m have some vibration modes lower than 50 Hz. To obtain design loads and FRS for these walls, seismic analysis was performed using wall oscillators evaluated in the same manner as floor oscillators. The calculated wall oscillators are shown in the seismic analysis model of Figure 3A.7-4.

The maximum horizontal acceleration of the wall out-of-plane oscillators are shown for each site condition of Case RU-7 in Table 3A.8.10-1. The results for the cracked Case RL-6 are shown in Table 3A.8.10-2. The design loads and FRS for these walls are determined by enveloping these response results (Section 3A.9).

3A.8.11 Effect of Structure-Structure Interaction

The RBFB effects on CB are more significant than the CB effects on RBFB, because the size of RBFB is much larger than that of CB. To evaluate the RBFB effects on CB, the analyses are performed by the following two steps.

(1) Perform the RBFB SASSI analysis to obtain the ground surface response at the CB location.

(2) Perform the CB SASSI analysis using the input motion obtained in Step 1.

For the comparison of without and with structure-structure interaction effect, Case CL-2 layered site was selected, because the CB shows the largest responses at Case CL-2 site among various layered sites. The corresponding RBFB case is Case RL-2. The CB case considering structure-structure interaction effect is called Case CL-6.

Comparisons of FRS at the top of CB are shown in Figures 3A.8.11-1 through 3A.8.11-3. The broadened envelope results of Case CU-3 (uniform site, single envelope input motion case) are also shown in the figures for comparison.

It is found from the results that the effect of structure-structure interaction is the largest in the Y direction (East-West) FRS, however, both FRS without and with structure-structure interaction effect are bounded by the broadened envelope responses of uniform site cases in the whole frequency range. Thus the effect of structure-structure interaction is included in the enveloping design loads (Section 3A.9).

Table 3A.8.1-1

Maximum Forces - X Direction (RU-1 and RU-2/CU-1 and CU-2)

Locations	Response Types	Soil Stiffness				
		SOFT	MEDIUM	HARD	FIX	North Anna
RPV	Shear	6	14	14	17	9
Support	Moment	24	65	108	117	120
RSW Base	Shear	5	13	17	20	10
	Moment	52	146	201	236	146
Vent Wall	Shear	8	16	16	19	11
Base	Moment	54	127	143	167	92
Pedestal	Shear	48	102	96	95	38
Base	Moment	712	1590	1494	1485	567
RCCV	Shear	119	255	240	237	92
Base	Moment	5148	10836	10483	9836	4039
RBFB	Shear	427	922	868	856	335
Base	Moment	16554	31489	32235	26978	9856
CB	Shear	64	74	73	59	80
Base	Moment	883	1062	1004	808	1428

Units: Shear Forces in MN; Moment in MN-m

Table 3A.8.1-2

Maximum Forces - Y Direction (RU-1 and RU-2/CU-1 and CU-2)

Locations	Response Types	Soil Stiffness				
		SOFT	MEDIUM	HARD	FIX	North Anna
RPV	Shear	6	12	11	12	11
Support	Moment	30	54	69	66	117
RSW Base	Shear	6	11	11	10	11
	Moment	66	122	128	116	136
Vent Wall	Shear	10	20	17	16	13
Base	Moment	77	165	148	126	79
Pedestal	Shear	55	121	97	88	41
Base	Moment	898	1963	1616	1455	580
RCCV	Shear	137	304	244	220	99
Base	Moment	6942	14200	11797	10876	4342
RBFB	Shear	477	1030	804	704	350
Base	Moment	17623	35275	28459	25566	8843
CB	Shear	67	72	73	62	72
Base	Moment	917	1000	977	803	979

Units: Shear Forces in MN; Moment in MN-m

Table 3A.8.2-1

Maximum Forces - X Direction (RU-3/ CU-3)

Locations	Response Types	Soil Stiffness			
		SOFT	MEDIUM	HARD	FIX
RPV	Shear	8	13	18	18
Support	Moment	35	64	101	128
RSW Base	Shear	7	11	15	16
	Moment	78	121	167	195
Vent Wall	Shear	10	18	17	22
Base	Moment	60	122	146	148
Pedestal	Shear	63	104	103	103
Base	Moment	931	1478	1521	1522
RCCV	Shear	157	256	260	258
Base	Moment	6243	10268	10170	9508
RBFB	Shear	563	917	930	921
Base	Moment	18839	31774	29695	26645
CB	Shear	73	67	83	85
Base	Moment	988	907	1245	1109

Units: Shear Forces in MN; Moment in MN-m

Table 3A.8.2-2

Maximum Forces - Y Direction (RU-3/ CU-3)

Locations	Response Types	Soil Stiffness			
		SOFT	MEDIUM	HARD	FIX
RPV	Shear	7	12	16	18
Support	Moment	41	73	124	122
RSW Base	Shear	6	11	15	14
	Moment	72	131	181	158
Vent Wall	Shear	12	19	20	23
Base	Moment	92	142	171	162
Pedestal	Shear	55	107	90	92
Base	Moment	944	1620	1451	1480
RCCV	Shear	138	267	223	229
Base	Moment	7671	12474	10856	10934
RBFB	Shear	474	907	736	790
Base	Moment	19908	30116	28273	25733
CB	Shear	63	74	80	82
Base	Moment	931	982	1072	1130

Units: Shear Forces in MN; Moment in MN-m

Table 3A.8.3-1

Maximum Forces - X Direction (RU-4)

Locations	Response Types	Soil Stiffness				Envelope
		SOFT	MEDIUM	HARD	FIX	RU-1,2 and 3
RPV	Shear	8	13	17	19	18
Support	Moment	34	64	100	129	128
RSW Base	Shear	7	11	15	16	20
	Moment	77	122	165	189	236
Vent Wall	Shear	10	19	18	23	22
Base	Moment	65	136	160	159	167
Pedestal	Shear	63	104	104	103	104
Base	Moment	936	1492	1531	1523	1590
RCCV	Shear	157	257	261	258	260
Base	Moment	6245	10317	10238	9605	10836
RBFB	Shear	564	921	934	921	930
Base	Moment	18888	31921	29920	26409	32235

Units: Shear Forces in MN; Moment in MN-m

Table 3A.8.3-2

Maximum Forces - Y Direction (RU-4)

Locations	Response Types	Soil Stiffness				Envelope
		SOFT	MEDIUM	HARD	FIX	RU-1,2 and 3
RPV Support	Shear	7	12	16	18	18
	Moment	42	71	123	122	124
RSW Base	Shear	6	11	15	14	15
	Moment	73	132	183	157	181
Vent Wall Base	Shear	13	21	21	24	23
	Moment	101	154	187	177	171
Pedestal Base	Shear	55	107	90	92	121
	Moment	953	1640	1463	1489	1963
RCCV Base	Shear	138	268	224	230	304
	Moment	7692	12513	10925	11013	14200
RBFB Base	Shear	477	911	737	793	1030
	Moment	19957	30244	28420	25929	35275

Units: Shear Forces in MN; Moment in MN-m

Table 3A.8.4-1

Maximum Forces - X Direction (RU-5)

Locations	Response Types	Soil Stiffness				Envelope
		SOFT	MEDIUM	HARD	FIX	RU-1,2 and 3
RPV	Shear	9	14	17	18	18
Support	Moment	35	60	100	141	128
RSW Base	Shear	7	12	17	19	20
	Moment	78	135	186	210	236
Vent Wall	Shear	16	29	30	30	22
Base	Moment	129	243	284	307	167
Pedestal	Shear	62	102	102	104	104
Base	Moment	962	1558	1592	1638	1590
RCCV	Shear	157	257	261	262	260
Base	Moment	6233	10356	10238	9473	10836
RBFB	Shear	563	919	931	930	930
Base	Moment	18888	31921	29665	26870	32235

Units: Shear Forces in MN; Moment in MN-m

Table 3A.8.4-2

Maximum Forces - Y Direction (RU-5)

Locations	Response Types	Soil Stiffness				Envelope
		SOFT	MEDIUM	HARD	FIX	RU-1,2 and 3
RPV	Shear	6	12	15	17	18
Support	Moment	43	66	128	133	124
RSW Base	Shear	7	10	16	16	15
	Moment	77	121	185	188	181
Vent Wall	Shear	20	33	35	35	23
Base	Moment	182	272	352	319	171
Pedestal	Shear	55	106	88	94	121
Base	Moment	1002	1690	1520	1485	1963
RCCV	Shear	138	268	224	233	304
Base	Moment	7682	12484	10925	10964	14200
RBFB	Shear	477	913	740	801	1030
Base	Moment	19937	30214	28233	25645	35275

Units: Shear Forces in MN; Moment in MN-m

Table 3A.8.5-1

Maximum Forces - X Direction (RU-6)

Locations	Response Types	Soil Stiffness				Envelope
		SOFT	MEDIUM	HARD	FIX	RU-1,2 and 3
RPV	Shear	8	13	17	18	18
Support	Moment	35	66	107	122	128
RSW Base	Shear	7	12	16	17	20
	Moment	80	130	174	194	236
Vent Wall	Shear	11	21	19	22	22
Base	Moment	65	132	157	148	167
Pedestal	Shear	61	105	104	104	104
Base	Moment	920	1491	1556	1553	1590
RCCV	Shear	153	258	263	260	260
Base	Moment	6175	10336	10189	9463	10836
RBFB	Shear	550	924	939	928	930
Base	Moment	19162	31989	29744	26762	32235

Units: Shear Forces in MN; Moment in MN-m

Table 3A.8.5-2

Maximum Forces - Y Direction (RU-6)

Locations	Response Types	Soil Stiffness				Envelope
		SOFT	MEDIUM	HARD	FIX	RU-1,2 and 3
RPV	Shear	7	13	16	18	18
Support	Moment	42	74	127	130	124
RSW Base	Shear	7	12	16	14	15
	Moment	75	136	190	164	181
Vent Wall	Shear	13	22	22	26	23
Base	Moment	98	148	173	166	171
Pedestal	Shear	55	107	90	92	121
Base	Moment	951	1630	1482	1484	1963
RCCV	Shear	138	269	225	230	304
Base	Moment	7657	12464	10885	10934	14200
RBFB	Shear	476	915	742	792	1030
Base	Moment	19908	30136	28263	25694	35275

Units: Shear Forces in MN; Moment in MN-m

Table 3A.8.7-1

Comparisons of RBFB Basemat Reaction Shear Force

Analysis Method	Effect of Embedment	Soft site (Vs 300 m/s) (MN)			Medium site (Vs 800 m/s) (MN)		
		Case	NS	EW	Case	NS	EW
DAC3N	Neglect	RU-3	900	760	RU-3	1450	1500
SASSI	Consider	RL-3	560	490	RL-4	1380	1310

Table 3A.8.8-1

Lateral Soil Pressure - RBFB

Floor Level	R1 and F3 Wall Soil Pressure (MPa)					RA and RG Wall Soil Pressure (MPa)					ASCE 4-98	Envelope (MPa)	
(m)	RL-1	RL-2	RL-3	RL-4	RL-5	RL-1	RL-2	RL-3	RL-4	RL-5	(MPa)	R1 and F3 Wall	RA and RG Wall
4.65													
Slab													
3.65 -1.00	0.20	0.19	0.24	0.19	0.21	0.27	0.17	0.33	0.19	0.22	0.30	0.30	0.33
Slab													
-2.00 -6.40	0.15	0.21	0.20	0.21	0.26	0.17	0.19	0.21	0.19	0.20	0.29	0.29	0.29
Slab													
-7.40 -11.50	0.19	0.21	0.20	0.21	0.25	0.18	0.19	0.18	0.20	0.20	0.23	0.25	0.23
Basemat	0.29	0.24	0.28	0.25	0.23	0.25	0.24	0.25	0.26	0.20	0.16	0.29	0.26

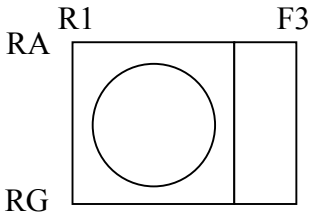

Table 3A.8.8-2

Lateral Soil Pressure - CB

Floor Level	C1 and C5 Wall Soil Pressure (MPa)						CA and CD Wall Soil Pressure (MPa)						ASCE 4-98	Envelope (MPa)	
(m)	CL-1	CL-2	CL-3	CL-4	CL-5	CL-6	CL-1	CL-2	CL-3	CL-4	CL-5	CL-6	(MPa)	C1 and C5 Wall	CA and CD Wall
4.65															
Slab															
3.95 -2.00	0.09	0.17	0.09	0.16	0.12	0.16	0.11	0.16	0.10	0.16	0.11	0.15	0.22	0.22	0.22
Slab															
-2.50 -7.40	0.10	0.14	0.09	0.14	0.14	0.13	0.10	0.14	0.10	0.14	0.13	0.13	0.18	0.18	0.18
Basemat	0.15	0.20	0.15	0.21	0.18	0.20	0.15	0.19	0.15	0.20	0.17	0.18	0.12	0.21	0.20

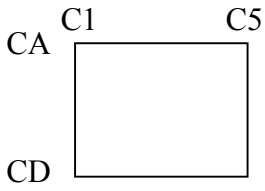

Table 3A.8.10-1
Maximum Horizontal Acceleration RBFB Wall Out-of-plane Oscillators (RU-7)

Locations	Wall Oscillator	Frequency (Hz)	Soil Stiffness			
			SOFT	MEDIUM	HARD	FIX
RB above EL34000 X direction	R1 and R7 wall (1)	15.87	0.69	1.14	1.54	1.53
	R1 and R7 wall (2)	35.22	0.62	1.23	1.22	1.30
	Node in RBFB Stick		0.61	1.11	1.12	1.19
RB above EL34000 Y direction	RB and RF wall (1)	14.14	0.74	1.22	1.54	1.71
	RB and RF wall (2)	24.51	0.76	1.29	1.47	1.56
	RB and RF wall (3)	43.36	0.75	1.22	1.25	1.14
	Node in RBFB Stick		0.74	1.21	1.22	1.08
FB above EL4650 X direction	F3 wall (1)	12.73	0.49	0.69	1.01	1.38
	F3 wall (2)	18.34	0.51	0.88	1.08	1.37
	F3 wall (3)	35.36	0.47	0.75	1.00	1.15
	F3 wall (4)	42.50	0.48	0.72	0.86	0.99
	Node in RBFB Stick		0.45	0.66	0.85	0.97
FB above EL4650 Y direction	FA and FF wall (1)	13.27	0.45	0.92	1.18	1.28
	FA and FF wall (2)	40.73	0.39	0.75	0.82	0.98
	Node in RBFB Stick		0.37	0.69	0.71	0.72

Unit: Acceleration in g.

Table 3A.8.10-2

Maximum Horizontal Acceleration RBFB Cracked Wall Out-of-plane Oscillators (RL-6)

Locations	Wall Oscillator	Frequency (Hz)	Site Case 2
RB above EL34000 X direction	R1 and R7 wall (1)	15.87	1.14
	R1 and R7 wall (2)	35.22	1.11
	Node in RBFB Stick		1.03
RB above EL34000 Y direction	RB and RF wall (1)	14.14	1.07
	RB and RF wall (2)	24.51	1.08
	RB and RF wall (3)	43.36	1.02
	Node in RBFB Stick		0.98
FB above EL4650 X direction	F3 wall (1)	12.73	0.67
	F3 wall (2)	18.34	0.72
	F3 wall (3)	35.36	0.68
	F3 wall (4)	42.50	0.63
	Node in RBFB Stick		0.61
FB above EL4650 Y direction	FA and FF wall (1)	13.27	0.61
	FA and FF wall (2)	40.73	0.67
	Node in RBFB Stick		0.55

Unit: Acceleration in g.

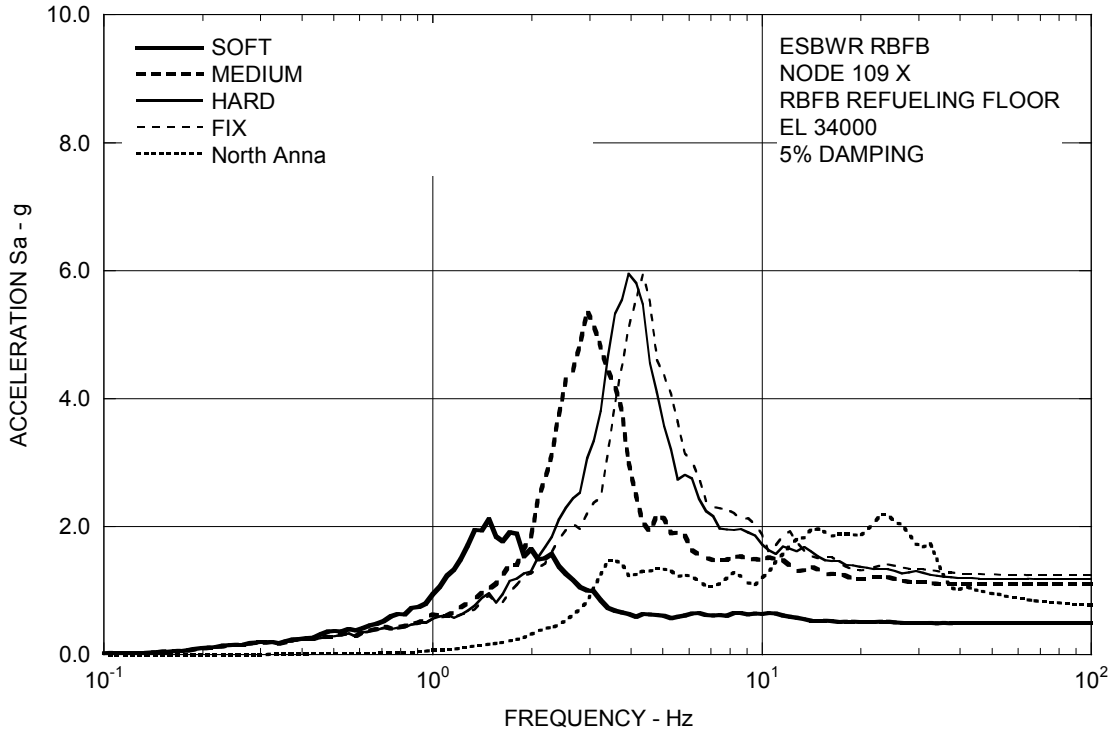

Figure 3A.8.1-1a. FRS (Effect of Soil Stiffness) – RBFB Refueling Floor X

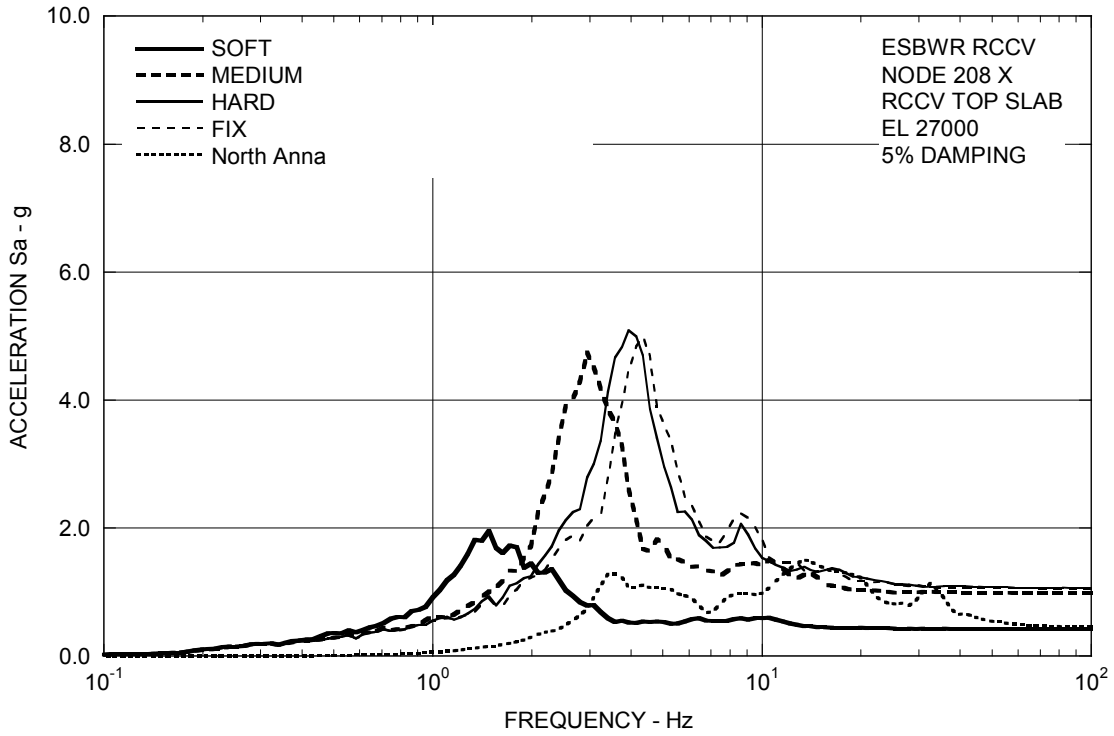

Figure 3A.8.1-1b. FRS (Effect of Soil Stiffness) – RCCV Top Slab X

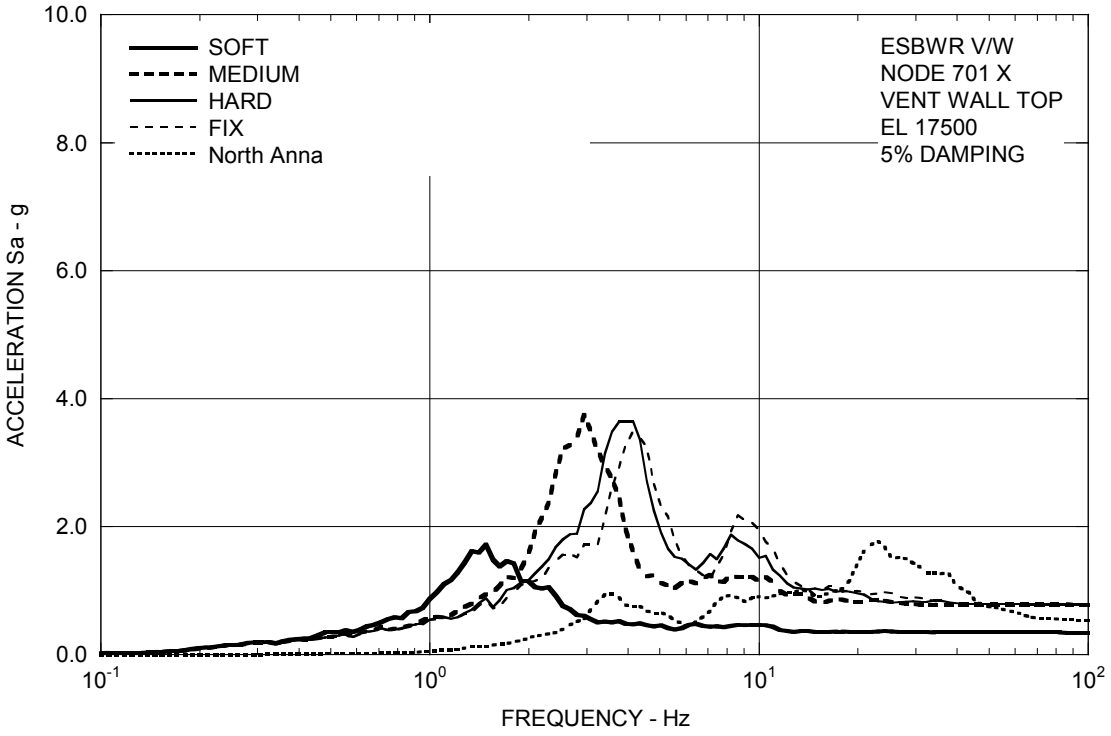

Figure 3A.8.1-1c. FRS (Effect of Soil Stiffness) – Vent Wall Top X

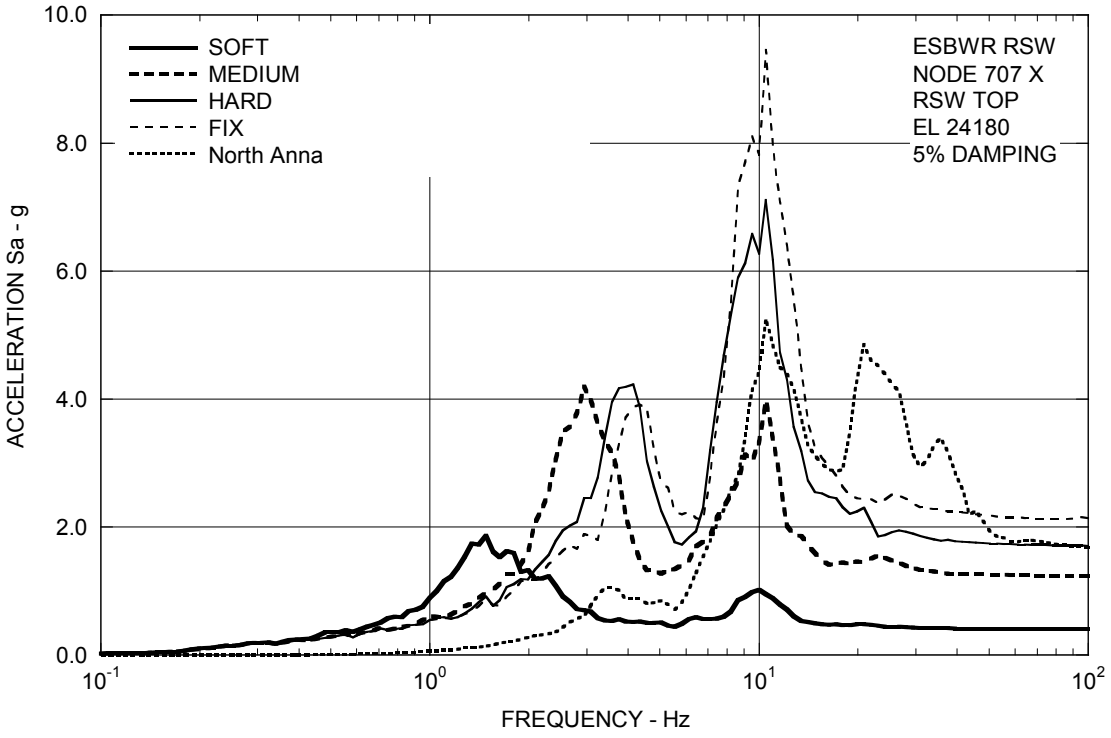

Figure 3A.8.1-1d. FRS (Effect of Soil Stiffness) – RSW Top X

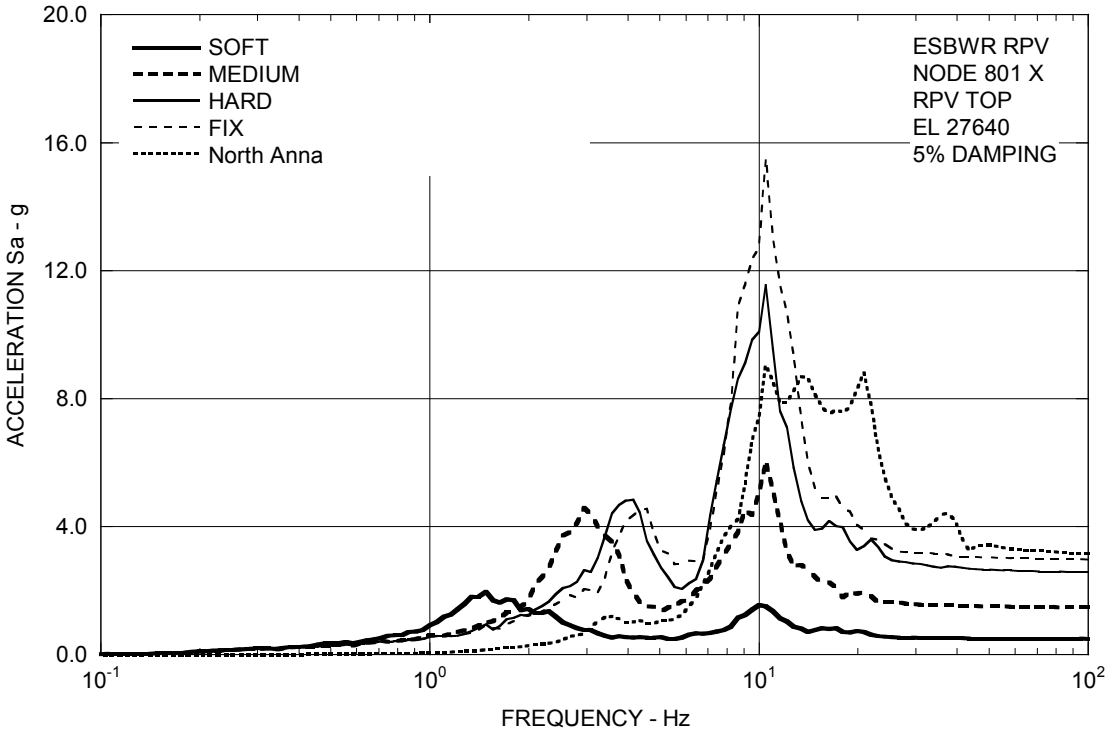

Figure 3A.8.1-1e. FRS (Effect of Soil Stiffness) – RPV Top X

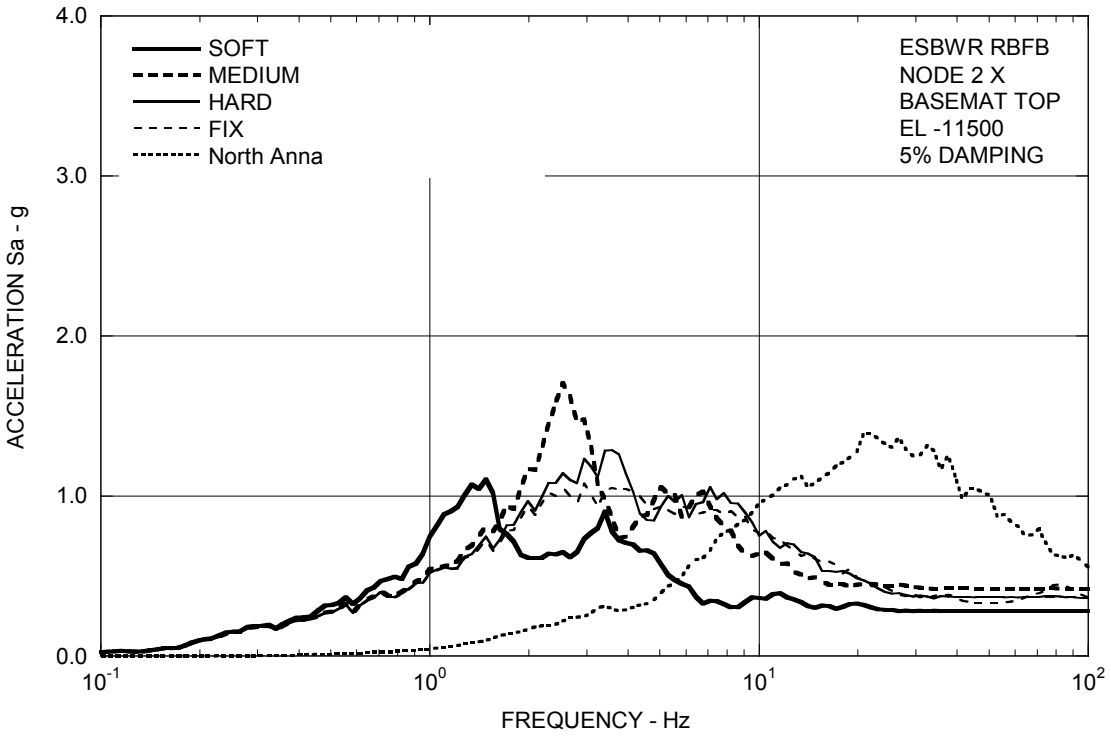

Figure 3A.8.1-1f. FRS (Effect of Soil Stiffness) – RBFB Basemat X

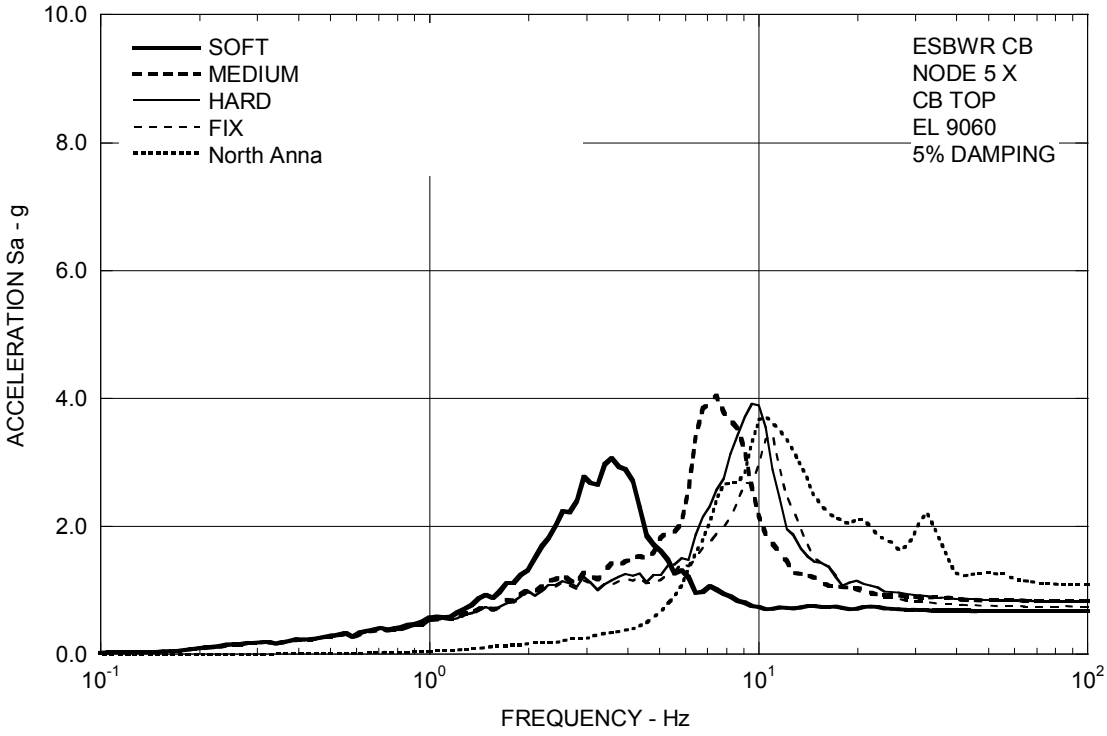

Figure 3A.8.1-1g. FRS (Effect of Soil Stiffness) – CB Top X

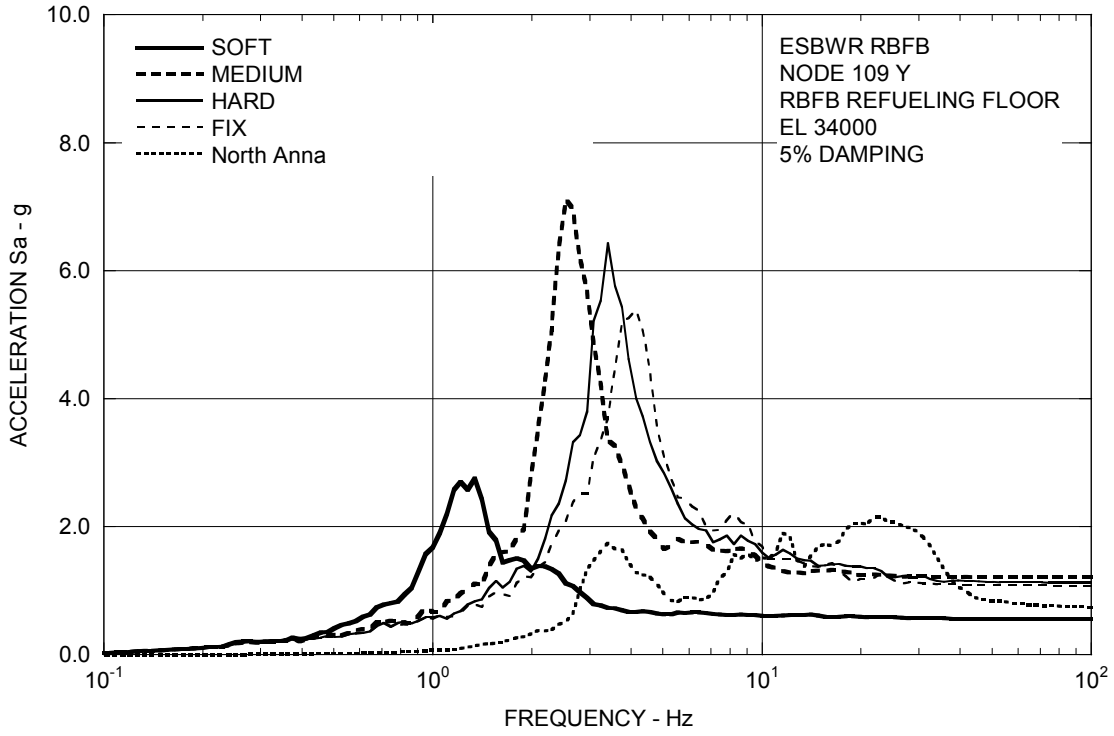

Figure 3A.8.1-2a. FRS (Effect of Soil Stiffness) – RBFB Refueling Floor Y

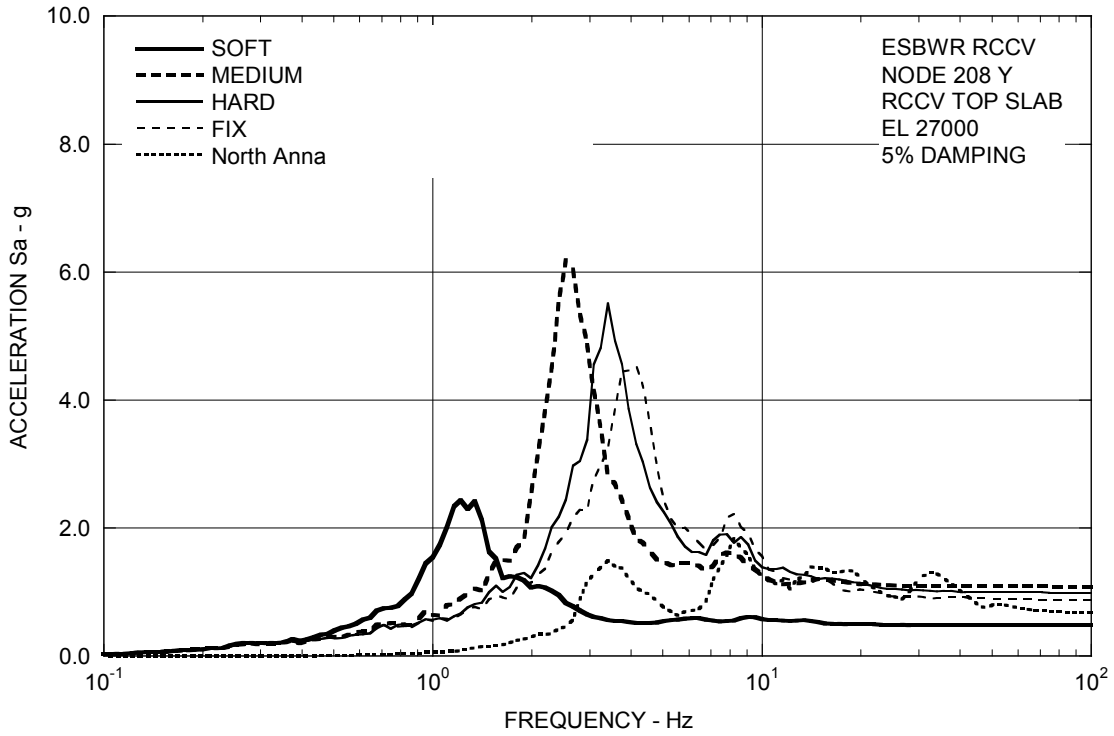

Figure 3A.8.1-2b. FRS (Effect of Soil Stiffness) – RCCV Top Slab Y

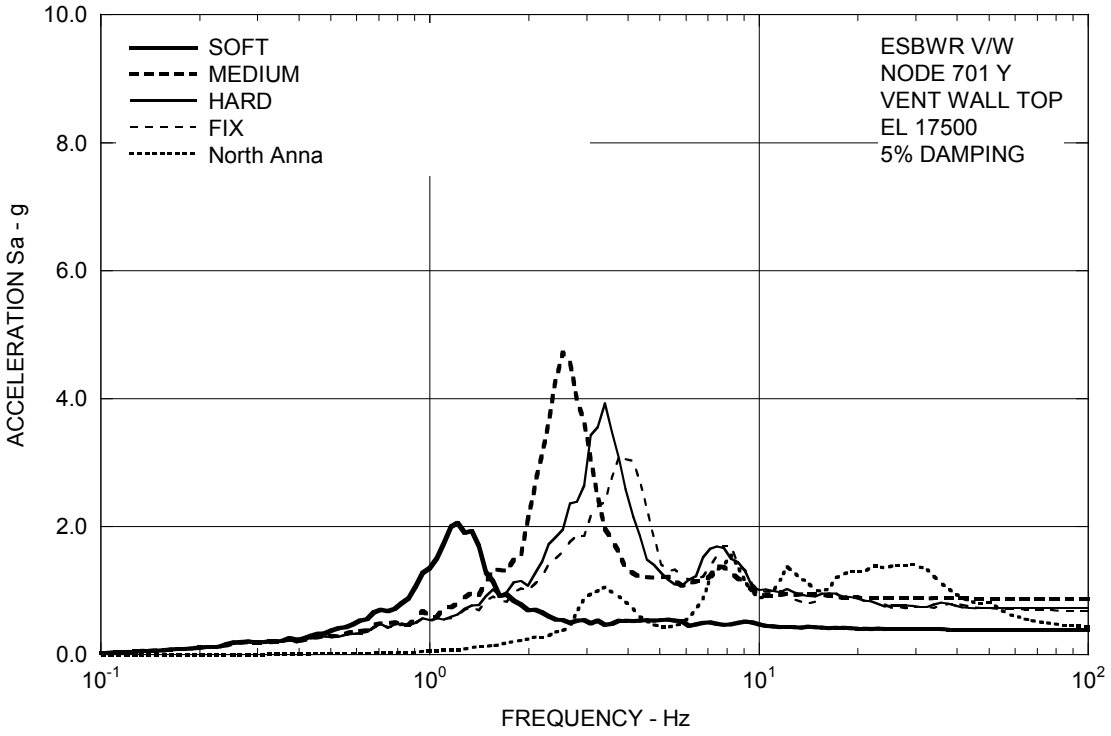

Figure 3A.8.1-2c. FRS (Effect of Soil Stiffness) – Vent Wall Top Y

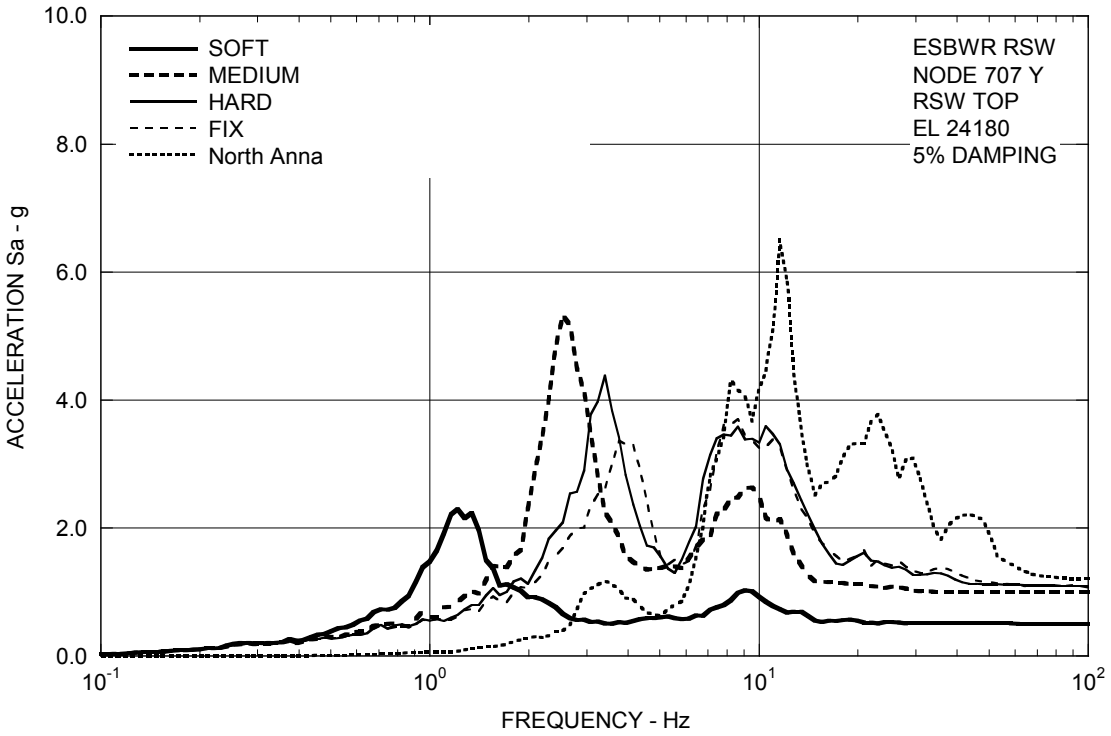

Figure 3A.8.1-2d. FRS (Effect of Soil Stiffness) – RSW Top Y

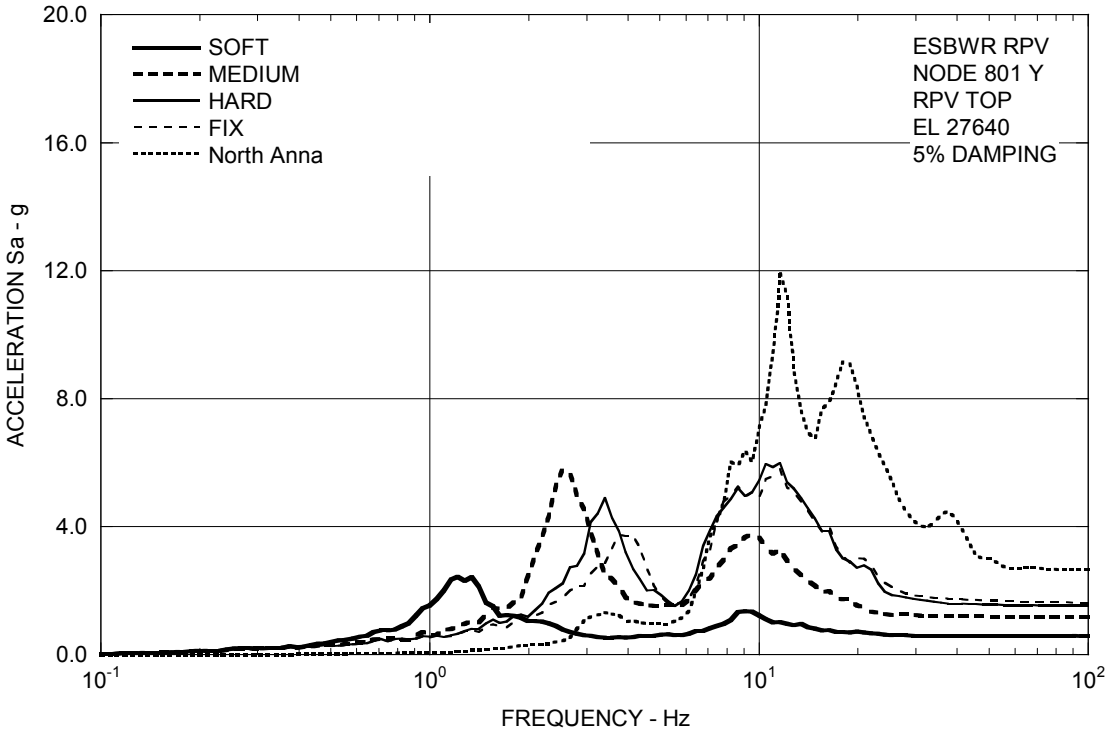

Figure 3A.8.1-2e. FRS (Effect of Soil Stiffness) – RPV Top Y

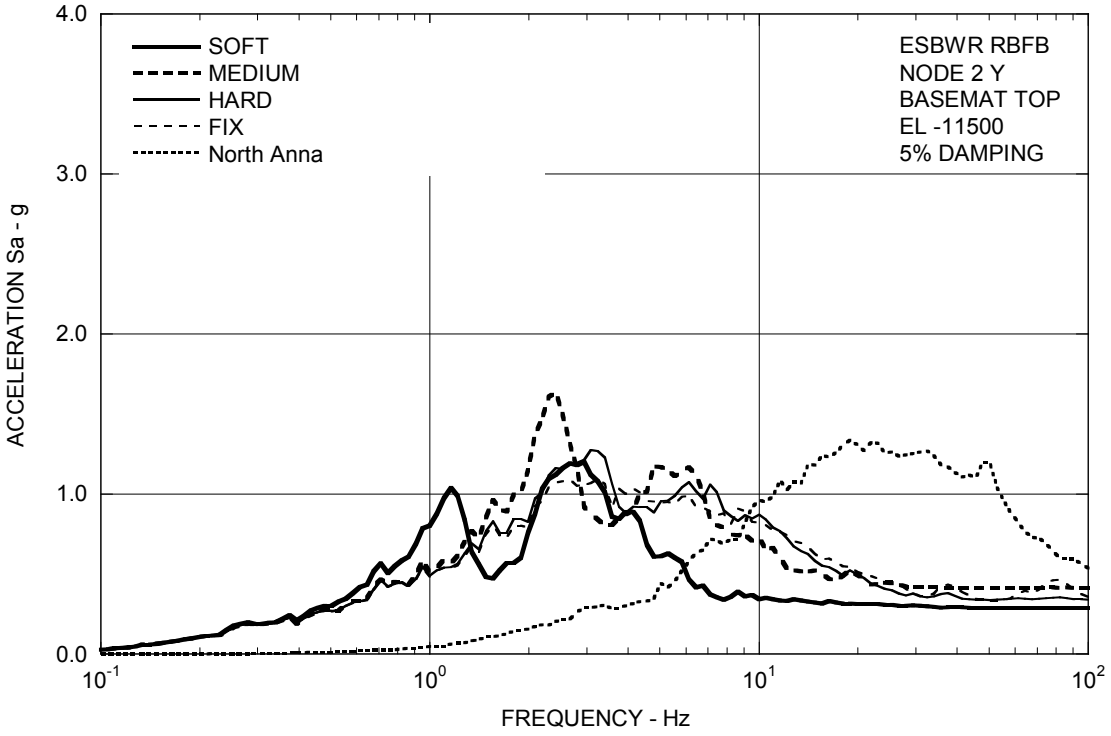

Figure 3A.8.1-2f. FRS (Effect of Soil Stiffness) – RBFB Basemat Y

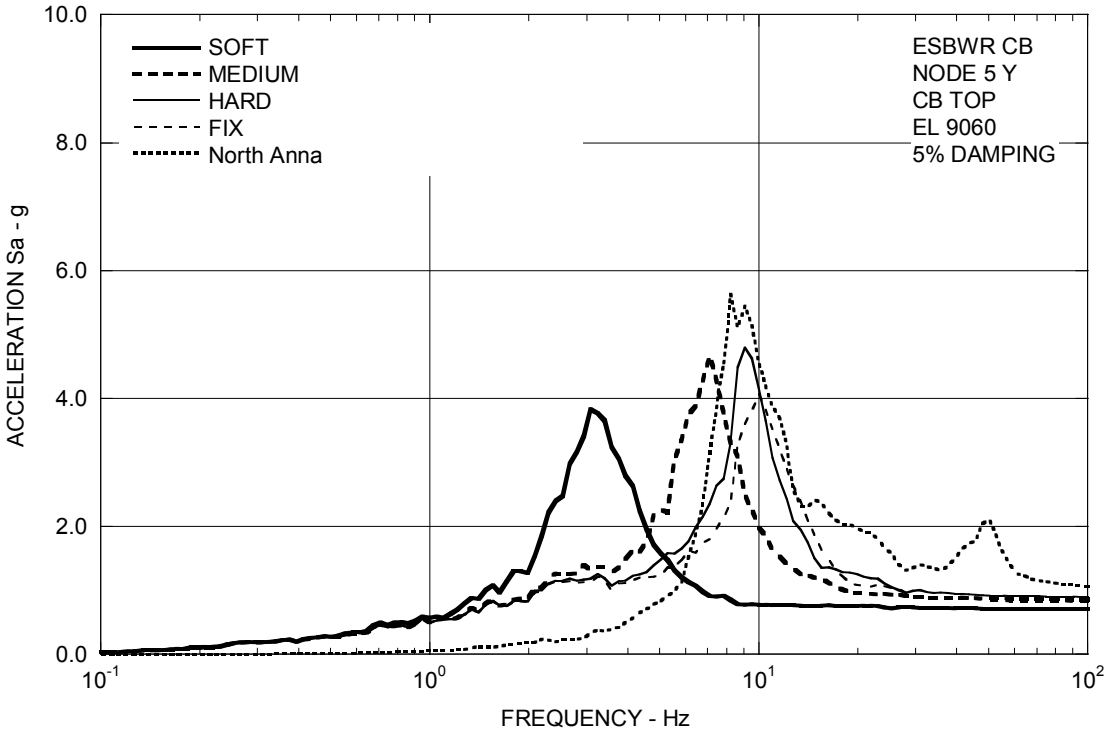

Figure 3A.8.1-2g. FRS (Effect of Soil Stiffness) – CB Top Y

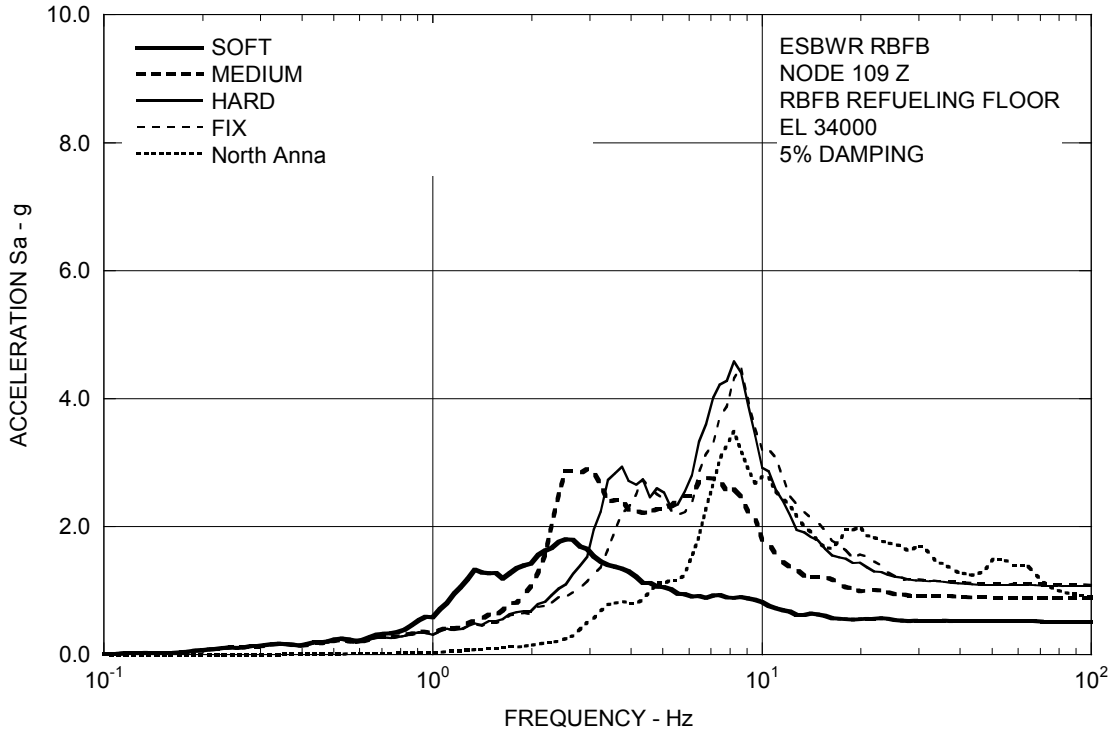

Figure 3A.8.1-3a. FRS (Effect of Soil Stiffness) – RBFB Refueling Floor Z

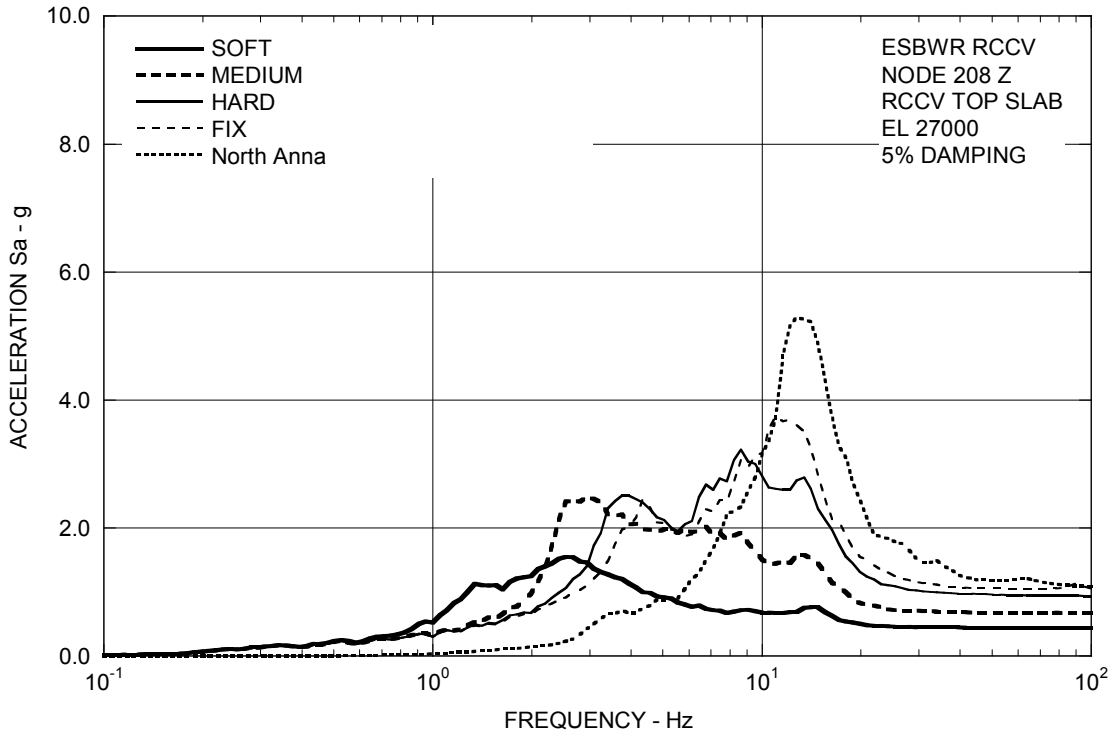

Figure 3A.8.1-3b. FRS (Effect of Soil Stiffness) – RCCV Top Slab Z

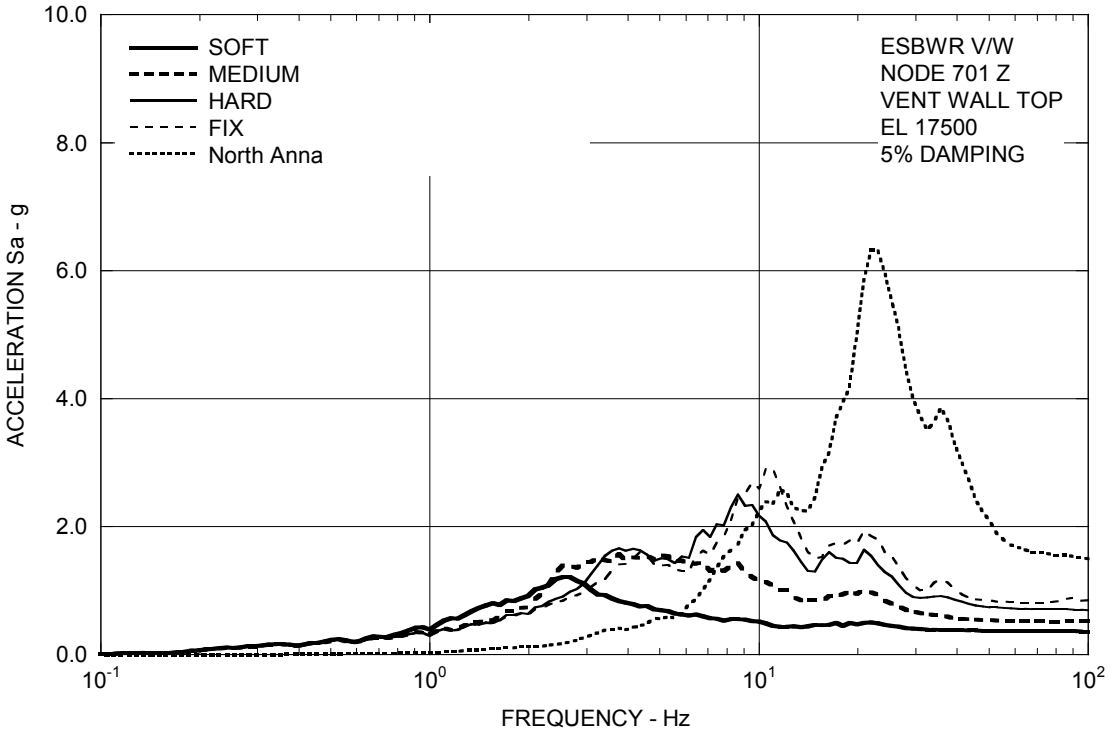

Figure 3A.8.1-3c. FRS (Effect of Stiffness) – Vent Wall Top Z

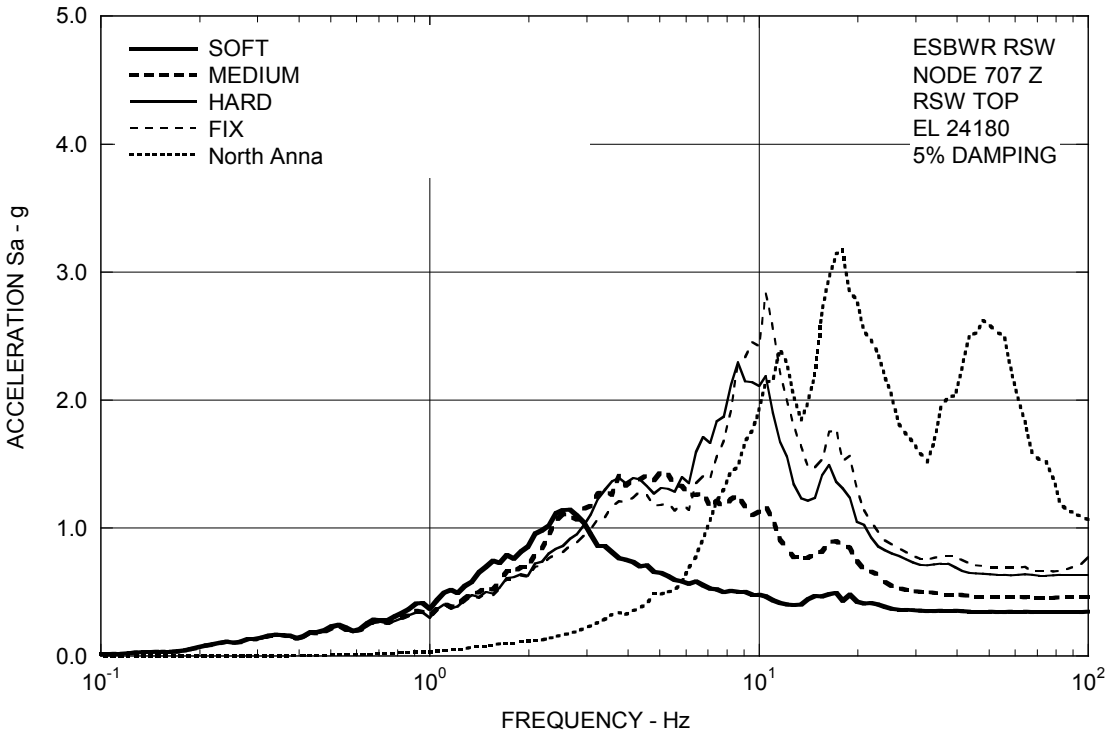

Figure 3A.8.1-3d. FRS (Effect of Soil Stiffness) – RSW Top Z

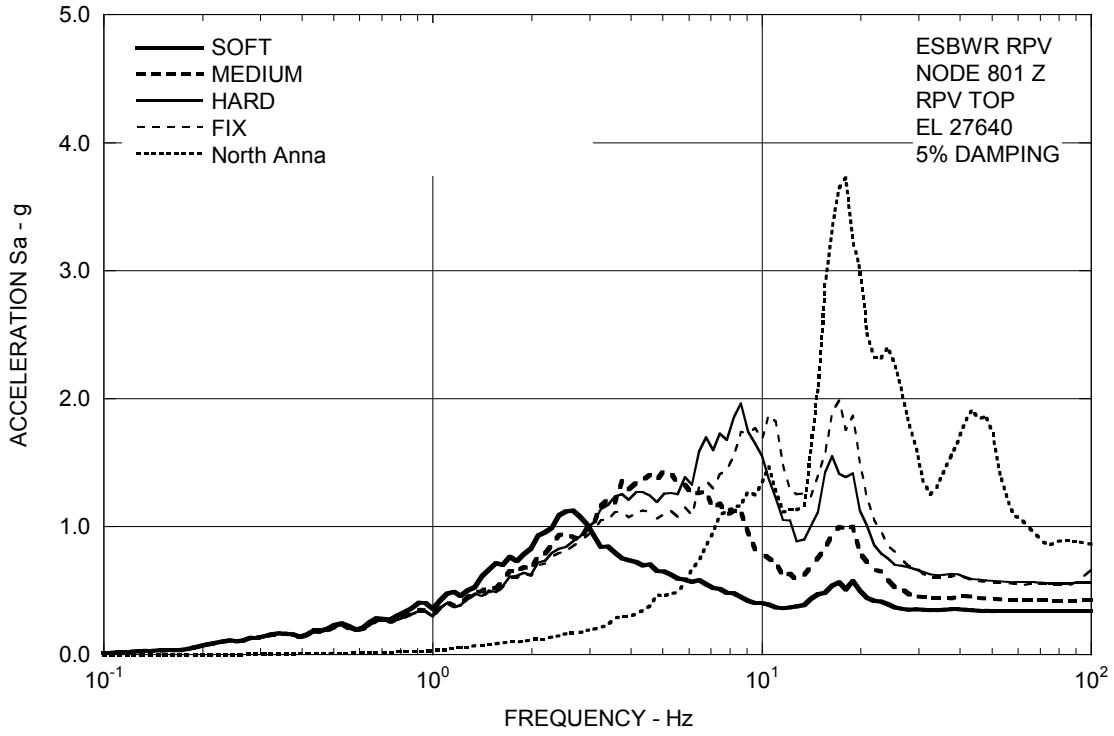

Figure 3A.8.1-3e. FRS (Effect of Soil Stiffness) – RPV Top Z

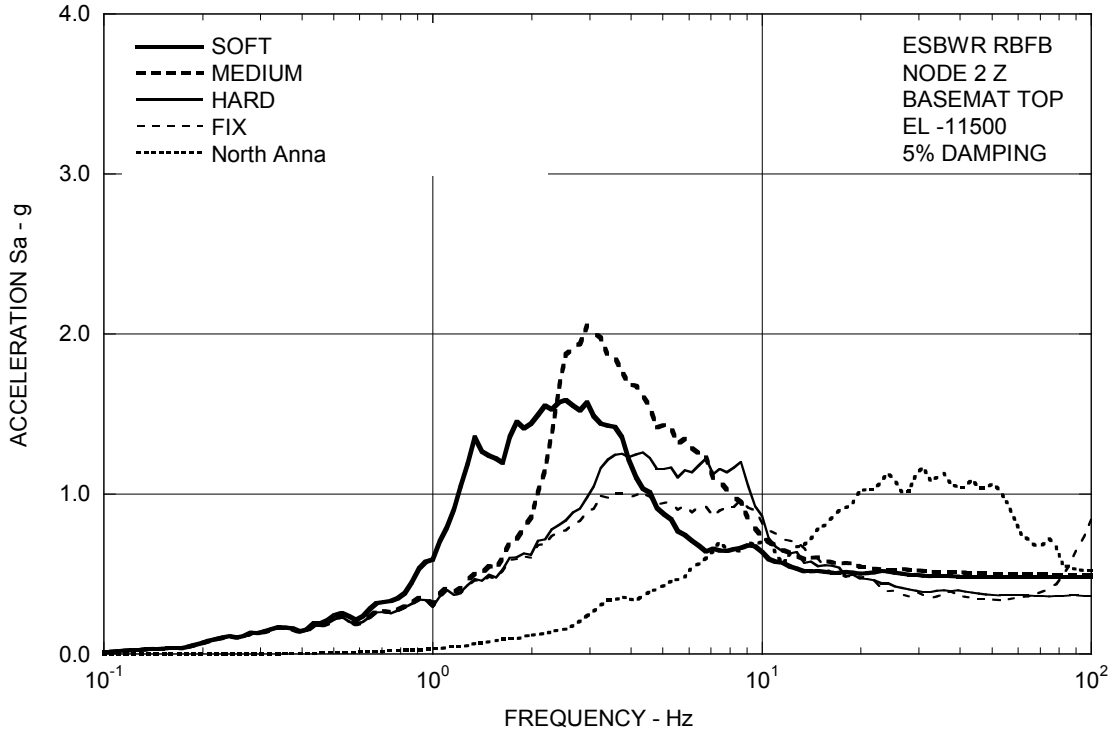

Figure 3A.8.1-3f. FRS (Effect of Soil Stiffness) – RBFB Basemat Z

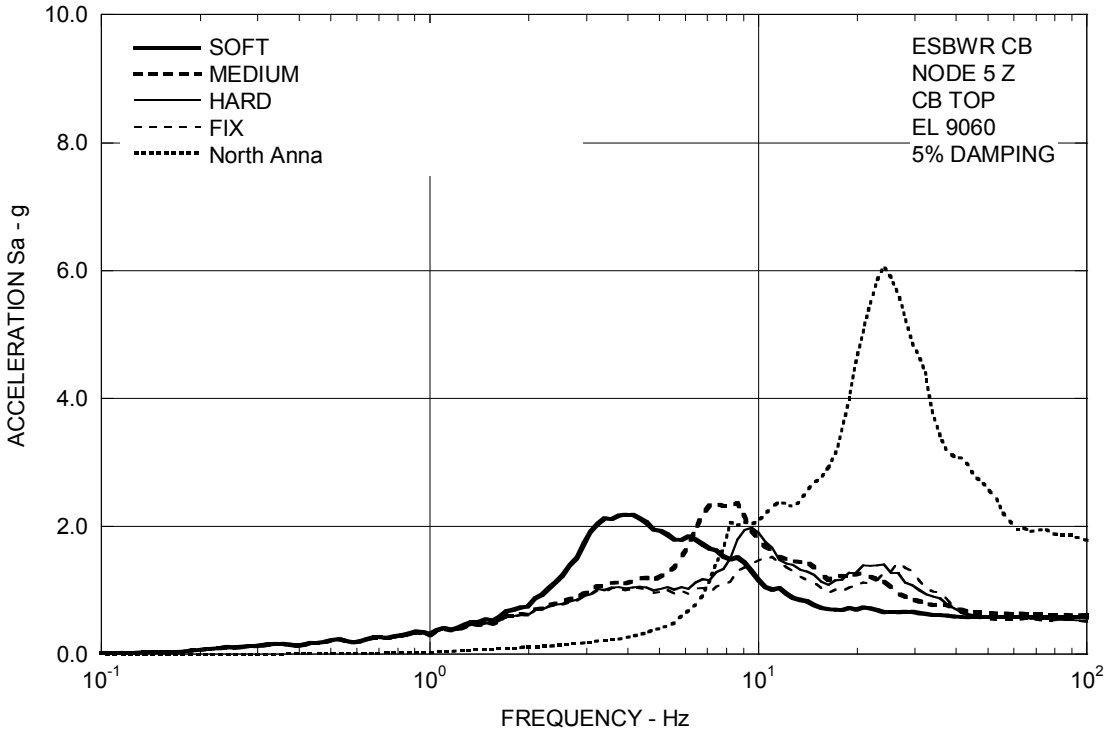

Figure 3A.8.1-3g. FRS (Effect of Soil Stiffness) – CB Top Z

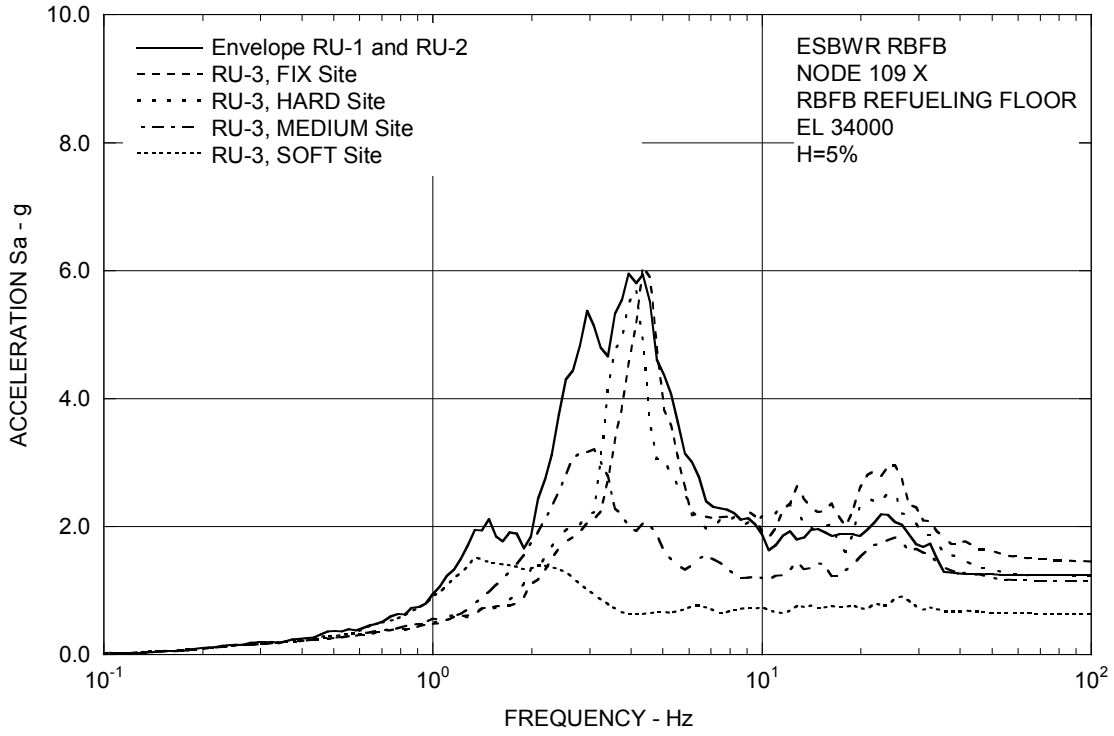

Figure 3A.8.2-1a. FRS (Effect of Single Envelope Ground Motion) – RBFB Refueling Floor X

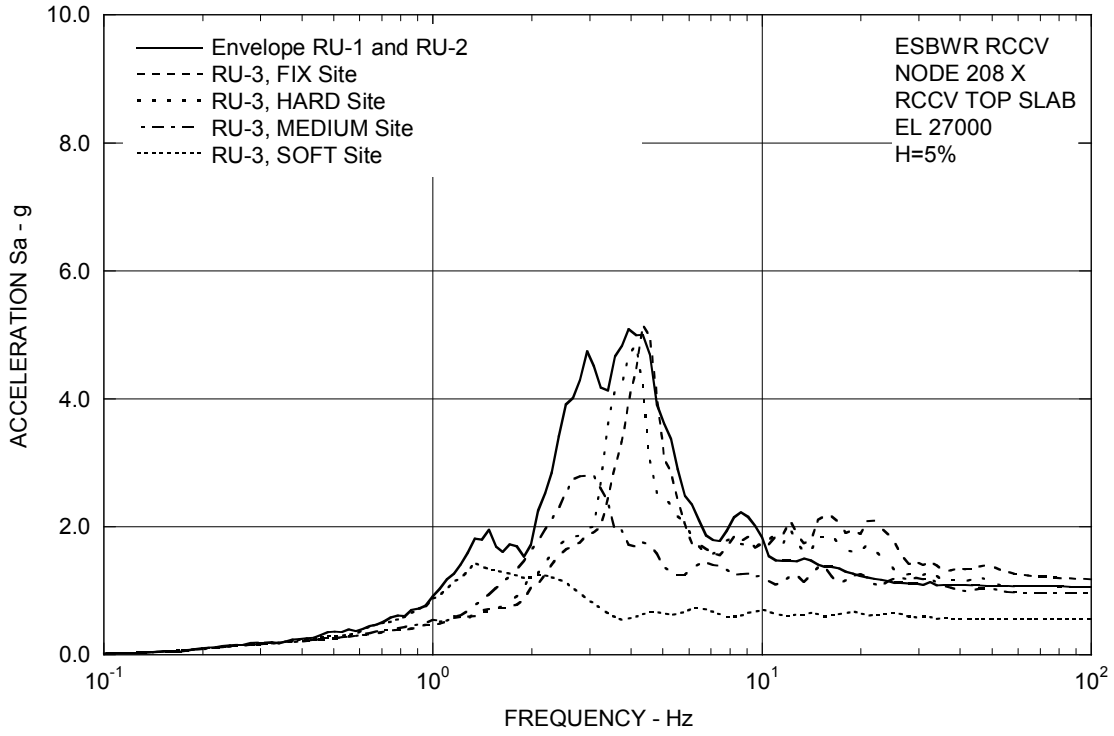

Figure 3A.8.2-1b. FRS (Effect of Single Envelope Ground Motion) – RCCV Top Slab X

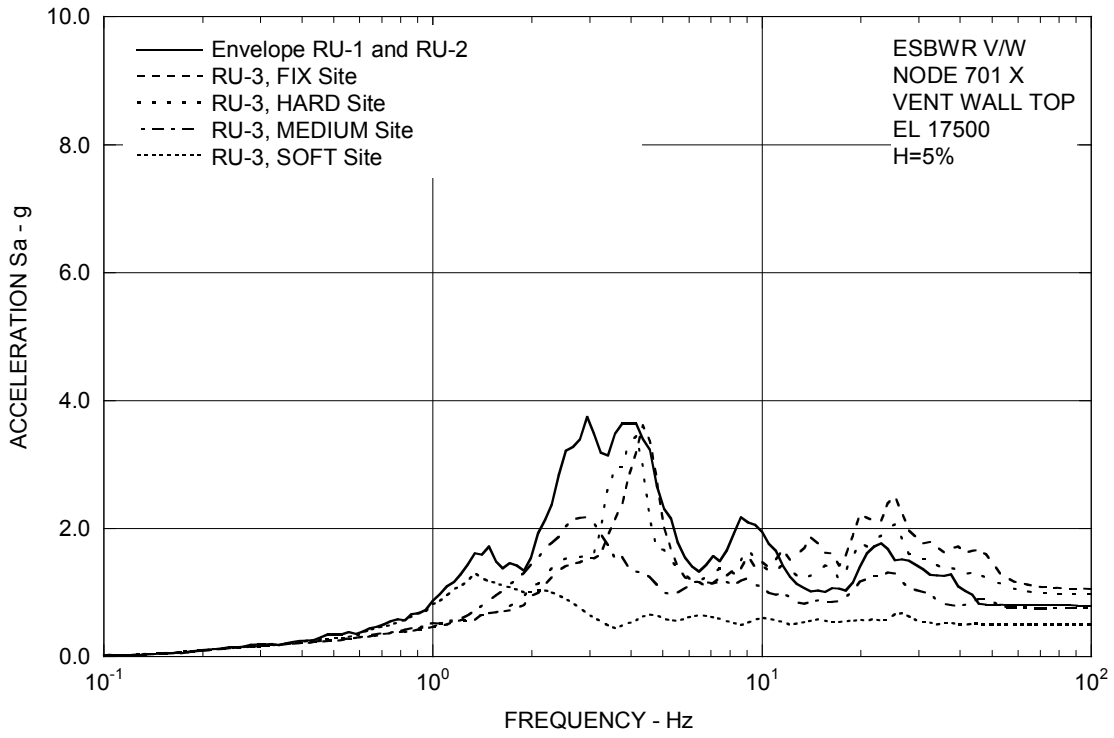

Figure 3A.8.2-1c. FRS (Effect of Single Envelope Ground Motion) – Vent Wall Top X

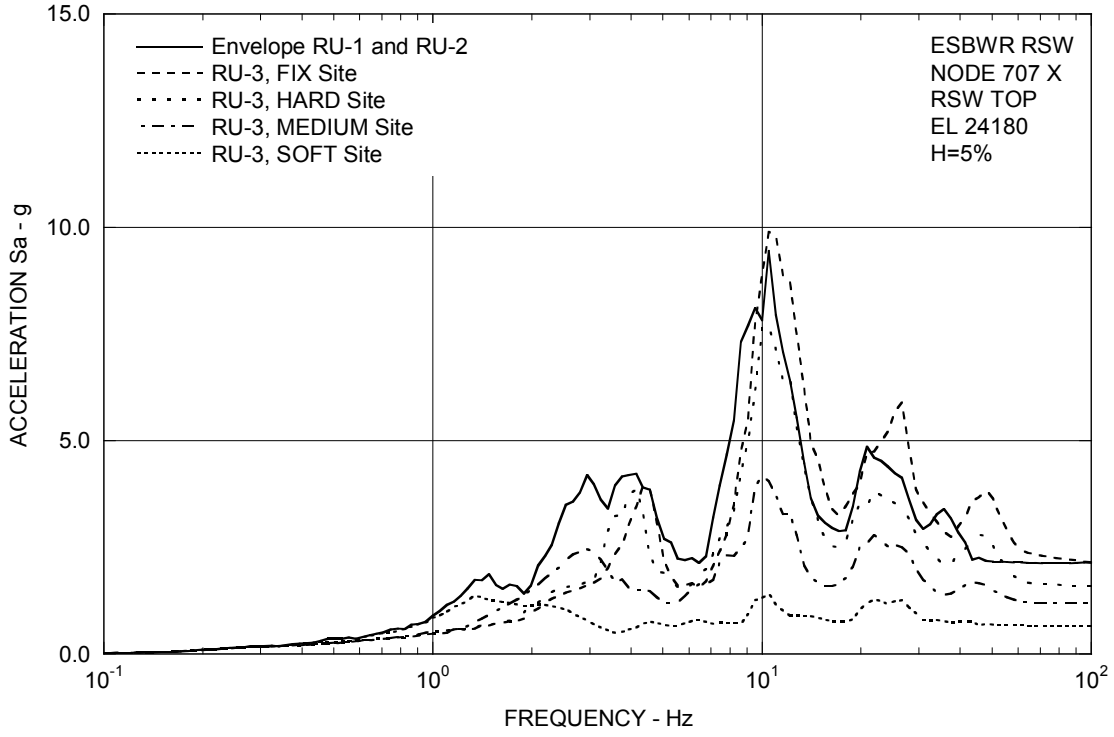

Figure 3A.8.2-1d. FRS (Effect of Single Envelope Ground Motion) – RSW Top X

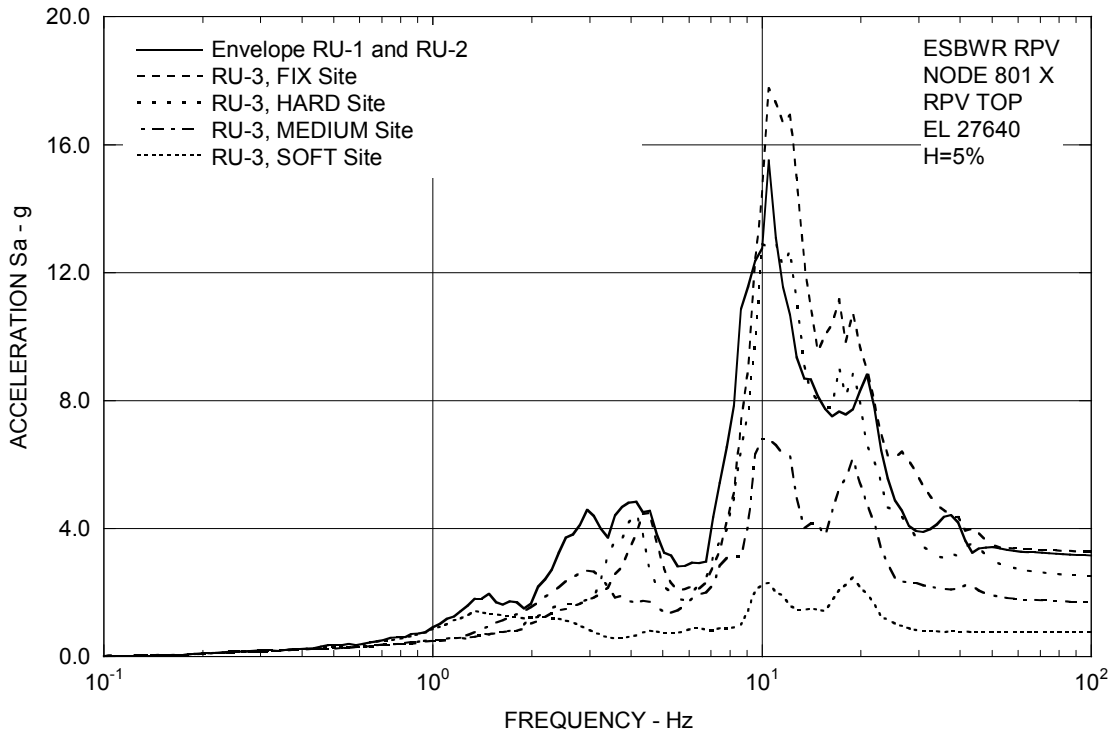

Figure 3A.8.2-1e. FRS (Effect of Single Envelope Ground Motion) – RPV Top X

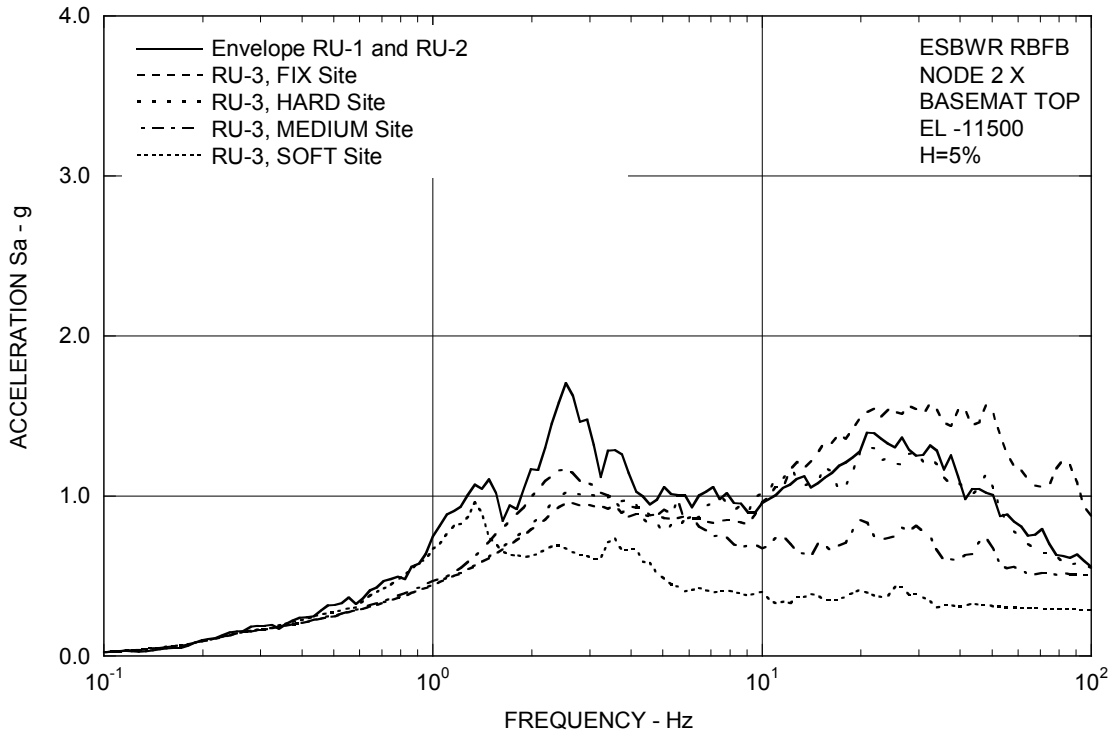

Figure 3A.8.2-1f. FRS (Effect of Single Envelope Ground Motion) – RBFB Basemat X

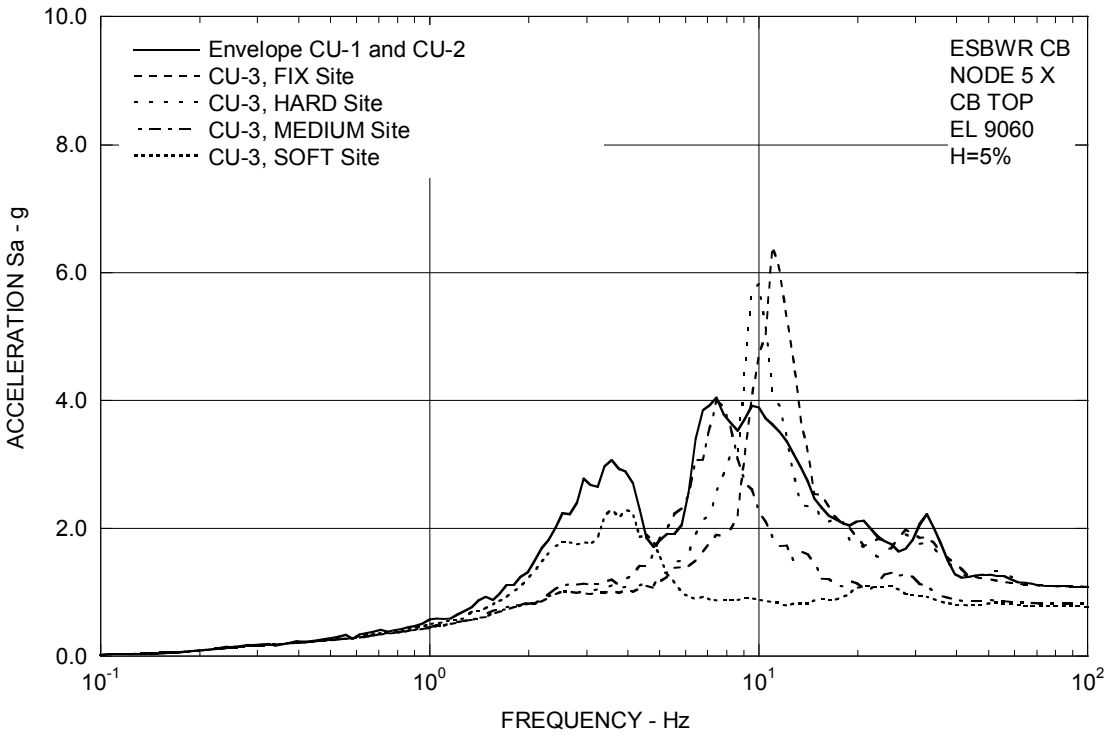

Figure 3A.8.2-1g. FRS (Effect of Single Envelope Ground Motion) – CB Top X

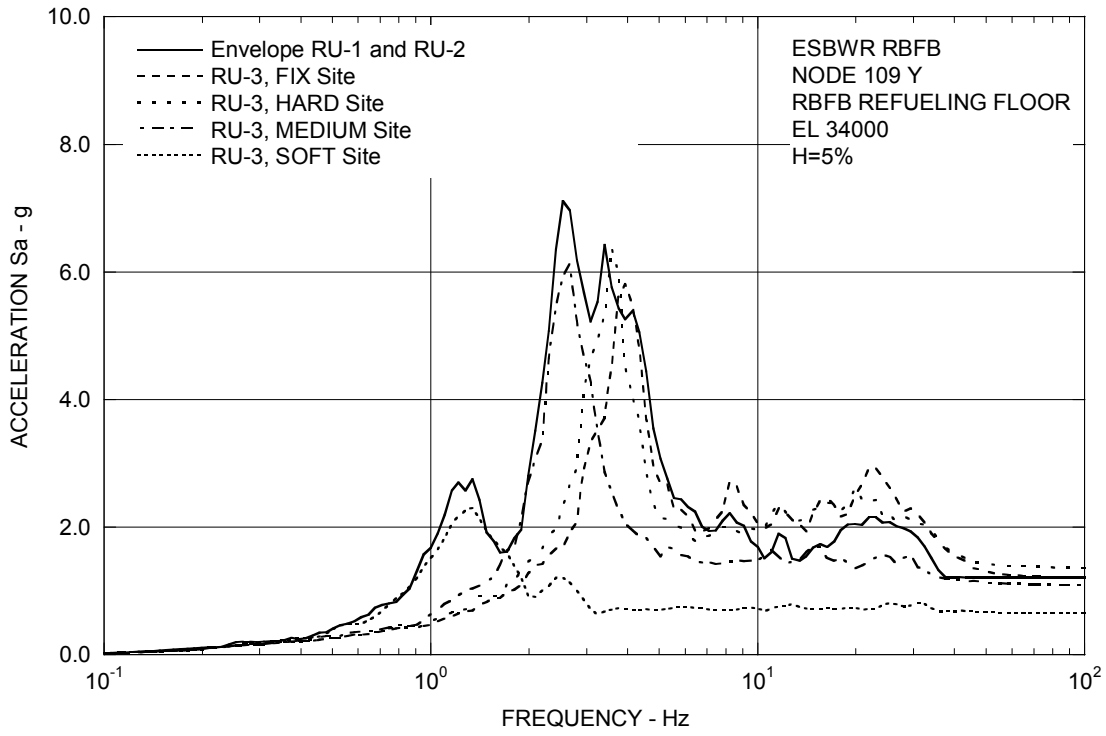

Figure 3A.8.2-2a. FRS (Effect of Single Envelope Ground Motion) – RBFB Refueling Floor Y

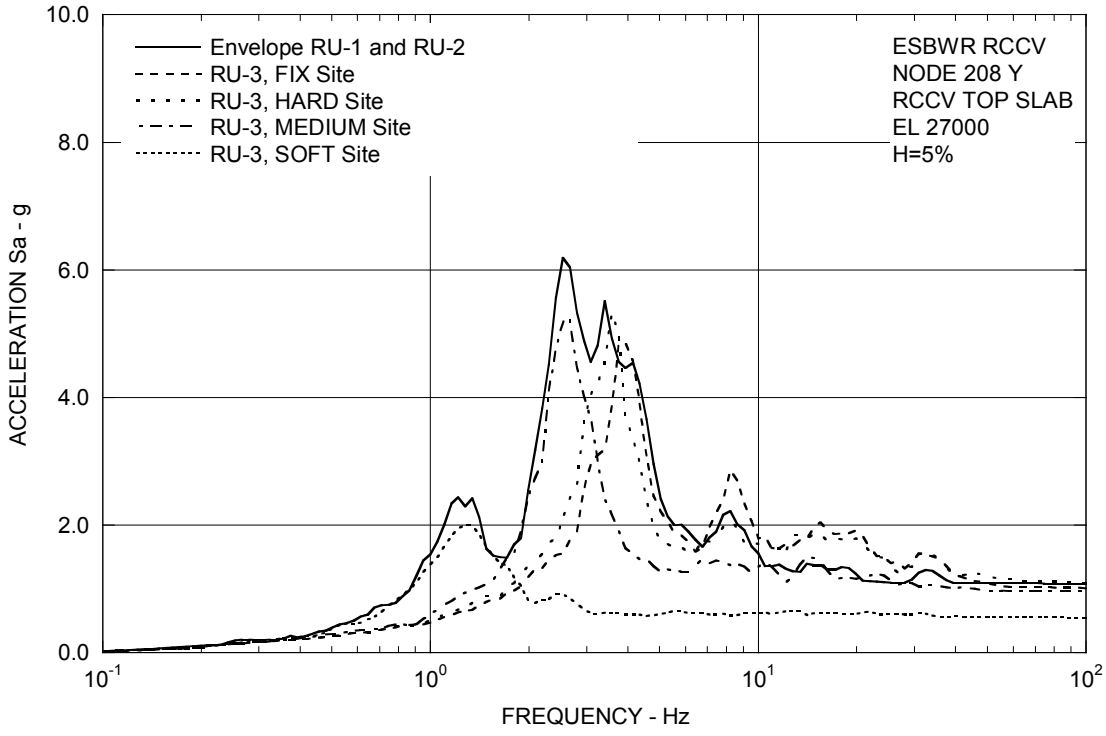

Figure 3A.8.2-2b. FRS (Effect of Single Envelope Ground Motion) – RCCV Top Slab Y

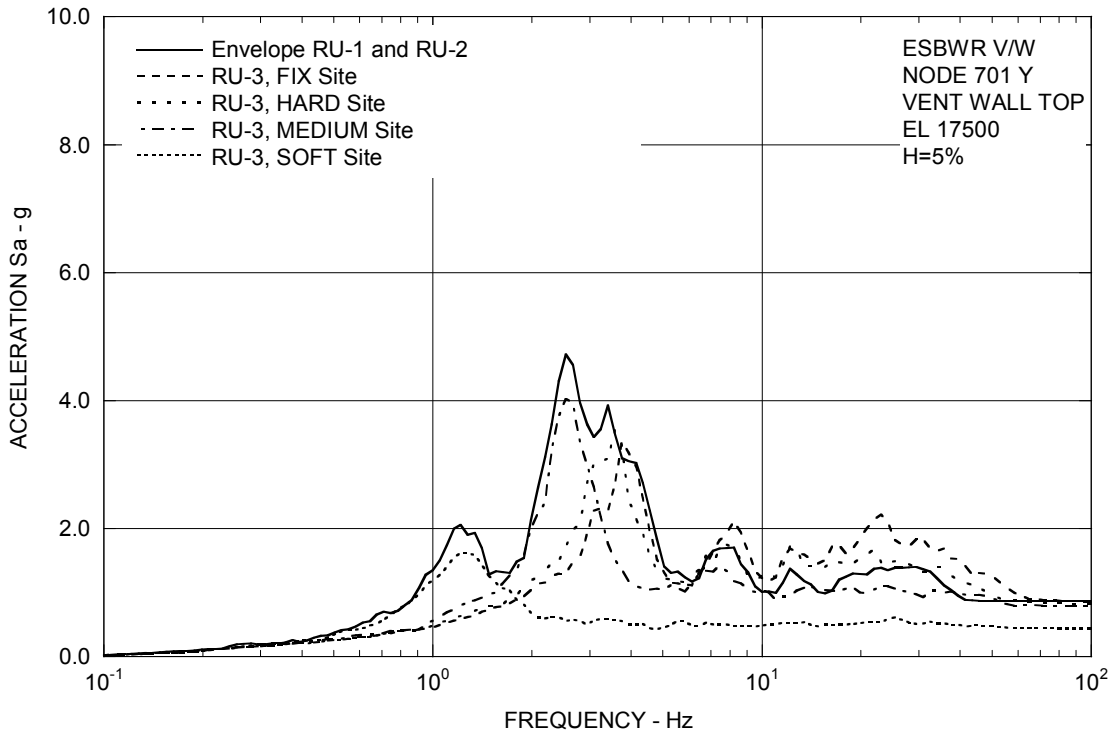

Figure 3A.8.2-2c. FRS (Effect of Single Envelope Ground Motion) – Vent Wall Top Y

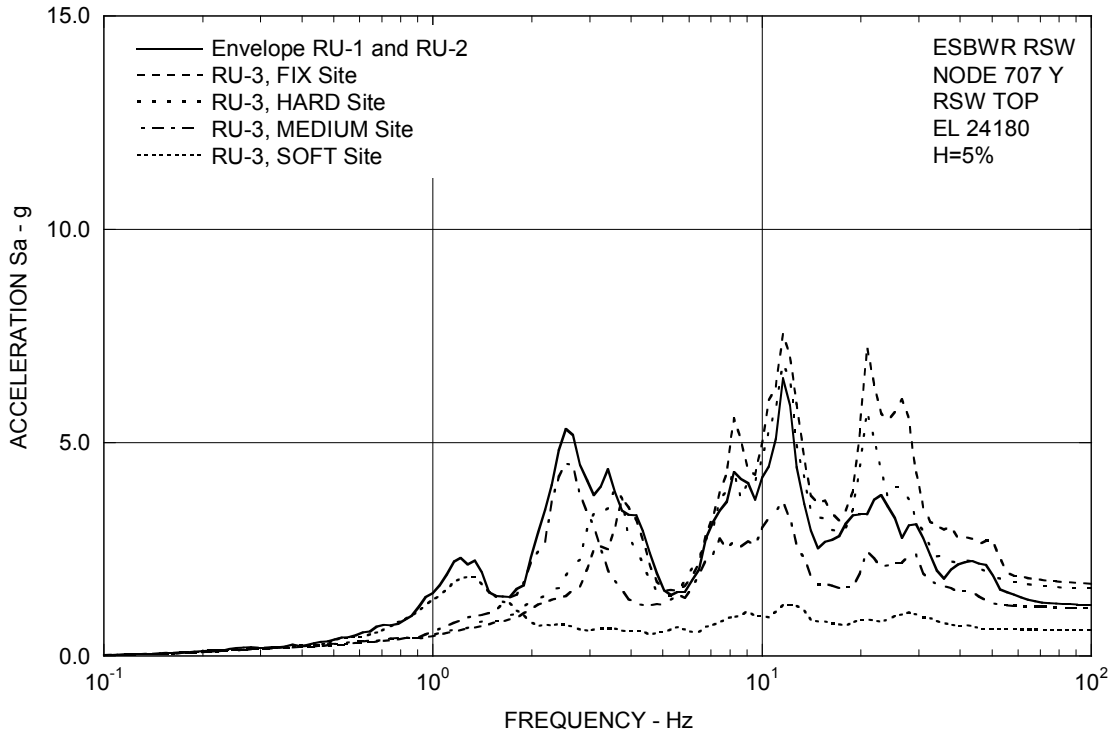

Figure 3A.8.2-2d. FRS (Effect of Single Envelope Ground Motion) – RSW Top Y

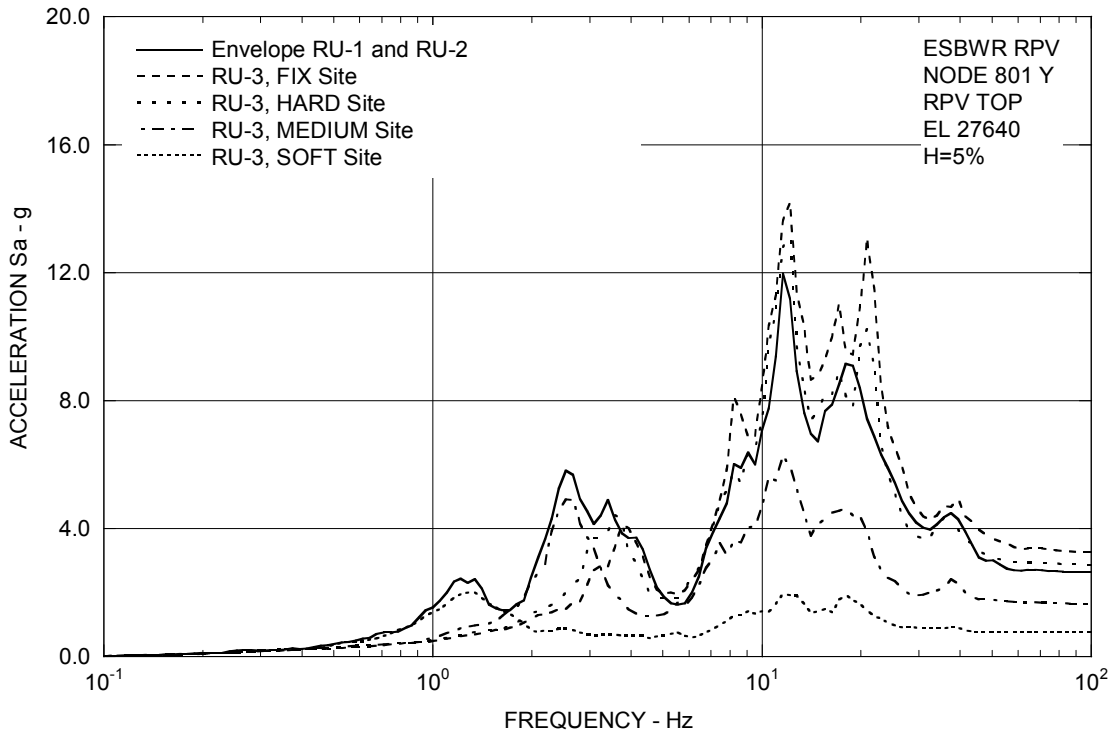

Figure 3A.8.2-2e. FRS (Effect of Single Envelope Ground Motion) – RPV Top Y

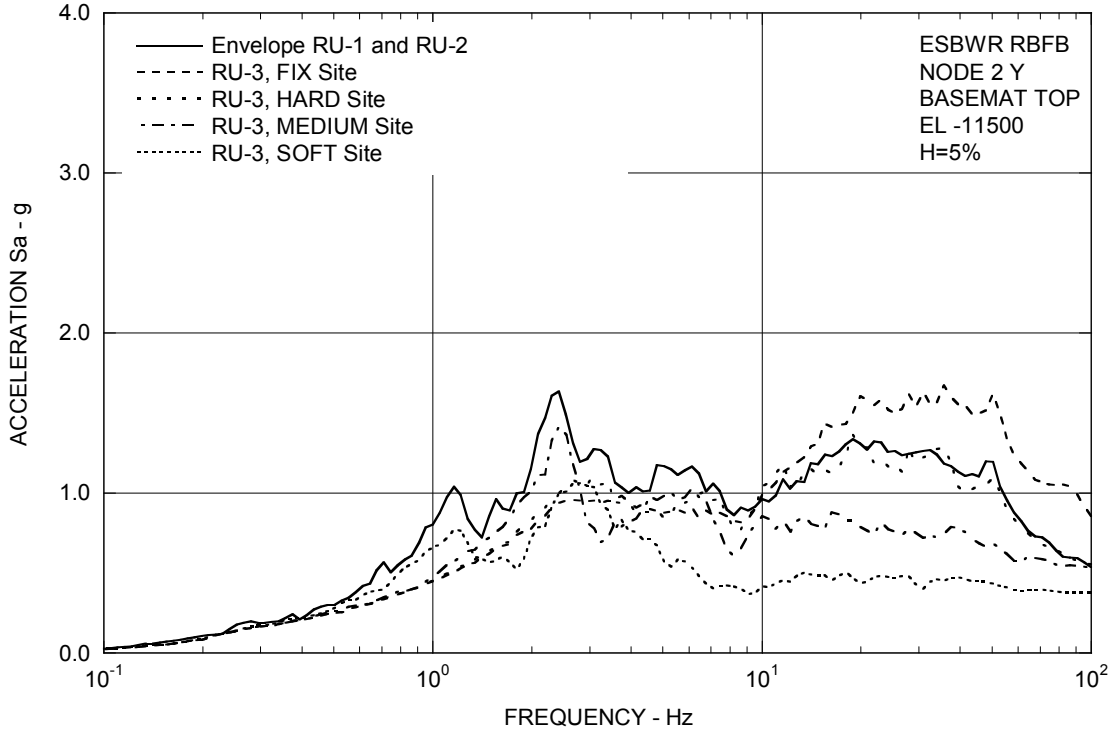

Figure 3A.8.2-2f. FRS (Effect of Single Envelope Ground Motion) – RBFB Basemat Y

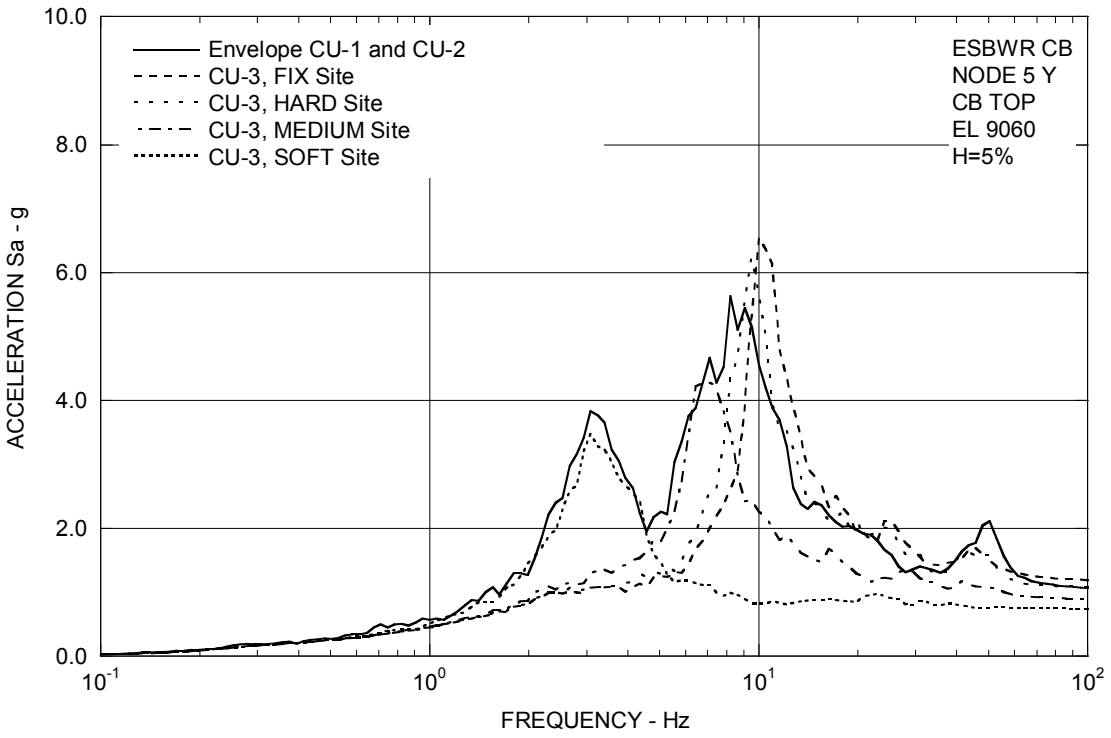

Figure 3A.8.2-2g. FRS (Effect of Single Envelope Ground Motion) – CB Top Y

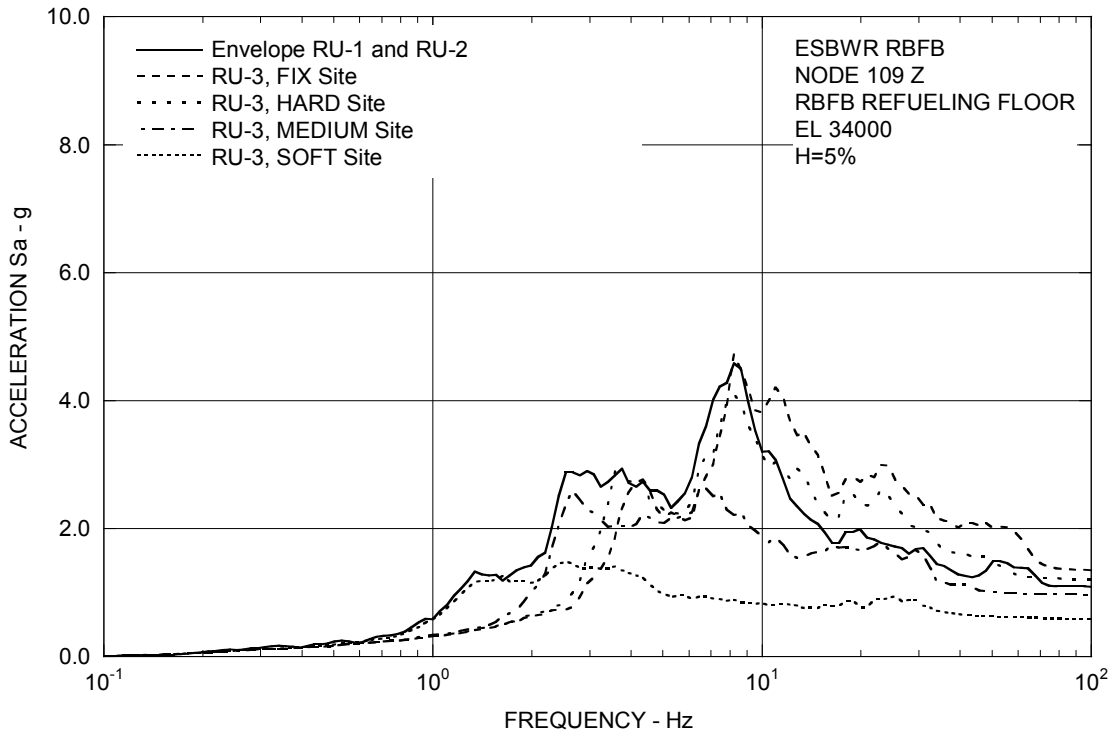

Figure 3A.8.2-3a. FRS (Effect of Single Envelope Ground Motion) – RBFB Refueling Floor Z

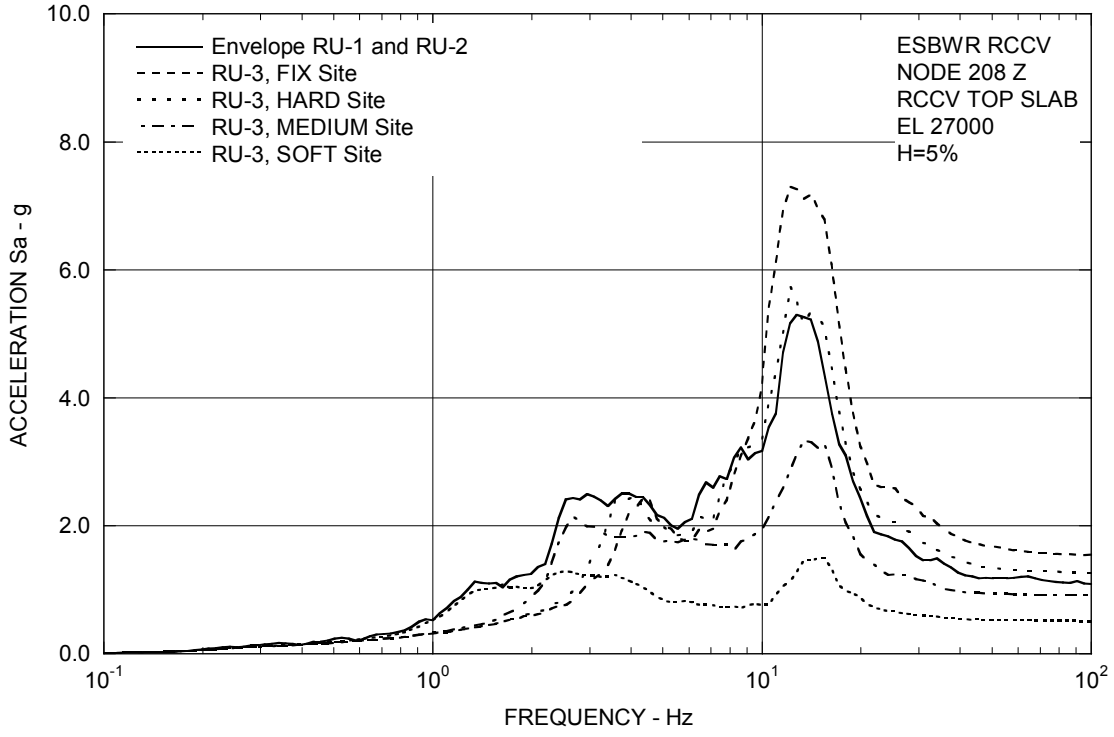

Figure 3A.8.2-3b. FRS (Effect of Single Envelope Ground Motion) – RCCV Top Slab Z

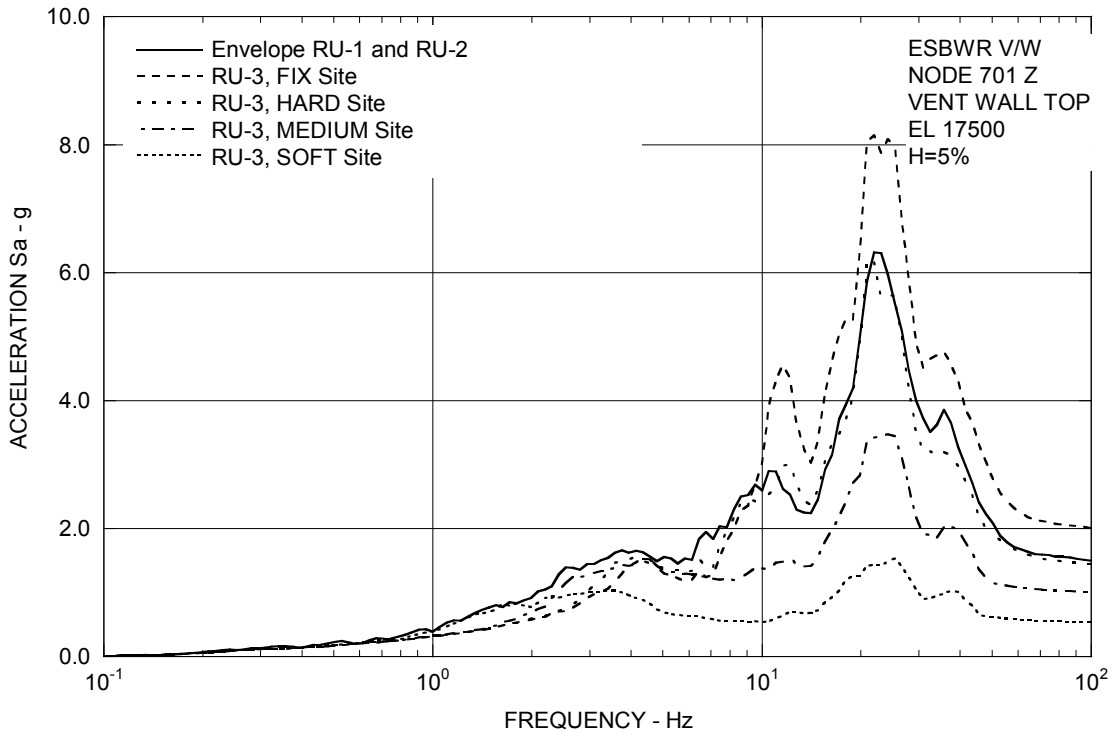

Figure 3A.8.2-3c. FRS (Effect of Single Envelope Ground Motion) – Vent Wall Top Z

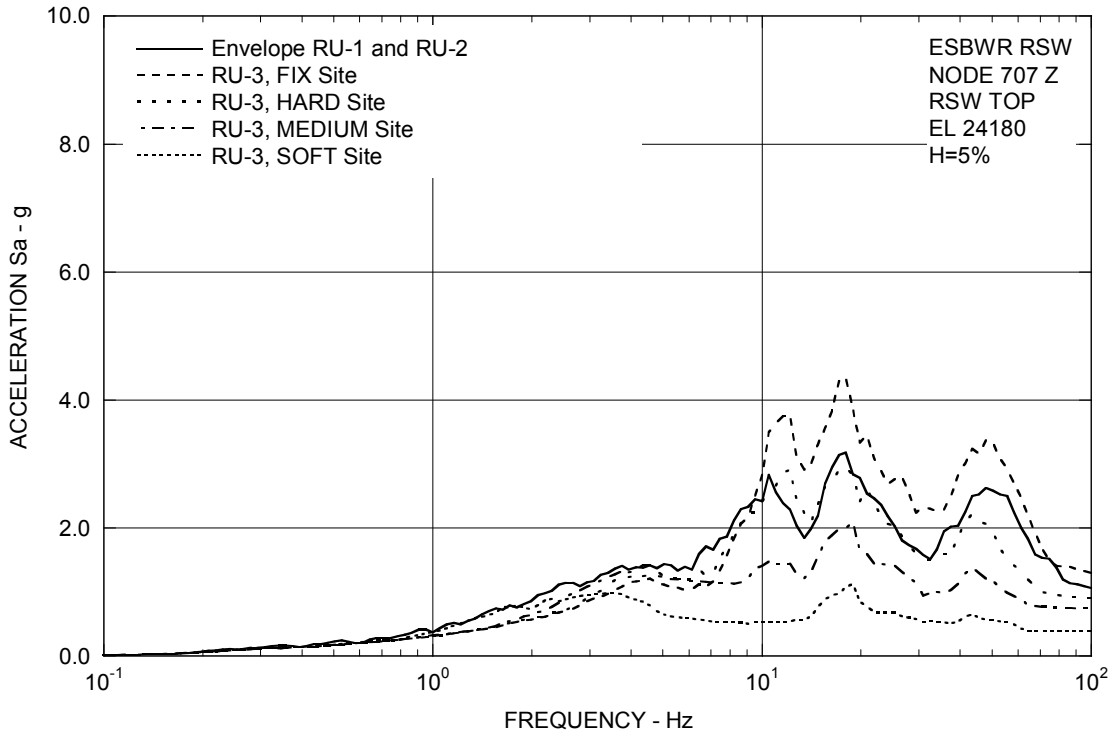

Figure 3A.8.2-3d. FRS (Effect of Single Envelope Ground Motion) – RSW Top Z

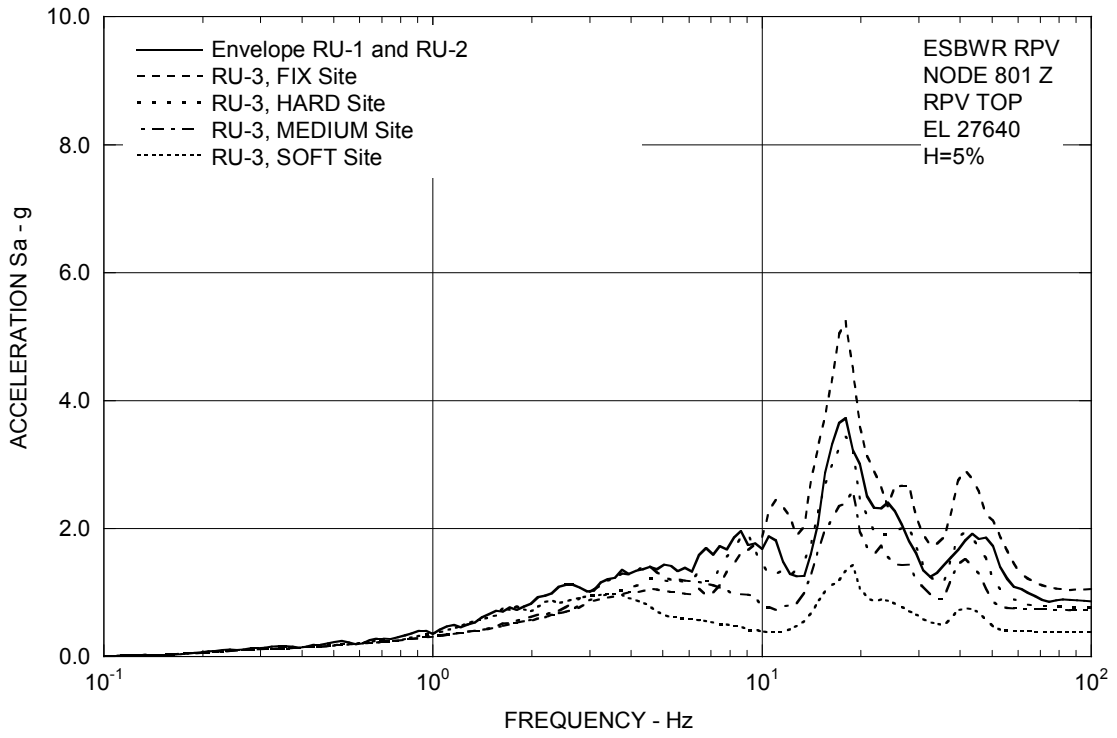

Figure 3A.8.2-3e. FRS (Effect of Single Envelope Ground Motion) – RPV Top Z

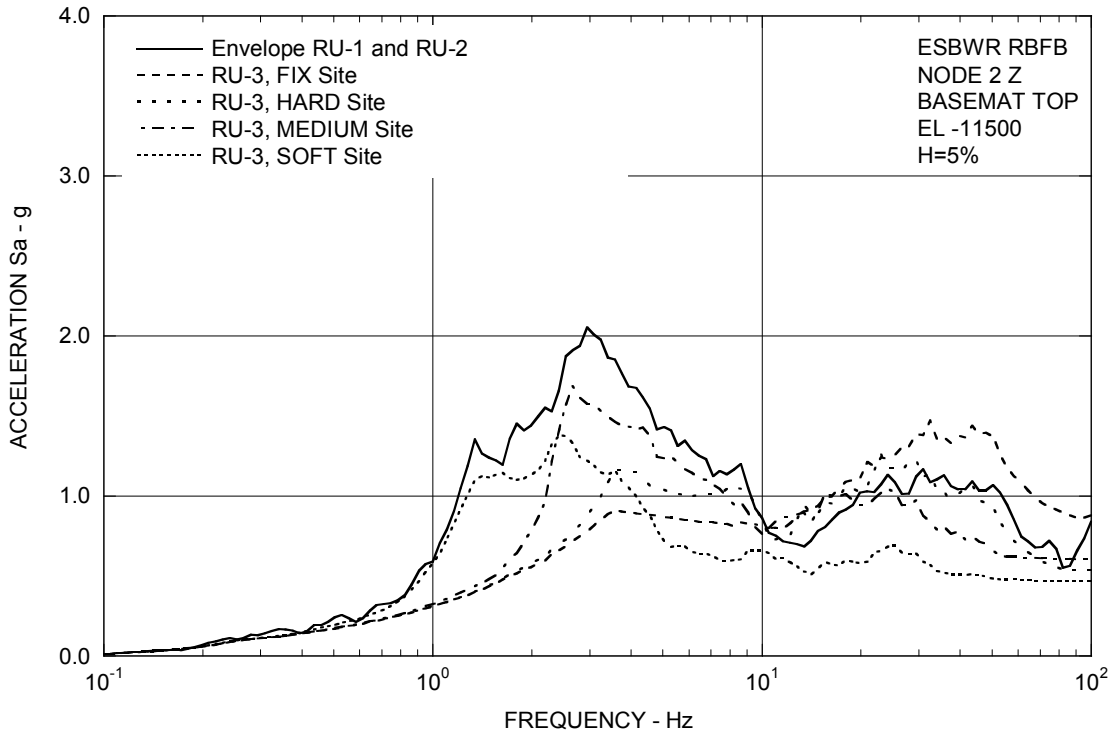

Figure 3A.8.2-3f. FRS (Effect of Single Envelope Ground Motion) – RBFB Basemat Z

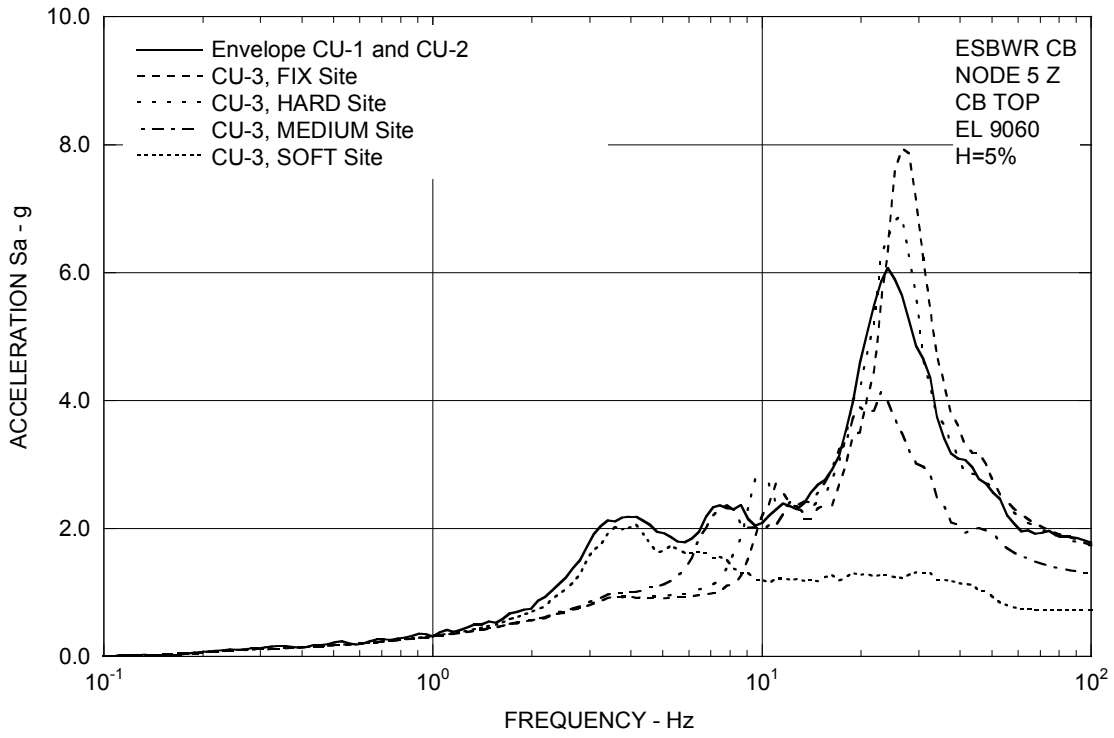

Figure 3A.8.2-3g. FRS (Effect of Single Envelope Ground Motion) – CB Top Z

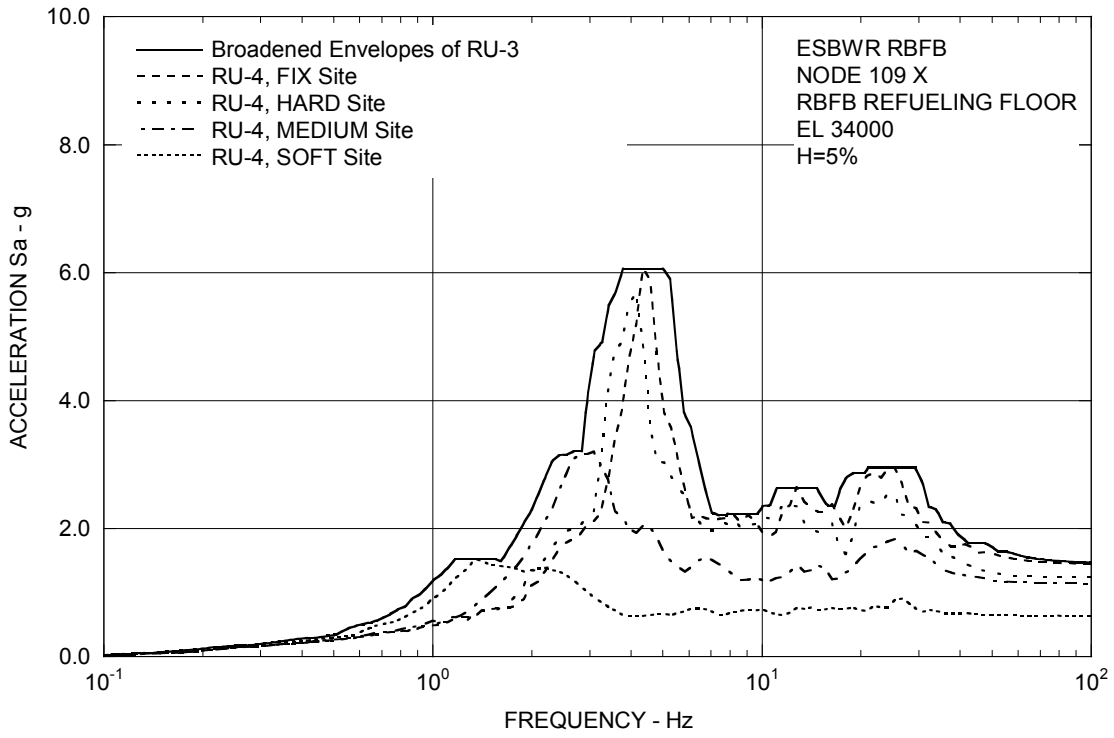

Figure 3A.8.3-1a. FRS (Effect of Updated Design of RSW and VW) – RBFB Refueling Floor X

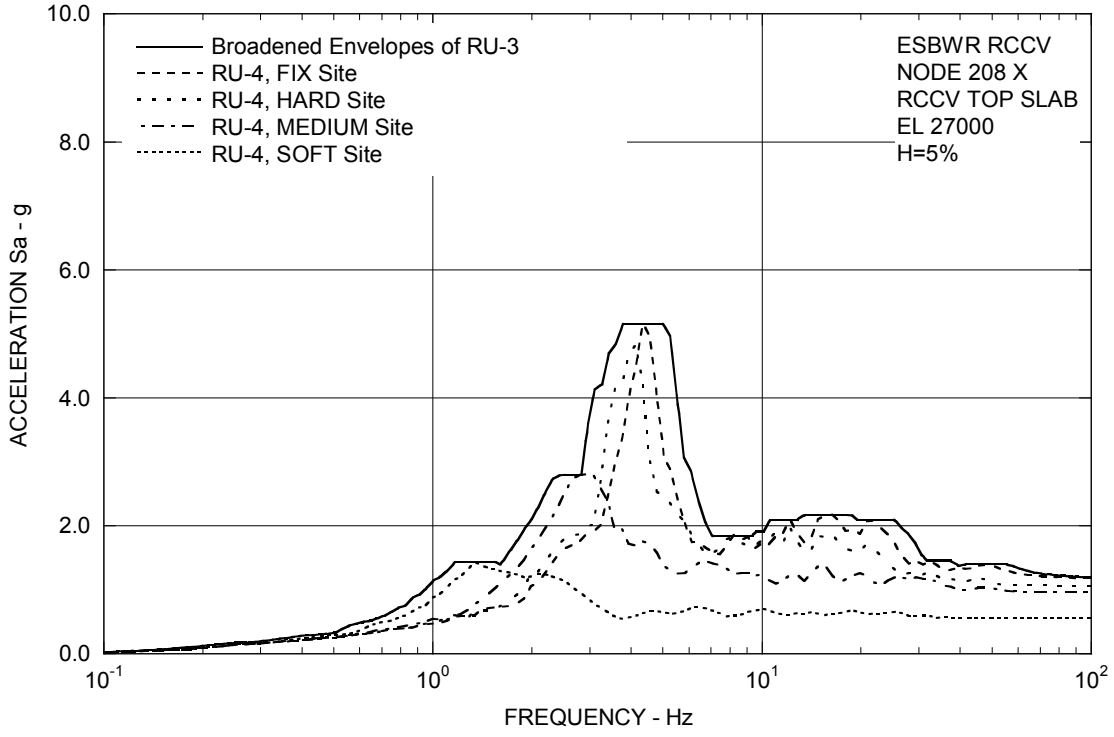

Figure 3A.8.3-1b. FRS (Effect of Updated Design of RSW and VW) – RCCV Top Slab X

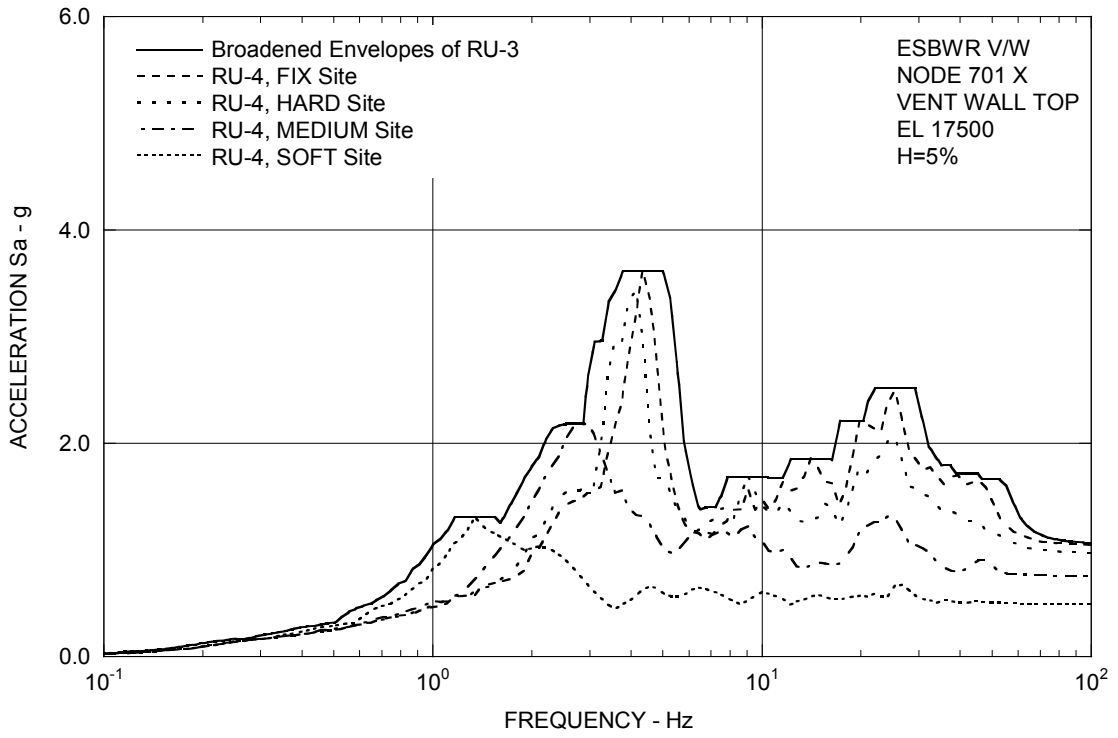

Figure 3A.8.3-1c. FRS (Effect of Updated Design of RSW and VW) – Vent Wall Top X

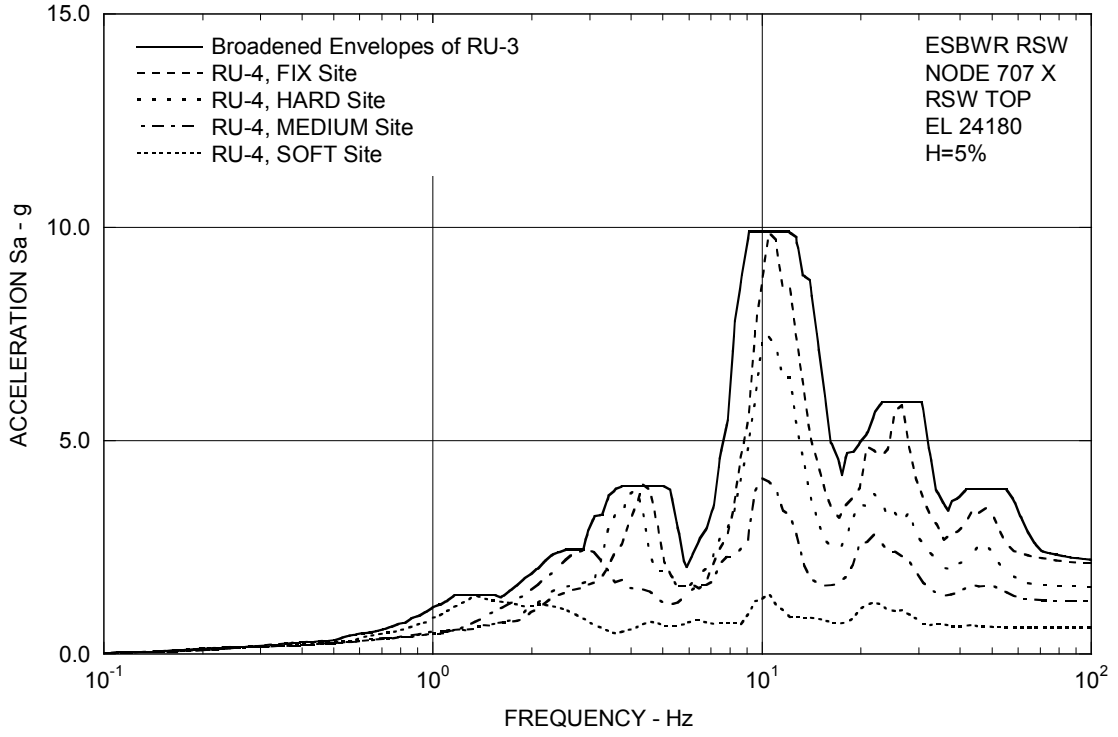

Figure 3A.8.3-1d. FRS (Effect of Updated Design of RSW and VW) – RSW Top X

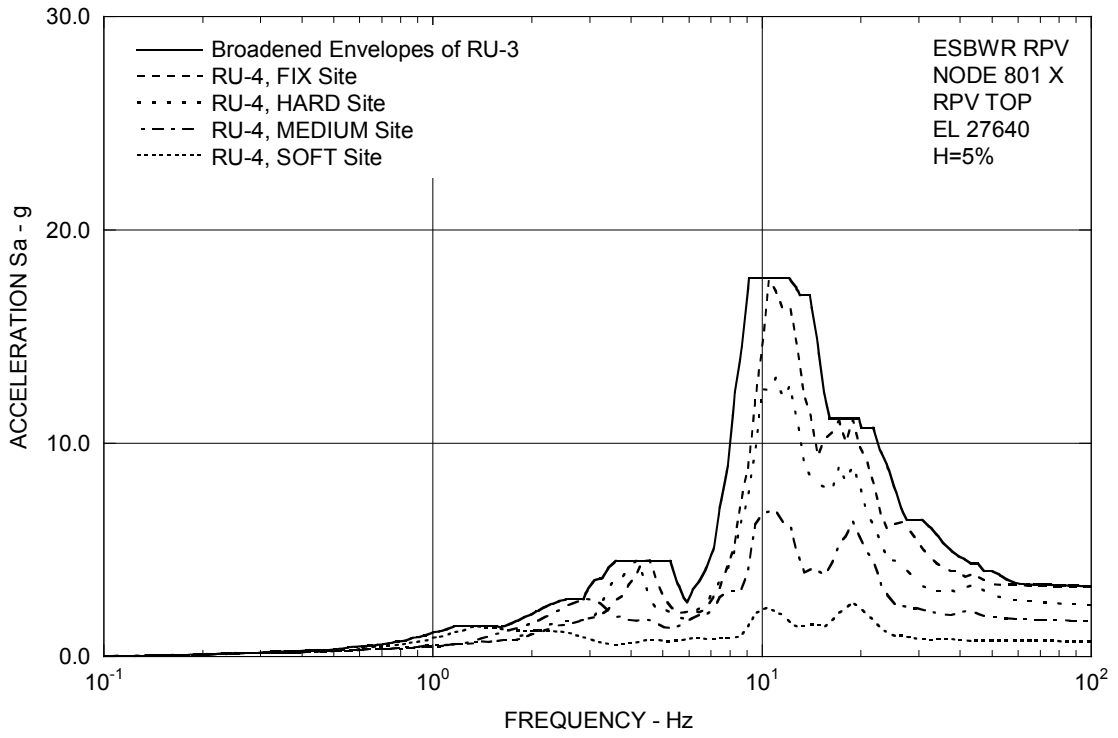

Figure 3A.8.3-1e. FRS (Effect of Updated Design of RSW and VW) – RPV Top X

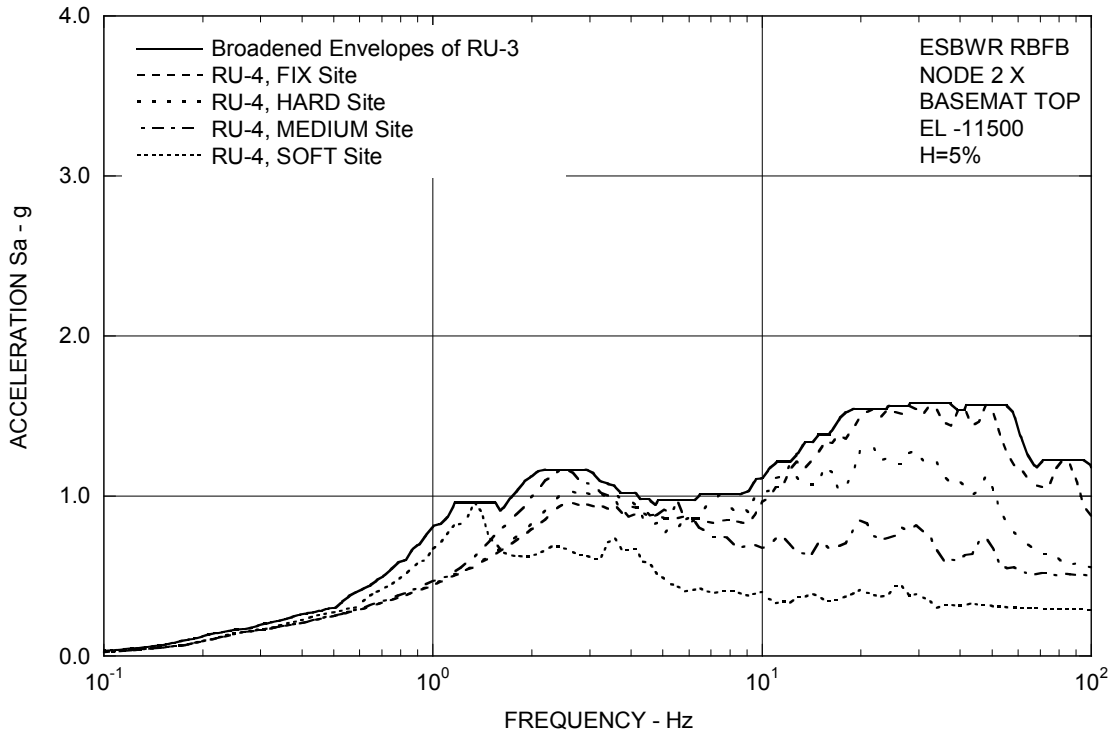

Figure 3A.8.3-1f. FRS (Effect of Updated Design of RSW and VW) – RBFB Basemat X

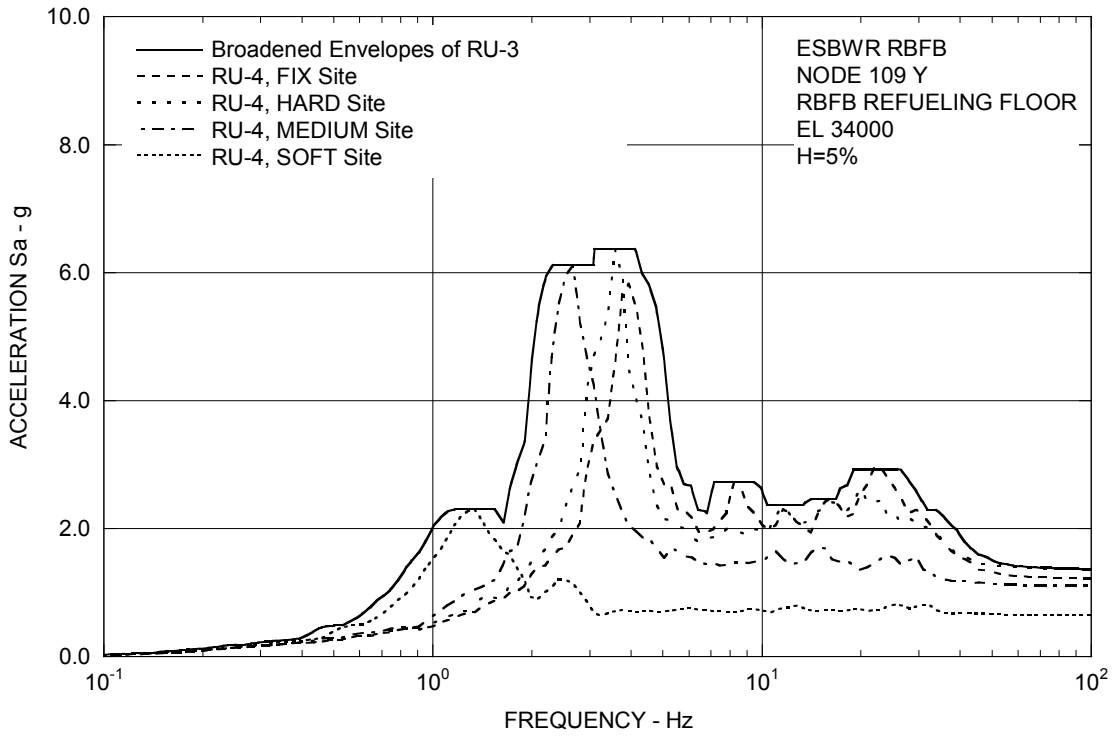

Figure 3A.8.3-2a. FRS (Effect of Updated Design of RSW and VW) – RBFB Refueling Floor Y

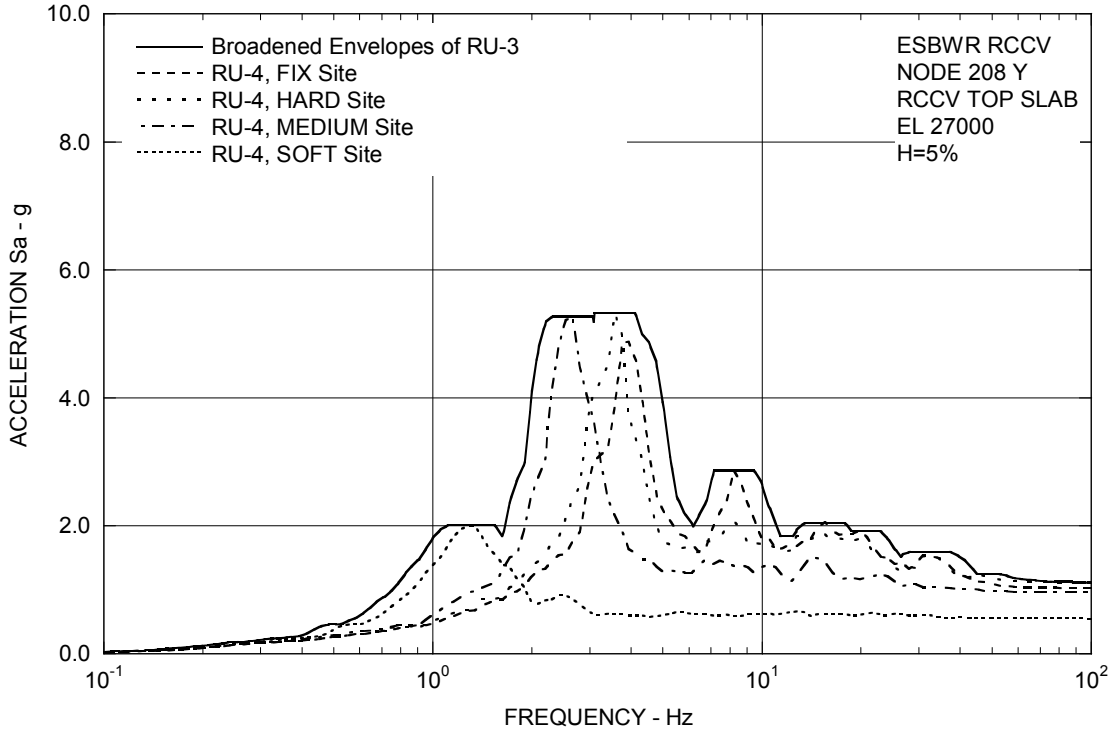

Figure 3A.8.3-2b. FRS (Effect of Updated Design of RSW and VW) – RCCV Top Slab Y

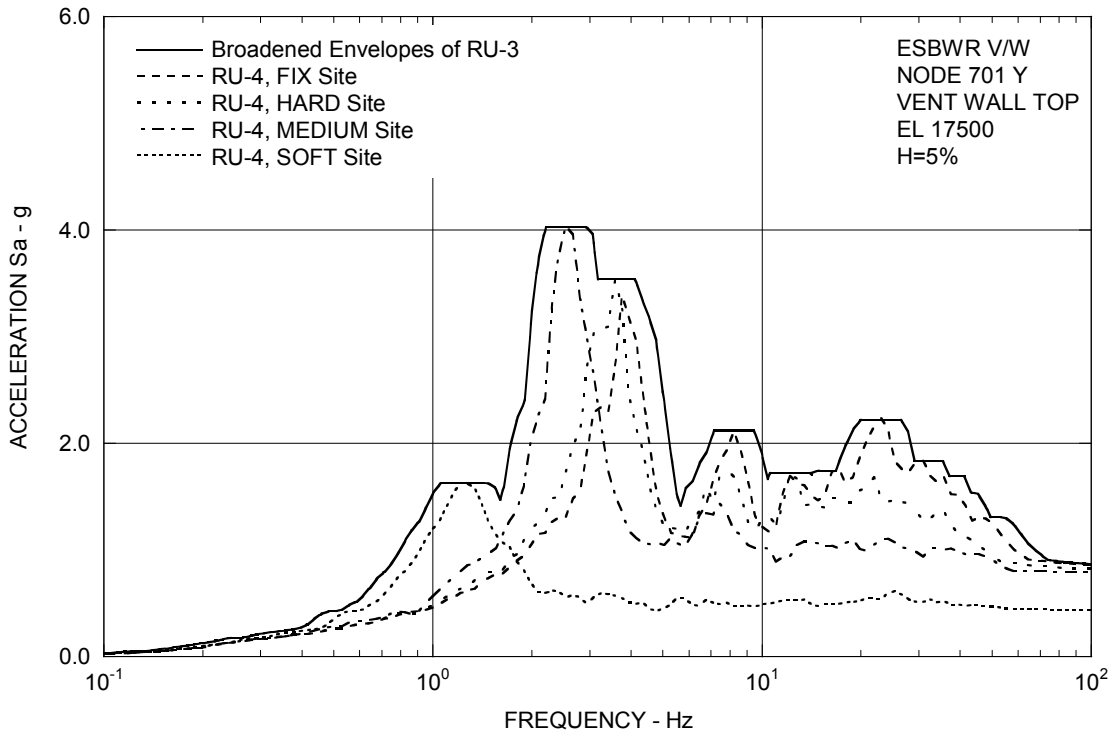

Figure 3A.8.3-2c. FRS (Effect of Updated Design of RSW and VW) – Vent Wall Top Y

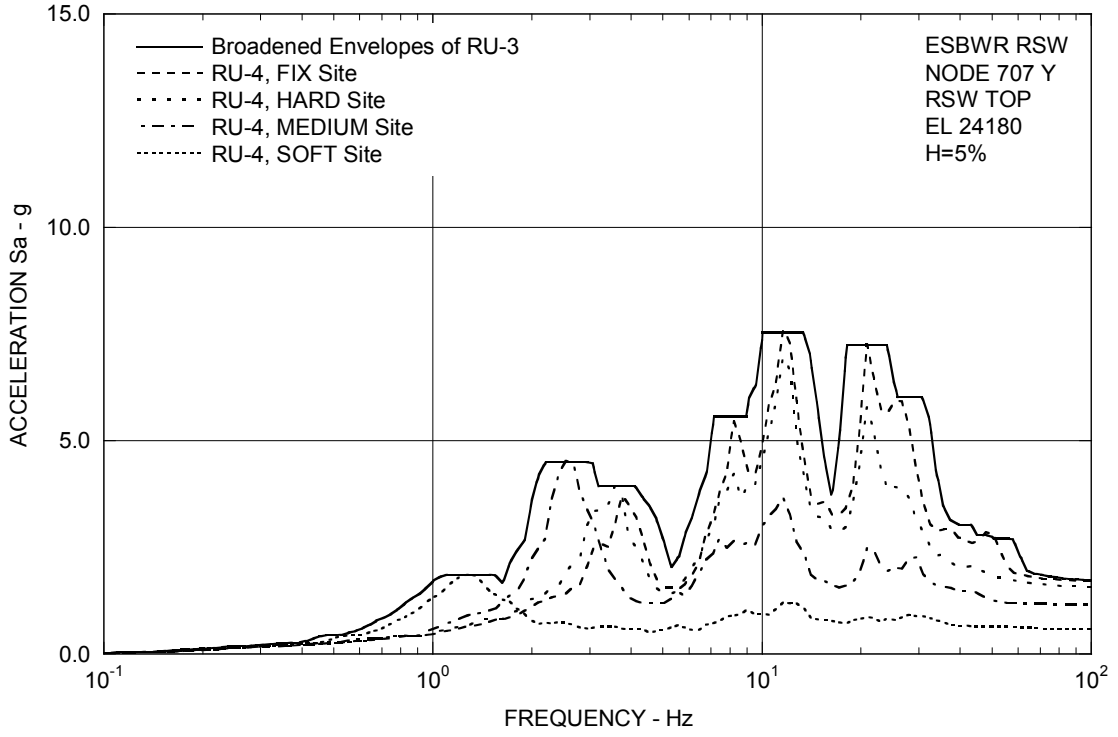

Figure 3A.8.3-2d. FRS (Effect of Updated Design of RSW and VW) – RSW Top Y

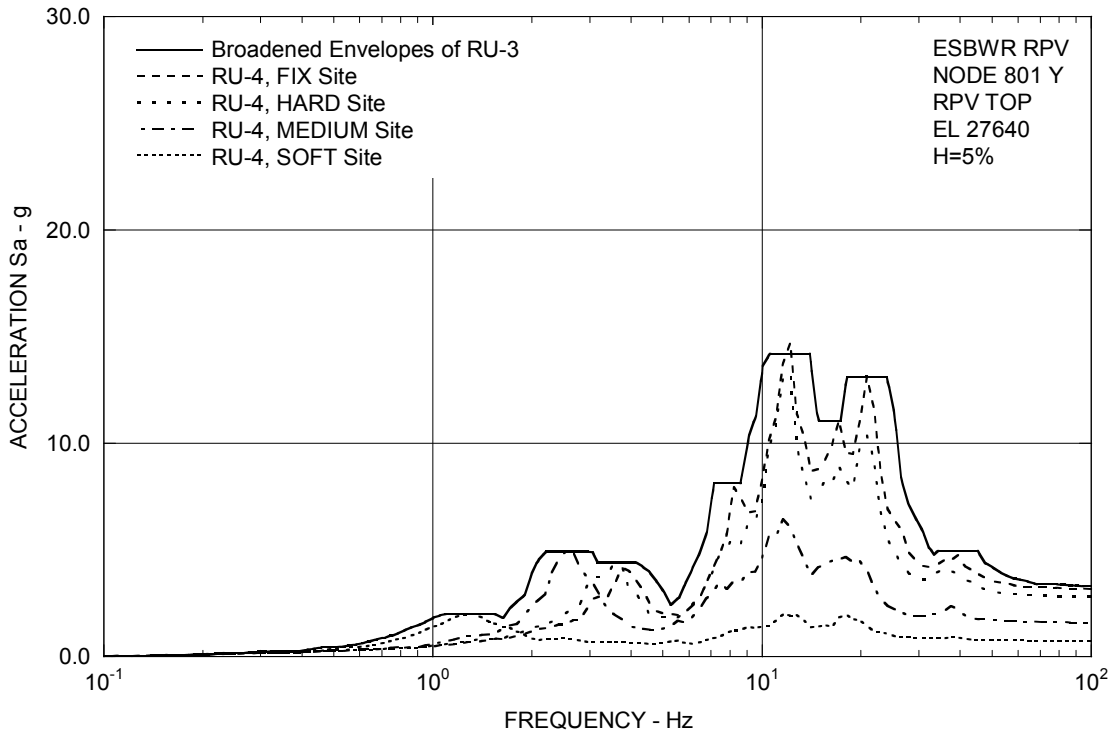

Figure 3A.8.3-2e. FRS (Effect of Updated Design of RSW and VW) – RPV Top Y

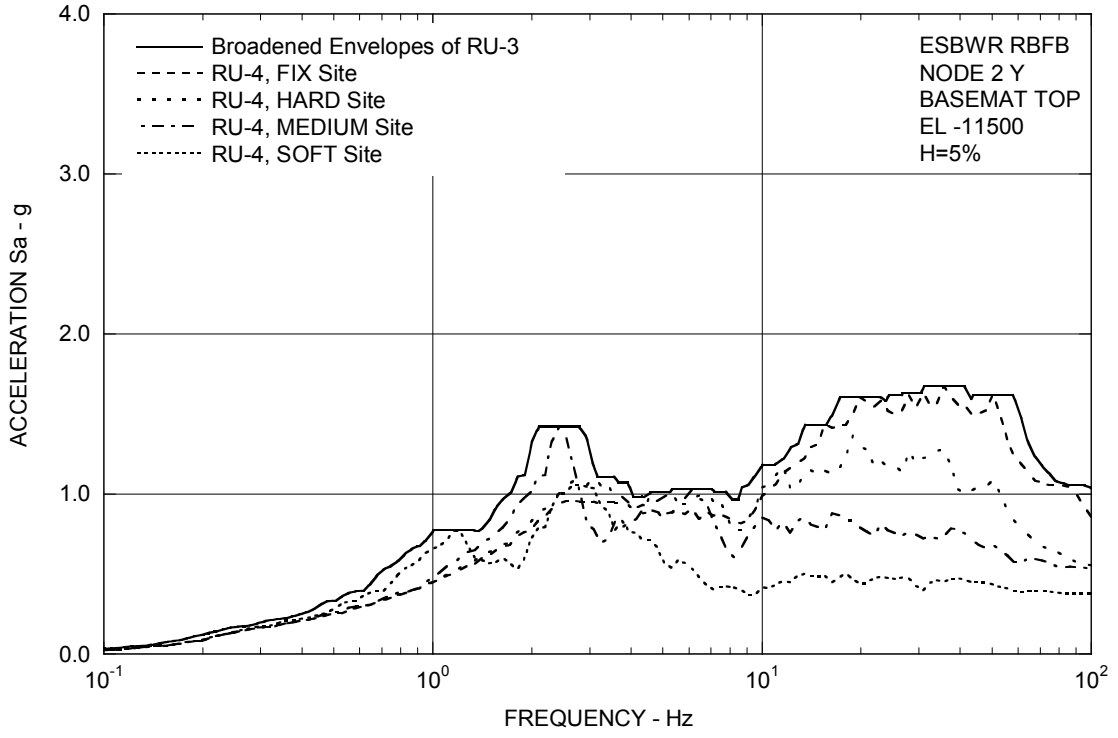

Figure 3A.8.3-2f. FRS (Effect of Updated Design of RSW and VW) – RBFB Basemat Y

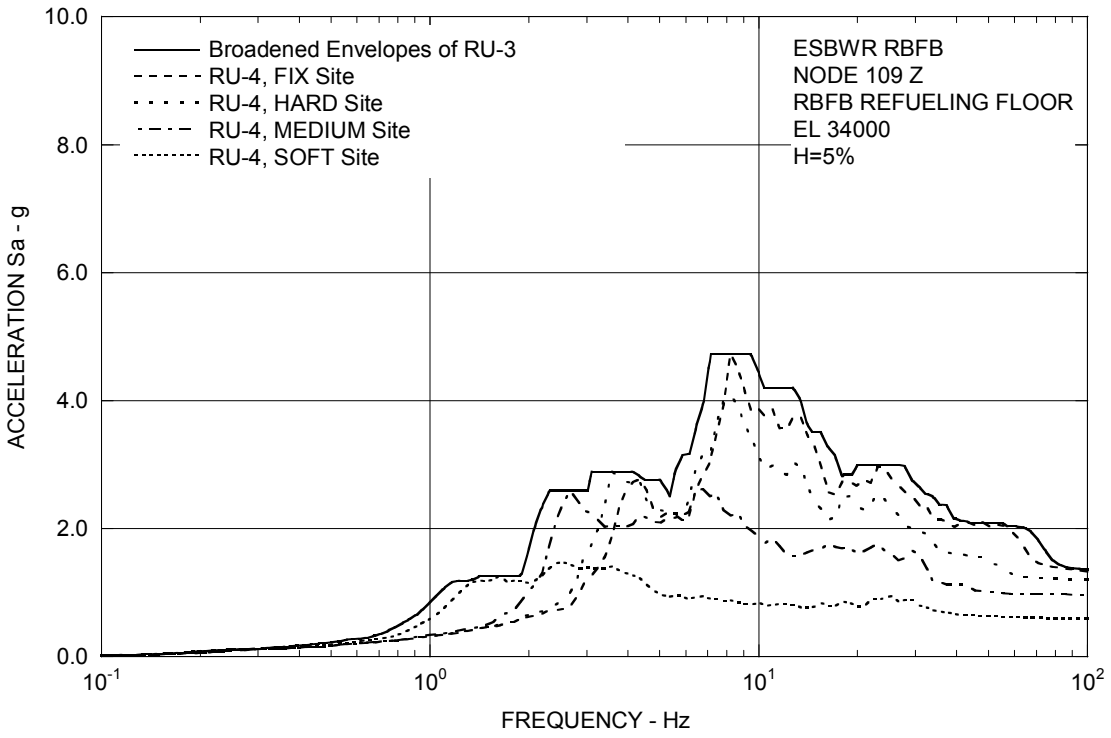

Figure 3A.8.3-3a. FRS (Effect of Updated Design of RSW and VW) – RBFB Refueling Floor Z

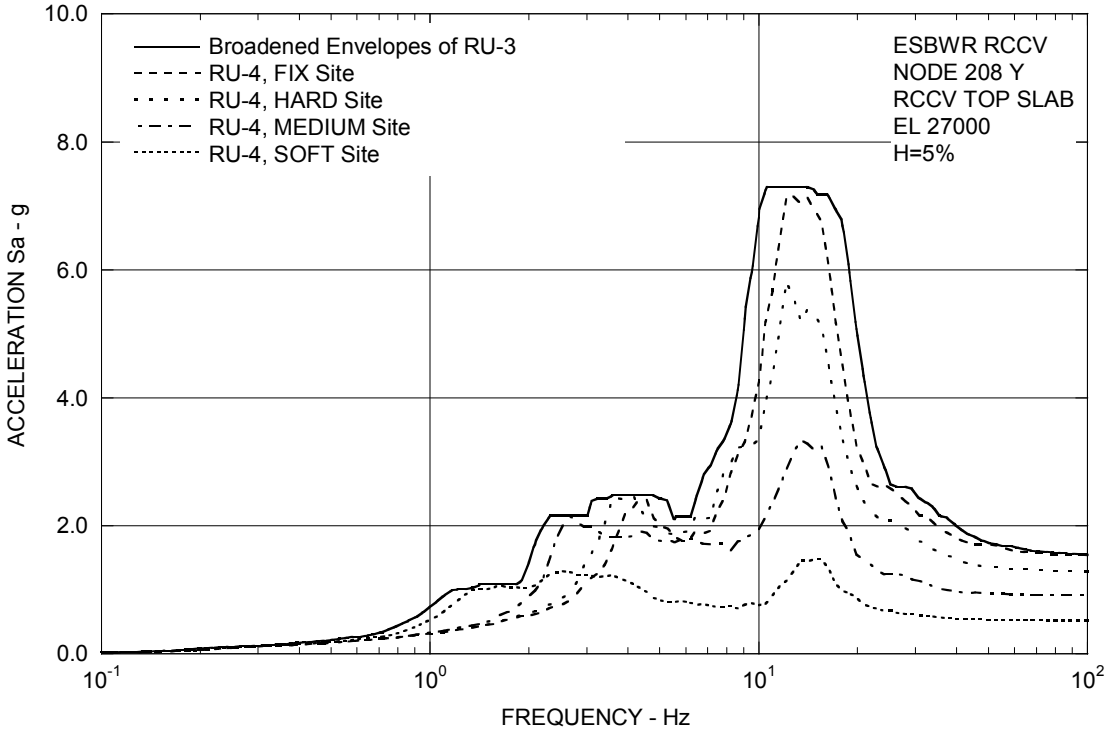

Figure 3A.8.3-3b. FRS (Effect of Updated Design of RSW and VW) – RCCV Top Slab Z

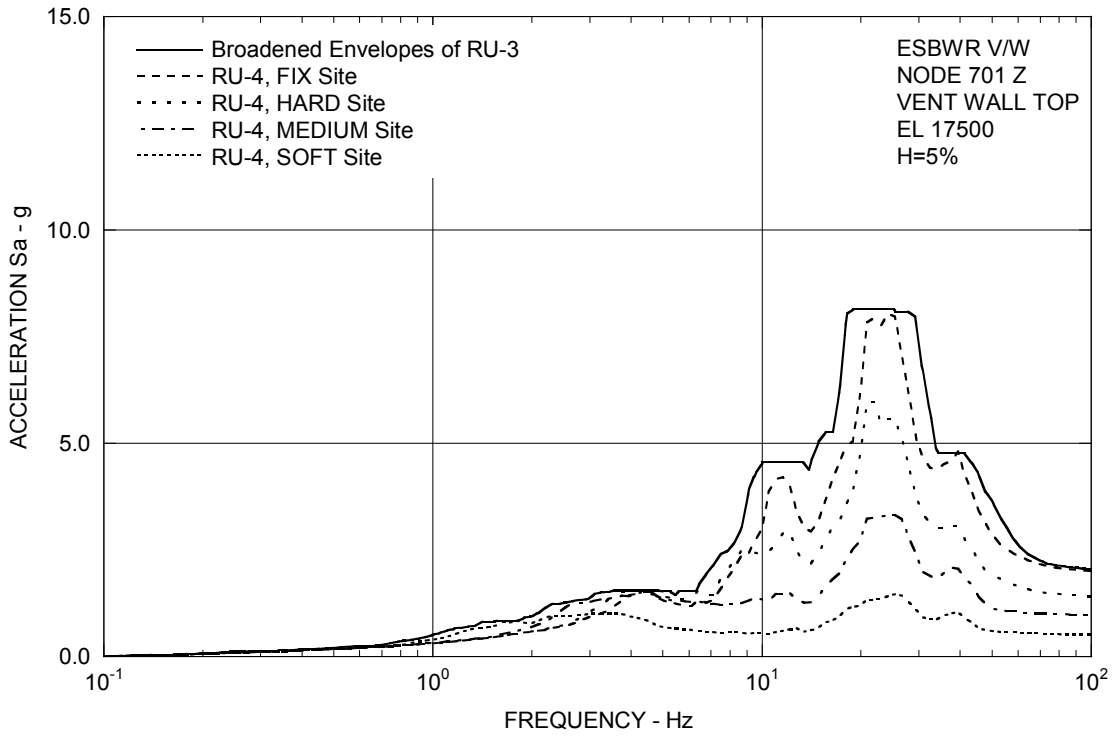

Figure 3A.8.3-3c. FRS (Effect of Updated Design of RSW and VW) – Vent Wall Top Z

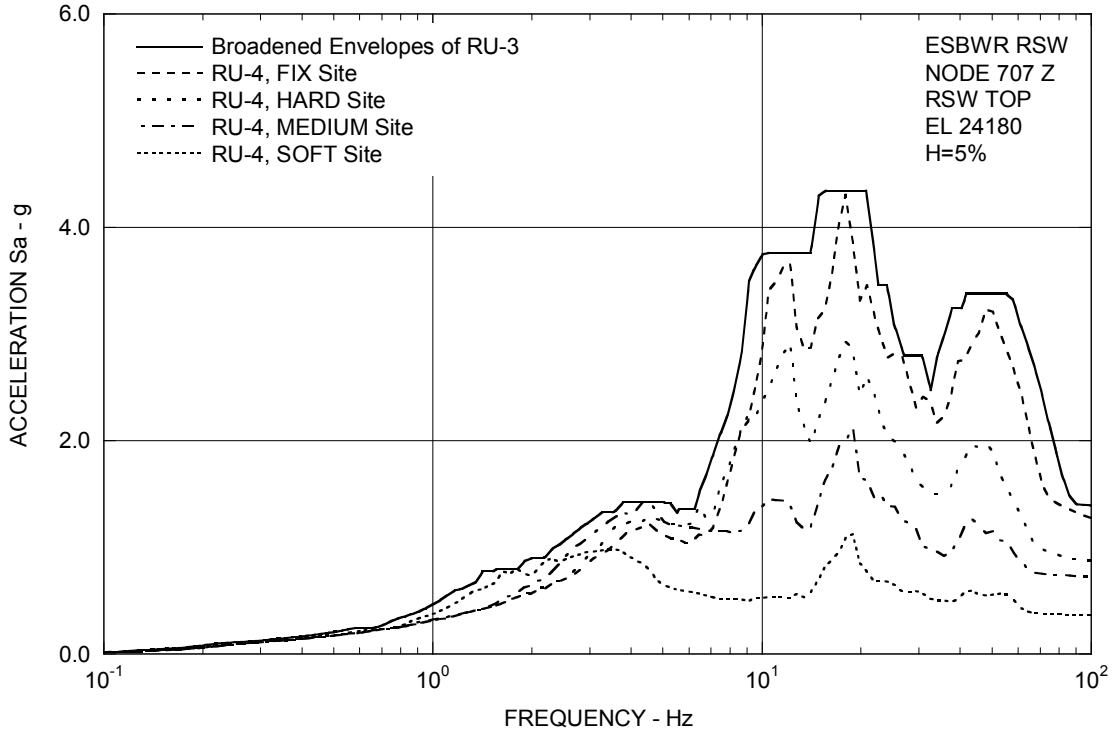

Figure 3A.8.3-3d. FRS (Effect of Updated Design of RSW and VW) – RSW Top Z

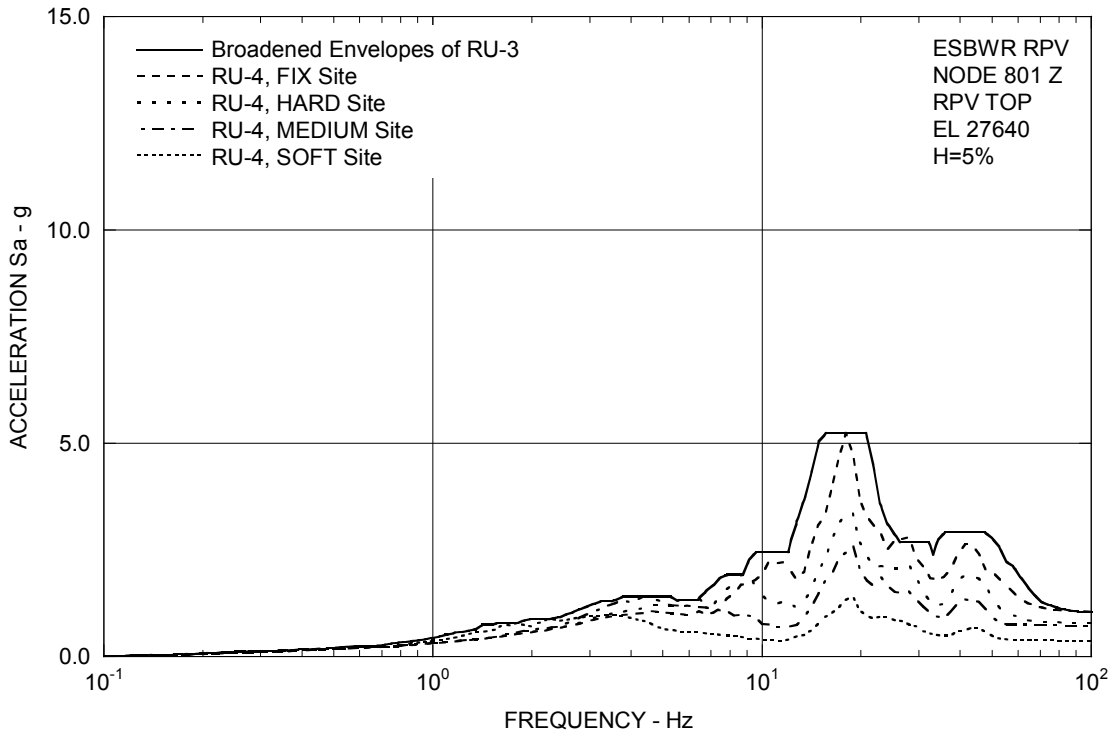

Figure 3A.8.3-3e. FRS (Effect of Updated Design of RSW and VW) – RPV Top Z

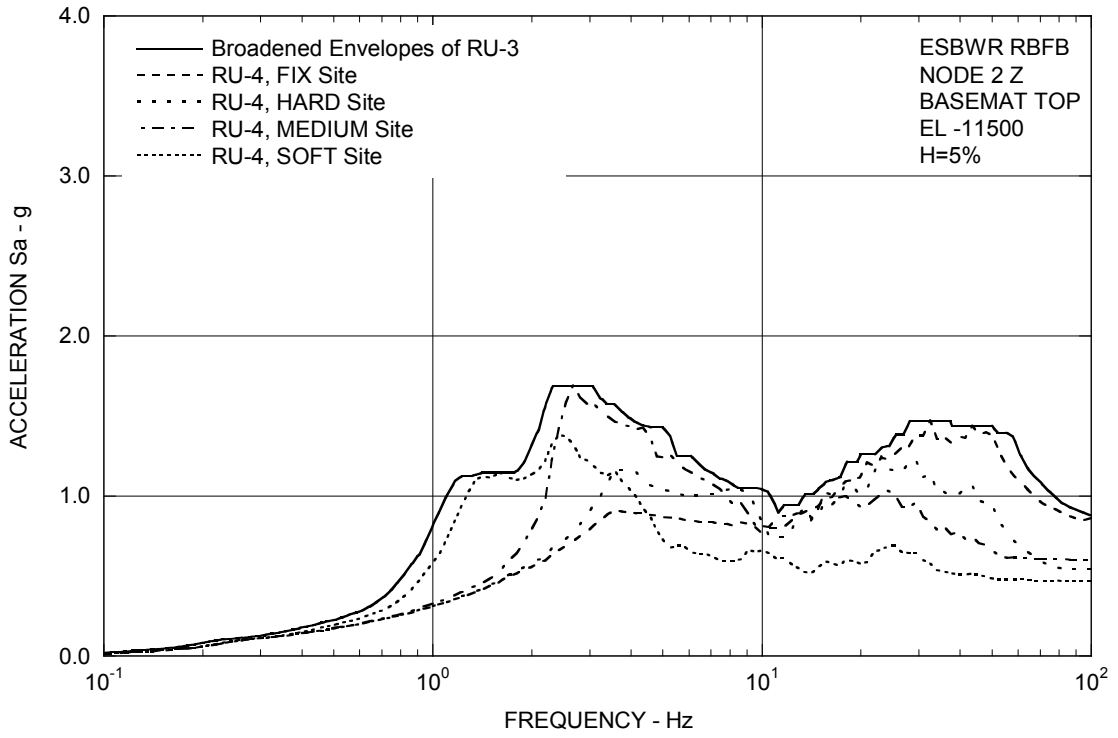

Figure 3A.8.3-3f. FRS (Effect of Updated Design of RSW and VW) – RBFB Basemat Z

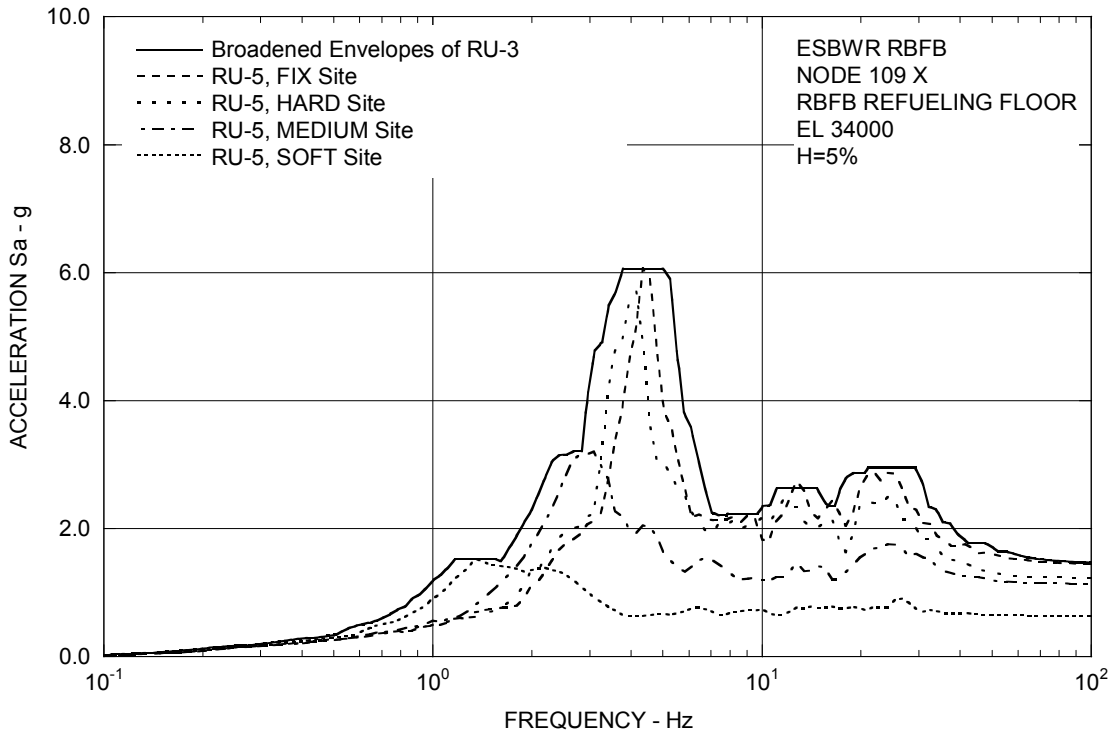

Figure 3A.8.4-1a. FRS (Effect of In-fill Concrete Stiffness of VW and DF) – RBFB Refueling Floor X

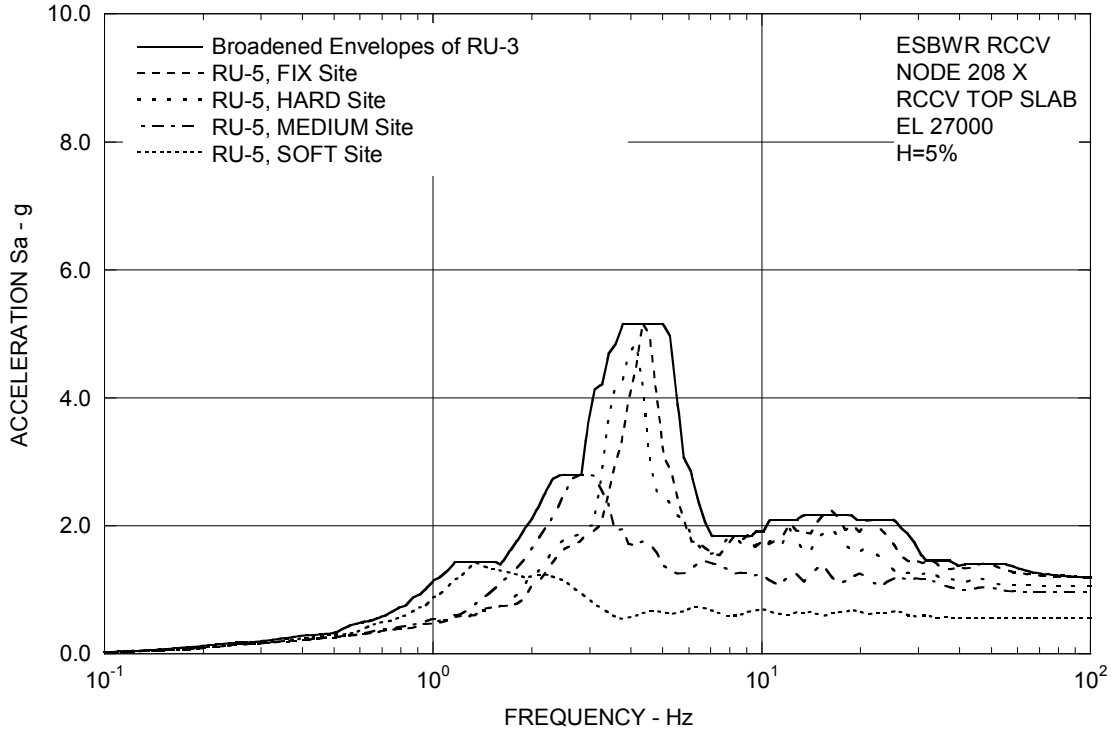

Figure 3A.8.4-1b. FRS (Effect of In-fill Concrete Stiffness of VW and DF) – RCCV Top Slab X

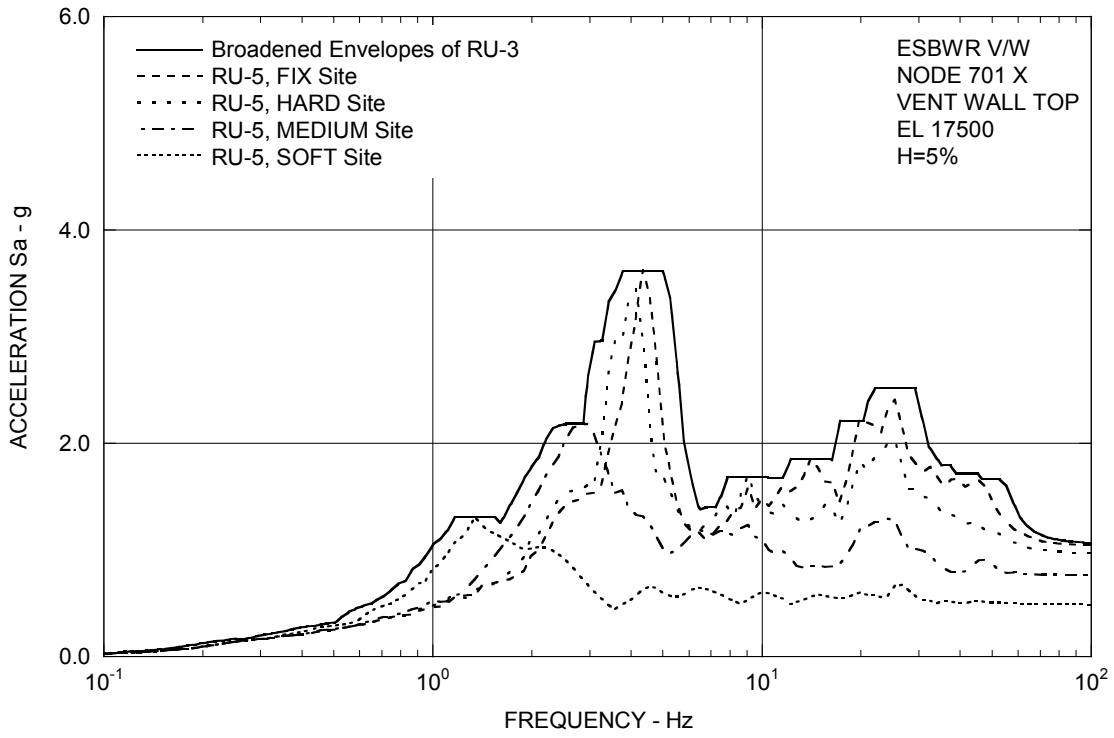

Figure 3A.8.4-1c. FRS (Effect of In-fill Concrete Stiffness of VW and DF) – Vent Wall Top X

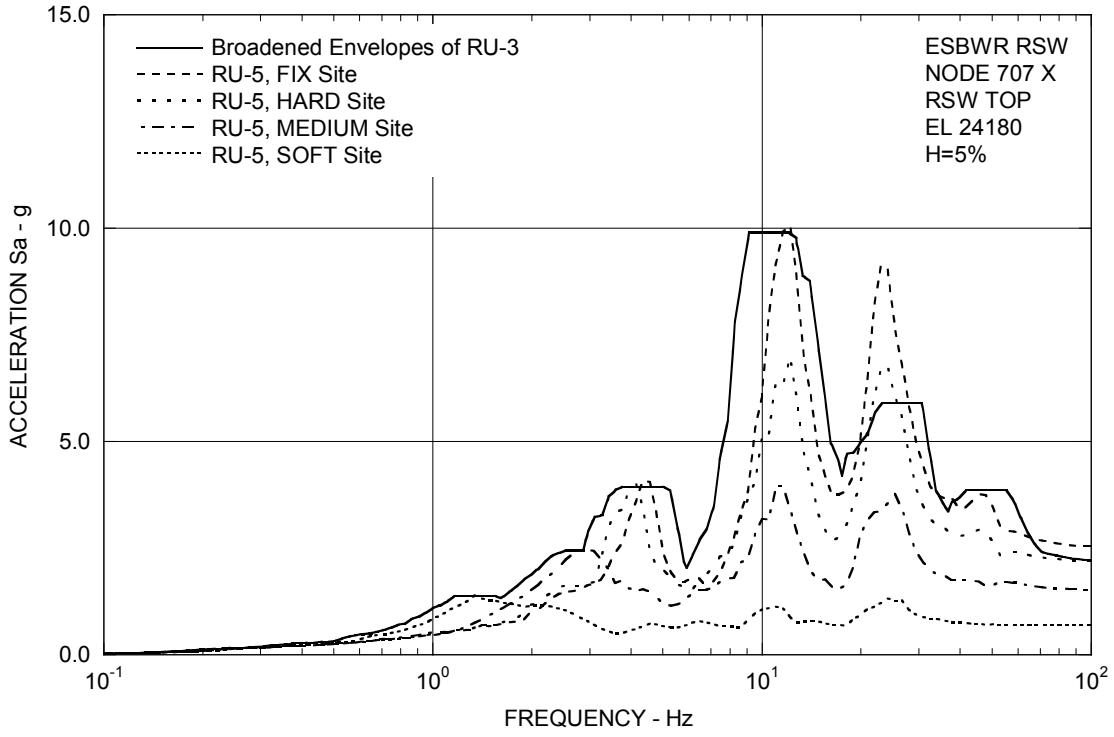

Figure 3A.8.4-1d. FRS (Effect of In-fill Concrete Stiffness of VW and DF) – RSW Top X

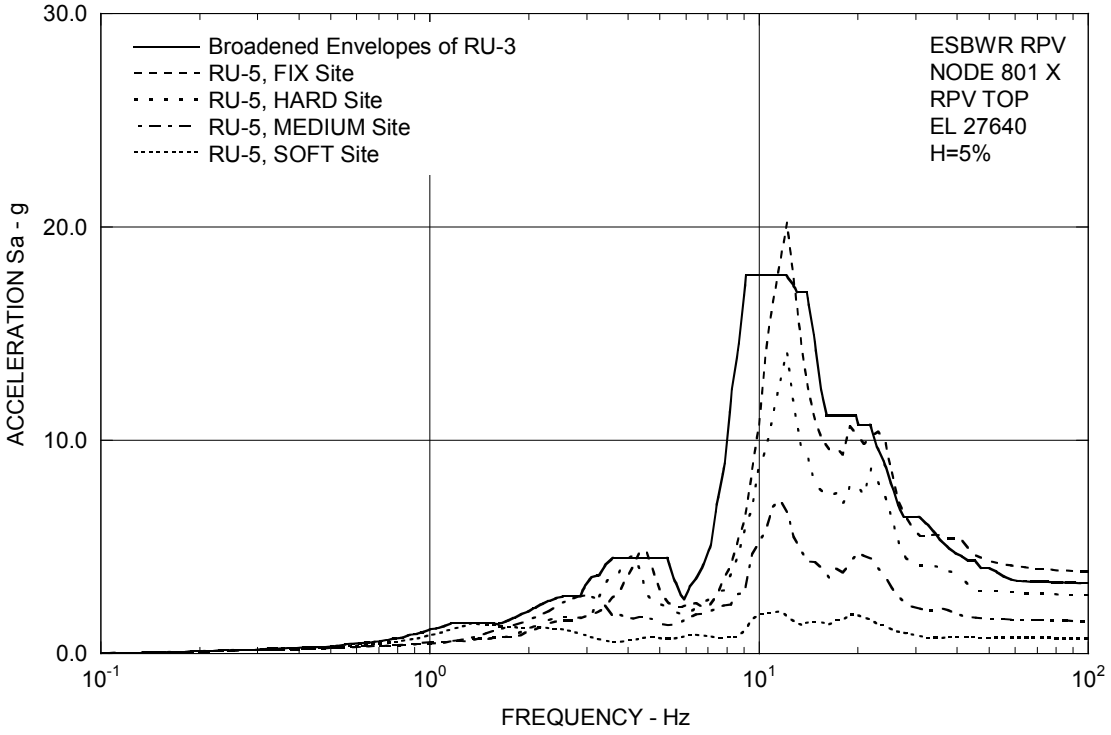

Figure 3A.8.4-1e. FRS (Effect of In-fill Concrete Stiffness of VW and DF) – RPV Top X

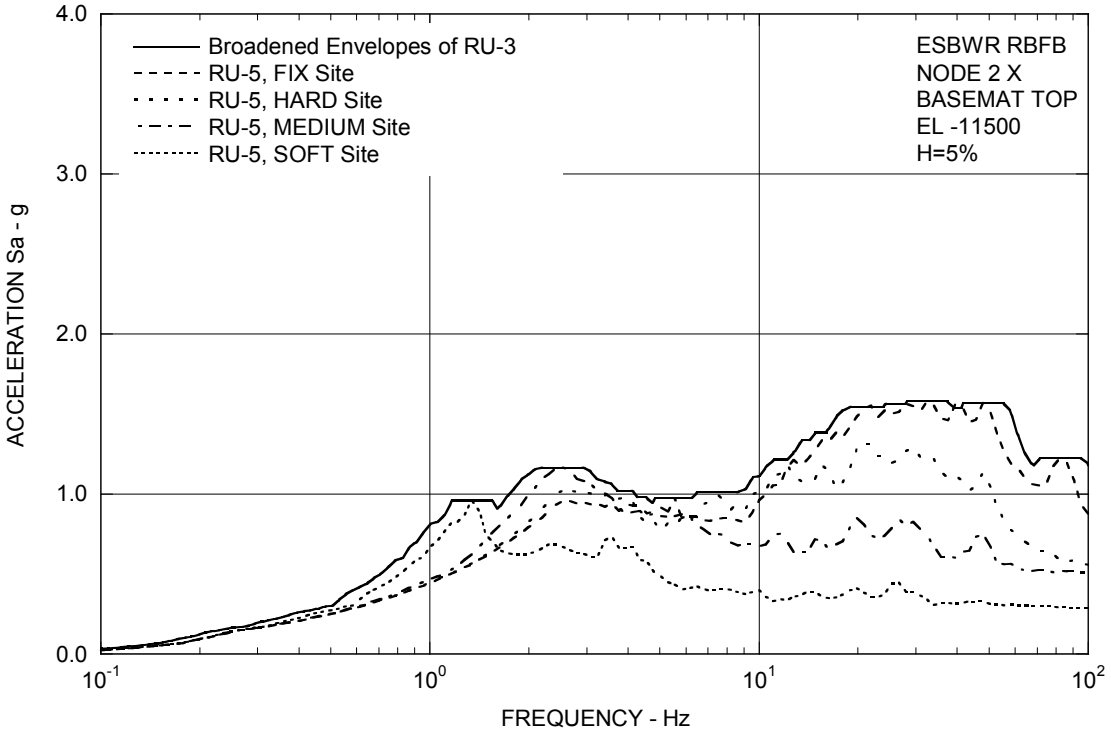

Figure 3A.8.4-1f. FRS (Effect of In-fill Concrete Stiffness of VW and DF) – RBFB Basemat X

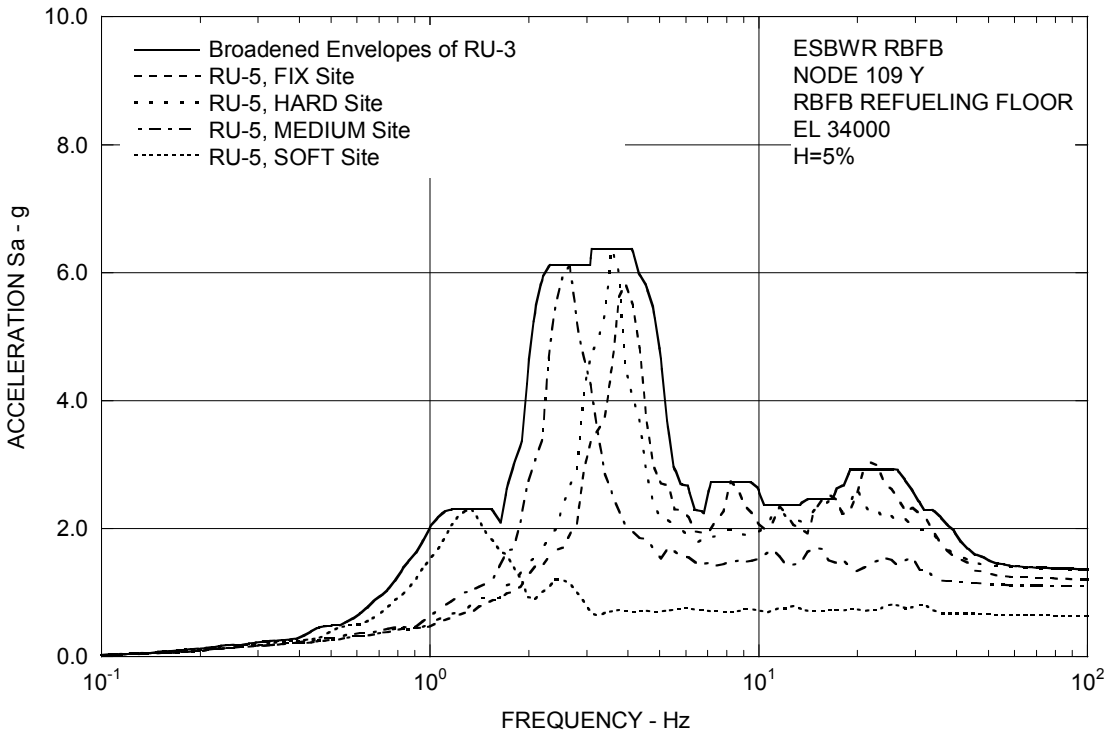

Figure 3A.8.4-2a. FRS (Effect of In-fill Concrete Stiffness of VW and DF) – RBFB Refueling Floor Y

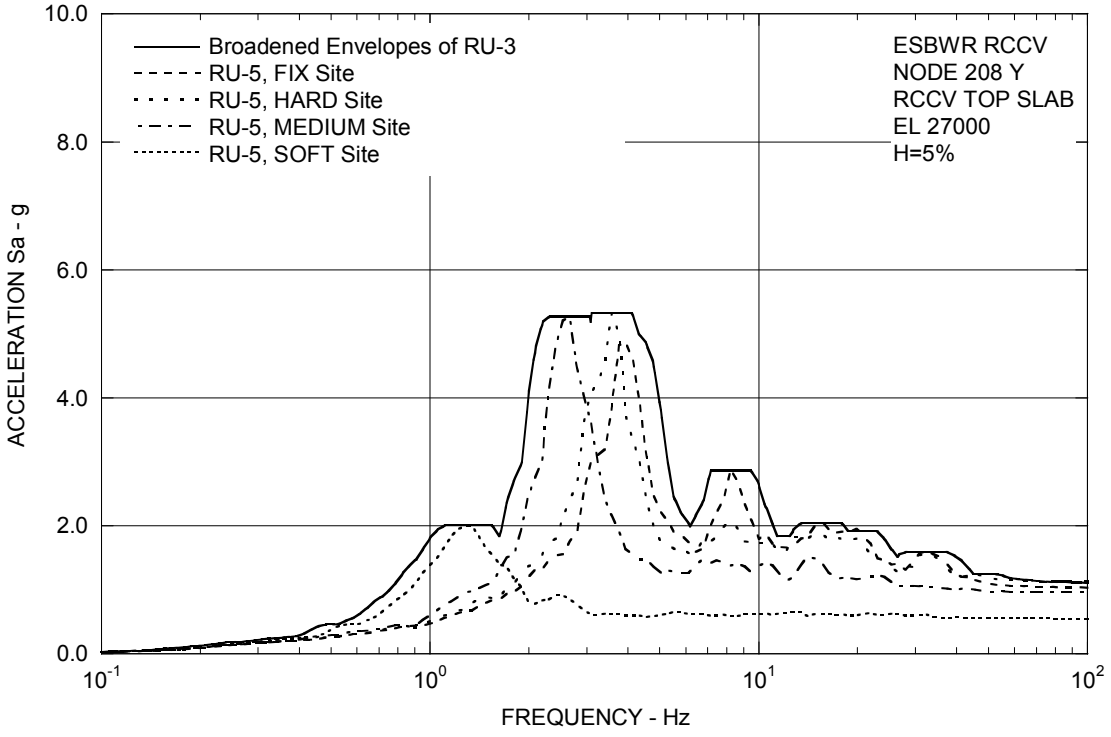

Figure 3A.8.4-2b. FRS (Effect of In-fill Concrete Stiffness of VW and DF) – RCCV Top Slab Y

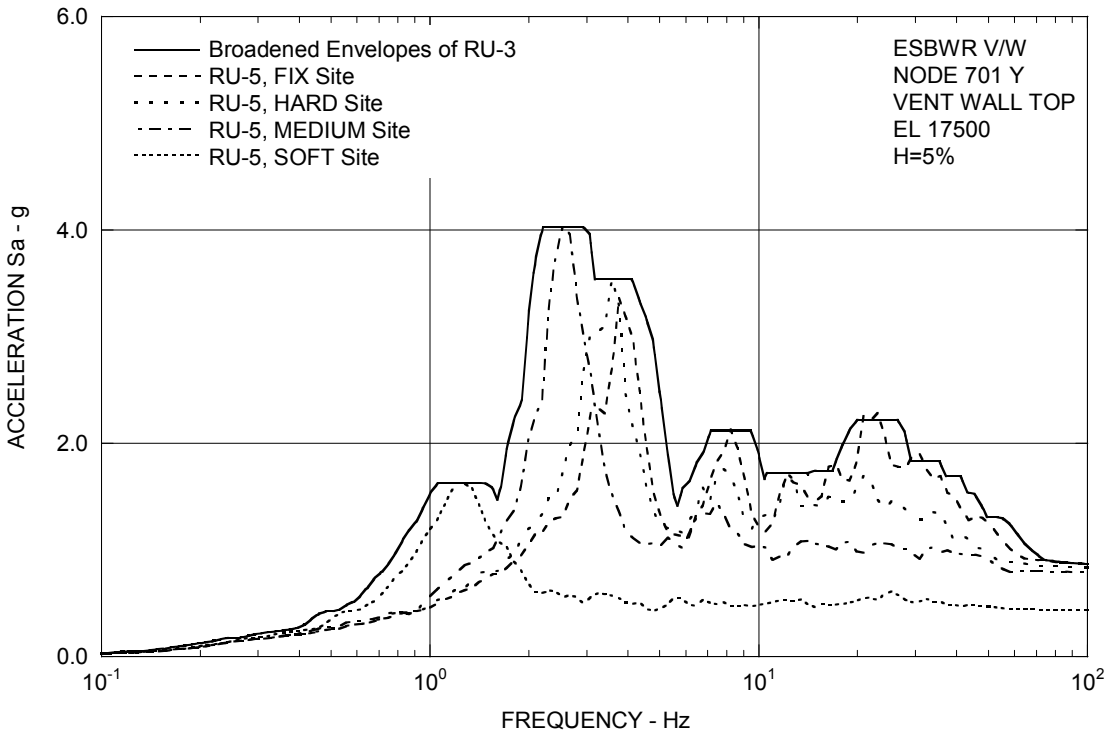

Figure 3A.8.4-2c. FRS (Effect of In-fill Concrete Stiffness of VW and DF) – Vent Wall Top Y

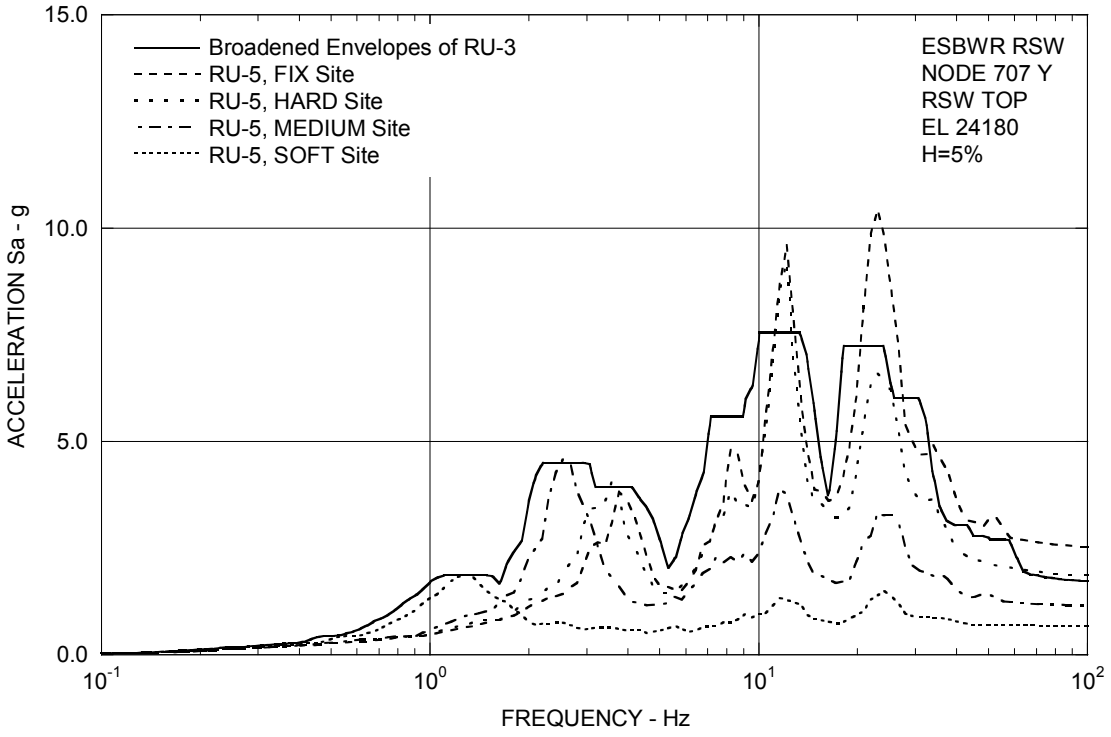

Figure 3A.8.4-2d. FRS (Effect of In-fill Concrete Stiffness of VW and DF) – RSW Top Y

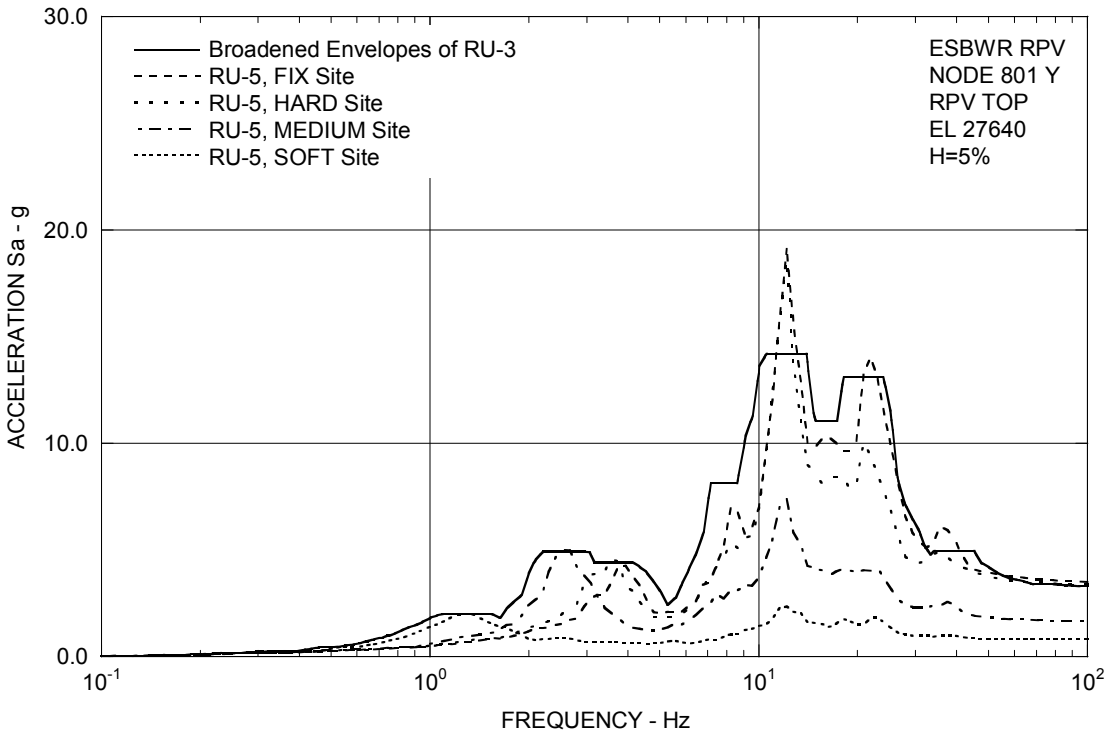

Figure 3A.8.4-2e. FRS (Effect of In-fill Concrete Stiffness of VW and DF) – RPV Top Y

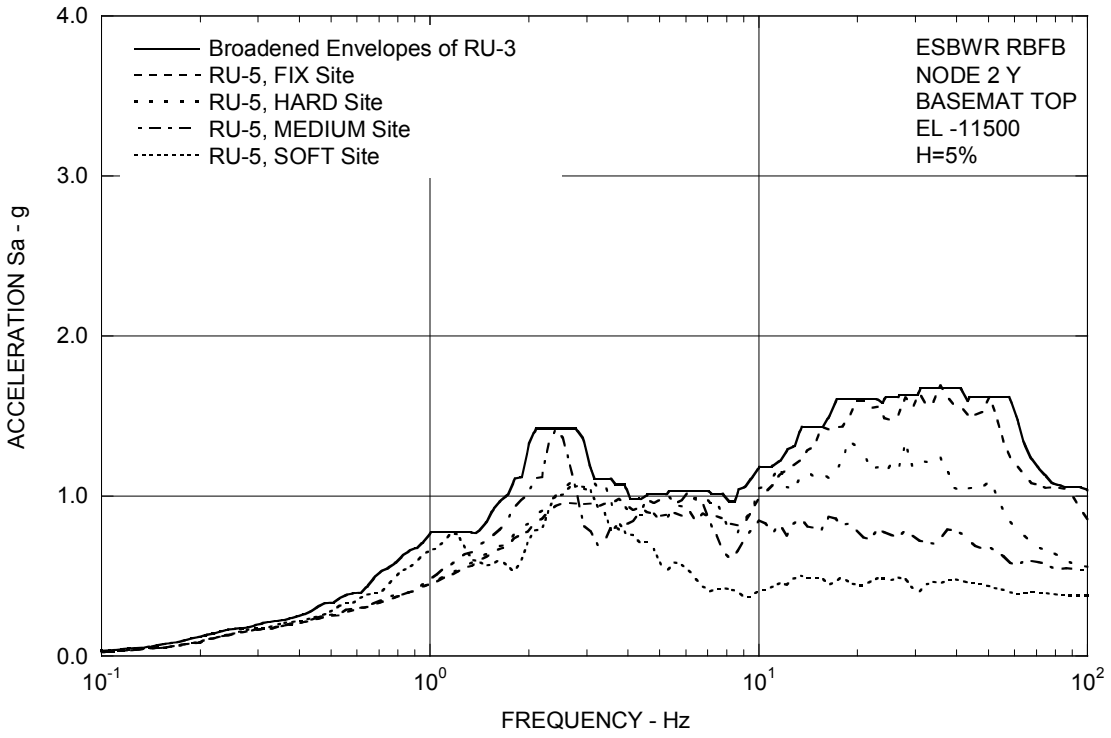

Figure 3A.8.4-2f. FRS (Effect of In-fill Concrete Stiffness of VW and DF) – RBFB Basemat Y

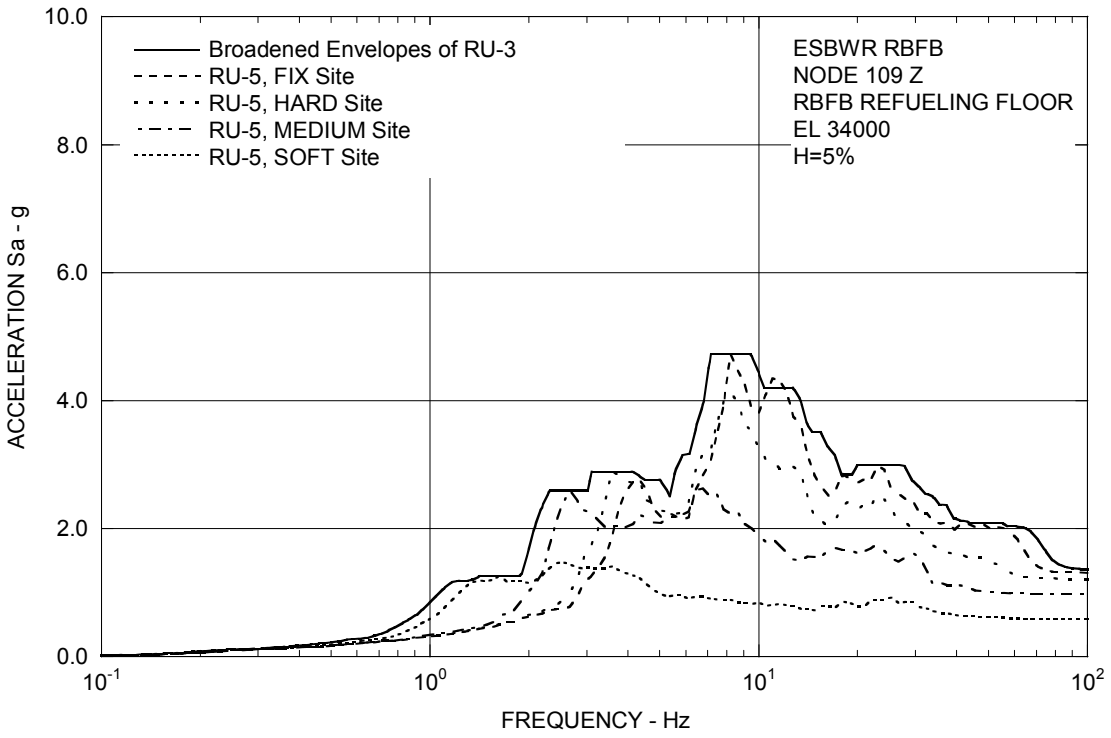

Figure 3A.8.4-3a. FRS (Effect of In-fill Concrete Stiffness of VW and DF) – RBFB Refueling Floor Z

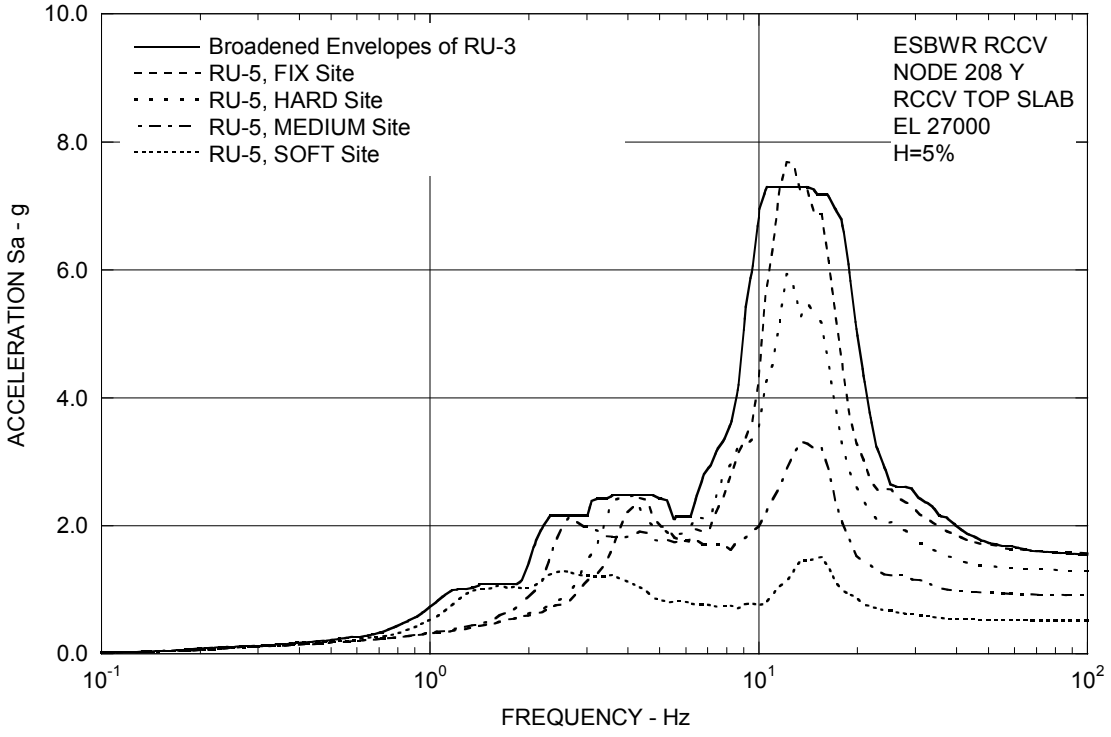

Figure 3A.8.4-3b. FRS (Effect of In-fill Concrete Stiffness of VW and DF) – RCCV Top Slab Z

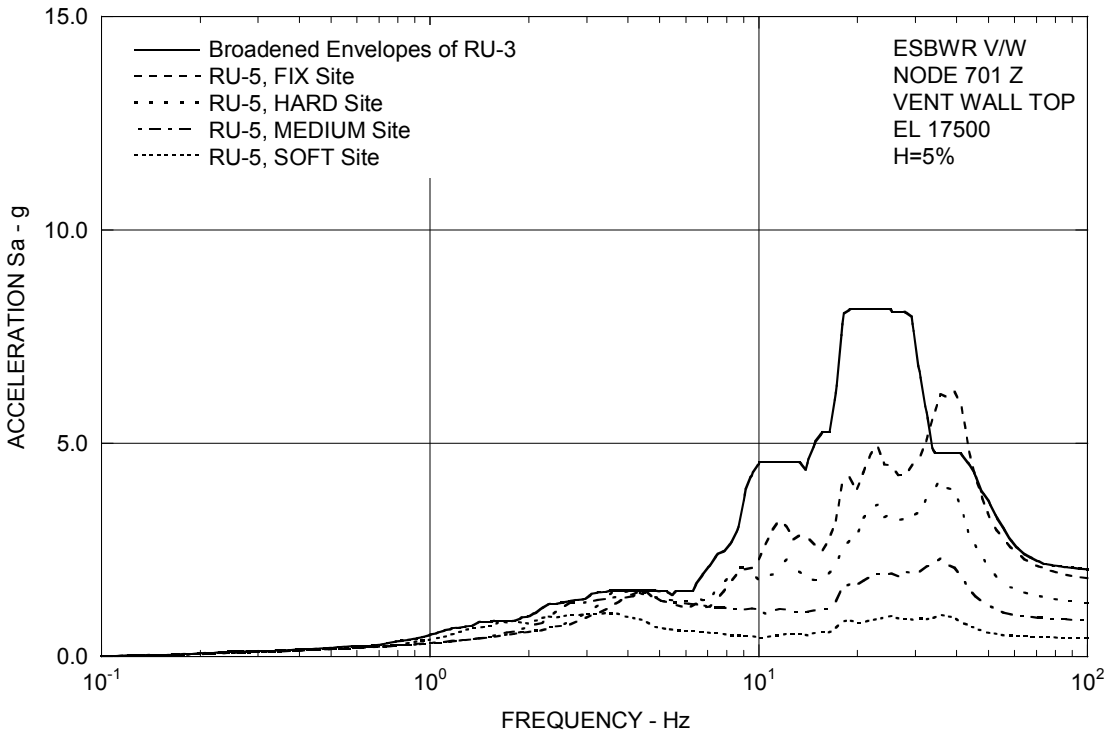

Figure 3A.8.4-3c. FRS (Effect of In-fill Concrete Stiffness of VW and DF) – Vent Wall Top Z

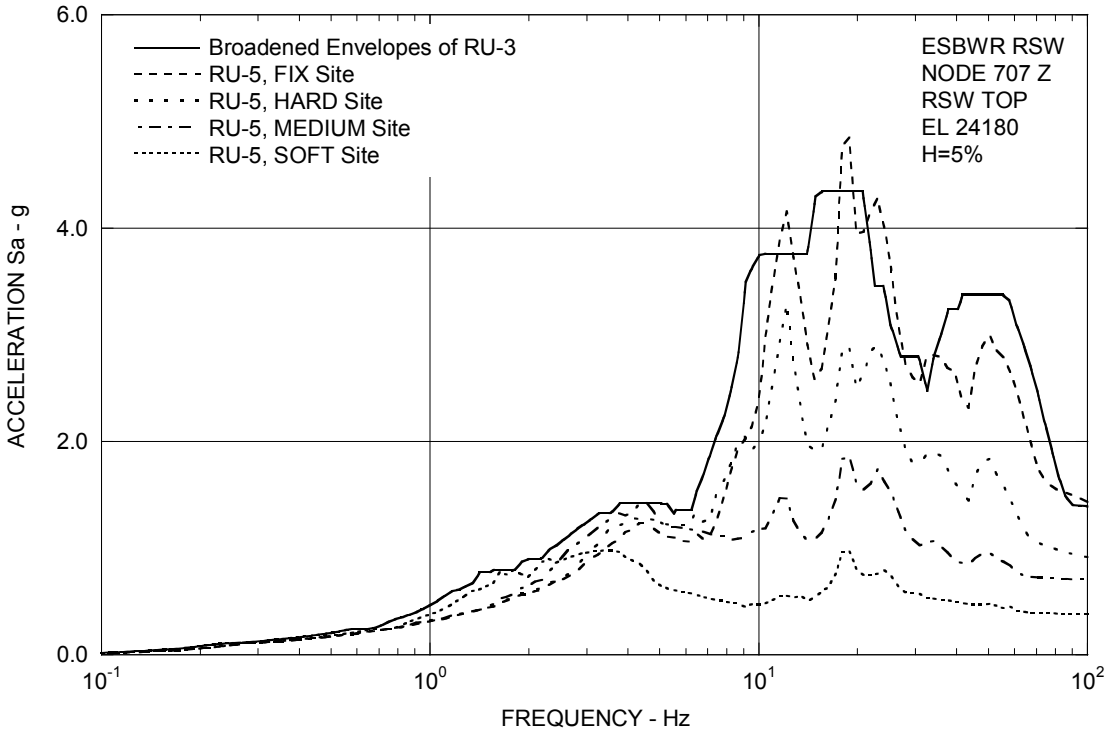

Figure 3A.8.4-3d. FRS (Effect of In-fill Concrete Stiffness of VW and DF) – RSW Top Z

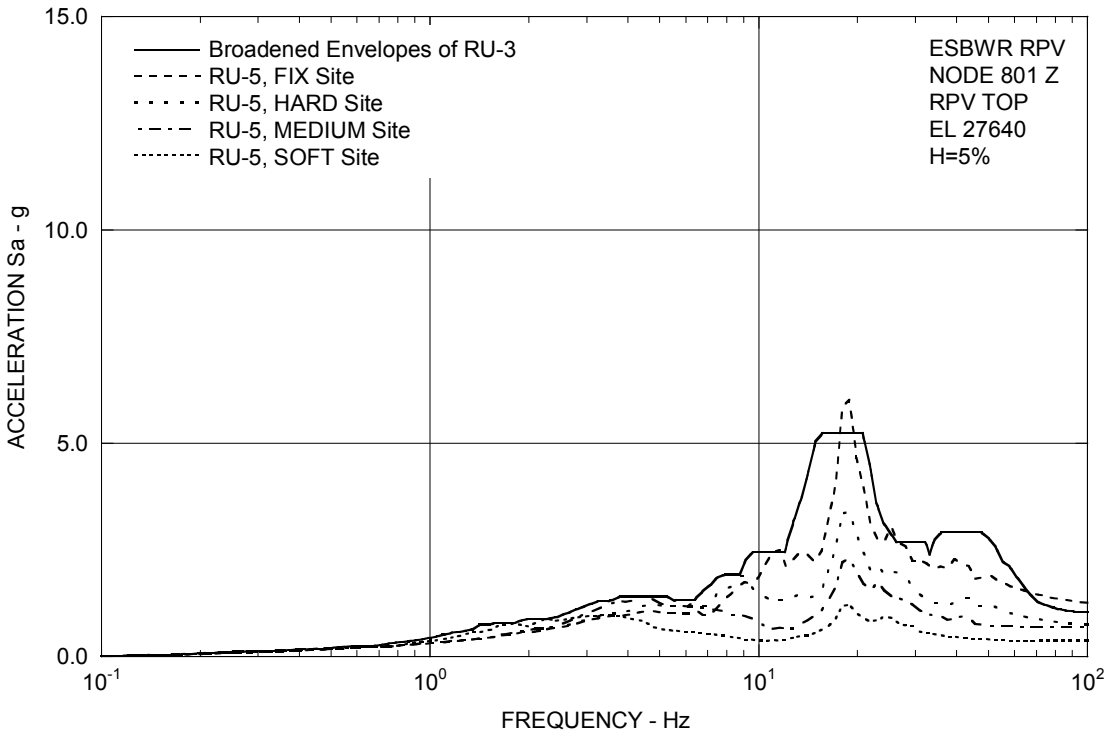

Figure 3A.8.4-3e. FRS (Effect of In-fill Concrete Stiffness of VW and DF) – RPV Top Z

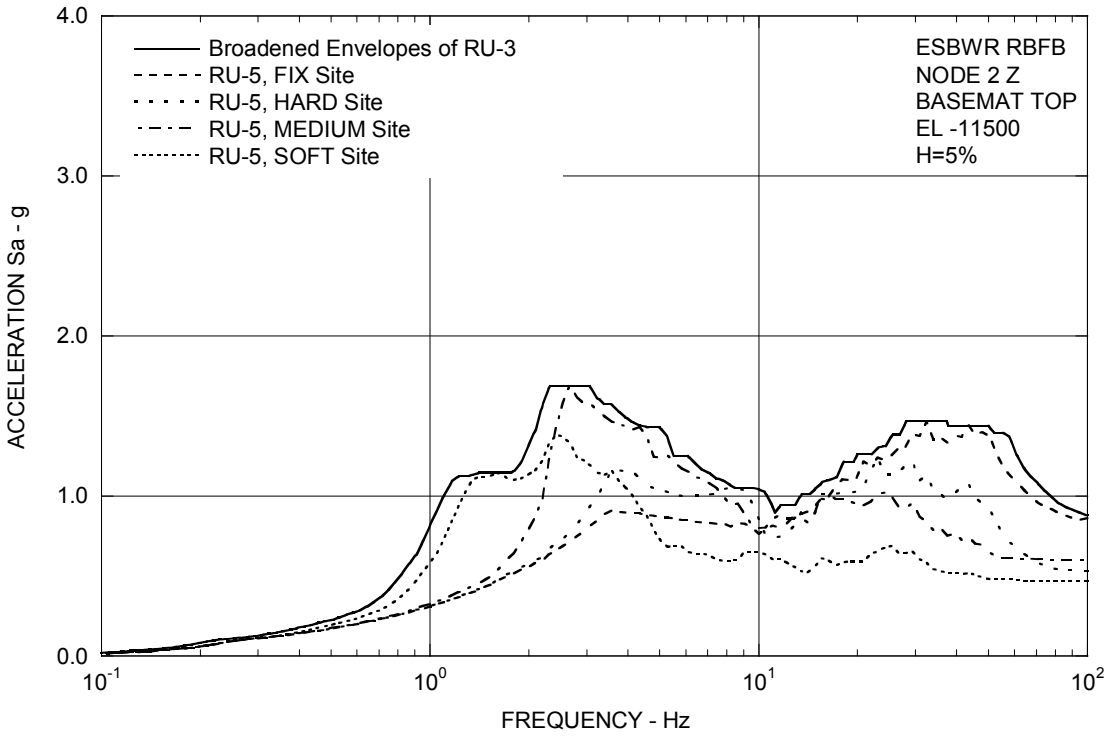

Figure 3A.8.4-3f. FRS (Effect of In-fill Concrete Stiffness of VW and DF) – RBFB Basemat Z

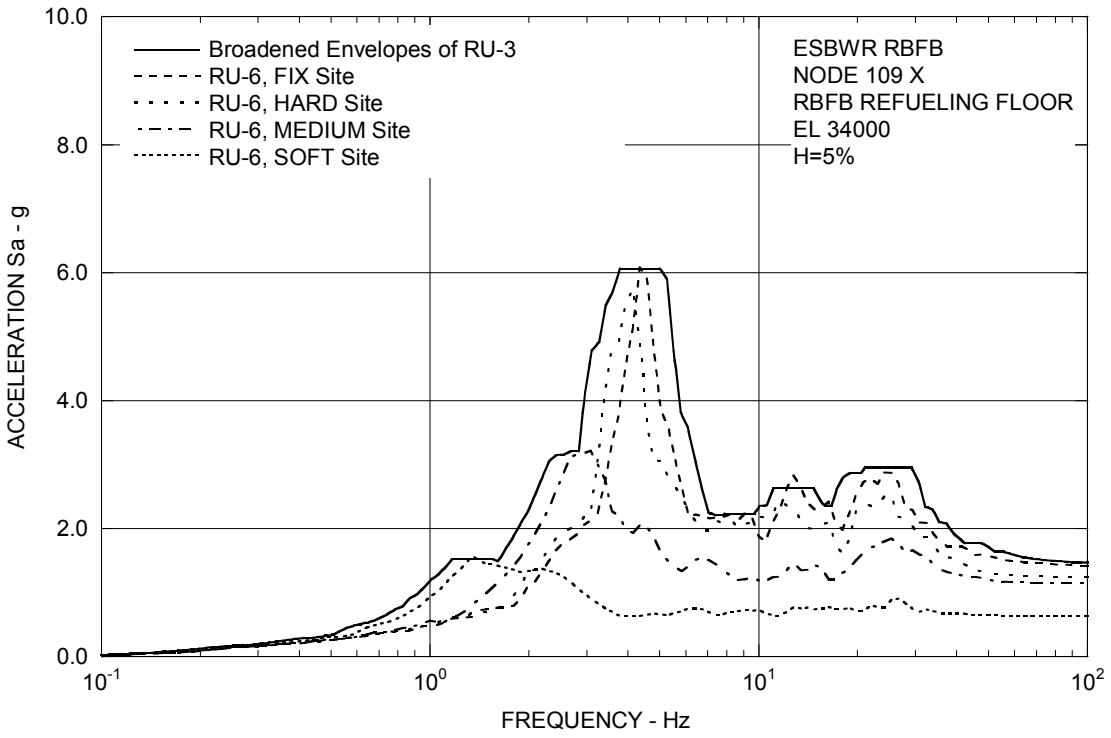

Figure 3A.8.5-1a. FRS (Effect of LOCA Flooding) – RBFB Refueling Floor X

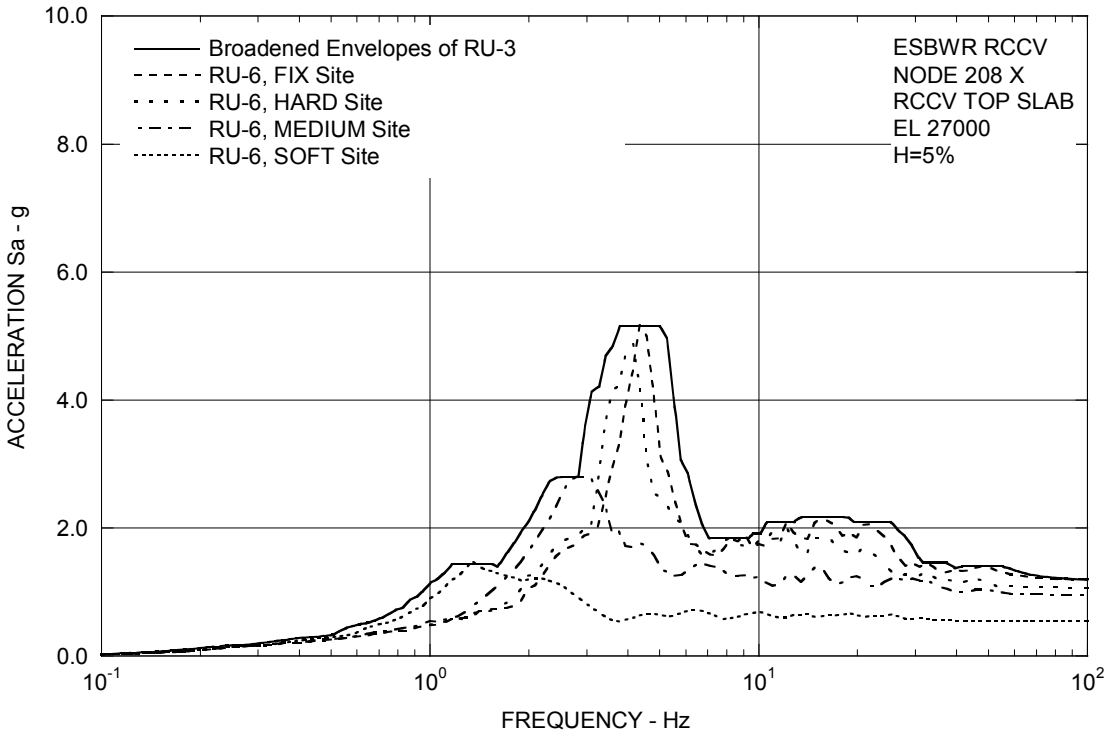

Figure 3A.8.5-1b. FRS (Effect of LOCA Flooding) – RCCV Top Slab X

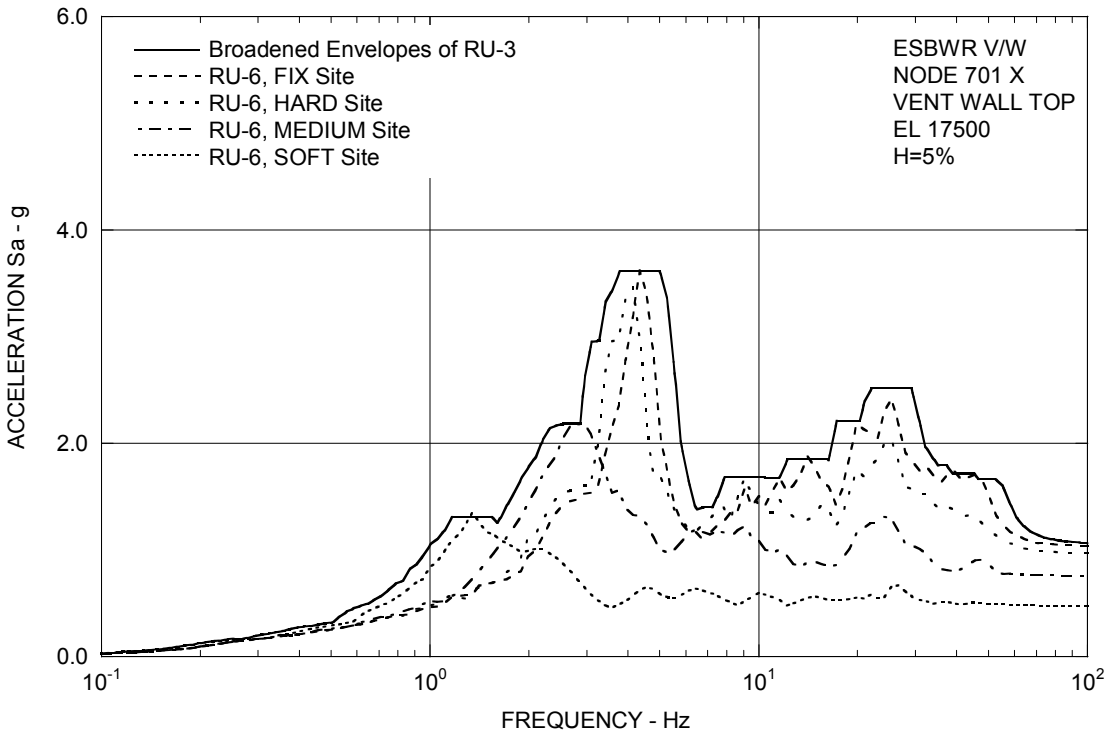

Figure 3A.8.5-1c. FRS (Effect of LOCA Flooding) – Vent Wall Top X

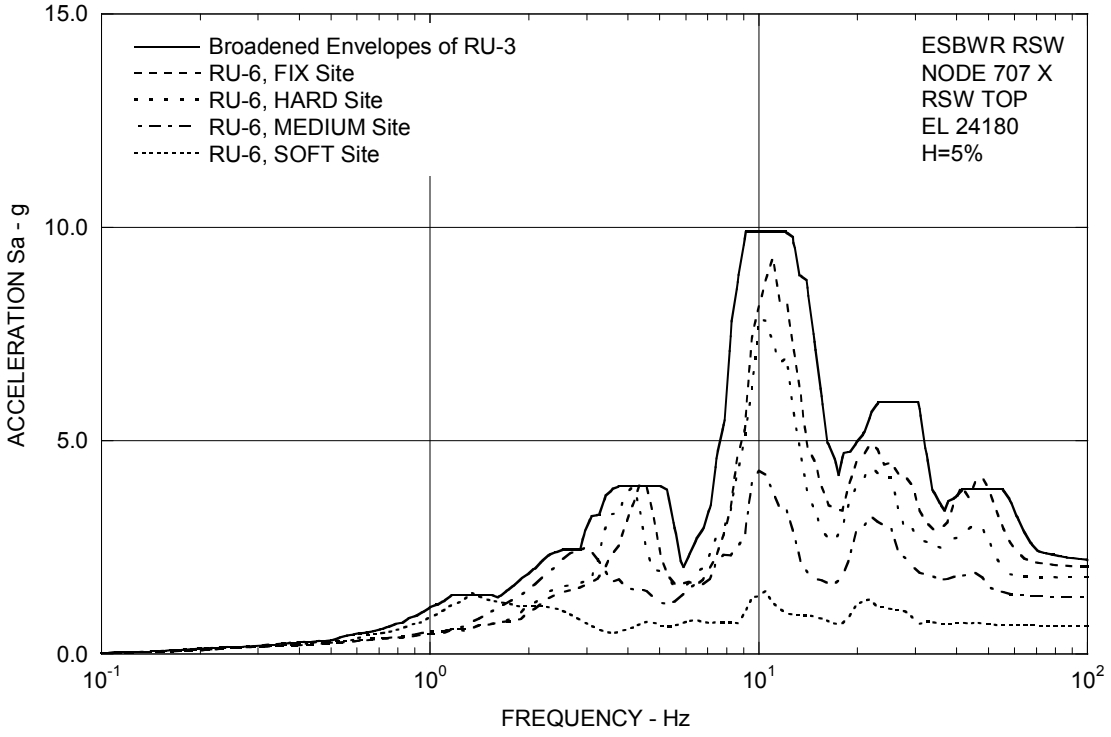

Figure 3A.8.5-1d. FRS (Effect of LOCA Flooding) – RSW Top X

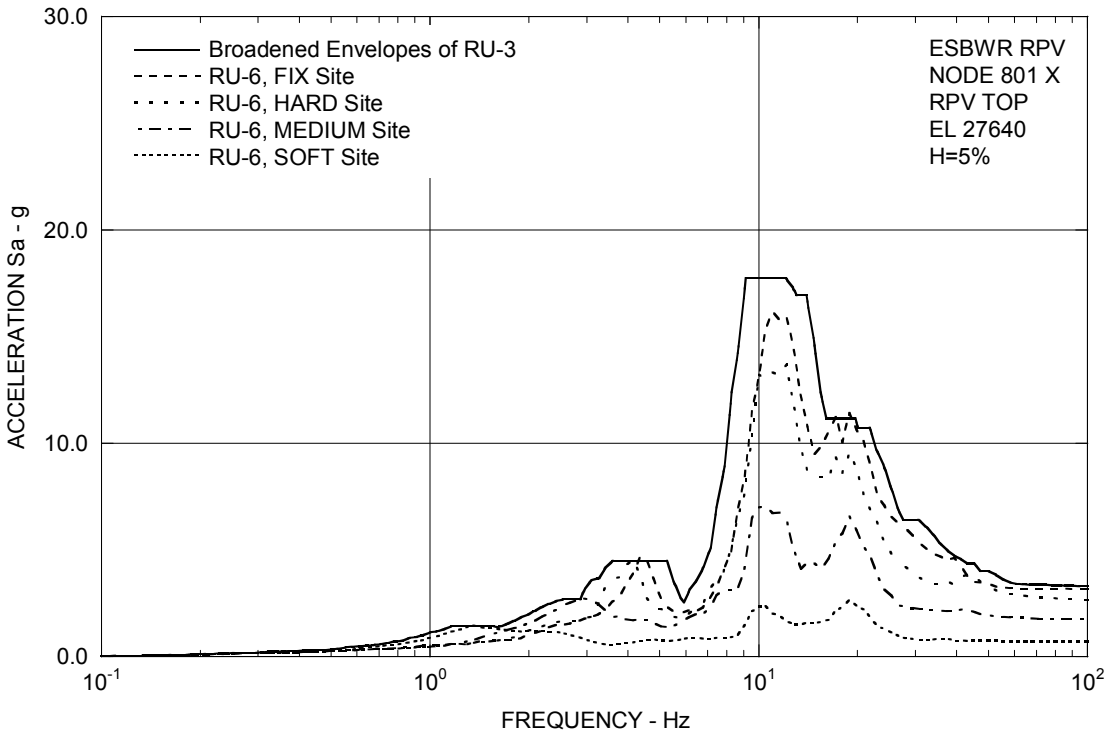

Figure 3A.8.5-1e. FRS (Effect of LOCA Flooding) – RPV Top X

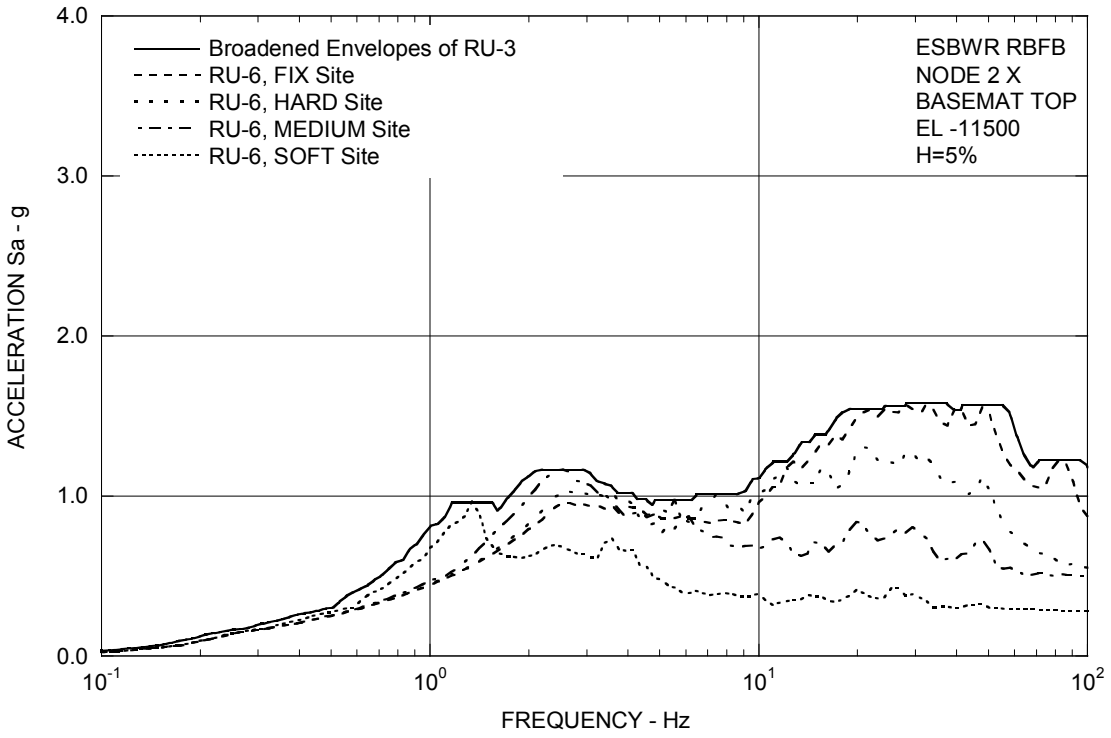

Figure 3A.8.5-1f. FRS (Effect of LOCA Flooding) – RBFB Basemat X

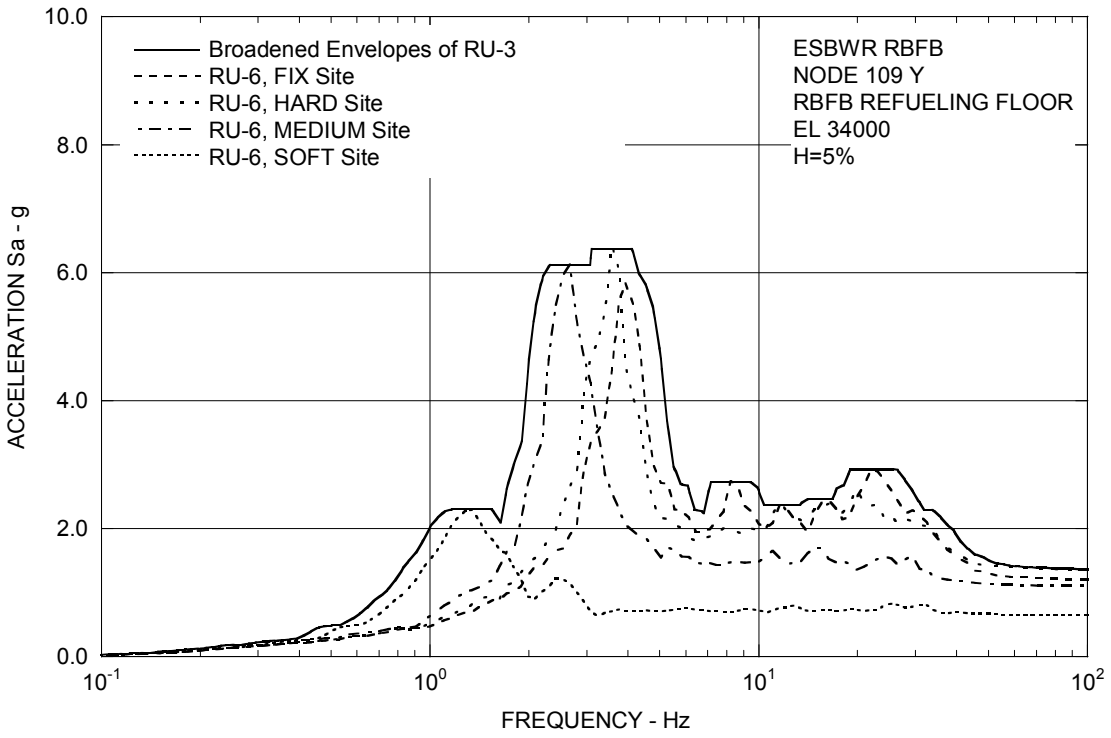

Figure 3A.8.5-2a. FRS (Effect of LOCA Flooding) – RBFB Refueling Floor Y

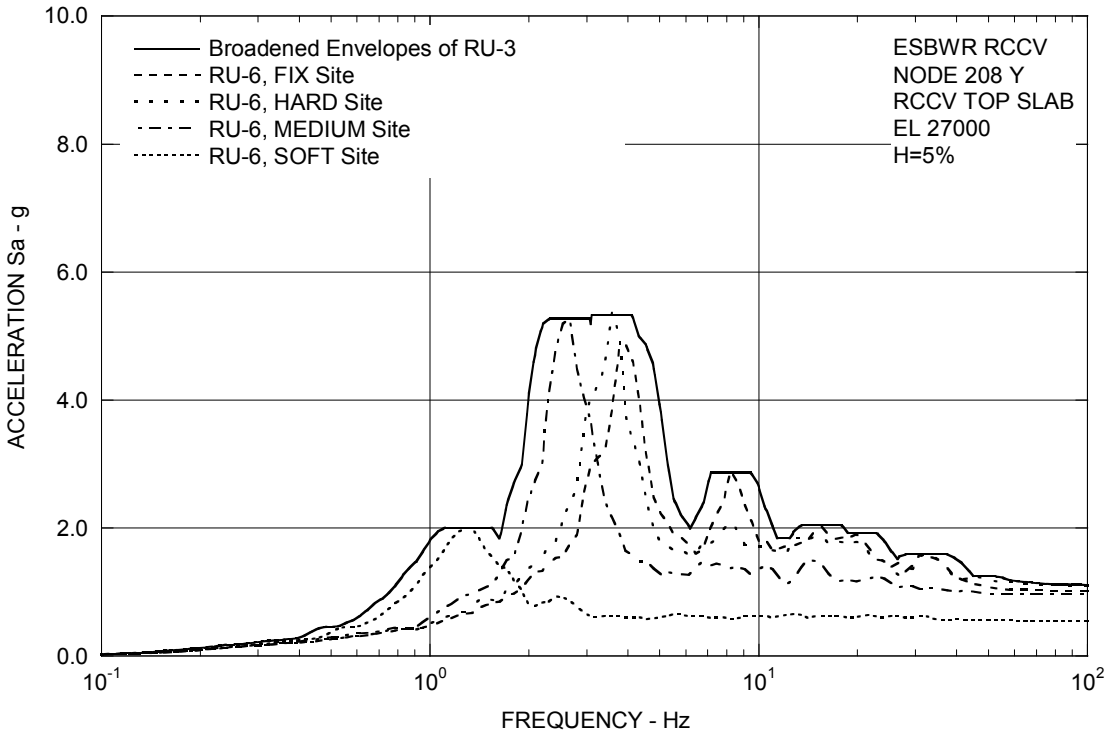

Figure 3A.8.5-2b. FRS (Effect of LOCA Flooding) – RCCV Top Slab Y

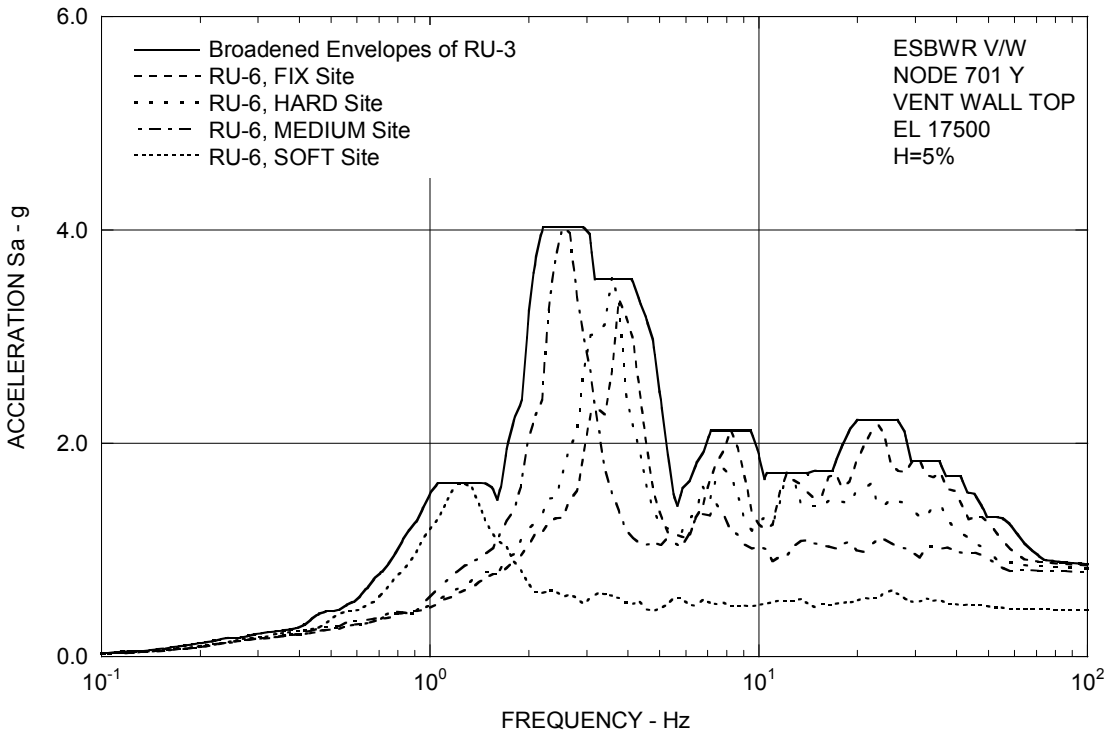

Figure 3A.8.5-2c. FRS (Effect of LOCA Flooding) – Vent Wall Top Y

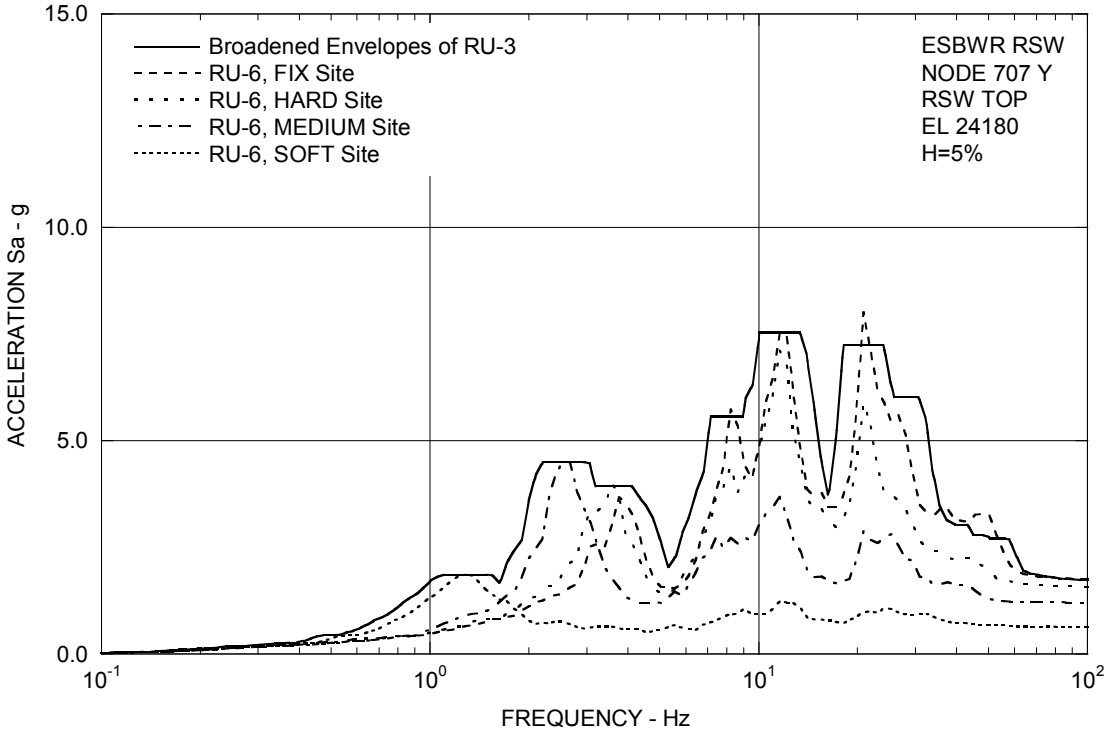

Figure 3A.8.5-2d. FRS (Effect of LOCA Flooding) – RSW Top Y

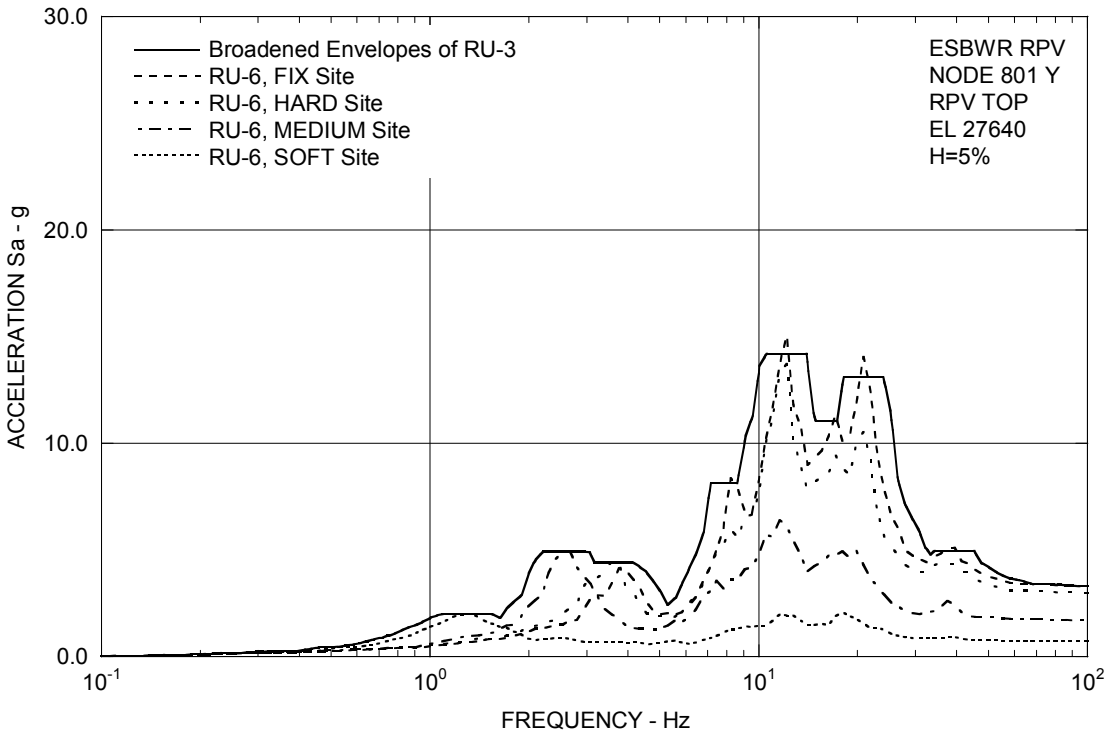

Figure 3A.8.5-2e. FRS (Effect of LOCA Flooding) – RPV Top Y

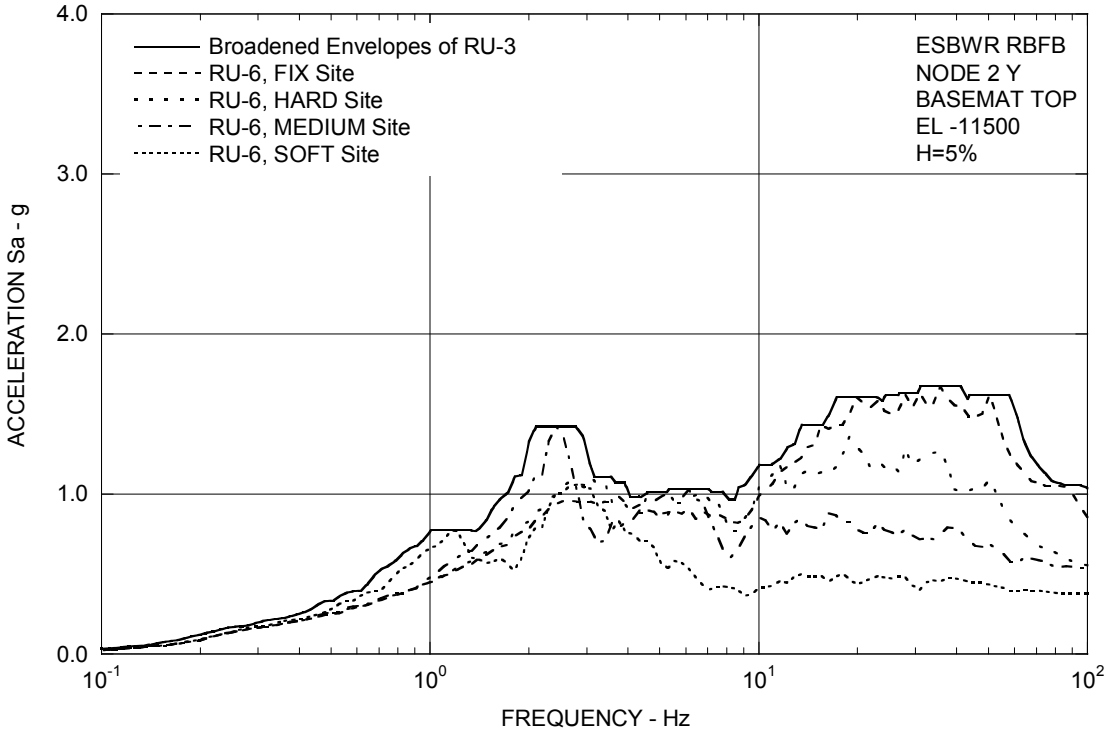

Figure 3A.8.5-2f. FRS (Effect of LOCA Flooding) – RBFB Basemat Y

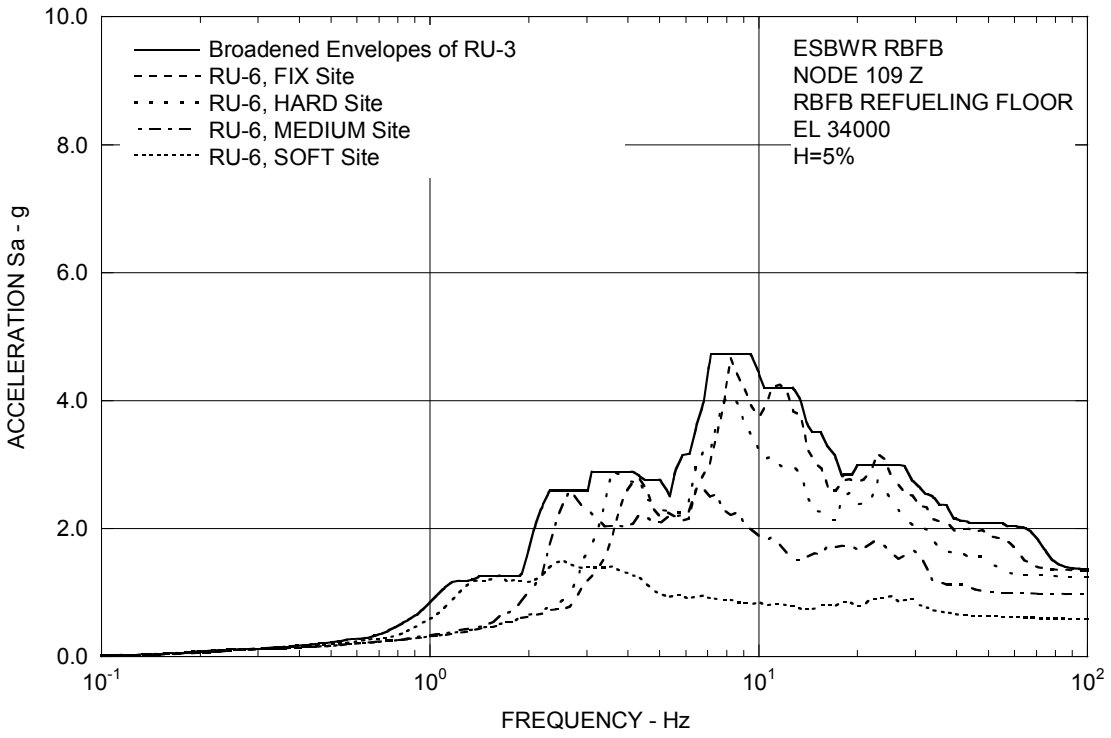

Figure 3A.8.5-3a. FRS (Effect of LOCA Flooding) – RBFB Refueling Floor Z

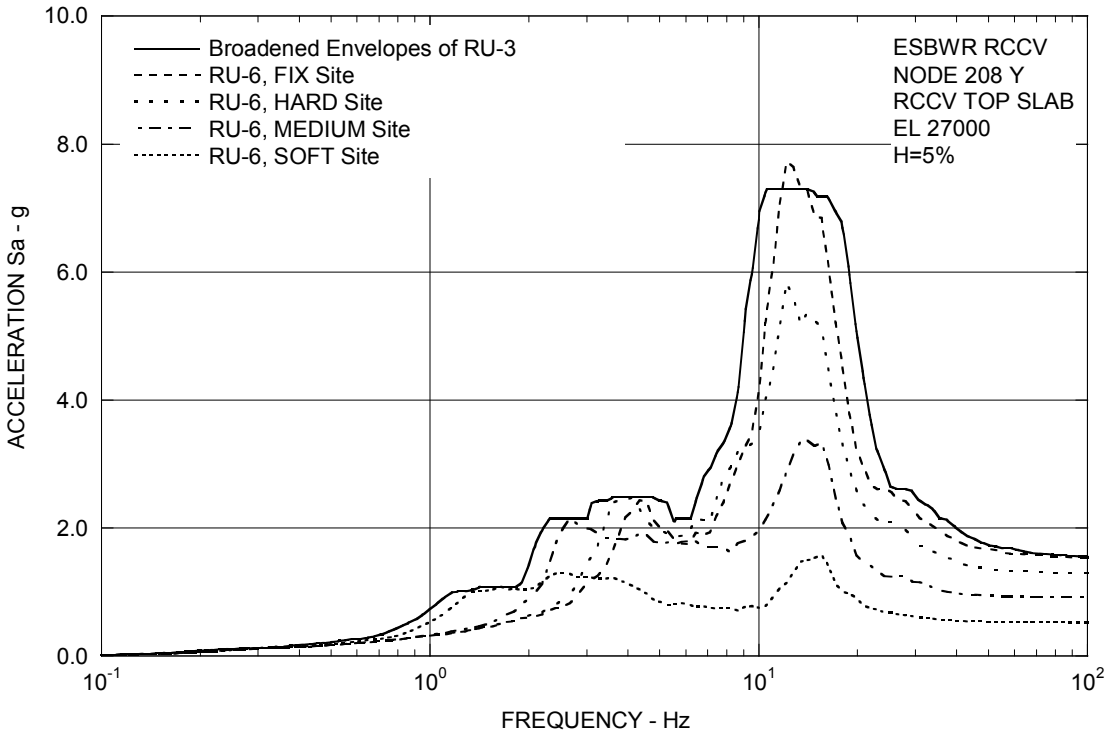

Figure 3A.8.5-3b. FRS (Effect of LOCA Flooding) – RCCV Top Slab Z

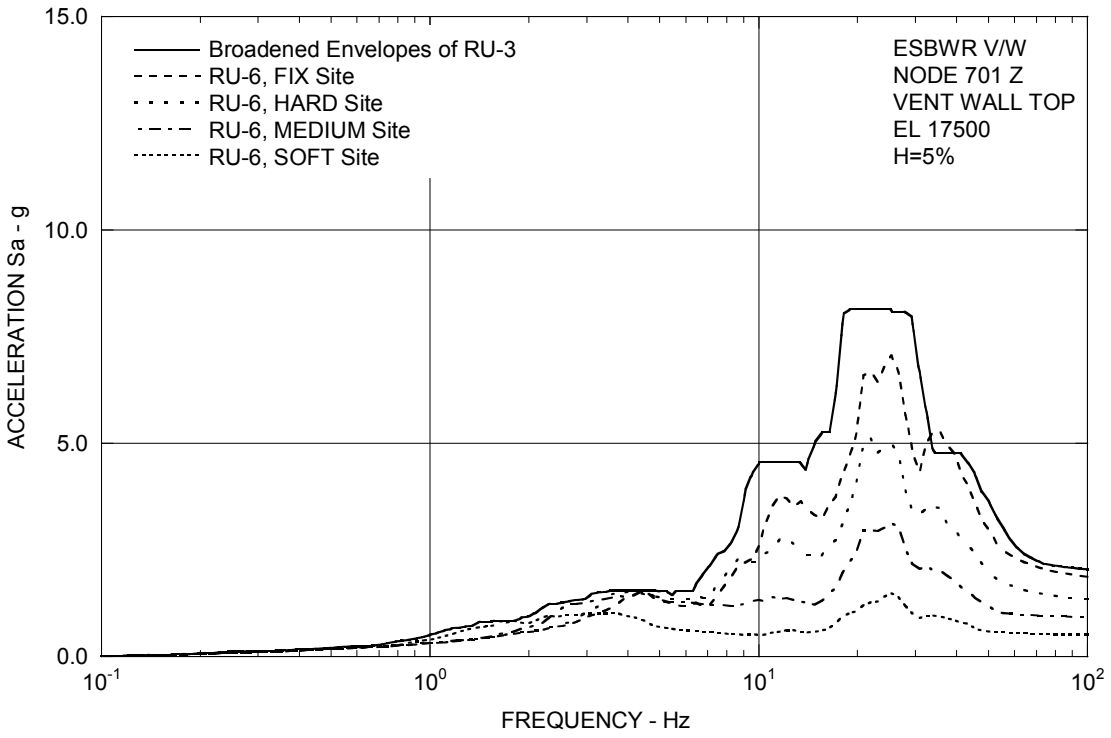

Figure 3A.8.5-3c. FRS (Effect of LOCA Flooding) – Vent Wall Top Z

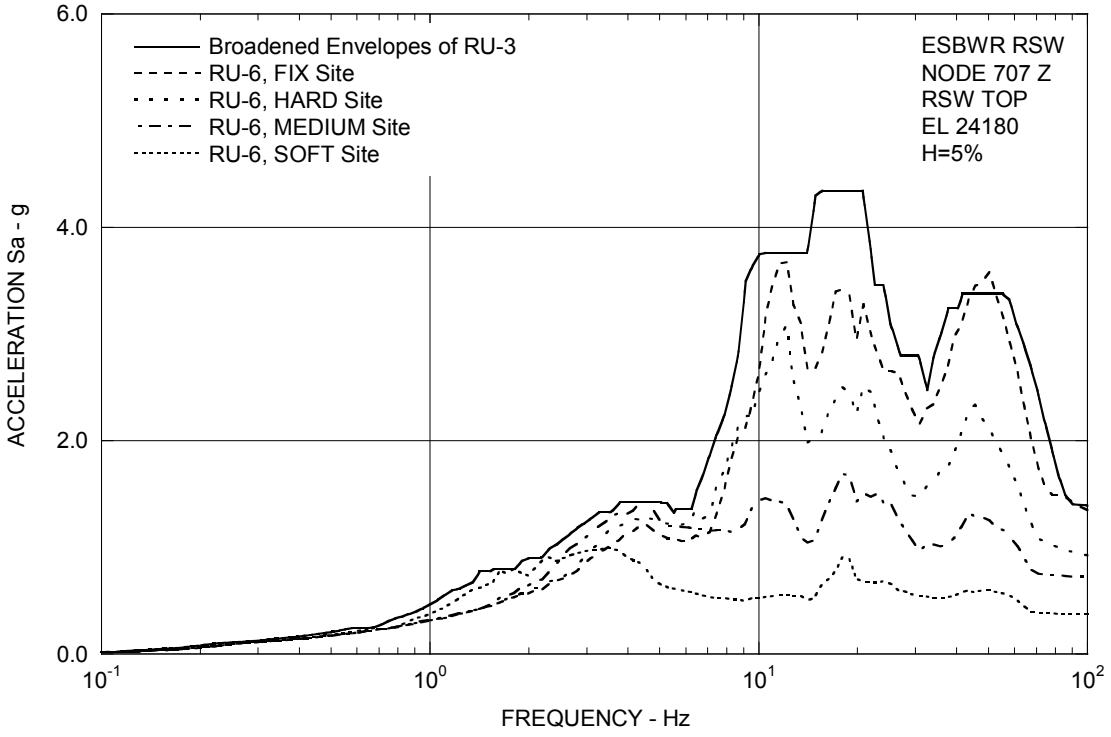

Figure 3A.8.5-3d. FRS (Effect of LOCA Flooding) – RSW Top Z

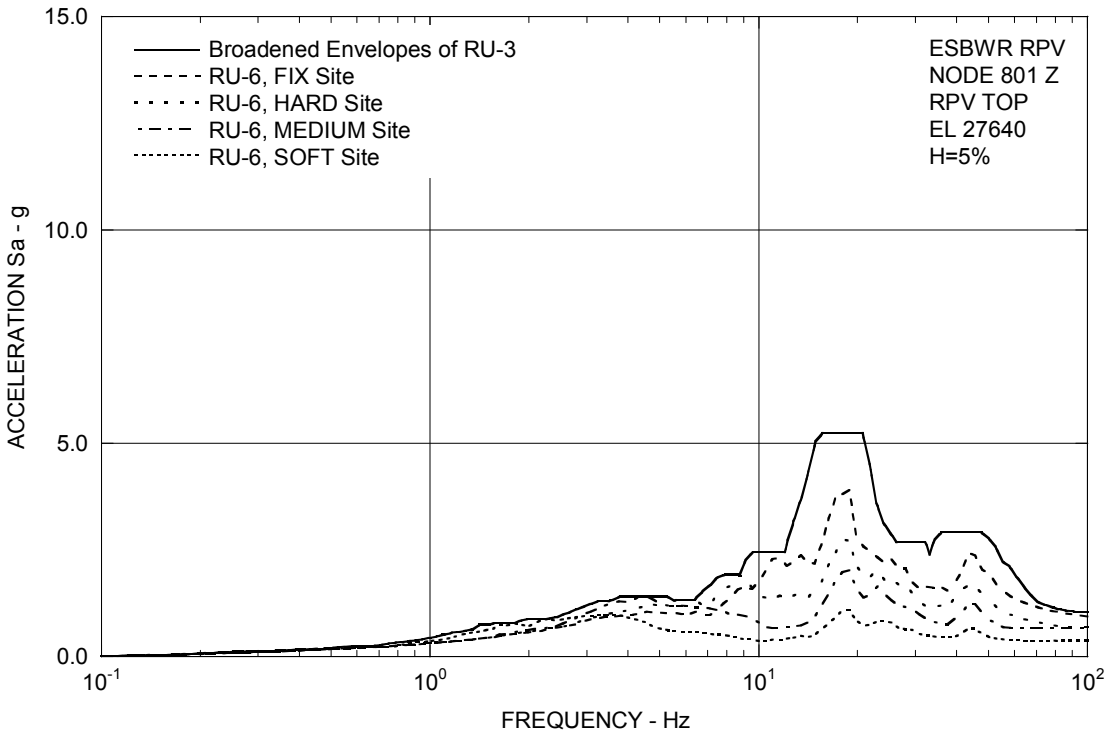

Figure 3A.8.5-3e. FRS (Effect of LOCA Flooding) – RPV Top Z

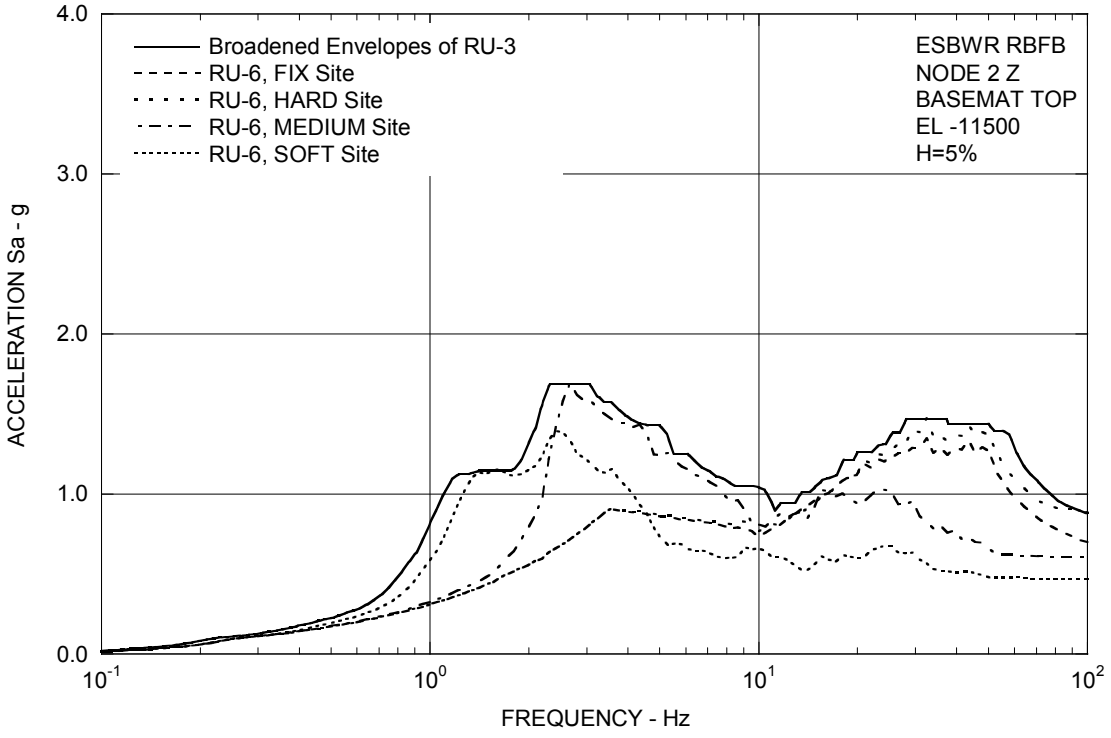

Figure 3A.8.5-3f. FRS (Effect of LOCA Flooding) – RBFB Basemat Z

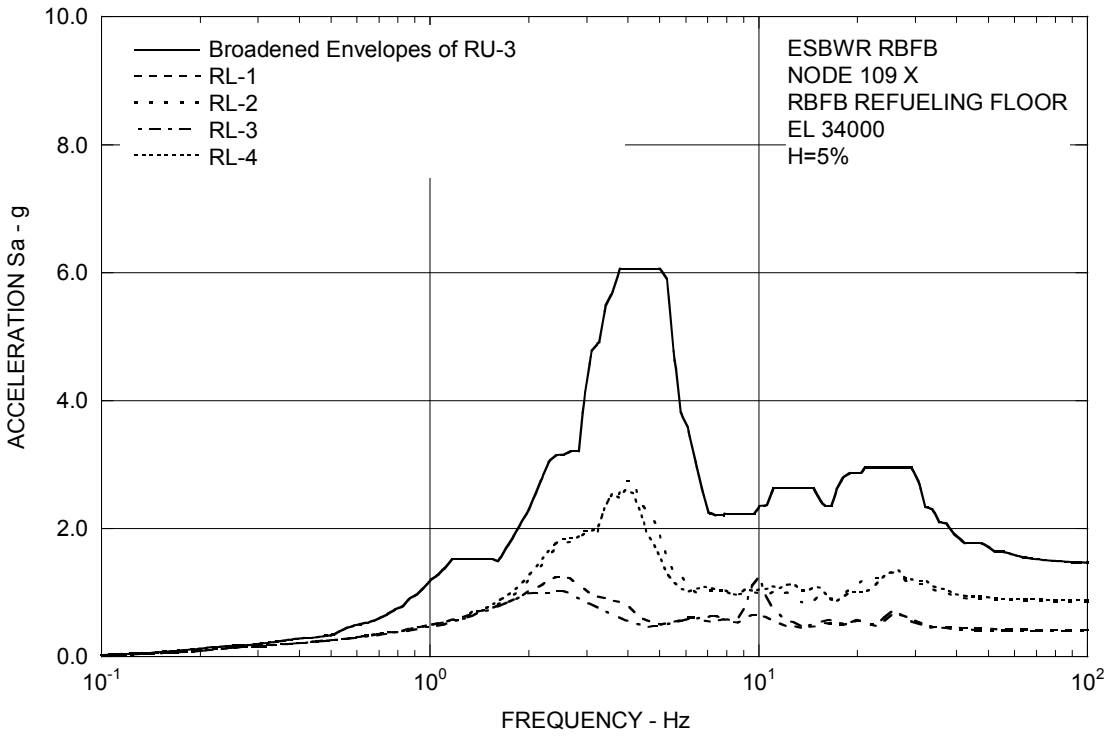

Figure 3A.8.6-1a. FRS (Effect of Layered Sites) – RBFB Refueling Floor X

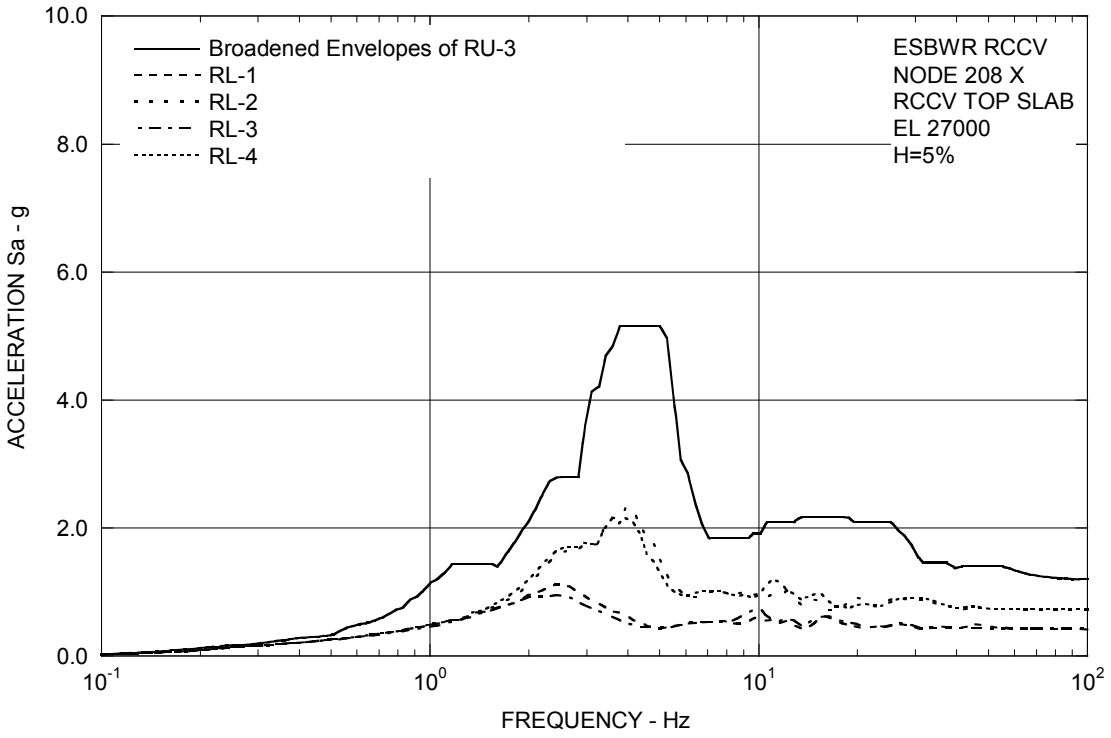

Figure 3A.8.6-1b. FRS (Effect of Layered Sites) – RCCV Top Slab X

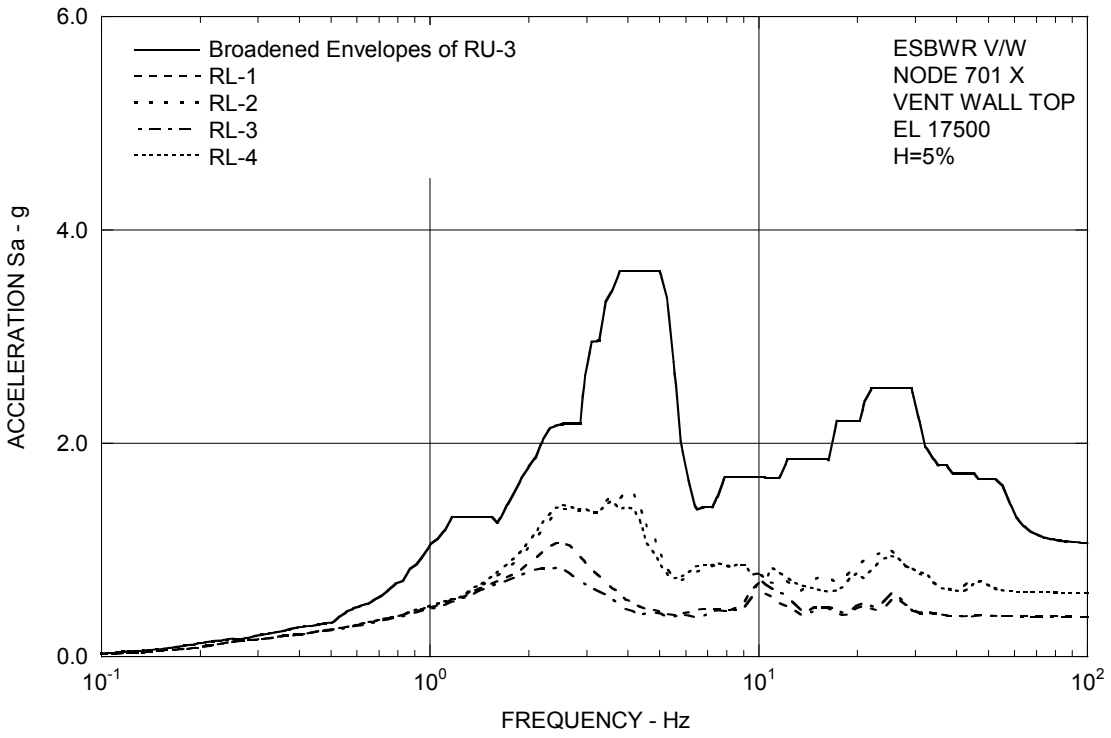

Figure 3A.8.6-1c. FRS (Effect of Layered Sites) – Vent Wall Top X

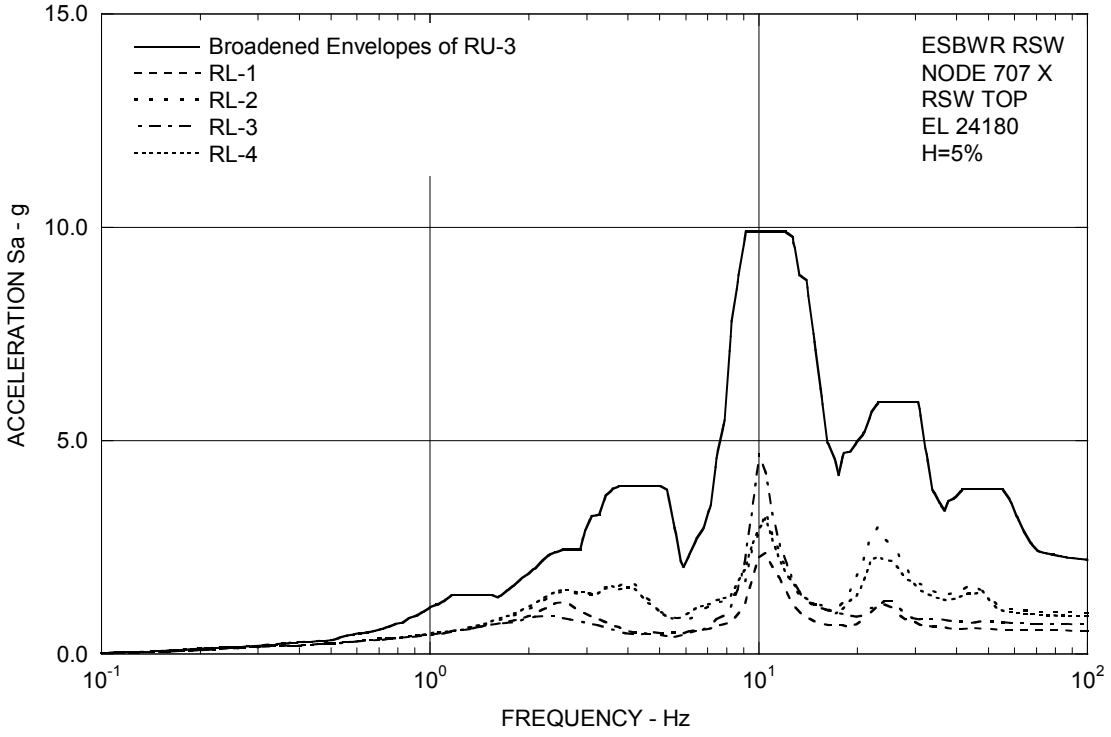

Figure 3A.8.6-1d. FRS (Effect of Layered Sites) – RSW Top X

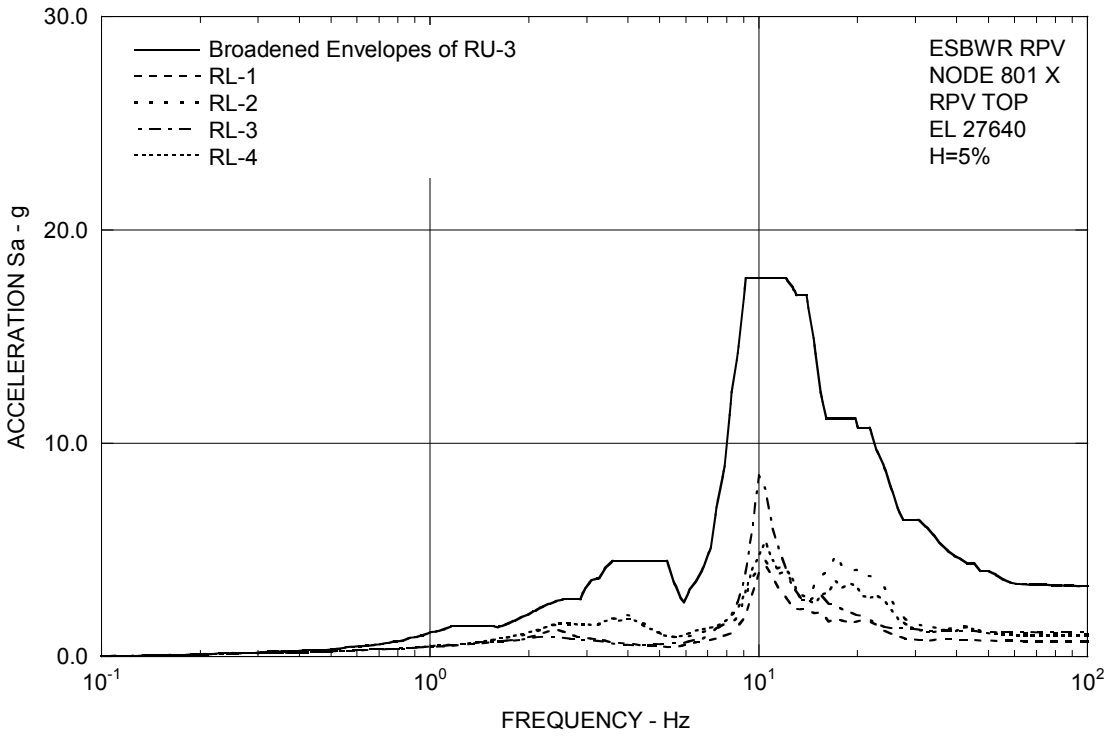

Figure 3A.8.6-1e. FRS (Effect of Layered Sites) – RPV Top X

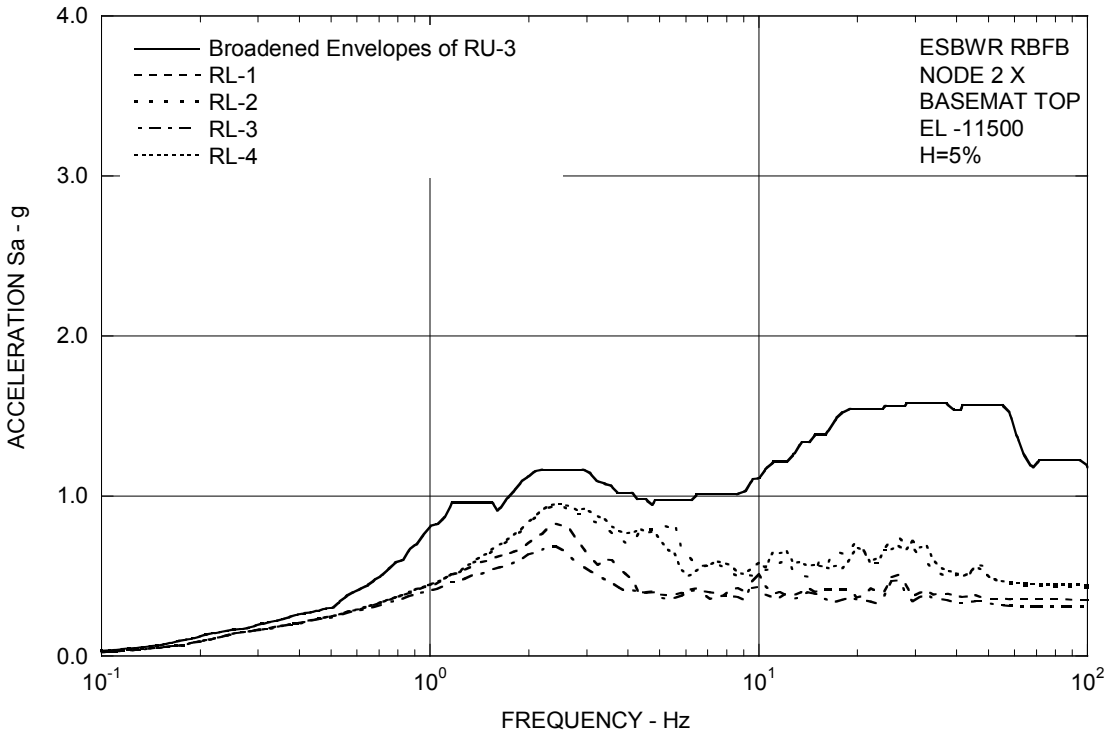

Figure 3A.8.6-1f. FRS (Effect of Layered Sites) – RBFB Basemat X

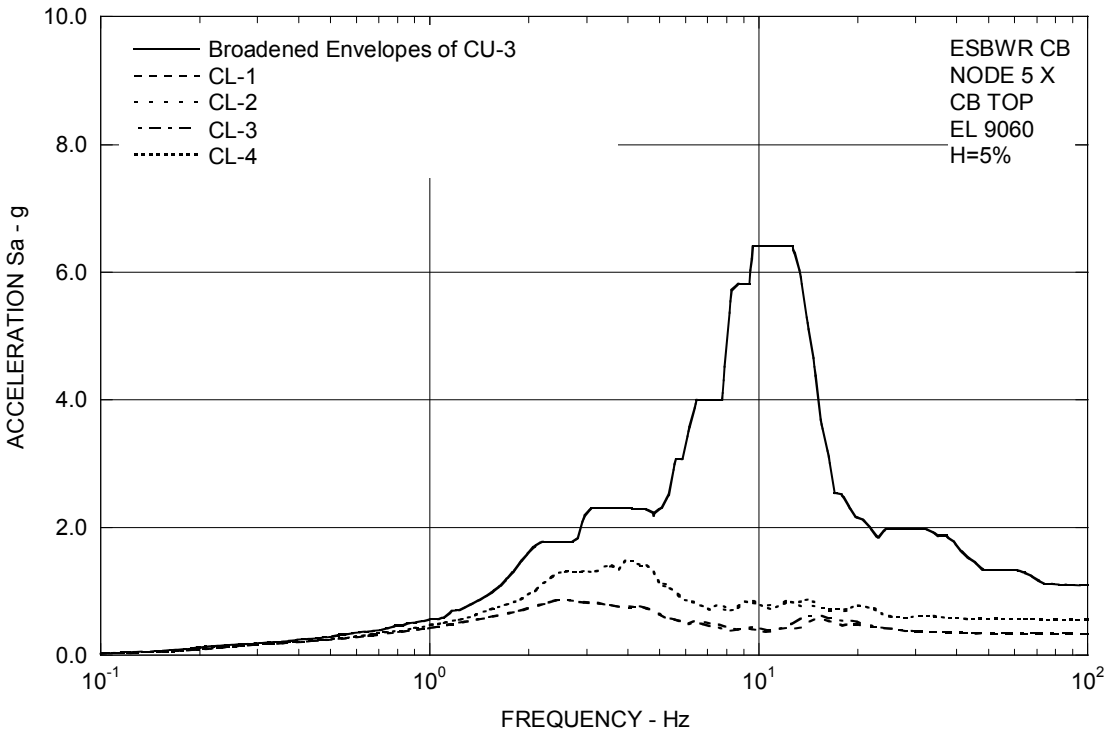

Figure 3A.8.6-1g. FRS (Effect of Layered Sites) – CB Top X

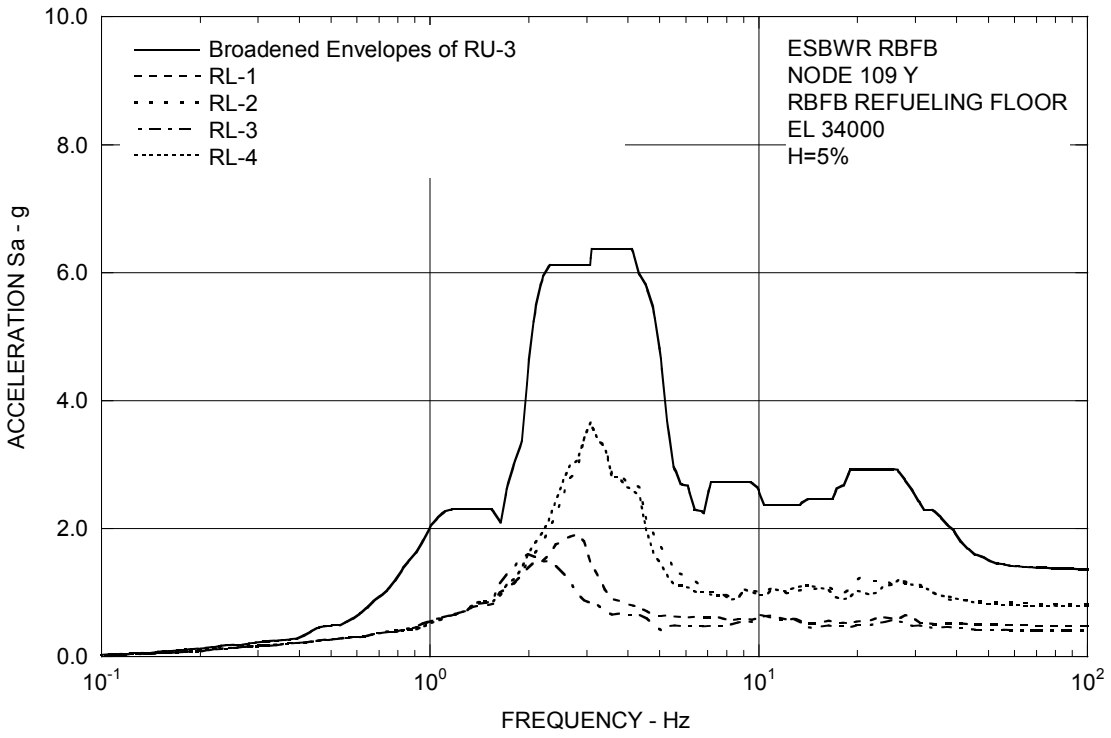

Figure 3A.8.6-2a. FRS (Effect of Layered Sites) – RBFB Refueling Floor Y

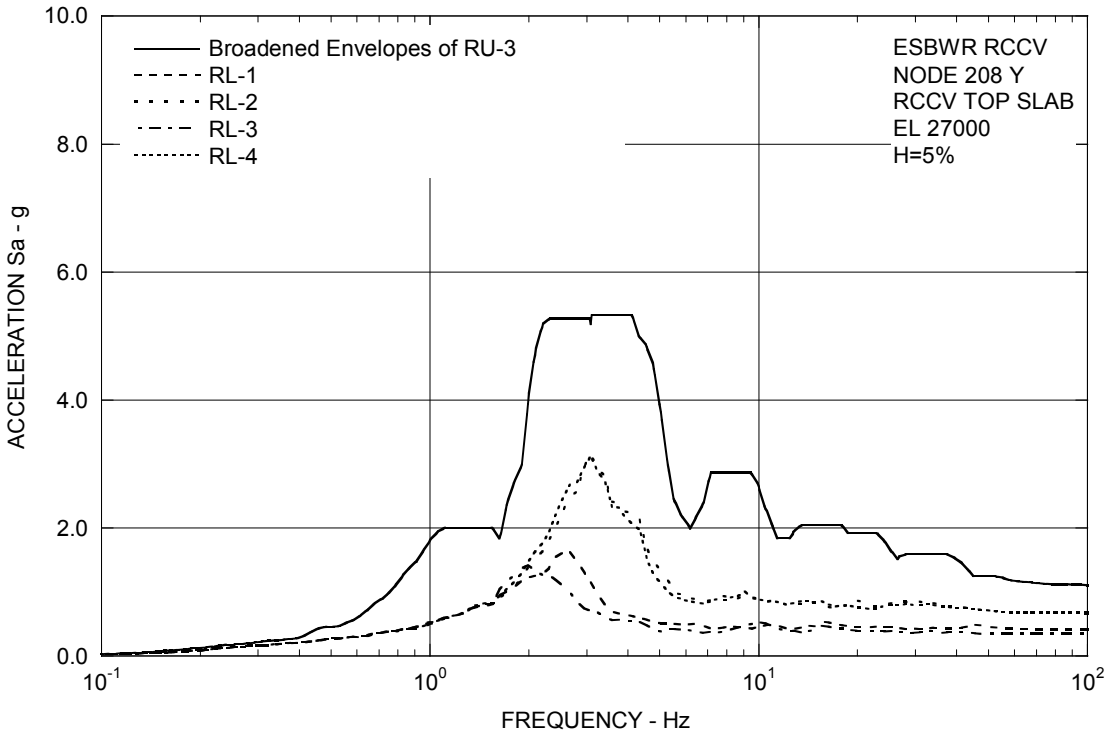

Figure 3A.8.6-2b. FRS (Effect of Layered Sites) – RCCV Top Slab Y

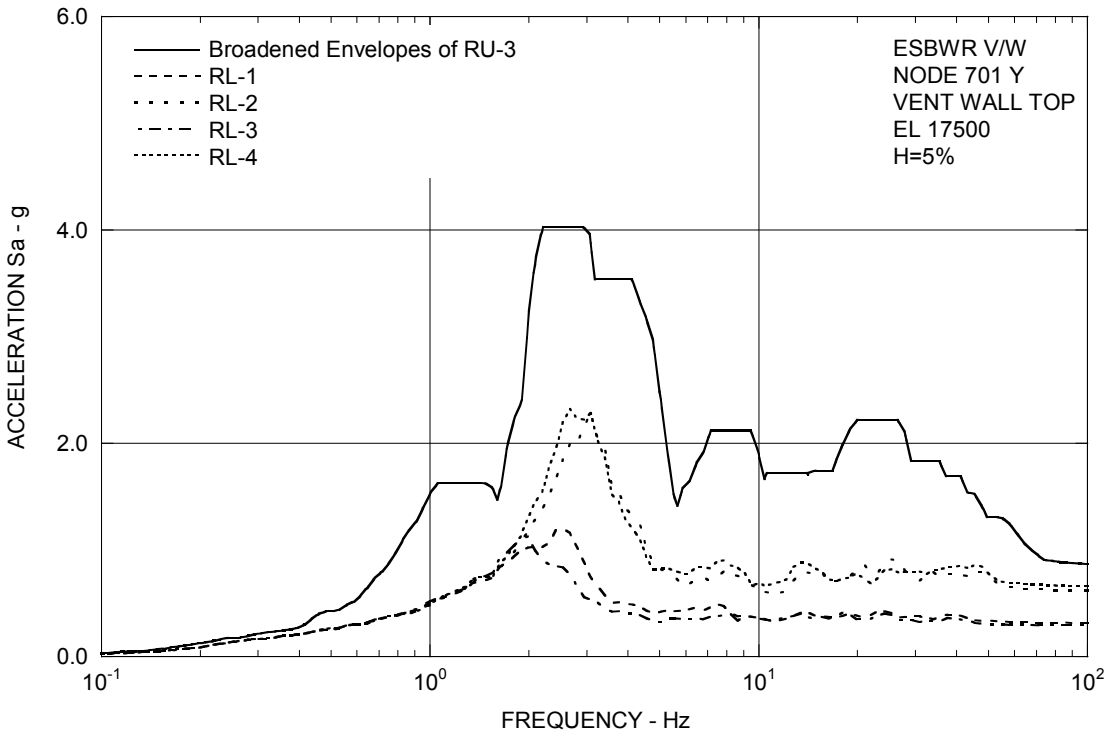

Figure 3A.8.6-2c. FRS (Effect of Layered Sites) – Vent Wall Top Y

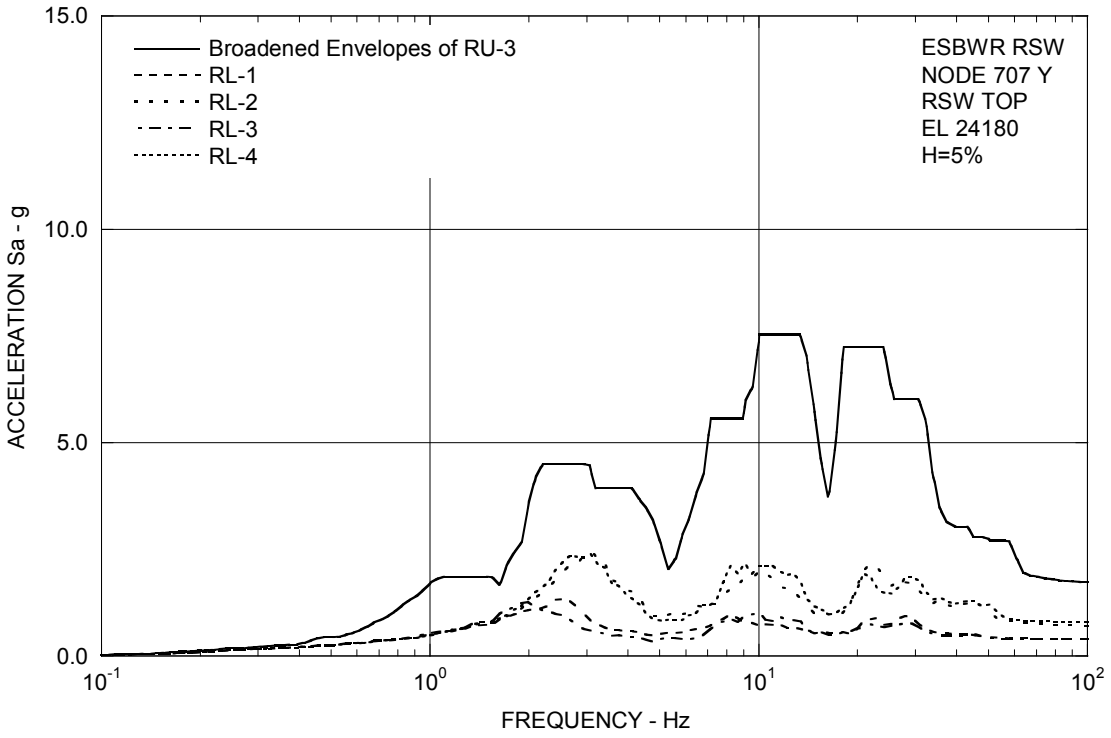

Figure 3A.8.6-2d. FRS (Effect of Layered Sites) – RSW Top Y

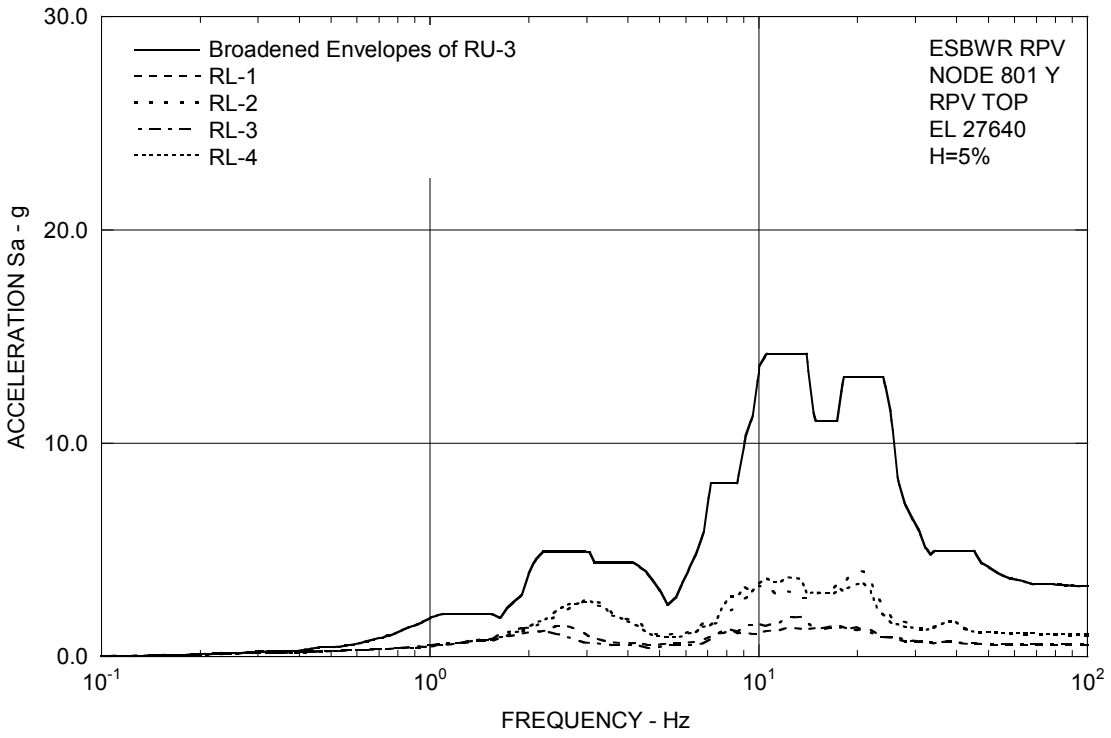

Figure 3A.8.6-2e. FRS (Effect of Layered Sites) – RPV Top Y

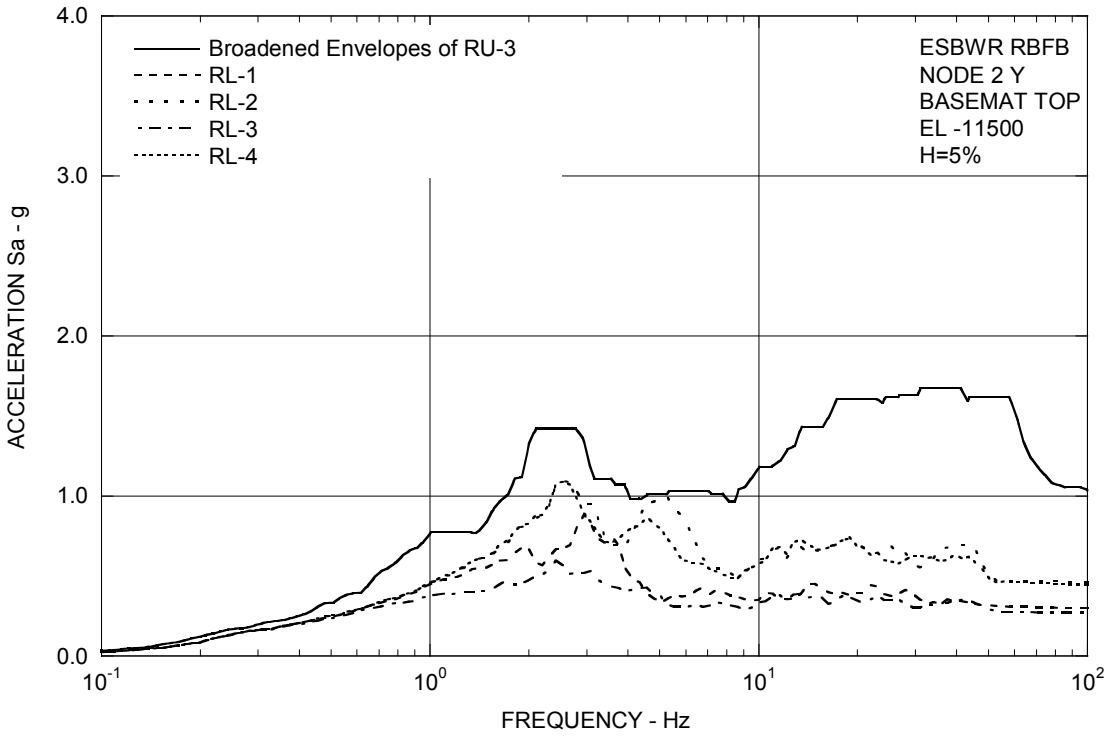

Figure 3A.8.6-2f. FRS (Effect of Layered Sites) – RBFB Basemat Y

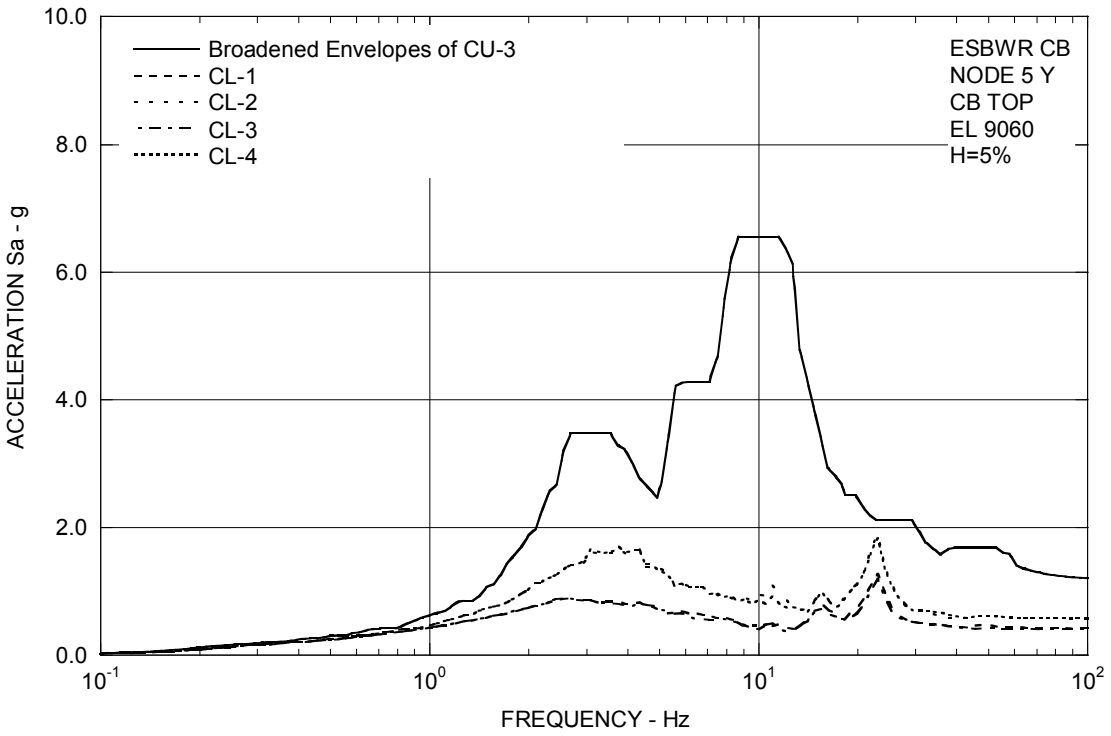

Figure 3A.8.6-2g. FRS (Effect of Layered Sites) – CB Top Y

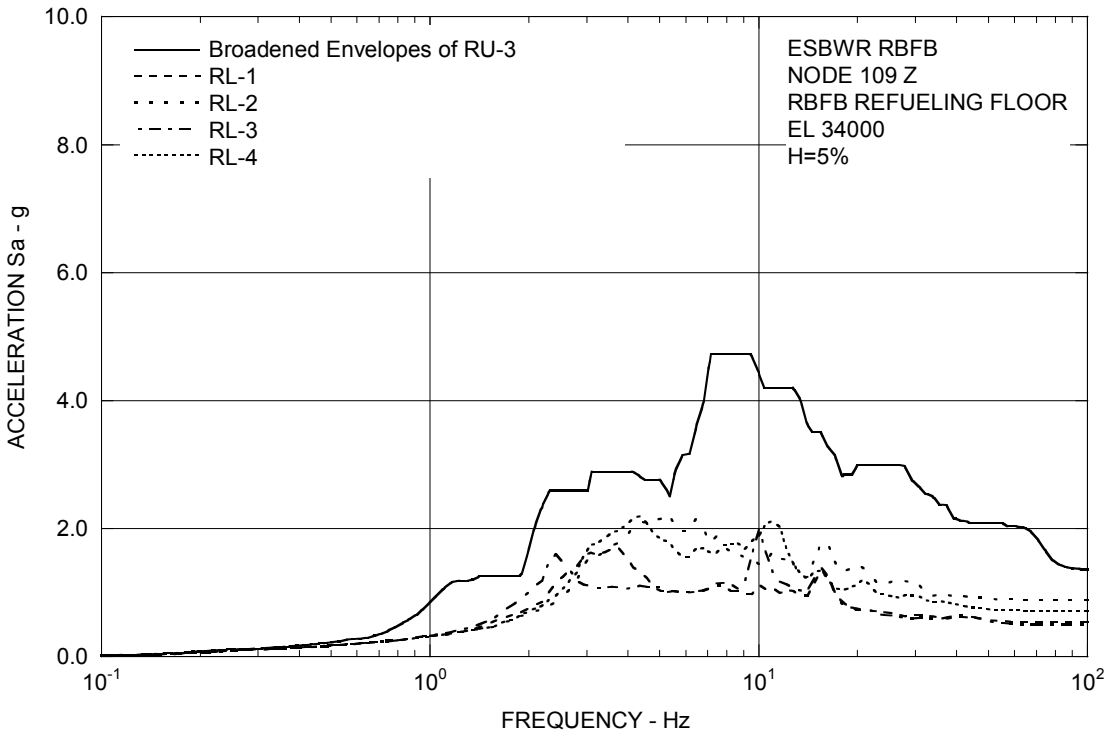

Figure 3A.8.6-3a. FRS (Effect of Layered Sites) – RBFB Refueling Floor Z

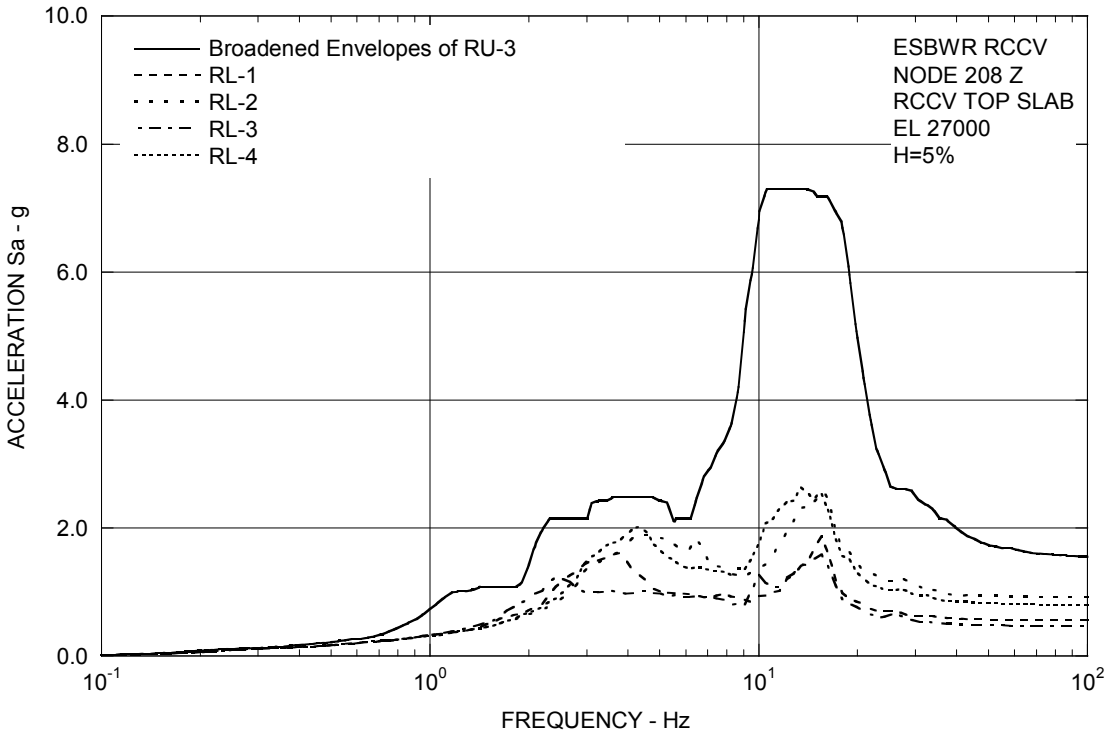

Figure 3A.8.6-3b. FRS (Effect of Layered Sites) – RCCV Top Slab Z

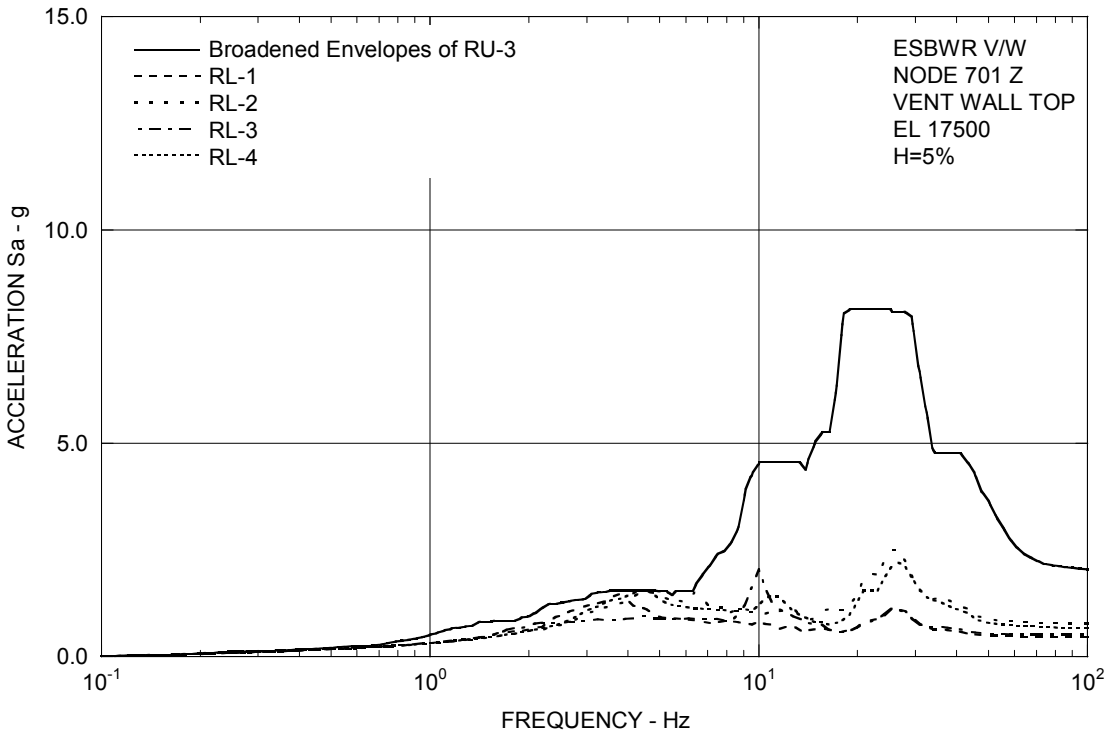

Figure 3A.8.6-3c. FRS (Effect of Layered Sites) – Vent Wall Top Z

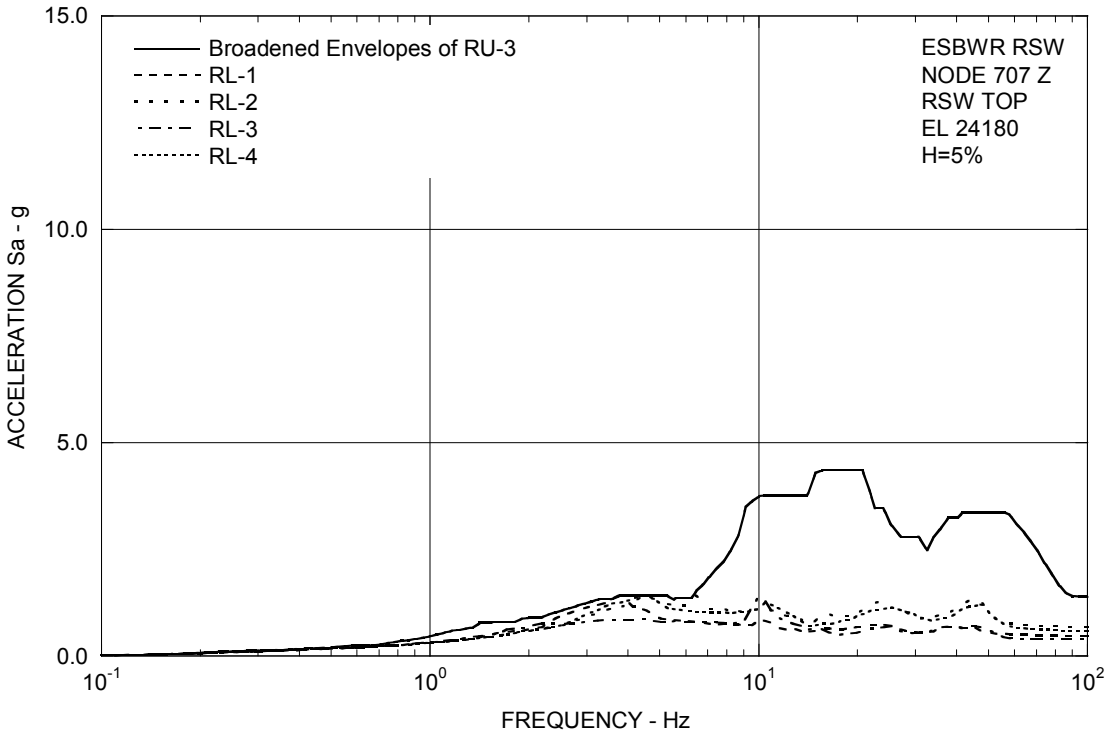

Figure 3A.8.6-3d. FRS (Effect of Layered Sites) – RSW Top Z

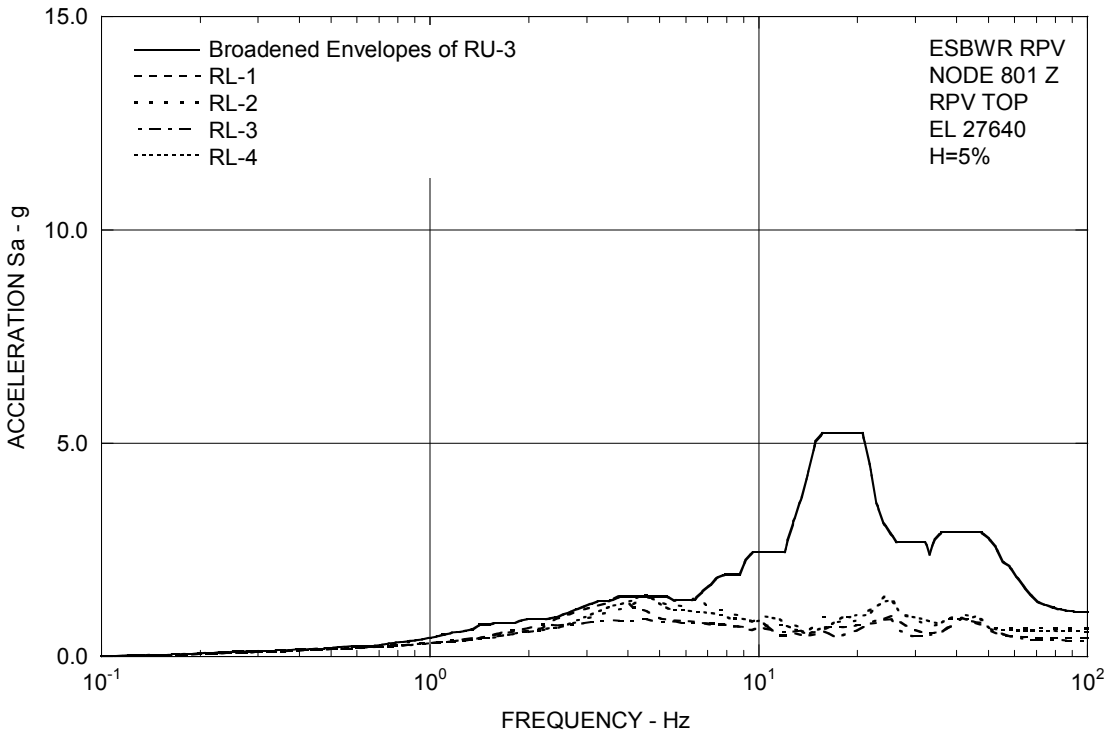

Figure 3A.8.6-3e. FRS (Effect of Layered Sites) – RPV Top Z

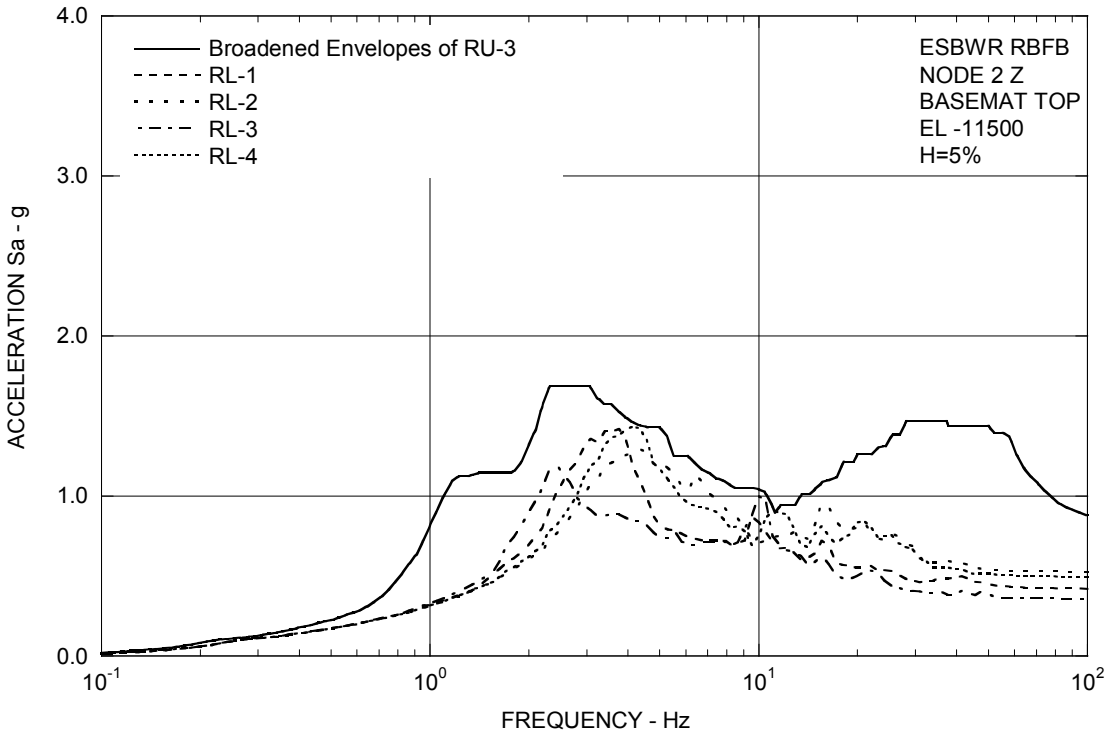

Figure 3A.8.6-3f. FRS (Effect of Layered Sites) – RBFB Basemat Z

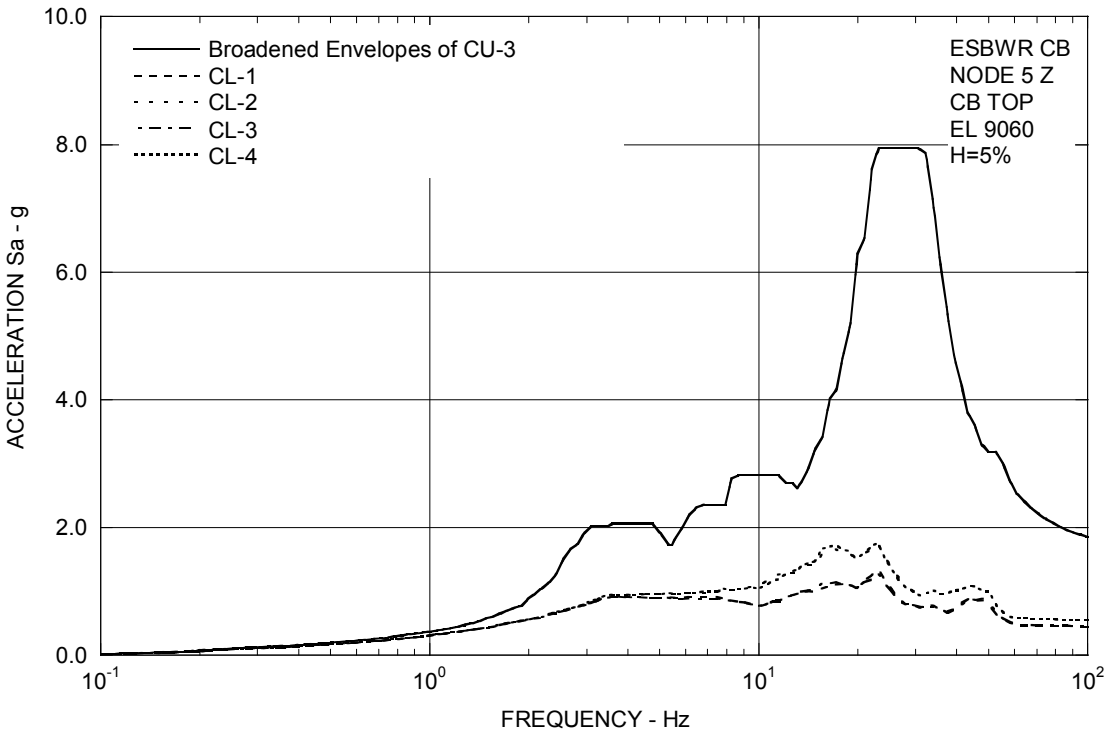

Figure 3A.8.6-3g. FRS (Effect of Layered Sites) – CB Top Z

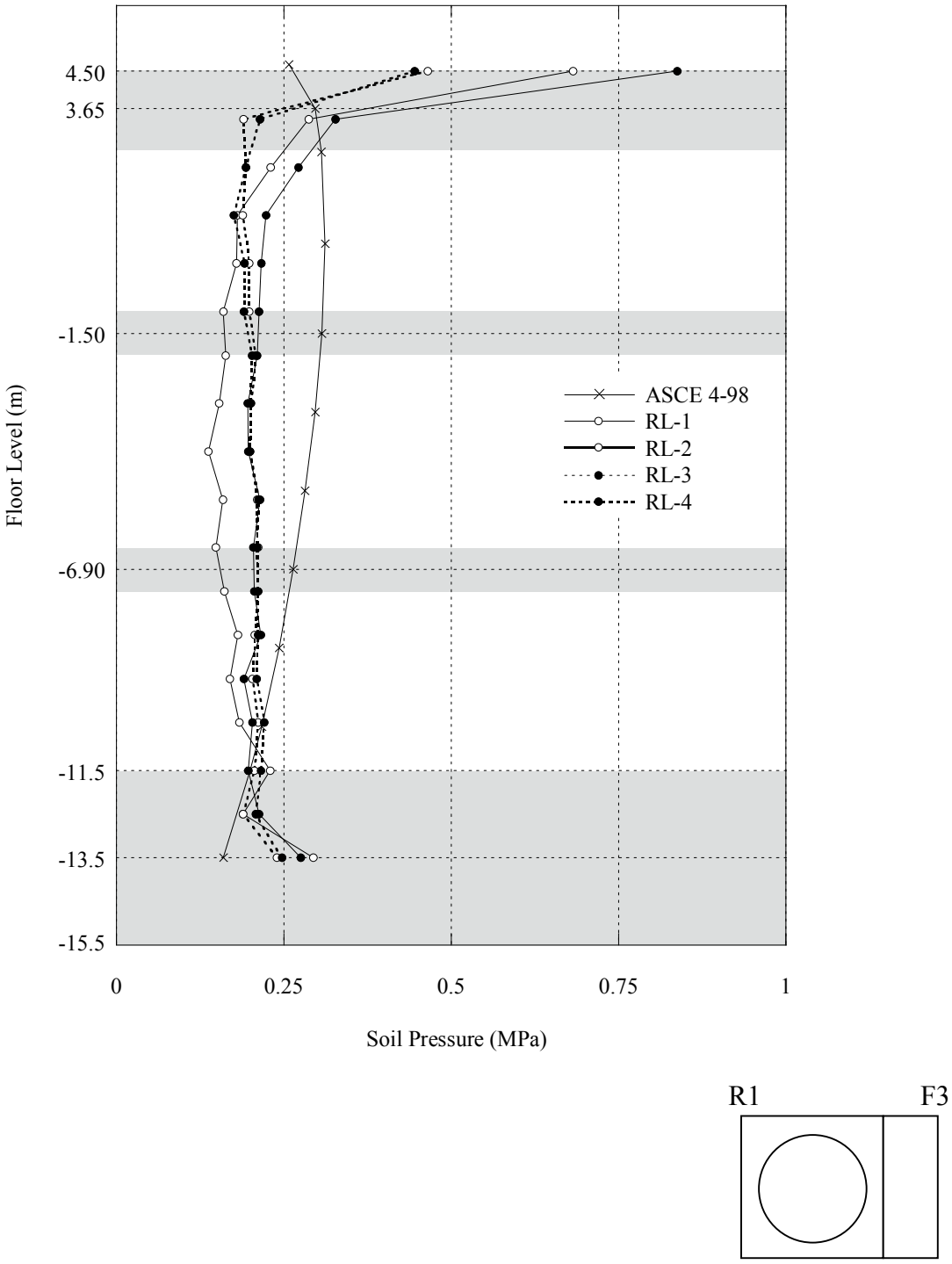

Note: The shaded area shows thickness of the floor slabs and basemat.

Figure 3A.8.8-1. Lateral Soil Pressure - RBFB R1 and F3 Wall

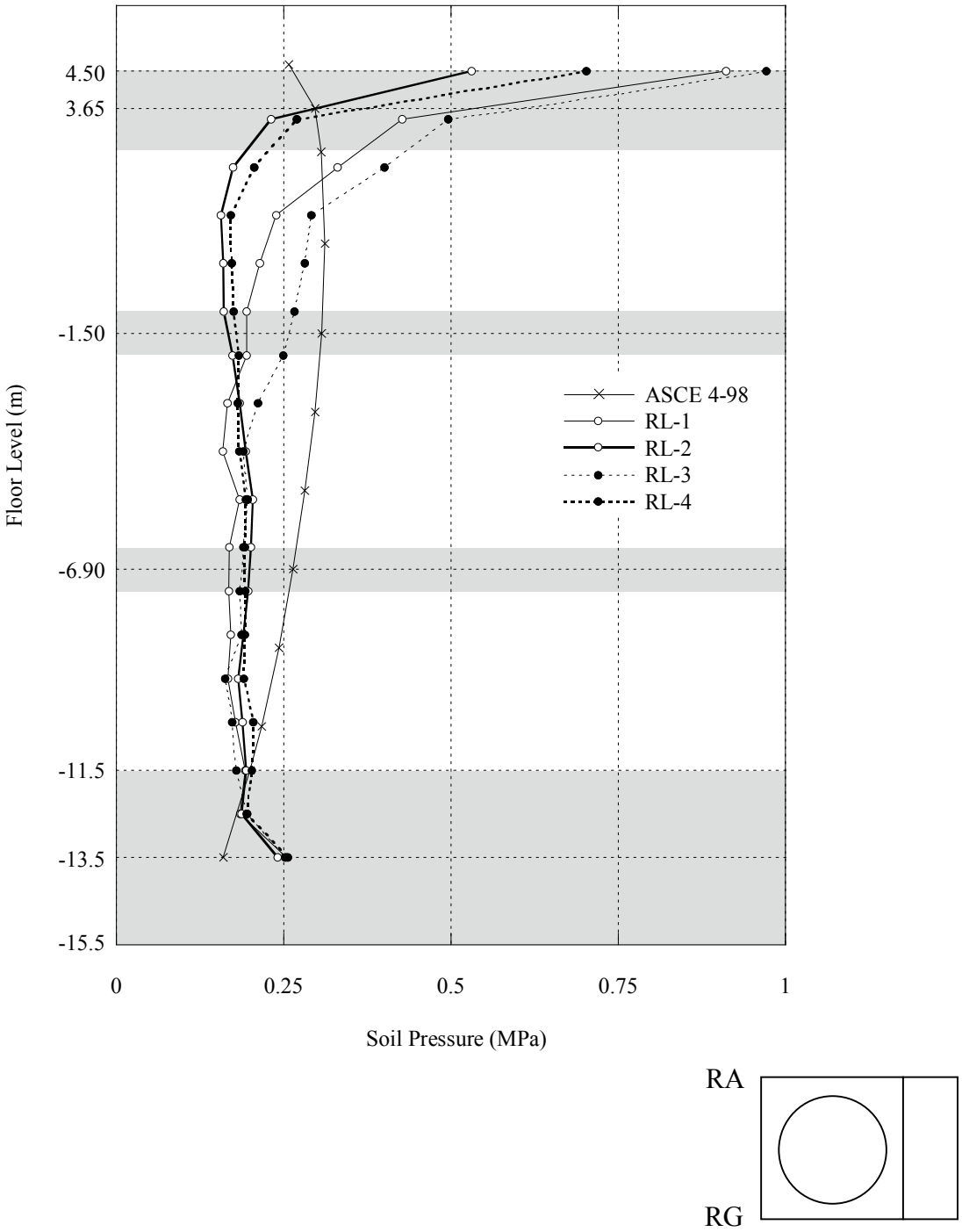

Note: The shaded area shows thickness of the floor slabs and basemat.

Figure 3A.8.8-2. Lateral Soil Pressure - RBFB RA and RG Wall

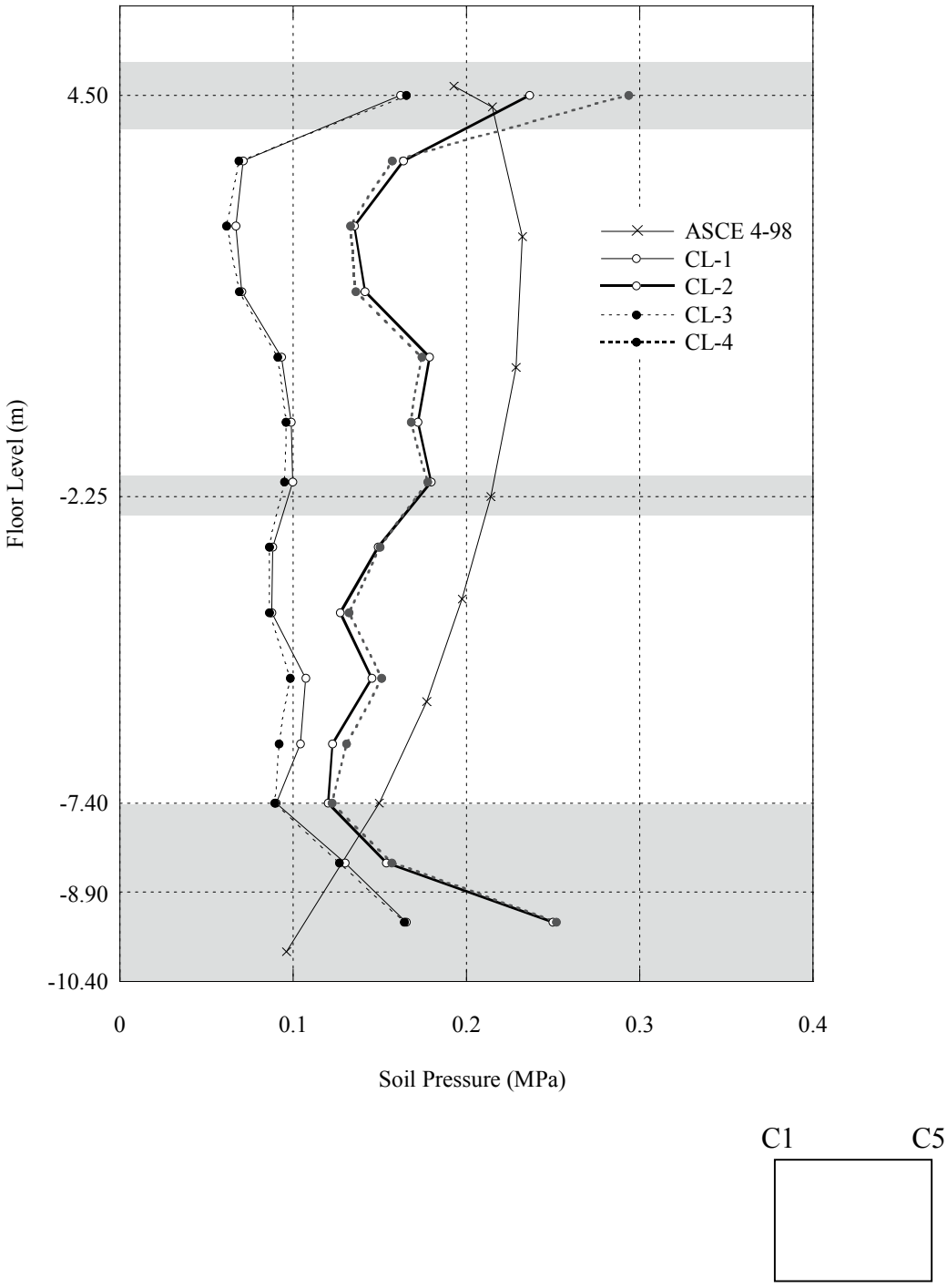

Note: The shaded area shows thickness of the floor slabs and basemat.

Figure 3A.8.8-3. Lateral Soil Pressure - CB C1 and C5 Wall

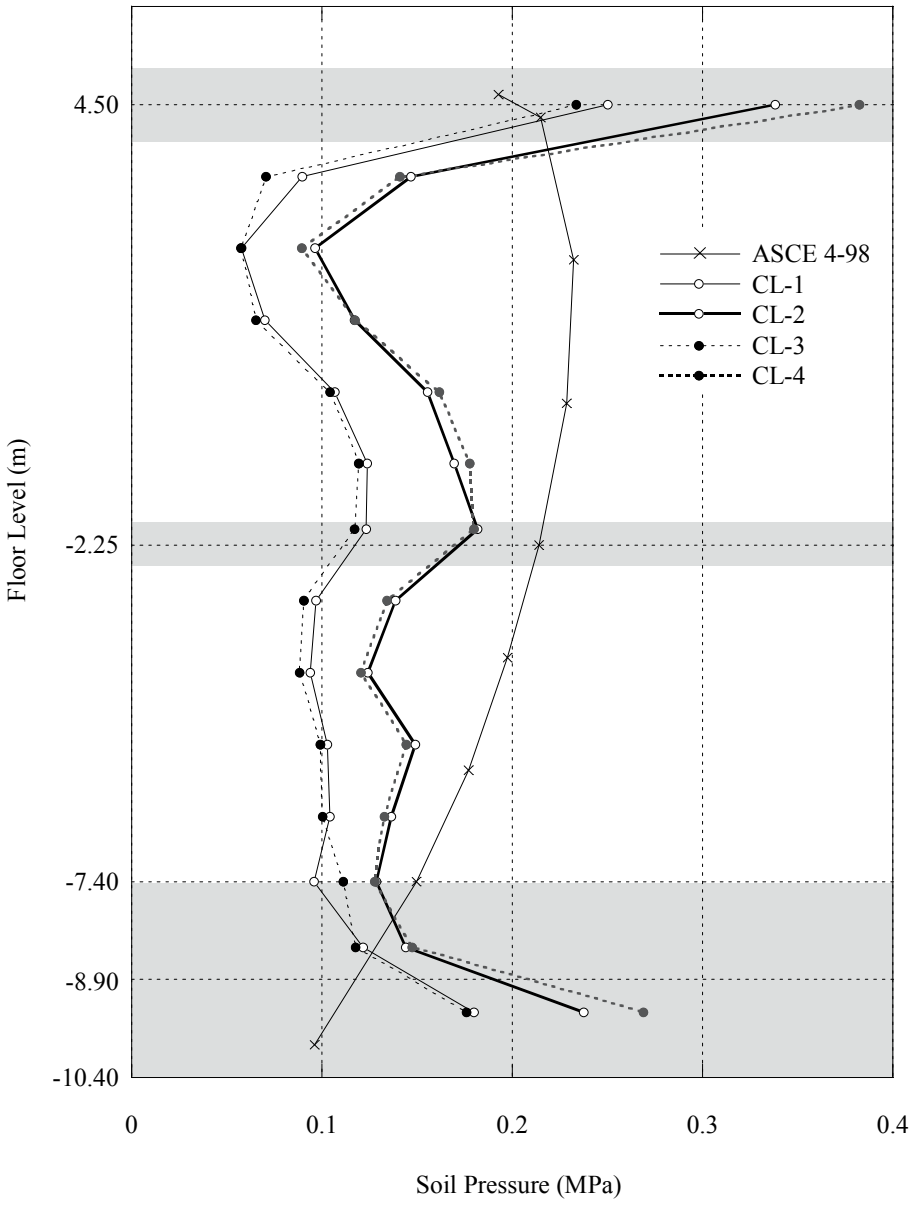

CA

CD

Note: The shaded area shows thickness of the floor slabs and basemat.

Figure 3A.8.8-4. Lateral Soil Pressure - CB CA and CD Wall

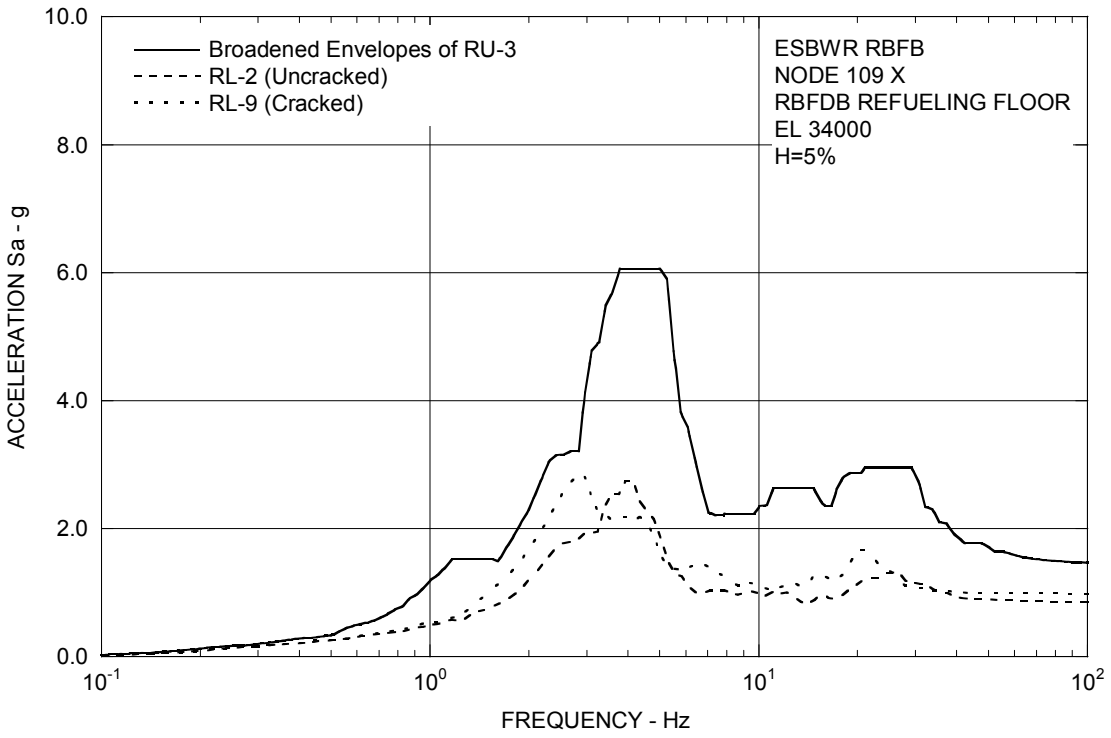

Figure 3A.8.9-1a. FRS (Effect of Concrete Cracking) – RBFB Refueling Floor X

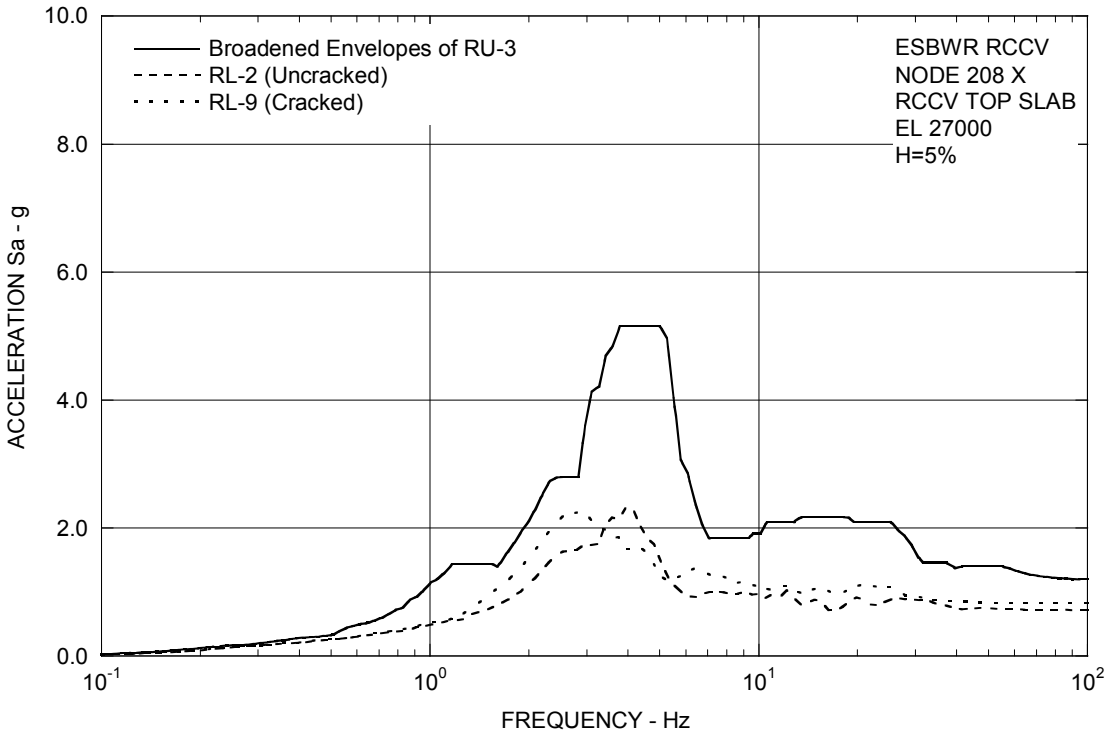

Figure 3A.8.9-1b. FRS (Effect of Concrete Cracking) – RCCV Top Slab X

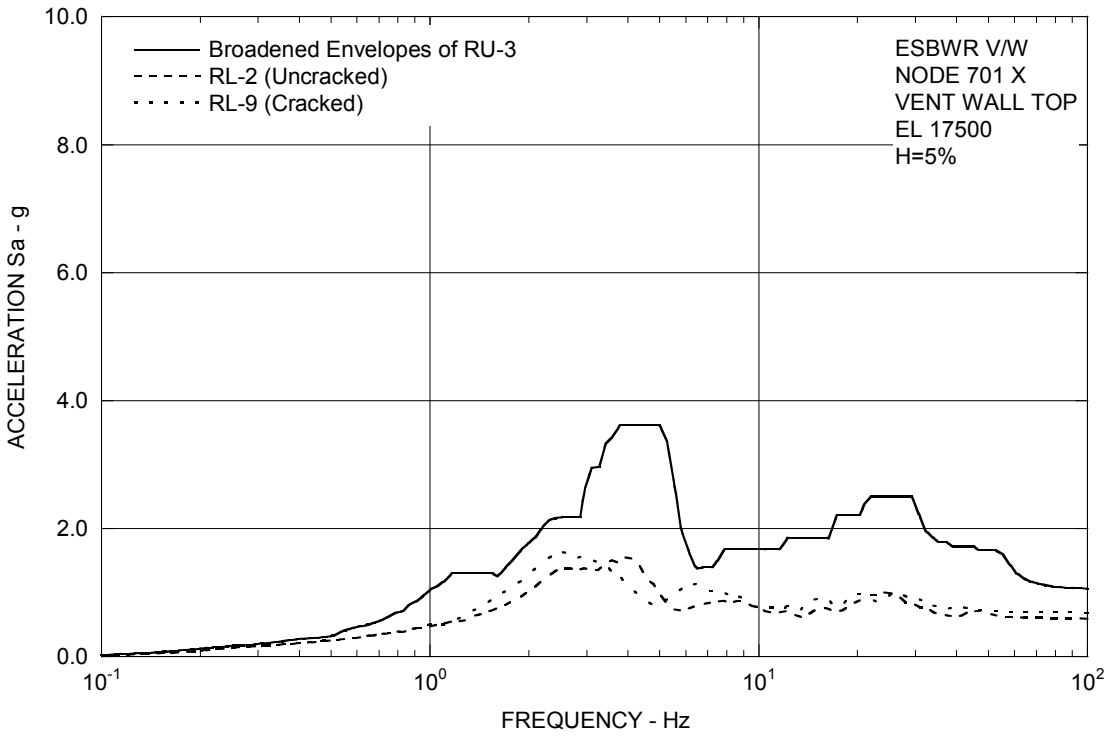

Figure 3A.8.9-1c. FRS (Effect of Concrete Cracking) – Vent Wall Top X

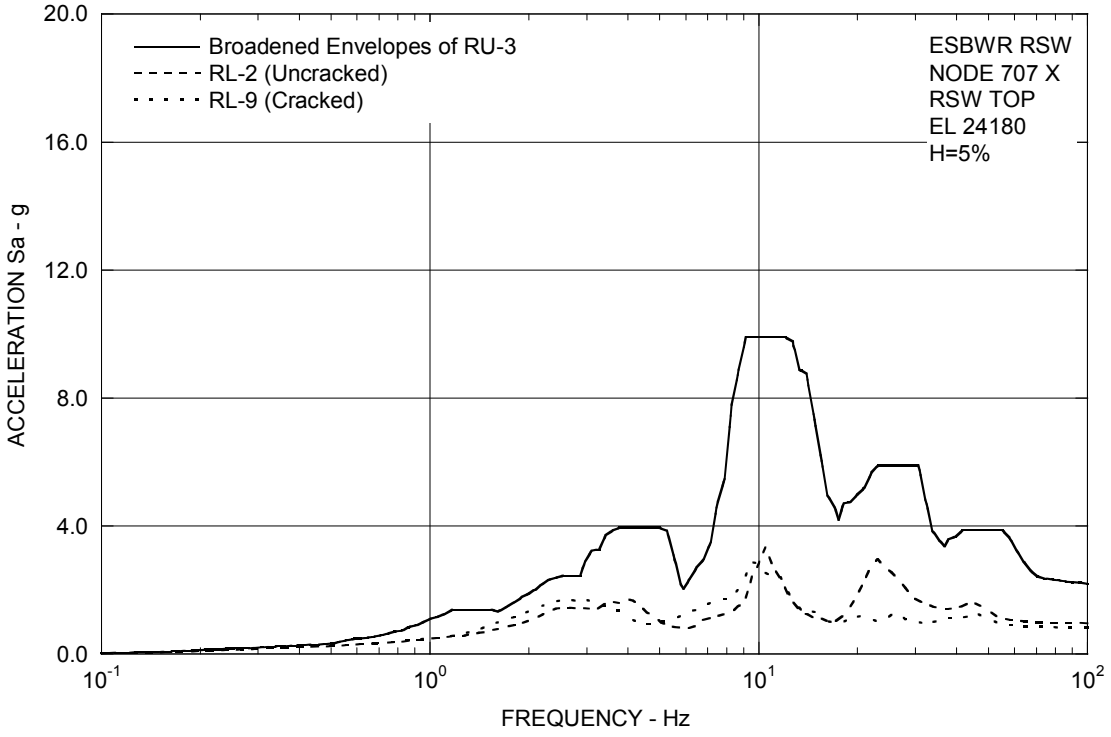

Figure 3A.8.9-1d. FRS (Effect of Concrete Cracking) – RSW Top X

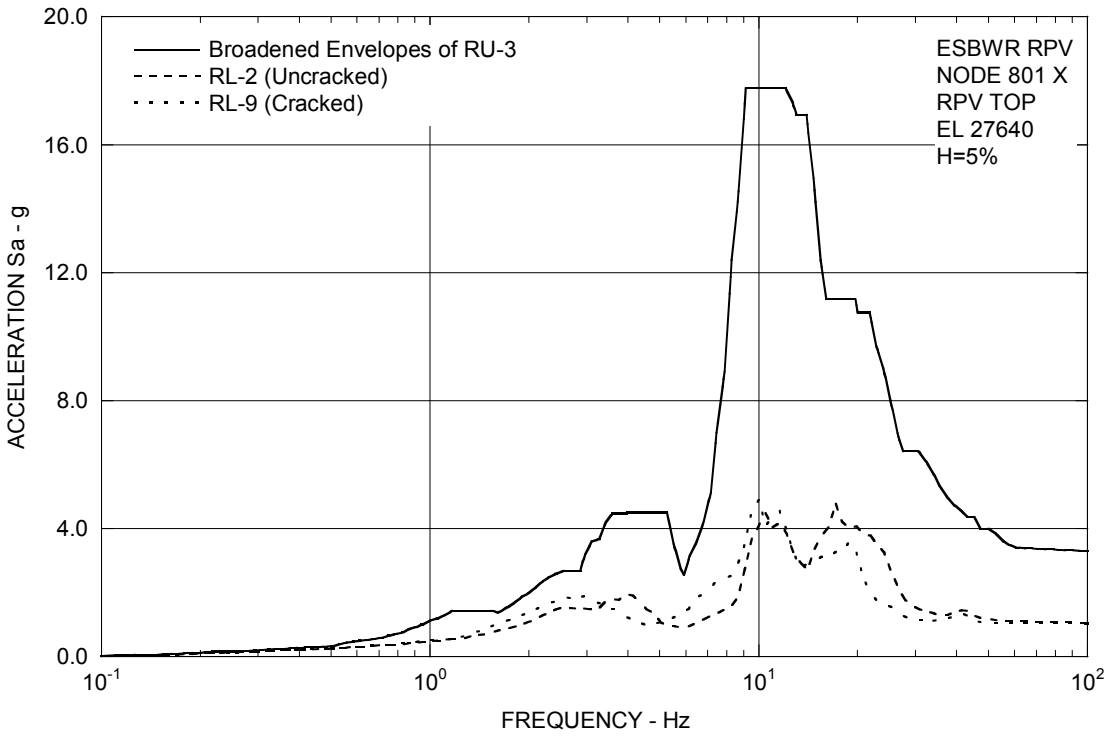

Figure 3A.8.9-1e. FRS (Effect of Concrete Cracking) – RPV Top X

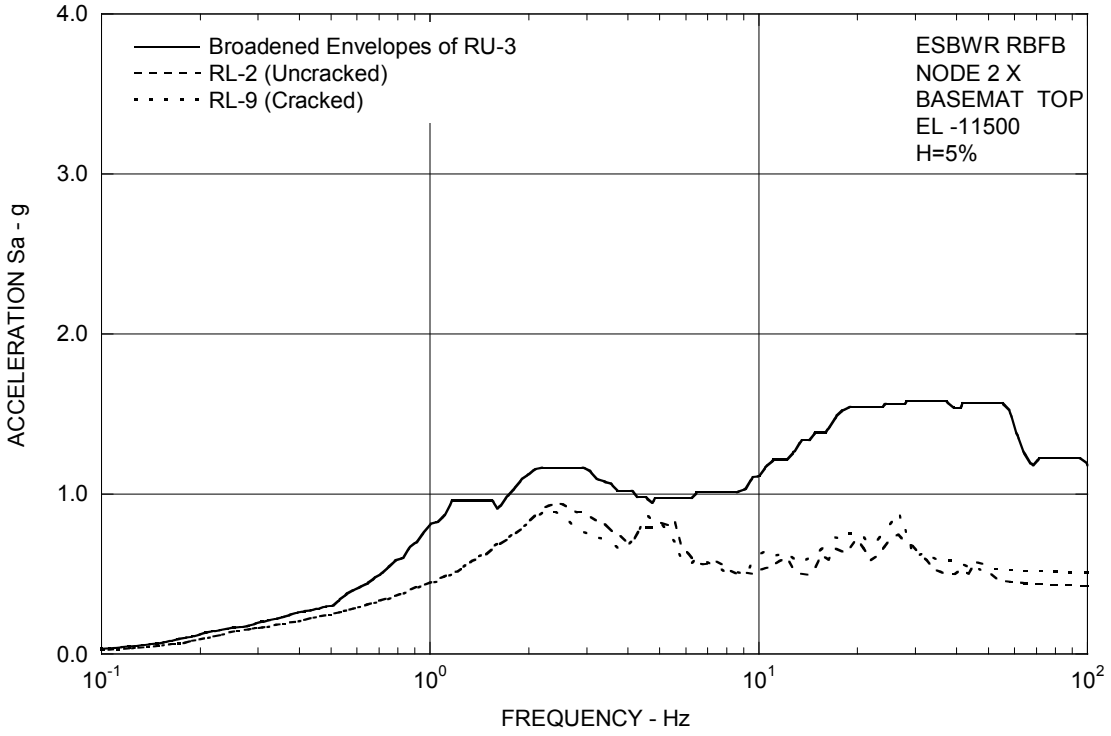

Figure 3A.8.9-1f. FRS (Effect of Concrete Cracking) – RBFB Basemat X

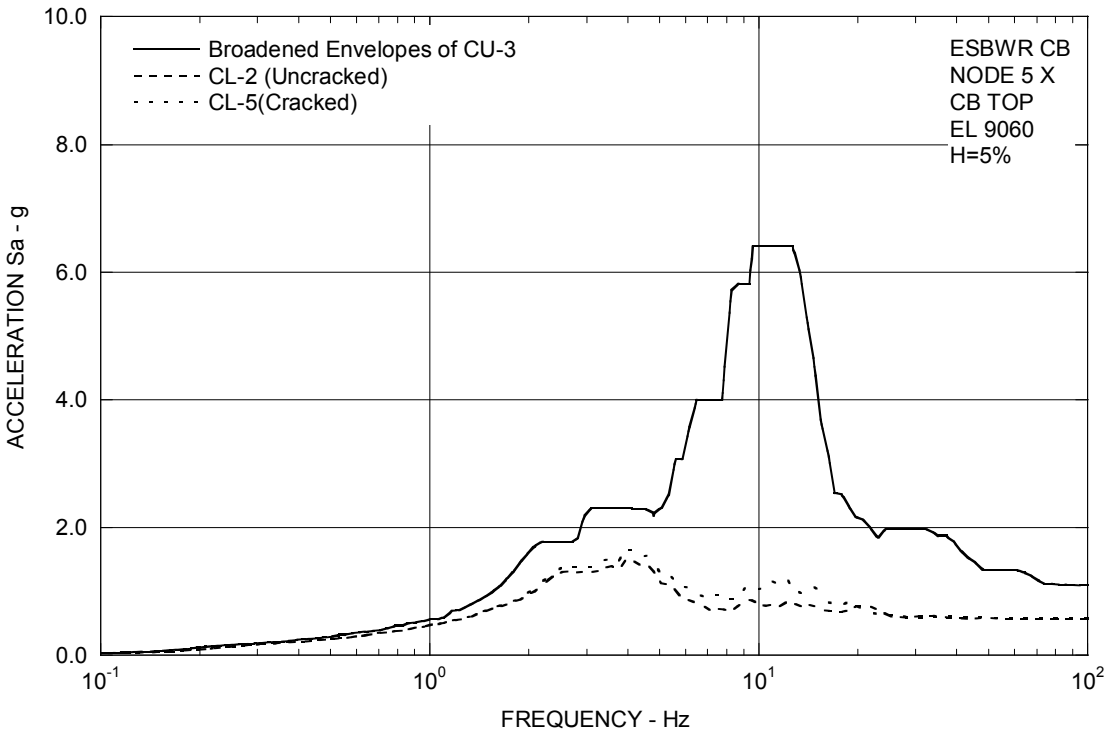

Figure 3A.8.9-1g. FRS (Effect of Concrete Cracking) – CB Top X

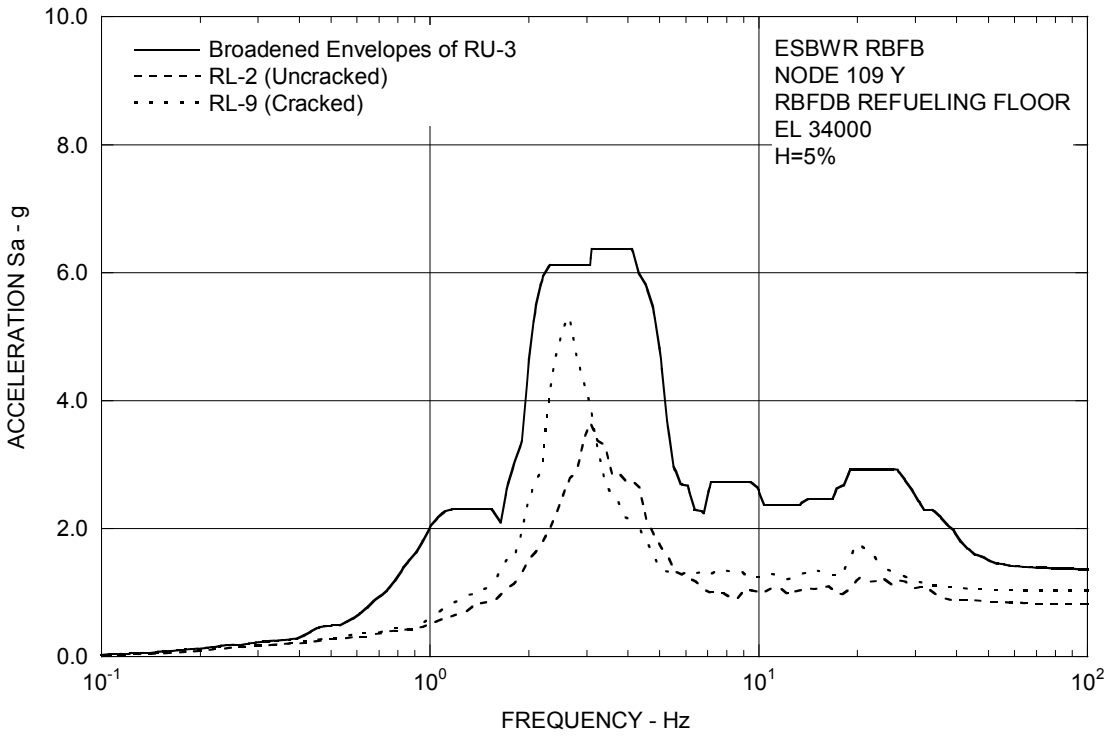

Figure 3A.8.9-2a. FRS (Effect of Concrete Cracking) – RBFB Refueling Floor Y

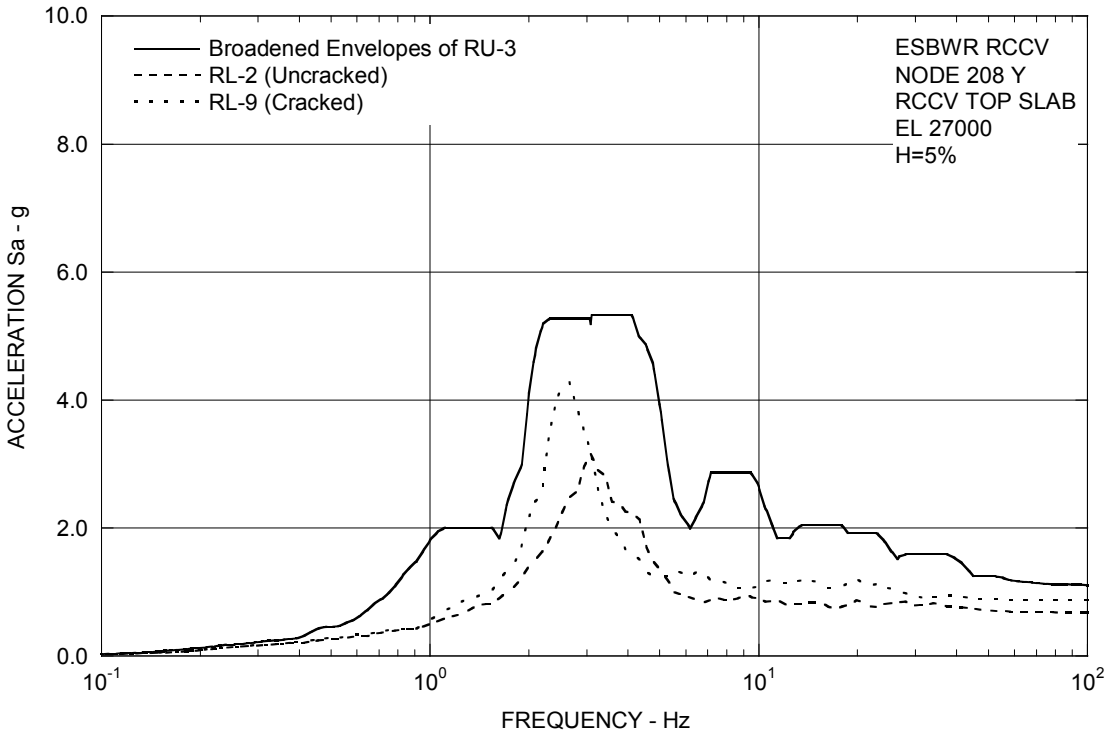

Figure 3A.8.9-2b. FRS (Effect of Concrete Cracking) – RCCV Top Slab Y

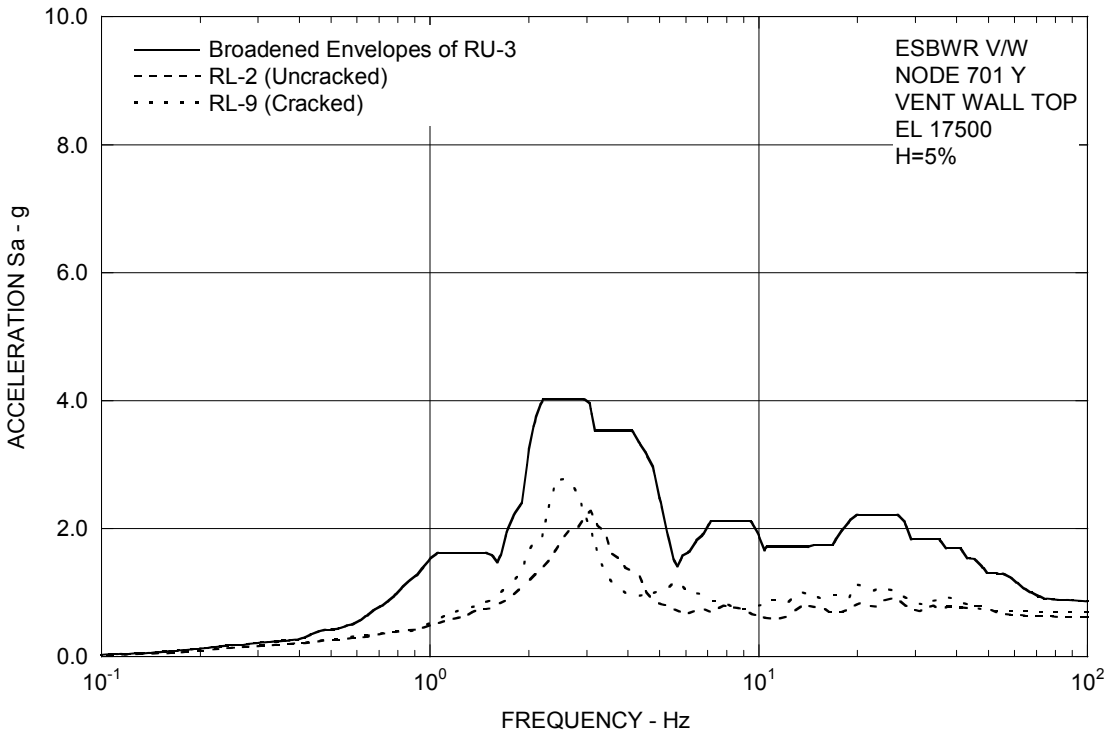

Figure 3A.8.9-2c. FRS (Effect of Concrete Cracking) – Vent Wall Top Y

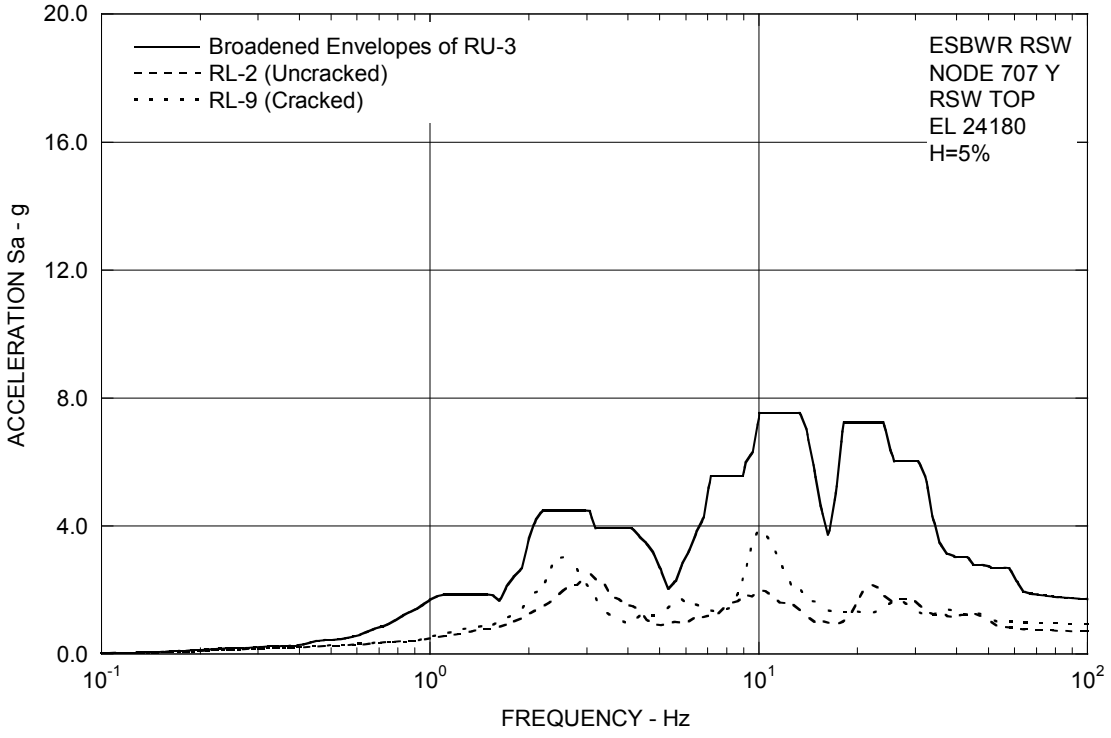

Figure 3A.8.9-2d. FRS (Effect of Concrete Cracking) – RSW Top Y

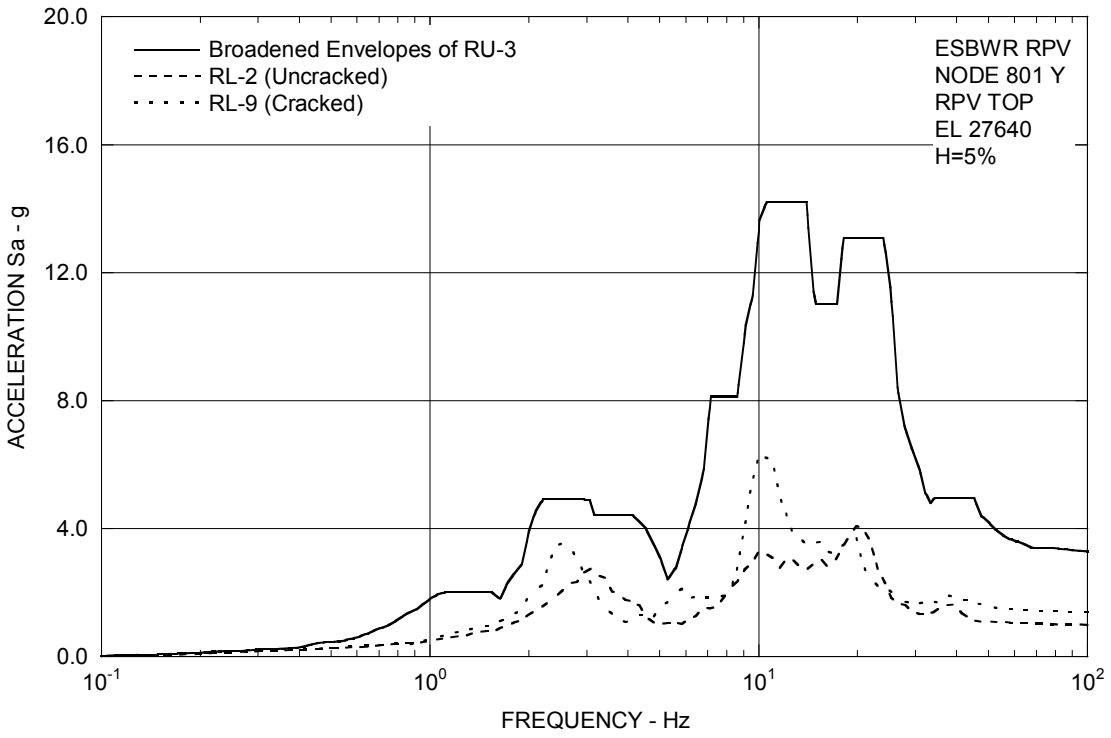

Figure 3A.8.9-2e. FRS (Effect of Concrete Cracking) – RPV Top Y

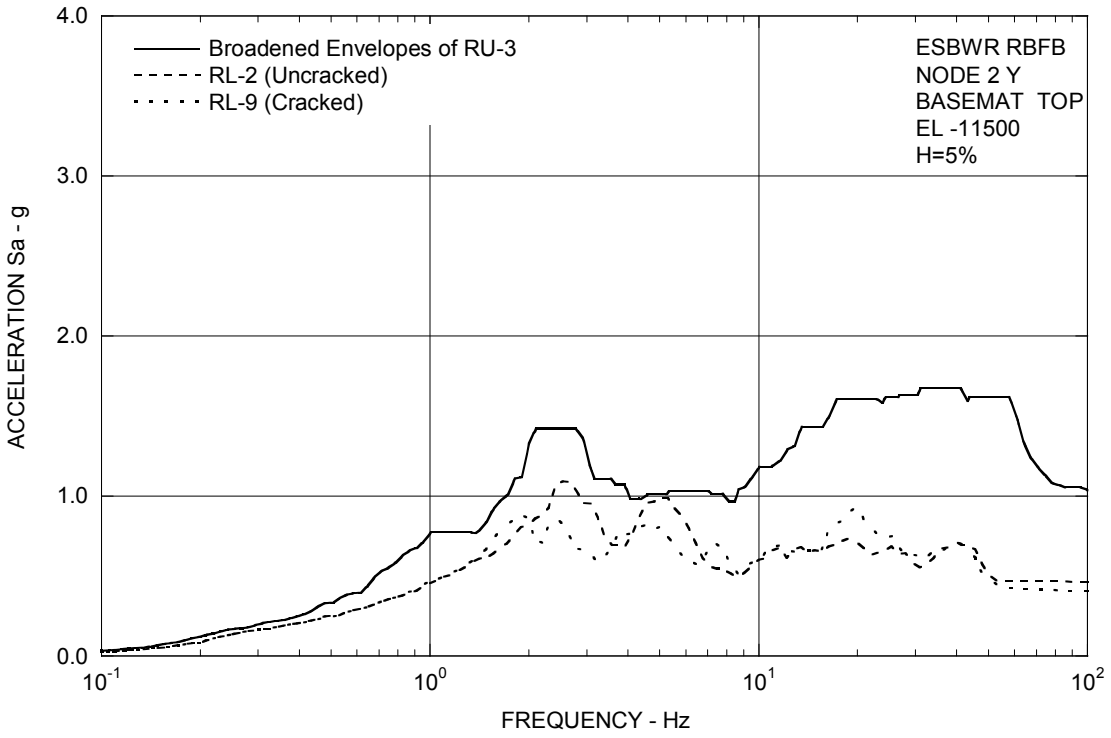

Figure 3A.8.9-2f. FRS (Effect of Concrete Cracking) – RBFB Basemat Y

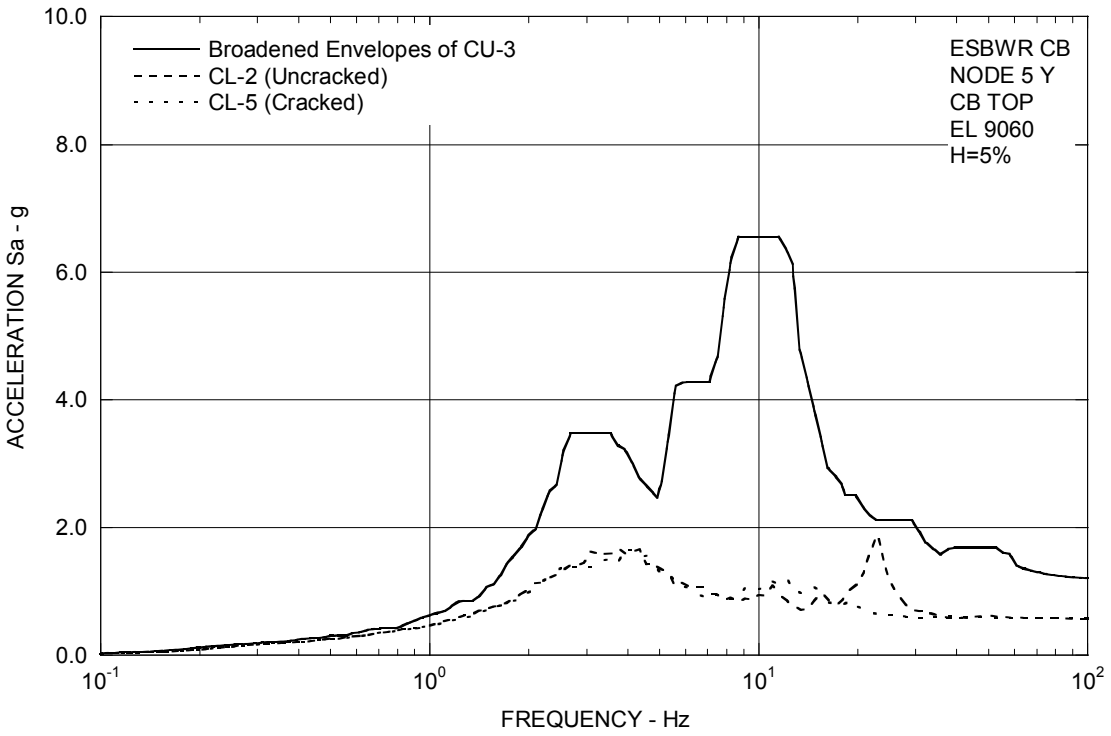

Figure 3A.8.9-2g. FRS (Effect of Concrete Cracking) – CB Top Y

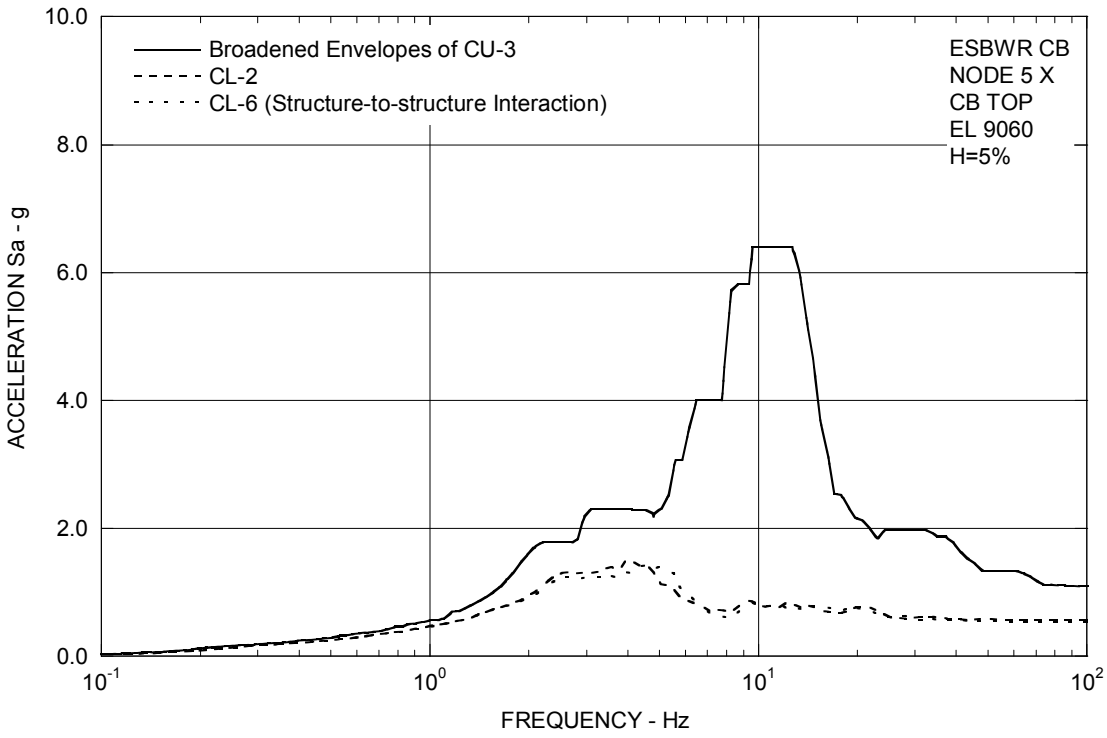

Figure 3A.8.11-1. FRS (Effect of Structure-Structure Interaction) – CB Top X

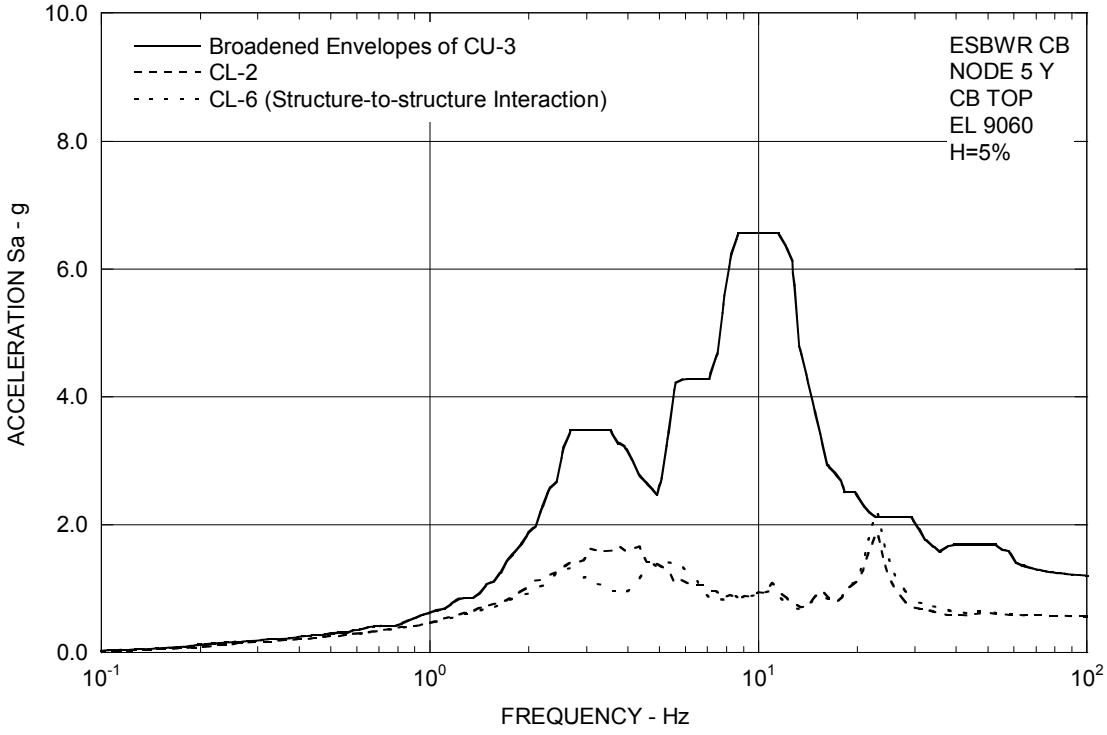

Figure 3A.8.11-2. FRS (Effect of Structure-Structure Interaction) – CB Top Y

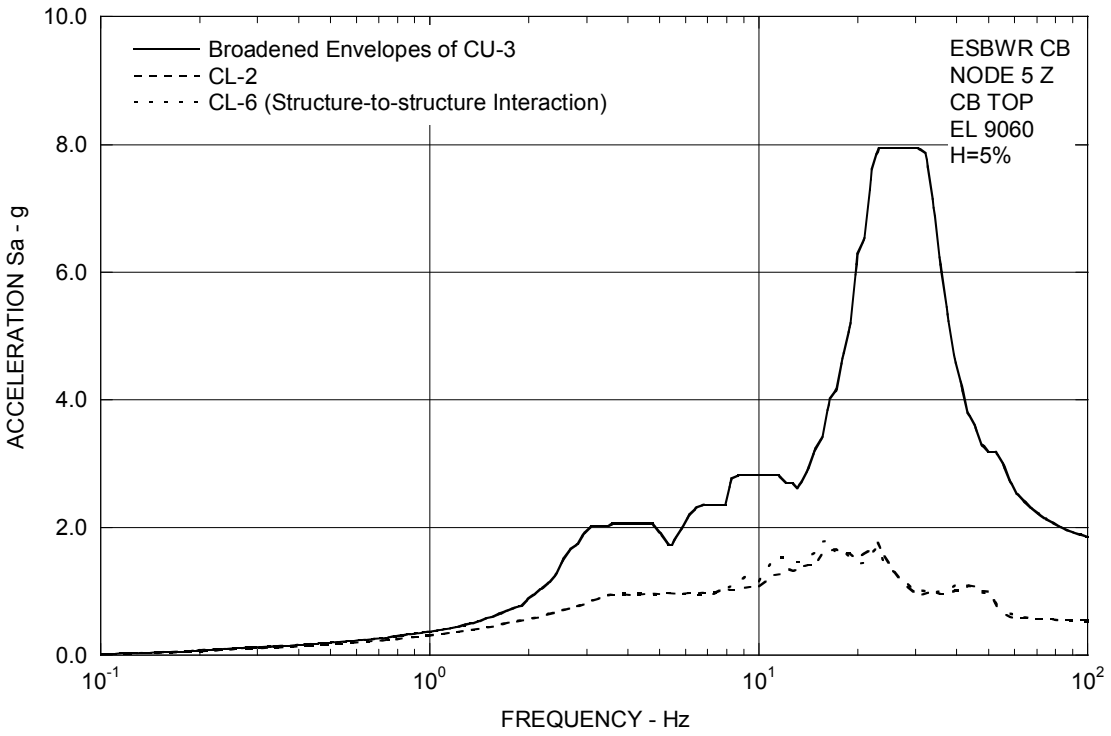

Figure 3A.8.11-3. FRS (Effect of Structure-Structure Interaction) – CB Top Z

3A.9 SITE ENVELOPE SEISMIC RESPONSES

The site-envelope seismic loads are established from the envelopes of all analysis results from SSI cases summarized in Table 3A.6-1. The site-envelope seismic loads obtained are applicable for the design of Seismic Category I (C-I) and II (C-II) structures, systems and components housed in the ESBWR standard plant.

3A.9.1 Enveloping Maximum Structural Loads

The enveloping maximum shear and moment distributions along the RBFB walls, RCCV, vent wall/pedestal, RSW, key RPV/internals, and the CB walls are shown in Tables 3A.9-1a through 3A.9-1f. These shears and moments are the envelope of all SSI cases, except for the LOCA flood case (RU-6). Tables 3A.9-2a through 3A.9-2e show enveloping maximum responses for the RBFB LOCA flood case (RU-6). The torsional moments for building structures are due to geometric eccentricities only. Additional torsion due to an accidental eccentricity of 5% of maximum floor dimension under consideration is added for the design of building structures.

The vertical loads are expressed in terms of enveloping absolute acceleration. The enveloping maximum acceleration values are shown in Tables 3A.9-3a through 3A.9-3g for all cases except for LOCA flood case (RU-6). Tables 3A.9-4a through 3A.9-4e show enveloping maximum responses for LOCA flood case (RU-6). These acceleration values do not include the coupling effect and are only applicable for structural analysis in combination with the seismic loads due to horizontal shakings.

3A.9.2 Enveloping Floor Response Spectra

The site-envelope SSE floor response spectra are obtained according to the following steps:

- For each soil case analyzed, the calculated co-directional floor response spectra in X, Y, and Z directions are combined by the SRSS method to obtain floor response spectra at the building edges considering the coupling effects between vertical and rocking and between lateral and torsion motions.
- Individual site responses are enveloped to form the site-envelope response spectra in each of the 3 directions.
- The envelope spectra are subsequently peak broadened by ±15%.

The site-envelope peak-broadened SSE floor response spectra at critical damping ratios 2, 3, 4, 5, 7, 10, and 20% for the RBFB and CB are shown in Figures 3A.9-1a through 3A.9-1g for the X direction, in Figures 3A.9-2a through 3A.9-2g for the Y direction, and in Figures 3A.9-3a through 3A.9-3g for the vertical direction. For seismic design of equipment and piping, the alternative seismic input can be the individual floor response spectra of each site condition considered in generating the site-envelope spectra.

Table 3A.9-1a

Enveloping Seismic Loads: RBFB Stick

Elev. (m)	Node No.	Elem No.	Shear		Moment		Torsion (MN-m)
			X-Dir. (MN)	Y-Dir. (MN)	X-Dir. (MN-m)	Y-Dir. (MN-m)	
52.40	110				1642	1808	
		1110	151.9	158.2	4303	4465	1379
34.00	109				5585	5497	
		1109	190.7	153.0	6477	6317	2405
27.00	108				7685	7106	
		1108	425.4	400.7	8964	8596	3329
22.50	107				9905	9193	
		1107	483.7	464.0	11464	11297	6093
17.50	106				12386	11935	
		1106	532.9	555.4	13778	13867	5068
13.57	105				14298	14377	
		1105	569.2	599.9	16593	16740	5245
9.06	104				16966	17191	
		1104	610.1	654.3	19378	19672	5985
4.65	103				19064	20192	
		1103	839.8	872.2	23163	24272	11425
-1.00	102				23673	24948	
		1102	871.4	938.5	27655	29263	11523
-6.40	101				28126	30038	
-11.50	2	1101	933.6	1029.7	32235	35275	11690

Note: Total torsional moments are obtained by the absolute sum of the accidental torsional moments and the values of the geometric torsional moments shown. The accidental torsional moment is the product of the horizontal force component and an eccentricity of 5% of the larger horizontal dimension at various elevations.

Table 3A.9-1b

Enveloping Seismic Loads: RCCV Stick

Elev. (m)	Node No.	Elem No.	Shear		Moment		Torsion (MN-m)
			X-Dir. (MN)	Y-Dir. (MN)	X-Dir. (MN-m)	Y-Dir. (MN-m)	
34.00	209				195	577	
		1209	137.0	183.2	1057	1496	36
27.00	208				1708	2532	
		1208	164.9	248.5	2959	4368	1814
17.50	206				3306	4715	
		1206	230.2	290.2	4147	5761	1982
13.57	205				4327	5949	
		1205	263.4	326.2	5404	7264	2186
9.06	204				5628	7519	
		1204	304.2	365.8	6785	8909	2616
4.65	203				6992	9171	
		1203	225.8	289.4	7958	10581	2870
-1.00	202				8076	10738	
		1202	271.7	330.6	9417	12523	2926
-6.40	201				9534	12651	
-11.50	2	1201	261.5	303.5	10836	14200	1962

Note: Total torsional moments are obtained by the absolute sum of the accidental torsional moments and the values of the geometric torsional moments shown. The accidental torsional moment is the product of the horizontal force component and an eccentricity of 5% of the larger horizontal dimension at various elevations.

Table 3A.9-1c

Enveloping Seismic Loads: VW/Pedestal Stick

Elev. (m)	Node No.	Elem No.	Shear		Moment		Torsion (MN-m)
			X-Dir. (MN)	Y-Dir. (MN)	X-Dir. (MN-m)	Y-Dir. (MN-m)	
17.50	701				78	85	
		701	28.0	28.4	100	122	73
14.50	702				119	139	
		702	29.5	30.5	184	217	75
11.50	703				185	225	
		703	30.1	33.2	276	316	77
8.50	704				276	320	
		704	30.4	35.3	307	352	78
7.4625	705				288	341	
		705	31.0	29.4	356	407	59
4.65	706,303				547	552	
		1303	32.8	44.8	567	594	142
2.4165	377				694	730	
		1377	48.1	66.3	748	868	172
-1.00	302				813	900	
		1302	65.6	81.4	903	1033	146
-2.75	376				903	1033	
		1376	66.0	81.7	1091	1330	146
-6.40	301				1131	1346	
-11.50	2	1301	104.4	121.2	1638	1963	118

Note: Total torsional moments are obtained by the absolute sum of the accidental torsional moments and the values of the geometric torsional moments shown. The accidental torsional moment is the product of the horizontal force component and an eccentricity of 5% of the larger horizontal dimension at various elevations.

Table 3A.9-1d

Enveloping Seismic Loads: RSW Stick

Elev. (m)	Node No.	Elem No.	Shear		Moment		Torsion (MN-m)
			X-Dir. (MN)	Y-Dir. (MN)	X-Dir. (MN-m)	Y-Dir. (MN-m)	
24.18	707				2.1	1.7	
		707	2.9	2.7	13.0	12.2	0.4
20.20	708				18.4	16.2	
		708	14.6	11.7	79.0	64.3	1.4
15.775	709				81.9	66.8	
		709	17.3	13.7	158.4	125.5	1.9
11.35	710				159.1	128.3	
		710	19.9	15.9	236.2	187.6	2.4
7.4625	711				197.0	183.6	
		711	41.1	35.6	292.4	251.3	22.0
4.65	712				117.5	118.8	
		712	14.3	19.5	126.3	136.0	30.3
2.4165	713				3.3	3.2	
		713	1.5	1.2	2.7	2.7	0.2
1.96	714				2.5	2.4	
-0.80	715	714	0.8	0.7	0.5	0.5	0.1

Note: Total torsional moments are obtained by the absolute sum of the accidental torsional moments and the values of the geometric torsional moments shown. The accidental torsional moment is the product of the horizontal force component and an eccentricity of 5% of the larger horizontal dimension at various elevations.

Table 3A.9-1e

Enveloping Seismic Loads: RPV Stick

Elev. (m)	Node No.	Elem No.	Axial (MN)	Shear		Moment	
				X-Dir. (MN)	Y-Dir. (MN)	X-Dir. (MN-m)	Y-Dir. (MN-m)
Shroud	845		8.58			16.2	14.3
Bottom	846	844	8.58	7.2	7.0	21.3	17.3
RPV	815		25.26			143.8	135.5
Support	711	871	25.26	18.6	17.9	141.3	132.9

Table 3A.9-1f

Enveloping Seismic Loads: CB Stick

Elev. (m)	Node No.	Elem No.	Shear		Moment		Torsion (MN-m)
			X-Dir. (MN)	Y-Dir. (MN)	X-Dir. (MN-m)	Y-Dir. (MN-m)	
13.50	6	--	13.6	15.1	--	--	--
9.06	5				184	132	
		5	43.6	45.2	300	289	35.6
4.65	4				450	389	
		4	72.5	69.8	897	768	49.4
-2.00	3				996	802	
		3	126.4	101.1	1428	1130	48.4
-7.40	2				1466	1136	
-10.40	1	2	96.2	94.6	1688	1362	49.8

Note: Total torsional moments are obtained by the absolute sum of the accidental torsional moments and the values of the geometric torsional moments shown. The accidental torsional moment is the product of the horizontal force component and an eccentricity of 5% of the larger horizontal dimension at various elevations.

Table 3A.9-2a

Enveloping Seismic Loads for LOCA Flooding: RBFB Stick

Elev. (m)	Node No.	Elem No.	Shear		Moment		Torsion (MN-m)
			X-Dir. (MN)	Y-Dir. (MN)	X-Dir. (MN-m)	Y-Dir. (MN-m)	
52.40	110				1588	1789	
		1110	129.4	159.9	3058	4465	1396
34.00	109				4290	5467	
		1109	189.5	150.2	4649	6094	2411
27.00	108				6201	7093	
		1108	420.7	356.7	7075	8018	3326
22.50	107				7903	8631	
		1107	472.9	398.8	8922	10425	5458
17.50	106				9973	11033	
		1106	507.1	471.9	11886	12690	4404
13.57	105				12494	13131	
		1105	536.2	506.5	14818	15142	4769
9.06	104				15328	15475	
		1104	574.7	548.2	17731	17564	5178
4.65	103				17613	17819	
		1103	813.1	723.7	21830	21065	10199
-1.00	102				22546	21467	
		1102	861.5	809.0	26988	25144	10689
-6.40	101				27557	25919	
		1101	938.7	914.9	31989	30136	11690
-11.50	2				43718	45297	
-15.50	1	1021	1443.5	1436.7	48837	50465	12082

Note: Total torsional moments are obtained by the absolute sum of the accidental torsional moments and the values of the geometric torsional moments shown. The accidental torsional moment is the product of the horizontal force component and an eccentricity of 5% of the larger horizontal dimension at various elevations.

Table 3A.9-2b

Enveloping Seismic Loads for LOCA Flooding: RCCV Stick

Elev. (m)	Node No.	Elem No.	Shear		Moment		Torsion (MN-m)
			X-Dir. (MN)	Y-Dir. (MN)	X-Dir. (MN-m)	Y-Dir. (MN-m)	
34.00	209				189	567	
		1209	118.5	178.7	890	1429	36
27.00	208				1643	2508	
		1208	161.9	245.7	2818	4006	1669
17.50	206				3208	4341	
		1206	225.8	267.5	3848	5170	1735
13.57	205				4051	5339	
		1205	252.2	287.6	4885	6484	1988
9.06	204				5107	6740	
		1204	302.8	302.0	6319	7994	2263
4.65	203				6517	8244	
		1203	225.8	250.6	7575	9506	2562
-1.00	202				7716	9681	
		1202	272.0	289.8	9007	11082	2714
-6.40	201				9126	11219	
-11.50	2	1201	262.8	269.2	10336	12464	1962

Note: Total torsional moments are obtained by the absolute sum of the accidental torsional moments and the values of the geometric torsional moments shown. The accidental torsional moment is the product of the horizontal force component and an eccentricity of 5% of the larger horizontal dimension at various elevations.

Table 3A.9-2c

Enveloping Seismic Loads for LOCA Flooding: VW/Pedestal Stick

Elev. (m)	Node No.	Elem No.	Shear		Moment		Torsion (MN-m)
			X-Dir. (MN)	Y-Dir. (MN)	X-Dir. (MN-m)	Y-Dir. (MN-m)	
17.50	701				55	60	
		701	15.8	18.5	66	72	30
14.50	702				85	91	
		702	14.4	16.0	100	123	31
11.50	703				107	127	
		703	17.4	22.6	143	158	34
8.50	704				144	159	
		704	22.4	25.9	157	173	36
7.4625	705				187	207	
		705	18.9	14.6	232	238	20
4.65	706,303				483	477	
		1303	31.0	38.2	505	512	126
2.4165	377				618	631	
		1377	47.7	57.5	682	781	154
-1.00	302				733	833	
		1302	65.6	71.4	820	933	136
-2.75	376				820	933	
		1376	66.0	71.5	1018	1141	136
-6.40	301				1052	1175	
-11.50	2	1301	104.5	107.4	1556	1630	118

Note: Total torsional moments are obtained by the absolute sum of the accidental torsional moments and the values of the geometric torsional moments shown. The accidental torsional moment is the product of the horizontal force component and an eccentricity of 5% of the larger horizontal dimension at various elevations.

Table 3A.9-2d

Enveloping Seismic Loads for LOCA Flooding: RSW Stick

Elev. (m)	Node No.	Elem No.	Shear		Moment		Torsion (MN-m)
			X-Dir. (MN)	Y-Dir. (MN)	X-Dir. (MN-m)	Y-Dir. (MN-m)	
24.18	707				2.0	1.5	
		707	2.2	1.9	10.4	8.9	0.3
20.20	708				16.0	12.8	
		708	12.2	12.0	65.5	63.5	1.2
15.775	709				67.5	65.1	
		709	13.8	13.9	127.1	126.0	1.7
11.35	710				129.3	128.1	
		710	16.8	16.4	194.1	190.0	2.4
7.4625	711				153.8	174.2	
		711	43.6	33.8	252.5	247.3	18.7
4.65	712				103.2	102.9	
		712	13.5	16.6	113.1	119.1	27.0
2.4165	713				5.4	5.0	
		713	2.4	2.2	4.5	4.1	0.4
1.96	714				3.9	3.7	
-0.80	715	714	1.3	1.2	0.7	0.8	0.2

Note: Total torsional moments are obtained by the absolute sum of the accidental torsional moments and the values of the geometric torsional moments shown. The accidental torsional moment is the product of the horizontal force component and an eccentricity of 5% of the larger horizontal dimension at various elevations.

Table 3A.9-2e

Enveloping Seismic Loads for LOCA Flooding: RPV Stick

Elev. (m)	Node No.	Elem No.	Axial (MN)	Shear		Moment	
				X-Dir. (MN)	Y-Dir. (MN)	X-Dir. (MN-m)	Y-Dir. (MN-m)
Shroud	845		6.22			18.0	13.7
Bottom	846	844	6.22	9.0	5.3	25.2	16.4
RPV	815		21.34			121.2	130.8
Support	711	871	21.34	18.5	17.8	122.3	130.4

Table 3A.9-3a

Enveloping Maximum Vertical Acceleration: RBFB

Elev. (m)	Node No.	Stick Model	Max. Vertical Acceleration (g)
52.40	110	RBFB	1.25
34.00	109	RBFB	0.83
27.00	108	RBFB	0.73
22.50	107	RBFB	0.73
17.50	106	RBFB	0.73
13.57	105	RBFB	0.74
9.06	104	RBFB	0.73
4.65	103	RBFB	0.78
-1.00	102	RBFB	0.76
-6.40	101	RBFB	0.68
-11.50	2	RBFB	0.63
-15.50	1	RBFB	0.51

Note:For structural design use only.

Table 3A.9-3b

Enveloping Maximum Vertical Acceleration: RCCV

Elev. (m)	Node No.	Stick Model	Max. Vertical Acceleration (g)
34.00	209	RCCV	0.90
27.00	208	RCCV	0.88
17.50	206	RCCV	0.73
13.57	205	RCCV	0.78
9.06	204	RCCV	0.65
4.65	203	RCCV	0.69
-1.00	202	RCCV	0.59
-6.40	201	RCCV	0.59

Note: For structural design use only.

Table 3A.9-3c

Enveloping Maximum Vertical Acceleration: VW/Pedestal

Elev. (m)	Node No.	Stick Model	Max. Vertical Acceleration (g)
17.50	701	VW	1.10
14.50	702	VW	1.04
11.50	703	VW	0.92
8.50	704	VW	0.77
7.4625	705	VW	0.70
4.65	706, 303	Pedestal	0.67
2.4165	377	Pedestal	0.64
-1.00	302	Pedestal	0.59
-2.753	376	Pedestal	0.51
-6.40	301	Pedestal	0.50

Note:For structural design use only.

Table 3A.9-3d

Enveloping Maximum Vertical Acceleration: RSW

Elev. (m)	Node No.	Stick Model	Max. Vertical Acceleration (g)
24.18	707	RSW	0.97
20.20	708	RSW	0.94
15.775	709	RSW	0.84
11.35	710	RSW	0.76
7.4625	711	RSW	0.70
4.65	712	RSW	0.67
2.4165	713	RSW	0.64
1.96	714	RSW	0.64
-0.80	715	RSW	0.65

Note:For structural design use only.

Table 3A.9-3e

Enveloping Maximum Vertical Acceleration: RBFB Flexible Slab Oscillators

Elev. (m)	Node No.	Stick Model	Max. Vertical Acceleration (g)
52.40	9101	Oscillator	1.20
	9102	Oscillator	1.82
	9103	Oscillator	3.14
	9104	Oscillator	2.26
	9105	Oscillator	2.32
	9106	Oscillator	2.99
	9107	Oscillator	2.80
	9108	Oscillator	2.61
34.00	9091	Oscillator	1.29
	9092	Oscillator	1.06
27.00	9081	Oscillator	1.16
	9082	Oscillator	0.99
	9083	Oscillator	1.09
	9084	Oscillator	1.31
	9085	Oscillator	0.97
22.50	9071	Oscillator	1.60
	9072	Oscillator	1.31
	9073	Oscillator	2.03
	9074	Oscillator	1.31
	9075	Oscillator	1.16
17.50	9061	Oscillator	1.79
	9062	Oscillator	1.49
	9063	Oscillator	0.82
	9064	Oscillator	1.84
	9065	Oscillator	1.42
	99064	Oscillator	1.07

Note:For structural design use only.

Table 3A.9-3e

Enveloping Maximum Vertical Acceleration: RBFB Flexible Slab Oscillators (Continued)

Elev. (m)	Node No.	Stick Model	Max. Vertical Acceleration (g)
13.57	9051	Oscillator	0.81
	9052	Oscillator	1.46
9.06	9041	Oscillator	0.88
	9042	Oscillator	1.42
4.65	9031	Oscillator	1.17
	9032	Oscillator	0.97
	9033	Oscillator	1.02
	9034	Oscillator	1.51
	9035	Oscillator	1.38
-1.00	9021	Oscillator	1.12
	9022	Oscillator	1.45
	9023	Oscillator	1.01
	9024	Oscillator	0.89
	9025	Oscillator	1.34
	9026	Oscillator	1.57
	9027	Oscillator	0.88
-6.40	9011	Oscillator	0.92
	9012	Oscillator	0.92
	9013	Oscillator	1.35

Note: For structural design use only.

Table 3A.9-3f

Enveloping Maximum Horizontal Acceleration: RBFB Wall Out-of-plane Oscillators

EL (m)	Node No.	Stick Model	Max. Horizontal Acceleration (g)
42.00	99981	Oscillator	1.54
(X-dir)	99982	Oscillator	1.30
42.00	99983	Oscillator	1.71
(Y-dir)	99984	Oscillator	1.56
	99985	Oscillator	1.25
13.57	99971	Oscillator	1.38
(X-dir)	99972	Oscillator	1.37
	99973	Oscillator	1.15
	99974	Oscillator	0.99
13.57	99975	Oscillator	1.28
(Y-dir)	99976	Oscillator	0.98

Note: For structural design use only.

Table 3A.9-3g

Enveloping Maximum Acceleration: CB

Elevation (m)	Node No.	Stick Model	Max. Vertical Acceleration (g)
9.06	5	CB	1.11
4.65	4	CB	0.96
-2.00	3	CB	0.63
-7.40	2	CB	0.52
-10.40	1	CB	0.46
9.06	9101	Oscillator	0.99
	9102	Oscillator	1.51
	9103	Oscillator	2.88
	9104	Oscillator	4.55
	9105	Oscillator	3.81
	9106	Oscillator	2.52
4.65	9201	Oscillator	1.99
-2.00	9301	Oscillator	0.64

Note:For structural design use only.

Table 3A.9-4a

Enveloping Maximum Vertical Acceleration for LOCA Flooding: RBFB

Elev. (m)	Node No.	Stick Model	Max. Vertical Acceleration (g)
52.40	110	RBFB	1.18
34.00	109	RBFB	0.82
27.00	108	RBFB	0.72
22.50	107	RBFB	0.66
17.50	106	RBFB	0.66
13.57	105	RBFB	0.65
9.06	104	RBFB	0.65
4.65	103	RBFB	0.69
-1.00	102	RBFB	0.65
-6.40	101	RBFB	0.56
-11.50	2	RBFB	0.54
-15.50	1	RBFB	0.51

Note: For structural design use only.

Table 3A.9-4b

Enveloping Maximum Vertical Acceleration for LOCA Flooding: RCCV

Elev. (m)	Node No.	Stick Model	Max. Vertical Acceleration (g)
34.00	209	RCCV	0.87
27.00	208	RCCV	0.86
17.50	206	RCCV	0.69
13.57	205	RCCV	0.62
9.06	204	RCCV	0.56
4.65	203	RCCV	0.52
-1.00	202	RCCV	0.50
-6.40	201	RCCV	0.49

Note: For structural design use only.

Table 3A.9-4c

Enveloping Maximum Vertical Acceleration for LOCA Flooding: VW/Pedestal

Elev. (m)	Node No.	Stick Model	Max. Vertical Acceleration (g)
17.50	701	VW	0.95
14.50	702	VW	0.87
11.50	703	VW	0.74
8.50	704	VW	0.62
7.4625	705	VW	0.62
4.65	706, 303	Pedestal	0.59
2.4165	377	Pedestal	0.56
-1.00	302	Pedestal	0.52
-2.753	376	Pedestal	0.50
-6.40	301	Pedestal	0.49

Note: For structural design use only.

Table 3A.9-4d

Enveloping Maximum Vertical Acceleration for LOCA Flooding: RSW

Elev. (m)	Node No.	Stick Model	Max. Vertical Acceleration (g)
24.18	707	RSW	0.84
20.20	708	RSW	0.82
15.775	709	RSW	0.74
11.35	710	RSW	0.63
7.4625	711	RSW	0.62
4.65	712	RSW	0.59
2.4615	713	RSW	0.56
1.96	714	RSW	0.56
-0.80	715	RSW	0.56

Note: For structural design use only.

Table 3A.9-4e

Enveloping Maximum Vertical Acceleration for LOCA Flooding: RBFB Flexible Slab Oscillators

Elev. (m)	Node No.	Stick Model	Max. Vertical Acceleration (g)
52.40	9101	Oscillator	1.02
	9102	Oscillator	1.53
	9103	Oscillator	3.08
	9104	Oscillator	2.32
	9105	Oscillator	2.29
	9106	Oscillator	2.82
	9107	Oscillator	2.76
	9108	Oscillator	2.61
34.00	9091	Oscillator	1.22
	9092	Oscillator	1.03
27.00	9081	Oscillator	1.15
	9082	Oscillator	0.97
	9083	Oscillator	1.06
	9084	Oscillator	1.27
	9085	Oscillator	0.95
22.50	9071	Oscillator	1.17
	9072	Oscillator	1.25
	9073	Oscillator	1.96
	9074	Oscillator	1.27
	9075	Oscillator	1.10
17.50	9061	Oscillator	1.75
	9062	Oscillator	1.40
	9063	Oscillator	0.79
	9064	Oscillator	1.51
	9065	Oscillator	1.38

Note: For structural design use only.

Table 3A.9-4e

Enveloping Maximum Vertical Acceleration for LOCA Flooding: RBFB Flexible Slab Oscillators (Continued)

Elev. (m)	Node No.	Stick Model	Max. Vertical Acceleration (g)
13.57	9051	Oscillator	0.83
	9052	Oscillator	1.42
9.06	9041	Oscillator	0.90
	9042	Oscillator	1.37
4.65	9031	Oscillator	1.20
	9032	Oscillator	0.97
	9033	Oscillator	0.88
	9034	Oscillator	1.47
	9035	Oscillator	1.32
-1.00	9021	Oscillator	1.11
	9022	Oscillator	1.41
	9023	Oscillator	1.01
	9024	Oscillator	0.88
	9025	Oscillator	1.26
	9026	Oscillator	1.43
	9027	Oscillator	0.93
-6.40	9011	Oscillator	0.92
	9012	Oscillator	0.88
	9013	Oscillator	1.27

Note: For structural design use only.

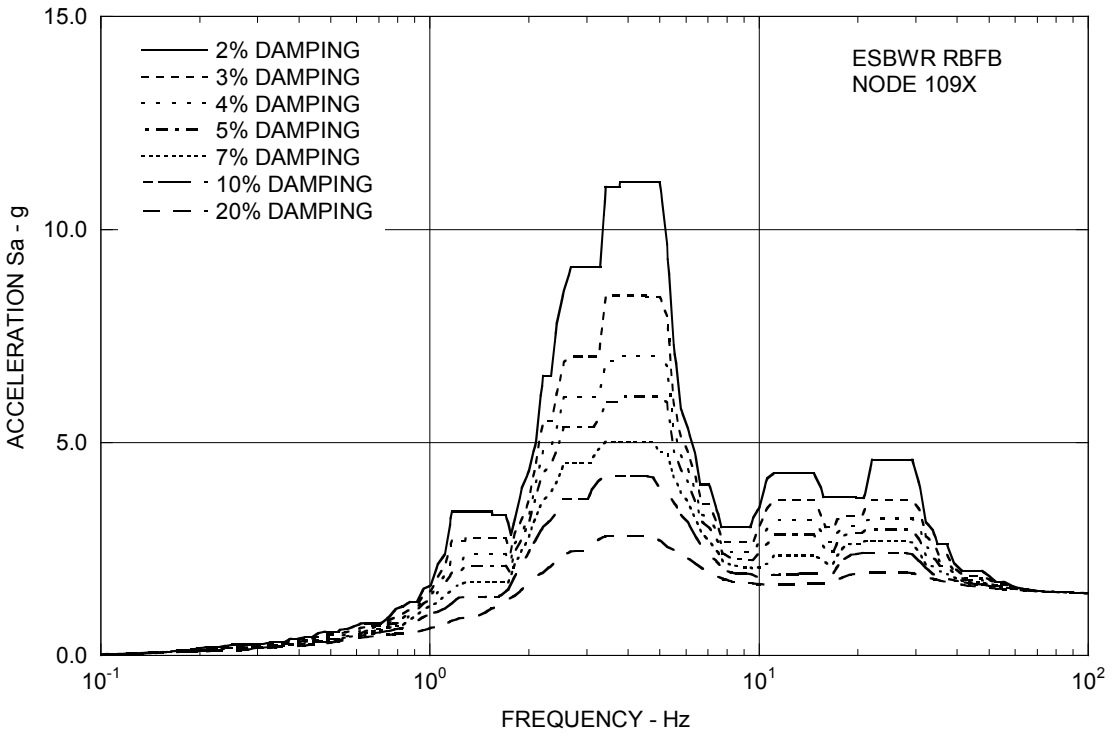

Figure 3A.9-1a. Enveloping Floor Response Spectra – RBFB Refueling Floor X

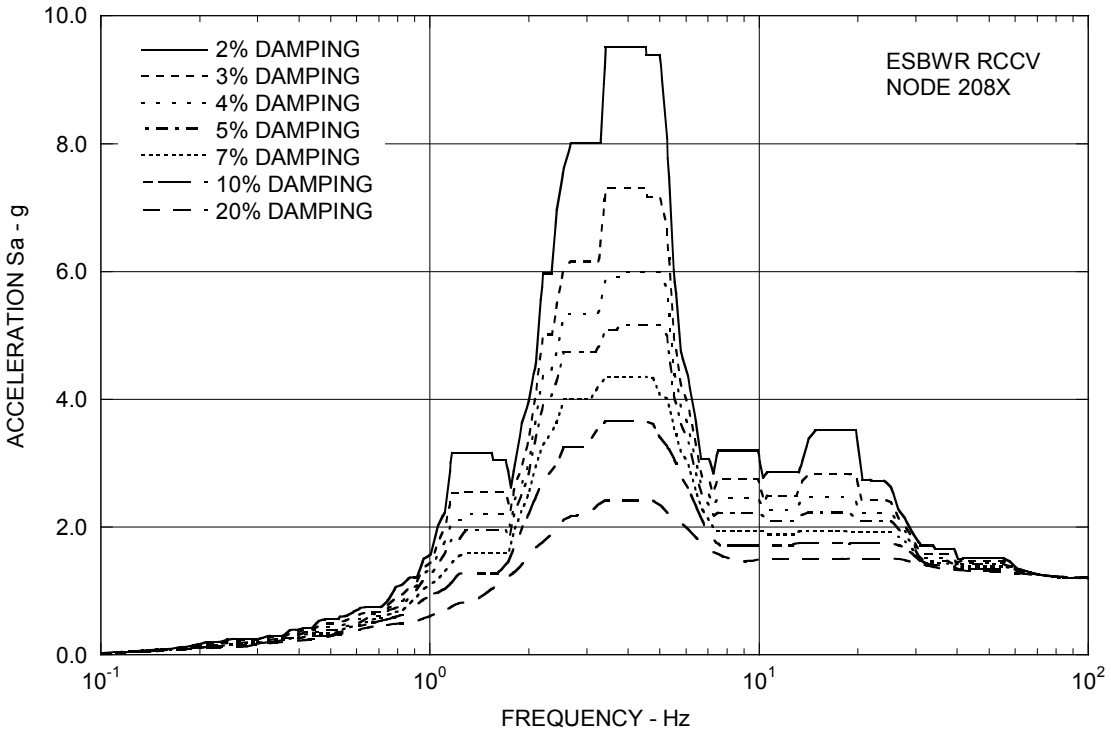

Figure 3A.9-1b. Enveloping Floor Response Spectra – RCCV Top Slab X

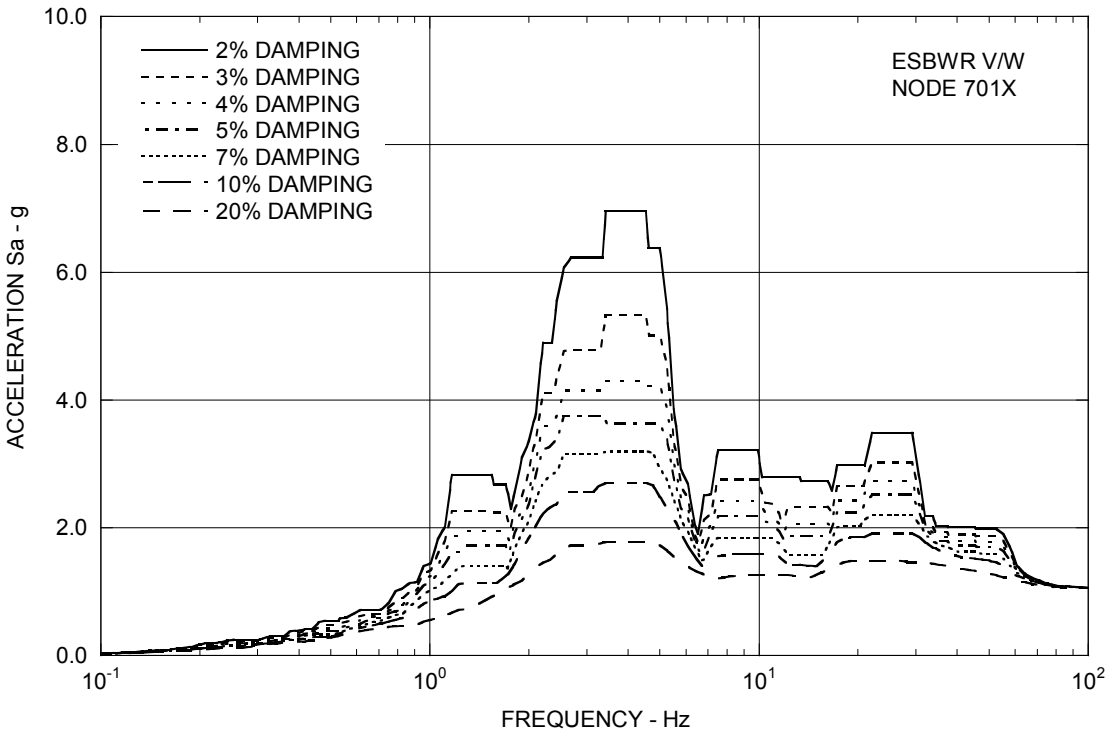

Figure 3A.9-1c. Enveloping Floor Response Spectra – Vent Wall Top X

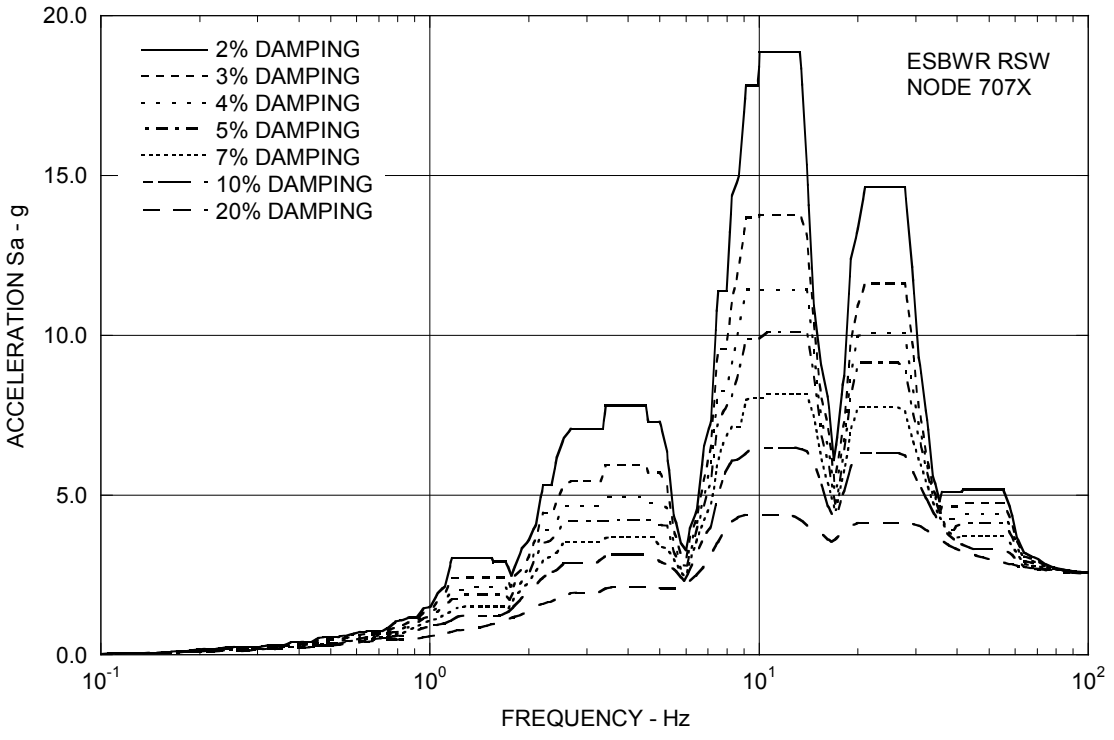

Figure 3A.9-1d. Enveloping Floor Response Spectra – RSW Top X

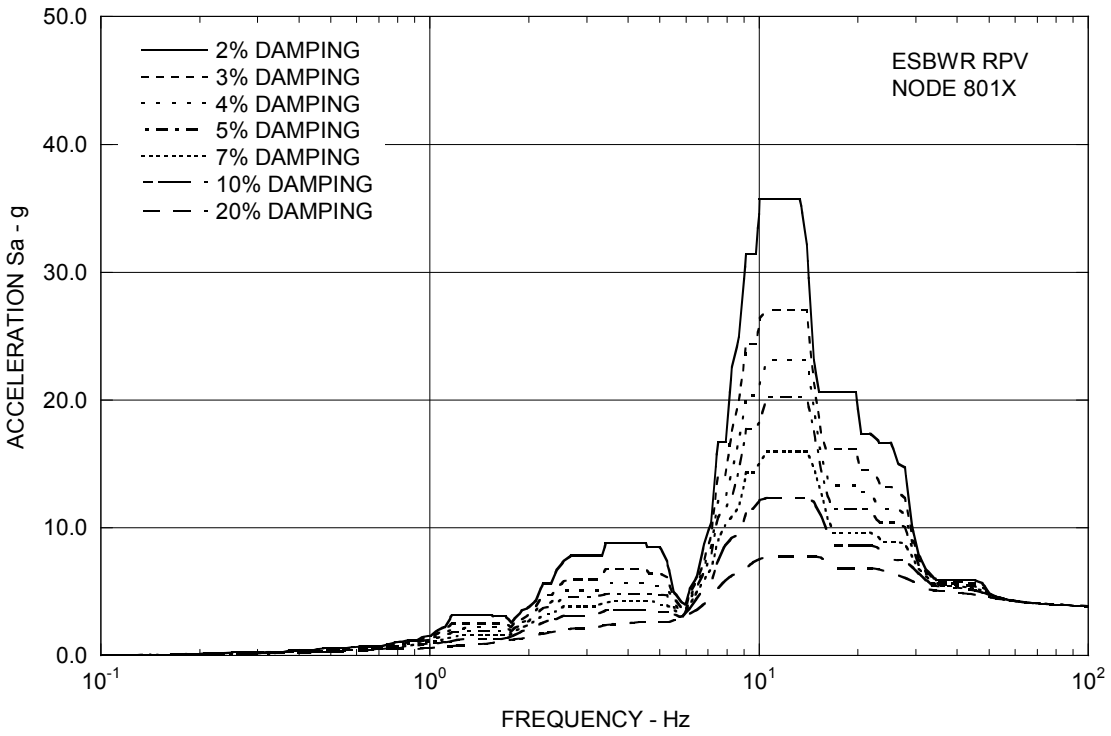

Figure 3A.9-1e. Enveloping Floor Response Spectra – RPV Top X

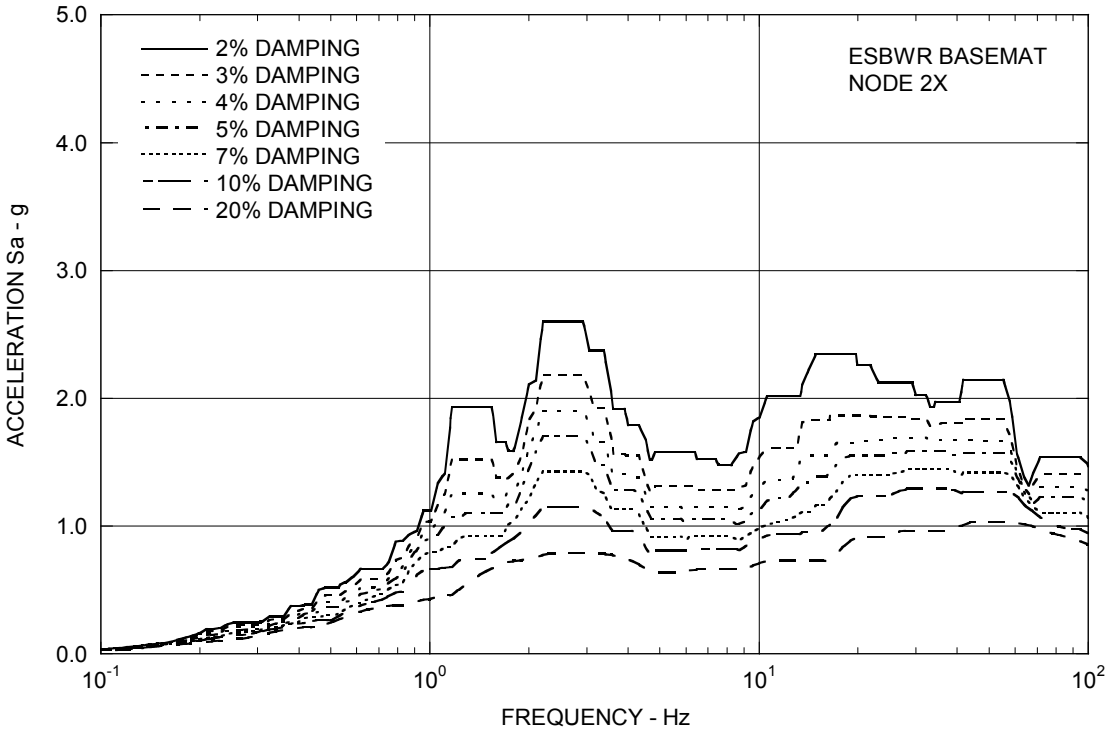

Figure 3A.9-1f. Enveloping Floor Response Spectra – RBFB Basemat X

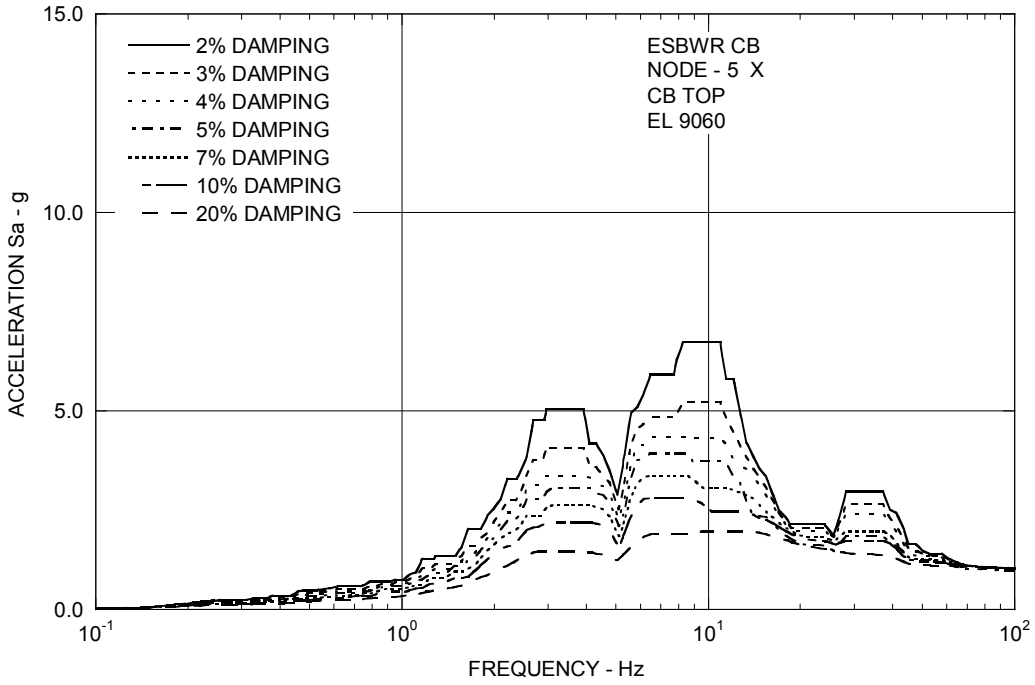

Figure 3A.9-1g. Enveloping Floor Response Spectra – CB Top X

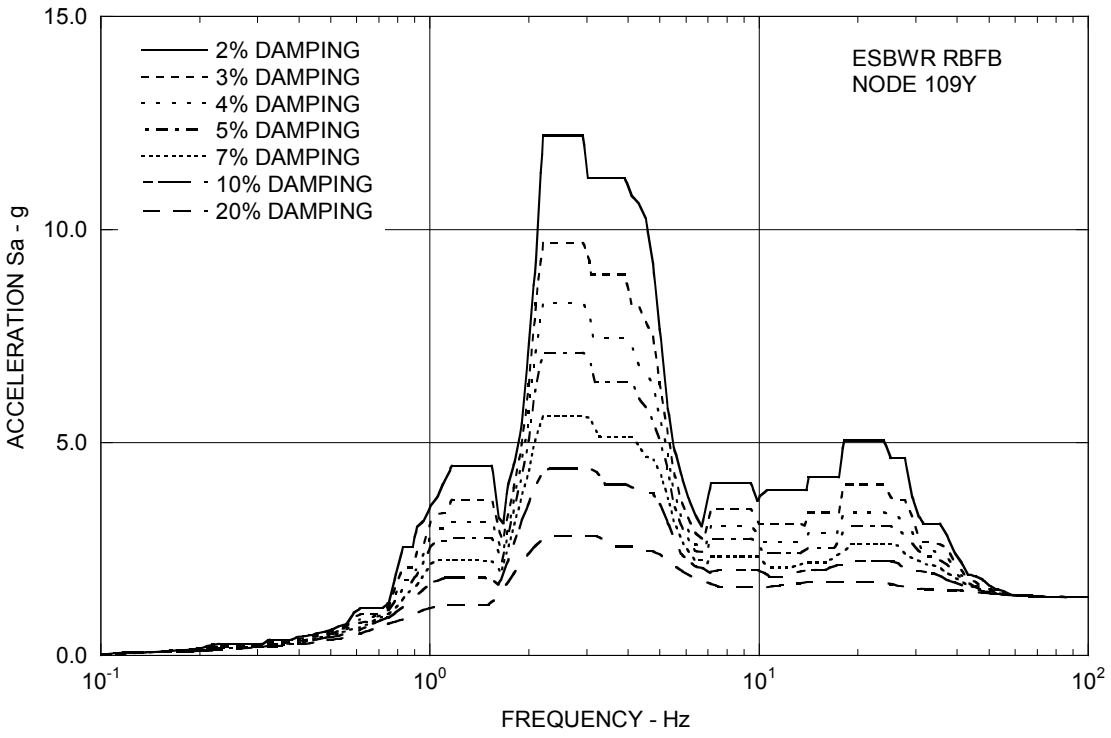

Figure 3A.9-2a. Enveloping Floor Response Spectra – RBFB Refueling Floor Y

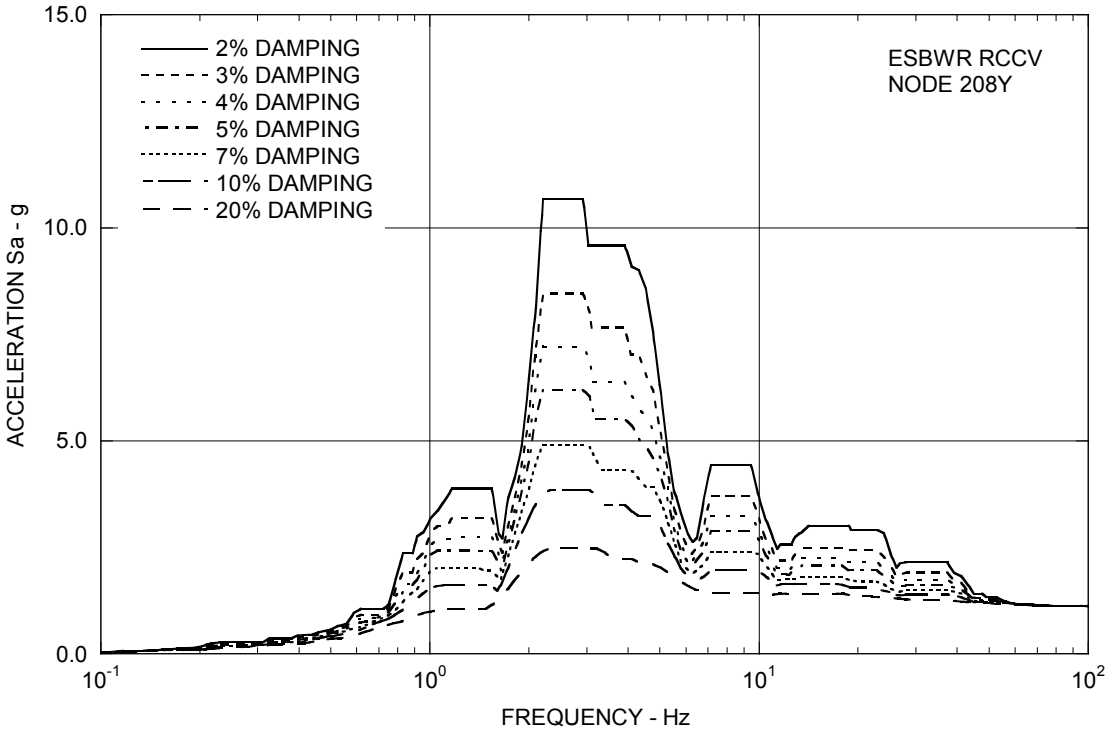

Figure 3A.9-2b. Enveloping Floor Response Spectra – RCCV Top Slab Y

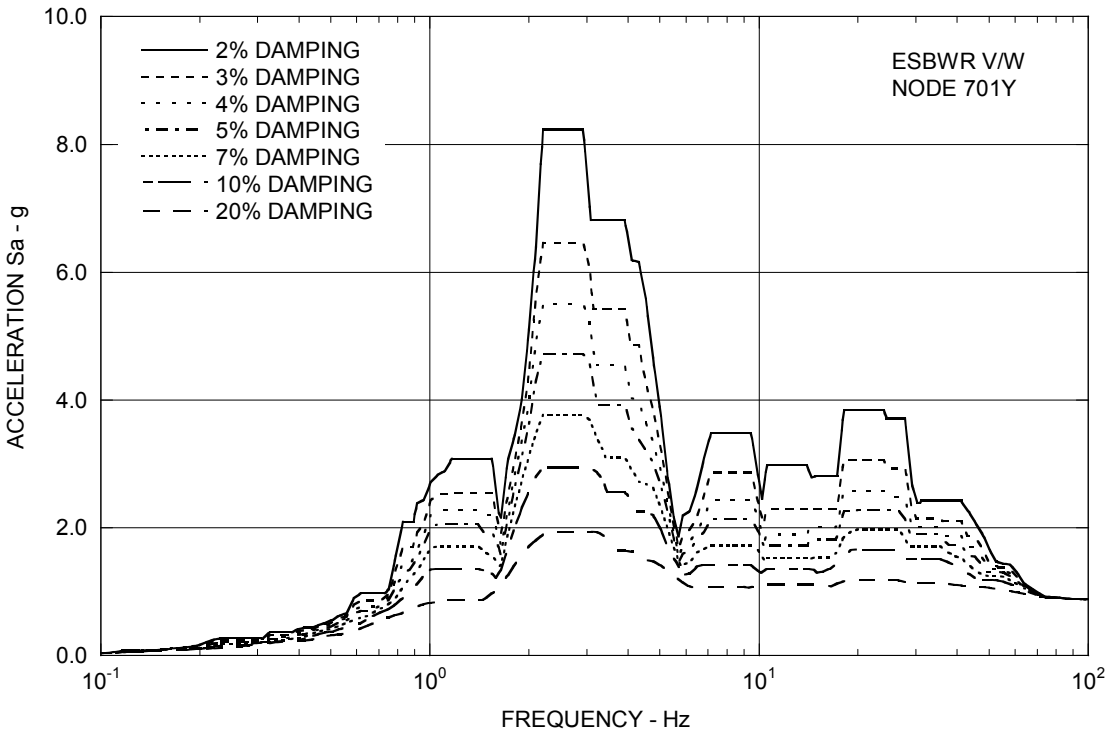

Figure 3A.9-2c. Enveloping Floor Response Spectra – Vent Wall Top Y

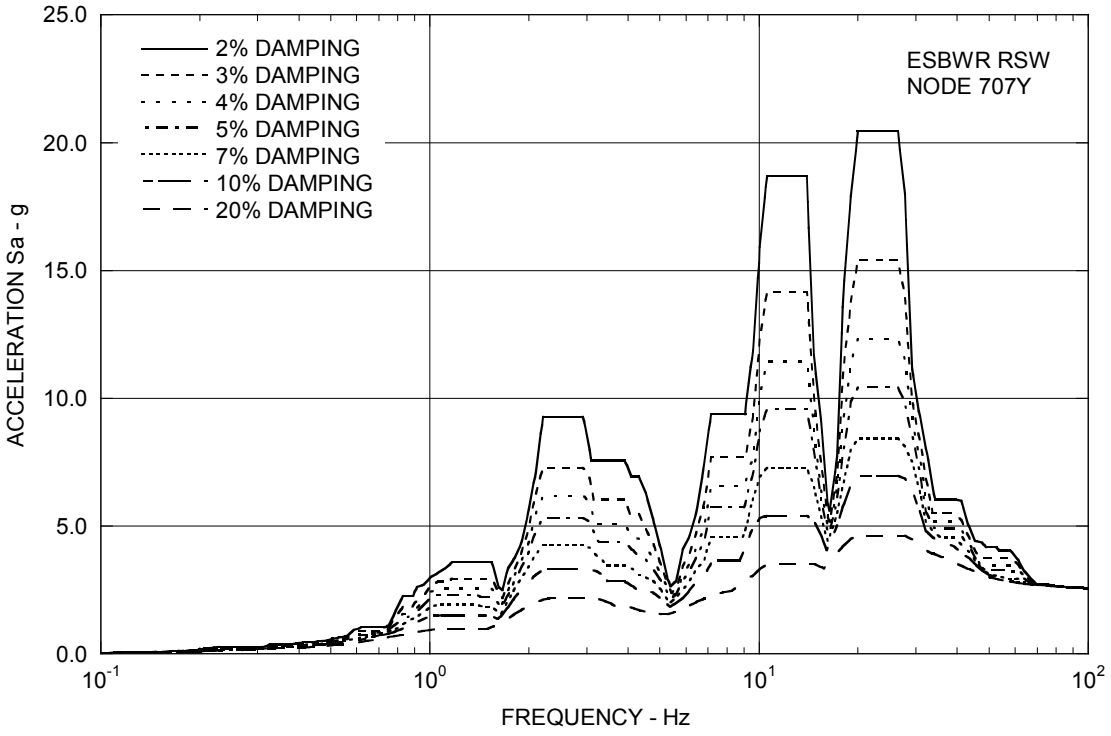

Figure 3A.9-2d. Enveloping Floor Response Spectra – RSW Top Y

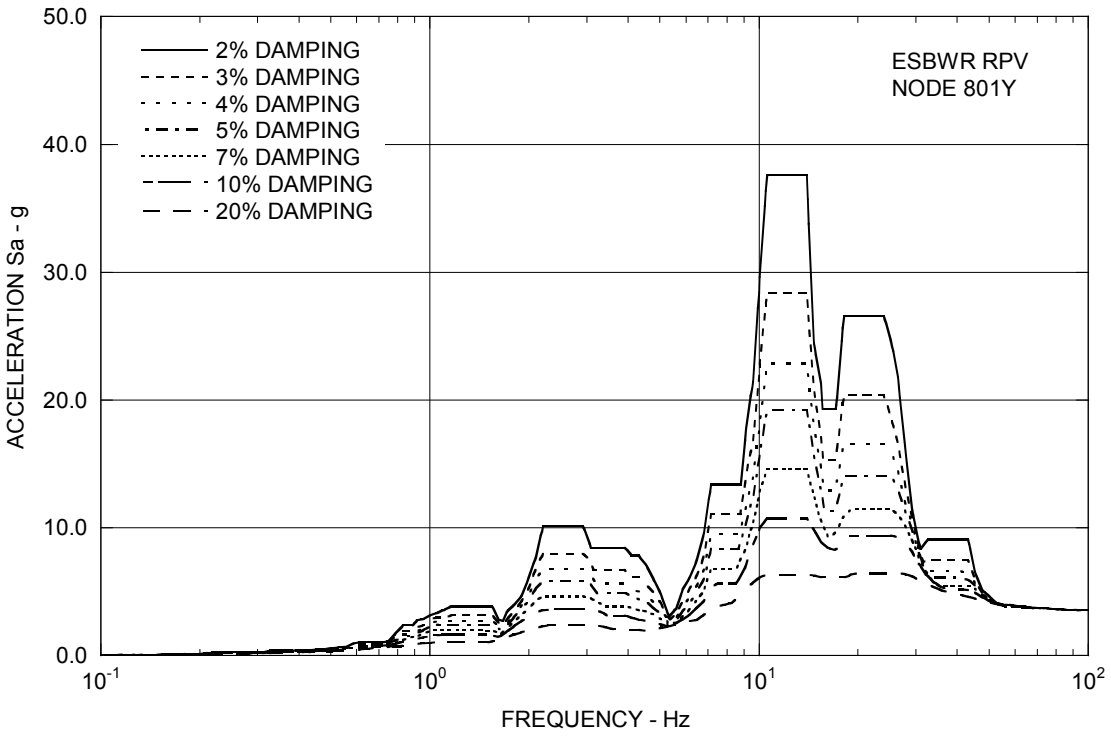

Figure 3A.9-2e. Enveloping Floor Response Spectra – RPV Top Y

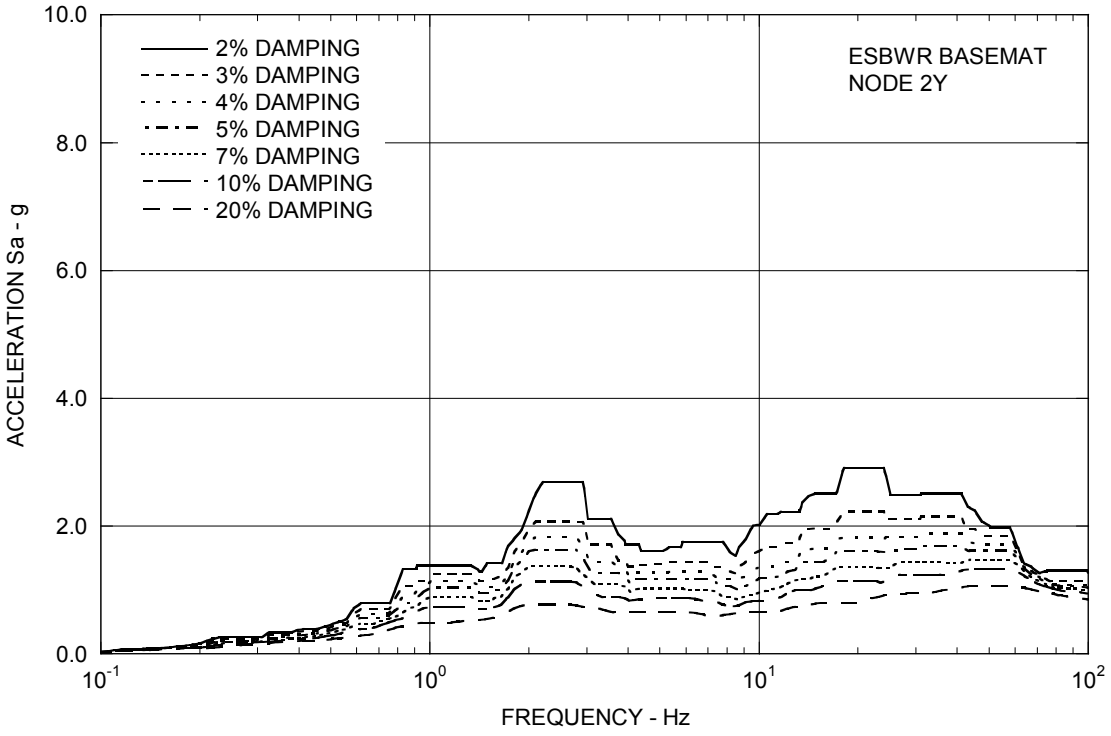

Figure 3A.9-2f. Enveloping Floor Response Spectra – RBFB Basemat Y

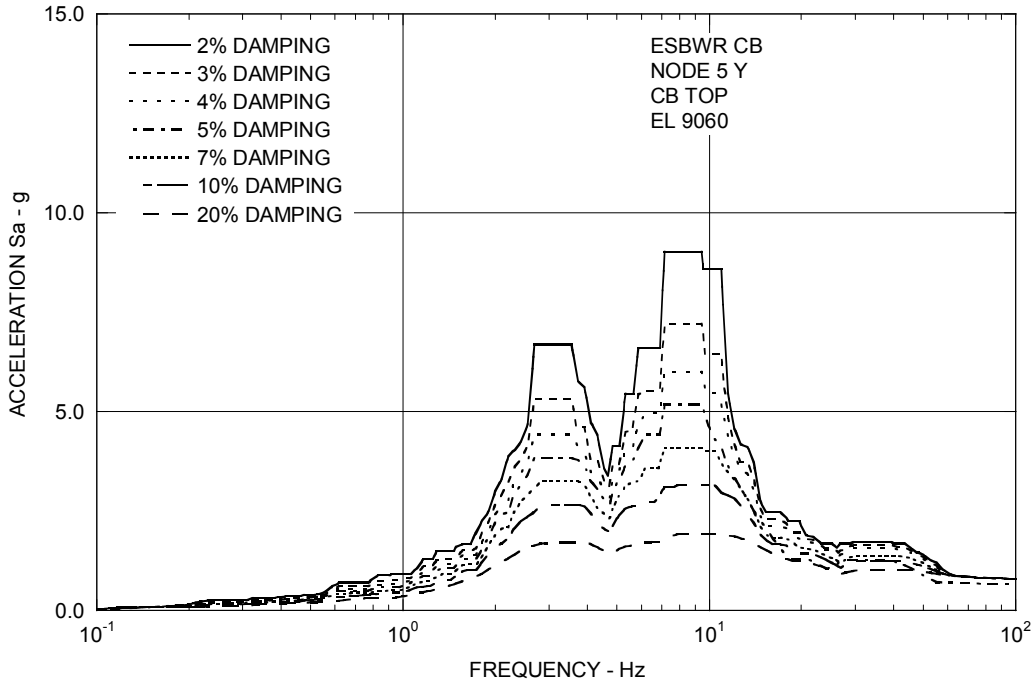

Figure 3A.9-2g. Enveloping Floor Response Spectra – CB Top Y

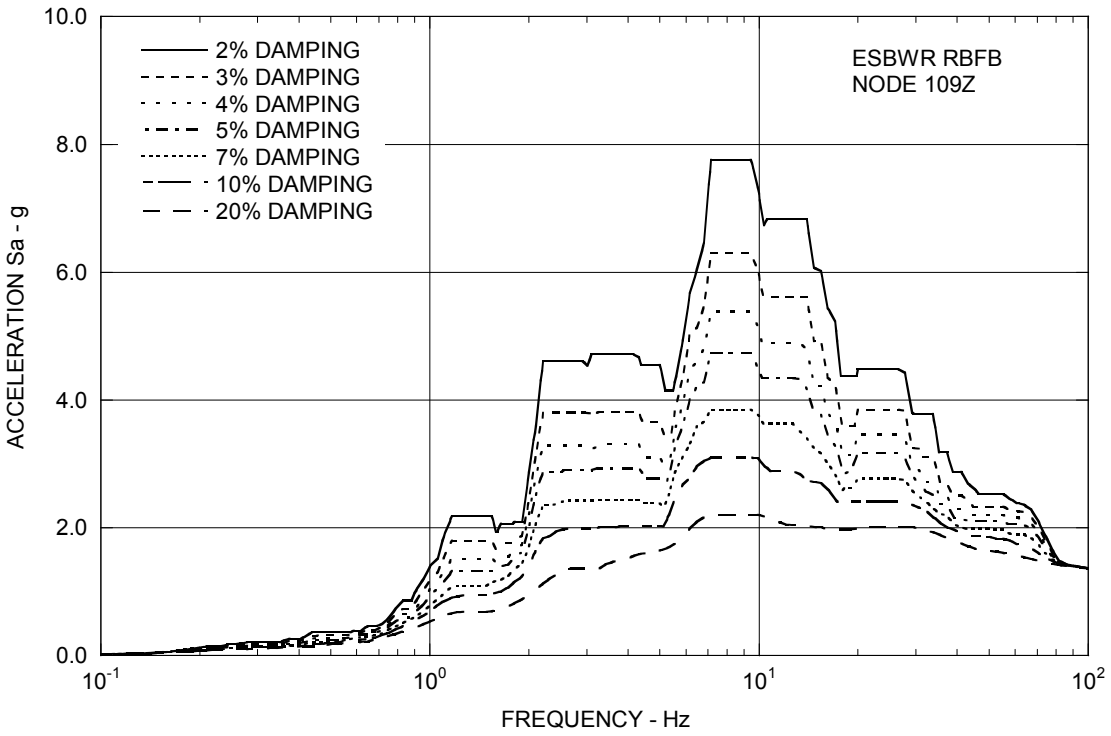

Figure 3A.9-3a. Enveloping Floor Response Spectra – RBFB Refueling Floor Z

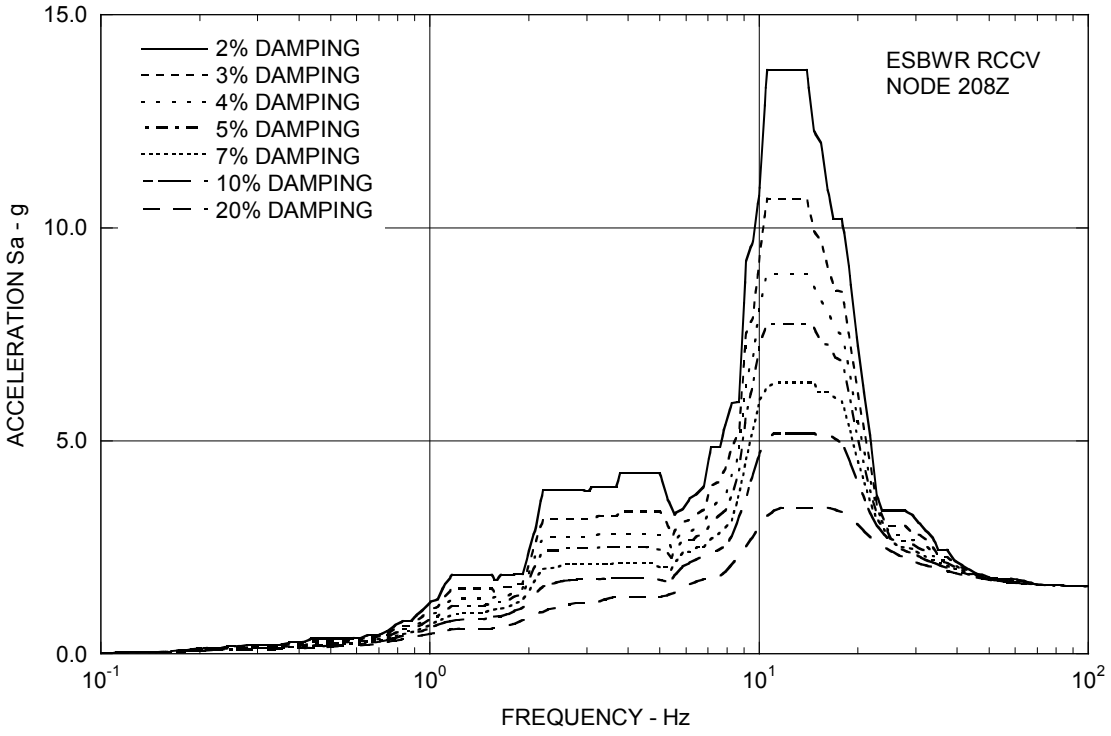

Figure 3A.9-3b. Enveloping Floor Response Spectra – RCCV Top Slab Z

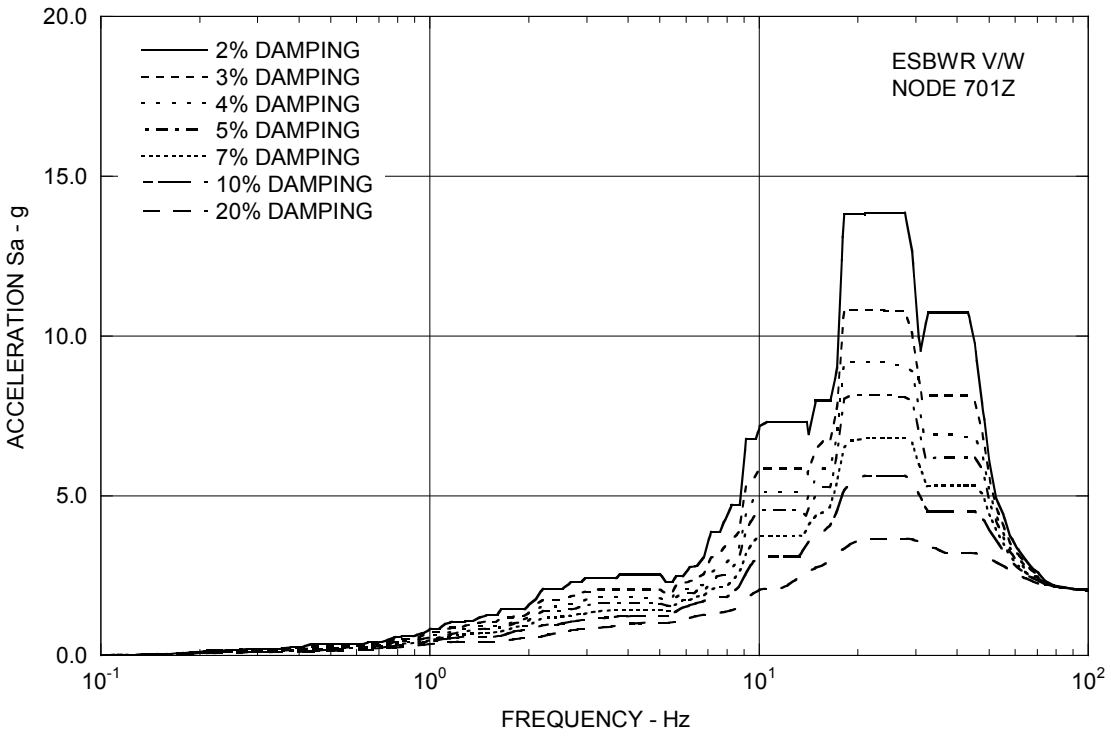

Figure 3A.9-3c. Enveloping Floor Response Spectra – Vent Wall Top Z

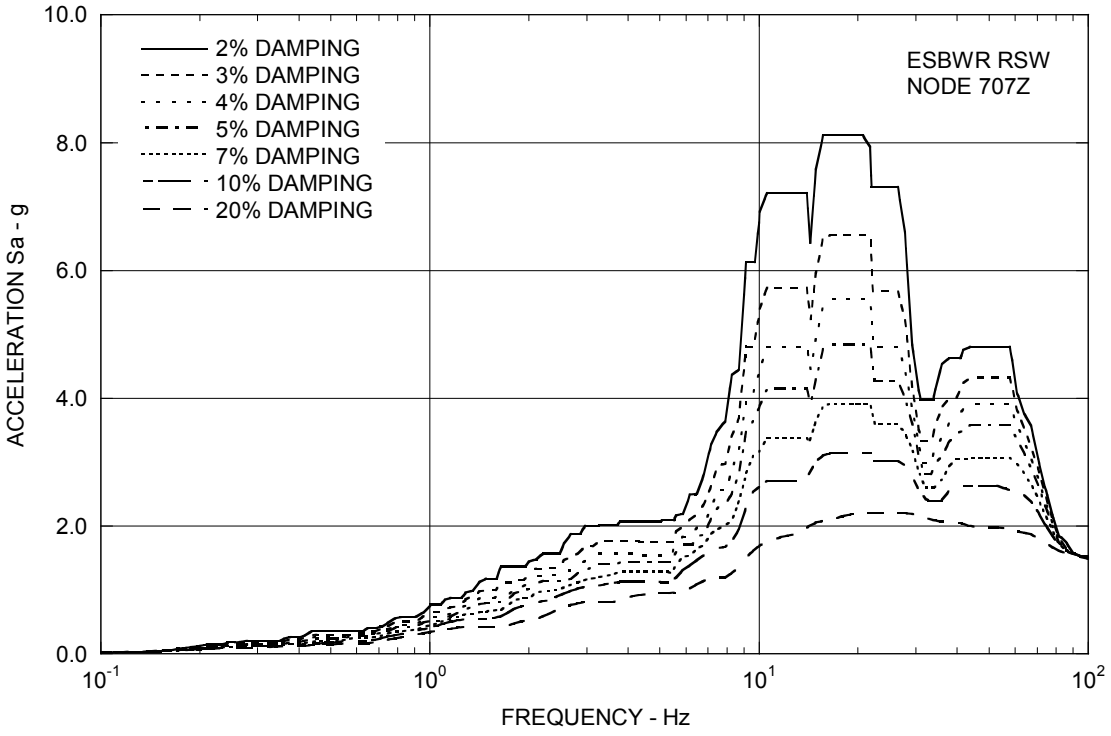

Figure 3A.9-3d. Enveloping Floor Response Spectra – RSW Top Z

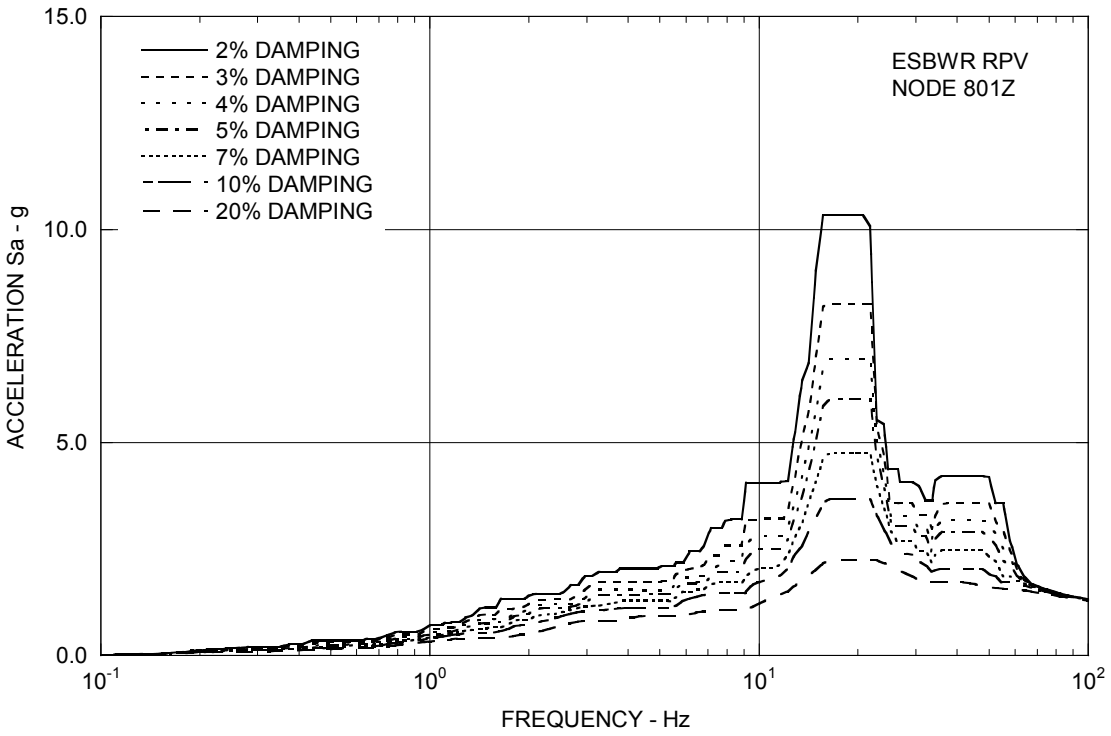

Figure 3A.9-3e. Enveloping Floor Response Spectra – RPV Top Z

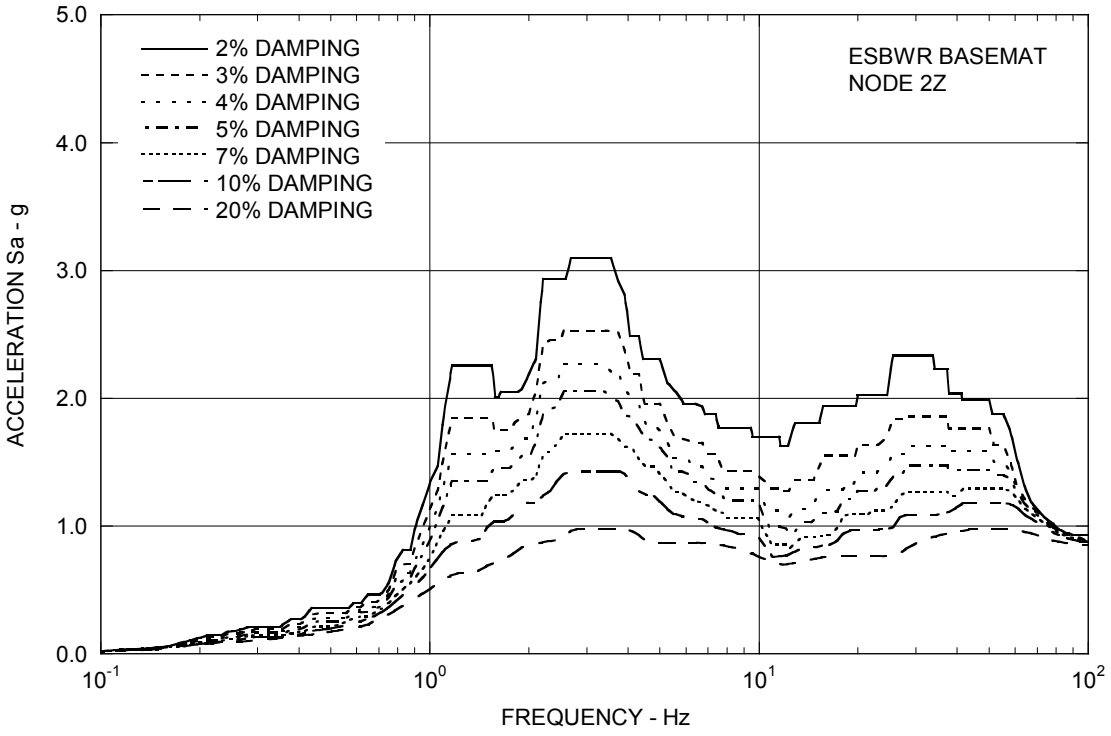

Figure 3A.9-3f. Enveloping Floor Response Spectra – RBFB Basemat Z

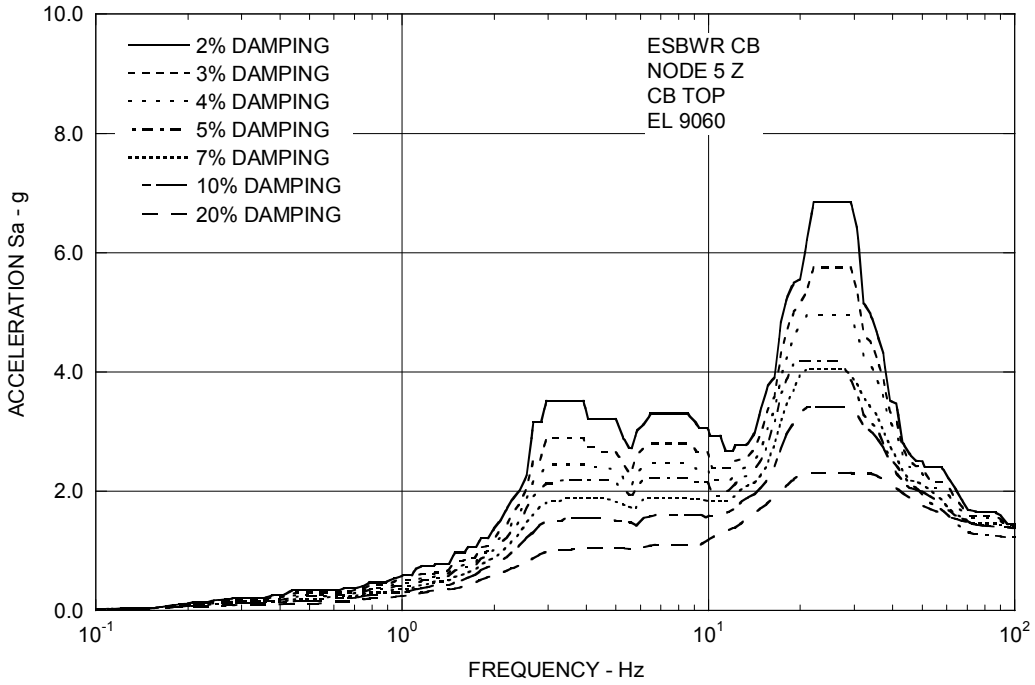

Figure 3A.9-3g. Enveloping Floor Response Spectra – CB Top Z

3B. CONTAINMENT HYDRODYNAMIC LOAD DEFINITIONS

This appendix provides the hydrodynamic loads applied in structural evaluations of the primary containment. The methodology used to develop these load definitions, and the justification for their applicability to ESBWR is given in Reference 3B-1.

3B.1 SAFETY RELIEF VALVE (SRV) LOADS

3B.1.1 Oscillating pressure load into the suppression pool from Safety Relief Valves (SRVs)

The distributions of SRV loads applied to structural evaluation of the boundary of the suppression pool are shown in Figure 3B-1.

3B.1.2 Pressure Time History

For acceleration response spectra generation, time histories of SRV are needed. Figure 3B-2 shows a typical pressure history applied to structural evaluation that is normalized to the maximum pressure value, with a frequency of 8 Hz. This pressure time history profile can be used in digitizing the pressure amplitude variation with time for other frequencies varying from 5 to 12 Hz. It should be noted that the bubble pressure decays to 1/3 Pmax with 5 cycles for any frequency between 5 and 12 Hz.

3B.2 ACCIDENT PRESSURE LOADS

During a LOCA, the suppression pool boundary is subjected to hydrodynamic loads, such as Pool Swell (PS), Condensation Oscillation (CO) and Chugging (CH) loads. These loads are not concurrent. The event-time relationship is shown in Figure 3B-3.

These pool swell boundary pressures shall be applied together with a drywell pressure of 345 kPag (50 psig). The pressure distribution is shown in Figure 3B-4.

The spatial distribution of CO and CH loads on the boundary of the suppression pool are shown in Figures 3B-5 and 3B-6, respectively. Dynamic load factors to convert the dynamic loads to static equivalent loads are also included in the RCCV and liner design.

For response spectra generation, pressure time histories of CO and CH are needed. There are five time histories of CO and eight time histories of CH required for the analysis. A typical pressure time history of CO and that of CH is shown in Figures 3B-7 and 3B-8, respectively.

For each chugging case, two sets of forcing frequencies shall be analyzed. The first forcing frequency is Figure 3B-8. The second forcing frequency is derived by adjusting the time scale of Figure 3B-8.

Each CO load is considered symmetric (in-phase for all vents). Each chugging load is considered symmetric (in-phase for all vents) and asymmetric (half of vents out-of-phase with other half).

In addition to CO and CH presented above, horizontal vent chugging and local CO loads are considered as follows:

A) Horizontal Vent Chugging

(1) Location: Each of top horizontal vents

(2) Loading: Triangular pulse in the upward direction as shown in Figure 3B-9 for global dynamic response analysis and Figure 3B-10 for vent pipe and pedestal design

(3) Phasing: Two cases, in-phase of all vents and half of vents 180 deg out-of phase with other half

(4) Combination with pool chugging: SRSS

B) Local Condensation Oscillation

(1) Location: Within 2 vent diameters for each of the bottom horizontal vents

(2) Loading: Triangular pulses as shown in Figure 3B-11

(3) Phasing: In-phase of all vents

(4) Combination with pool CO: Absolute sum (ABS)

The CO and chugging load magnitudes are proprietary information. The values shown in Figure 3B-7, 8, 9, 10 and 11 are normalized values. The proprietary magnitudes used in Appendices 3F and 3G are given in Reference 3B-1.

3B.3 REFERENCES

3B-1 GE Energy, "ESBWR Containment Load Definition," NEDE-33261P, Class III (proprietary), (May 2006), and NEDO-33261, Class I (non-proprietary), (May 2006).

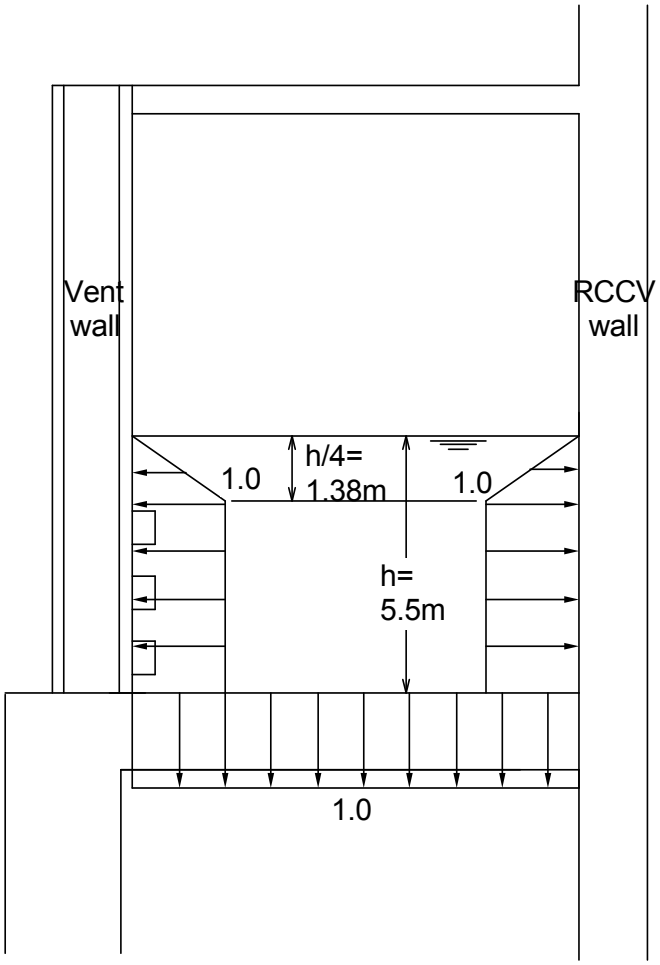

SRV Peak Positive Pressure = 152 kPag
SRV Peak Negative Pressure = -63 kPag
Dynamic Load Factor (DLF) = 2.0

Figure 3B-1. Safety Relief Valve (SRV) Pressure Loads

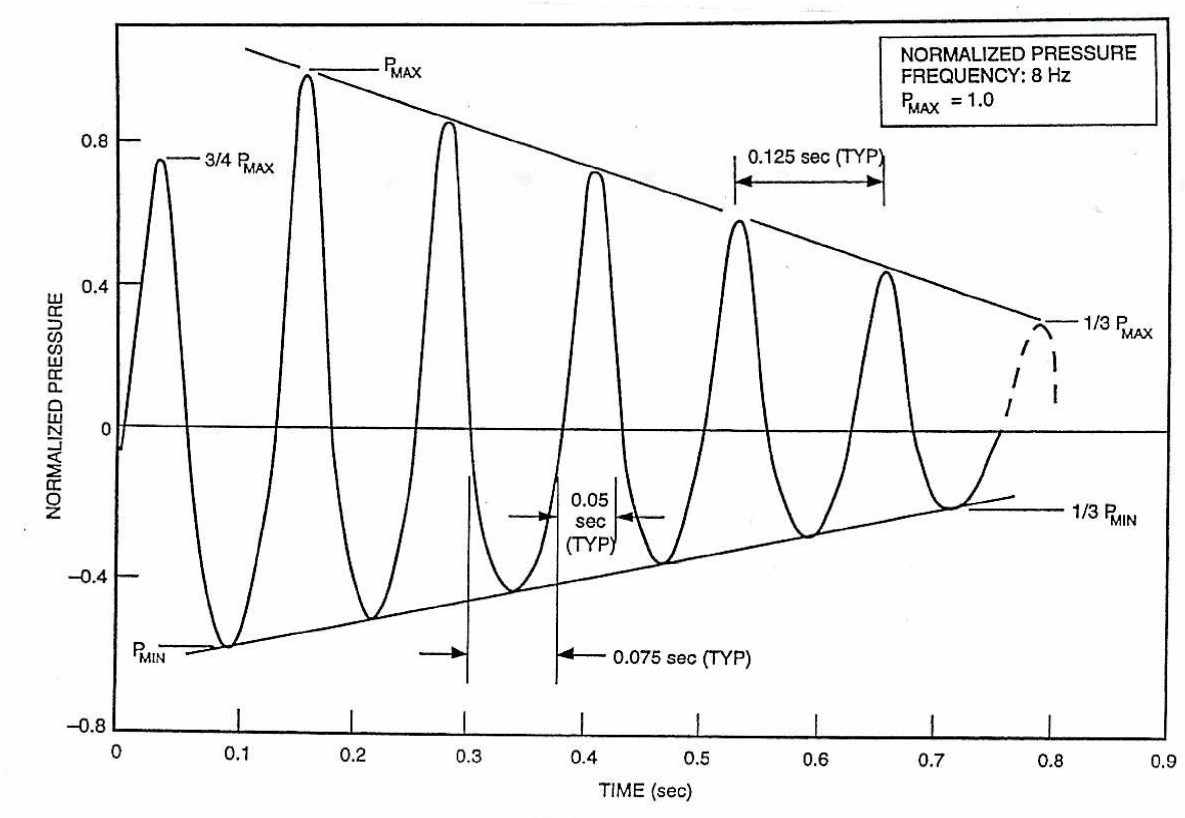

Figure 3B-2. Normalized SRV Pressure Time History (Idealized)

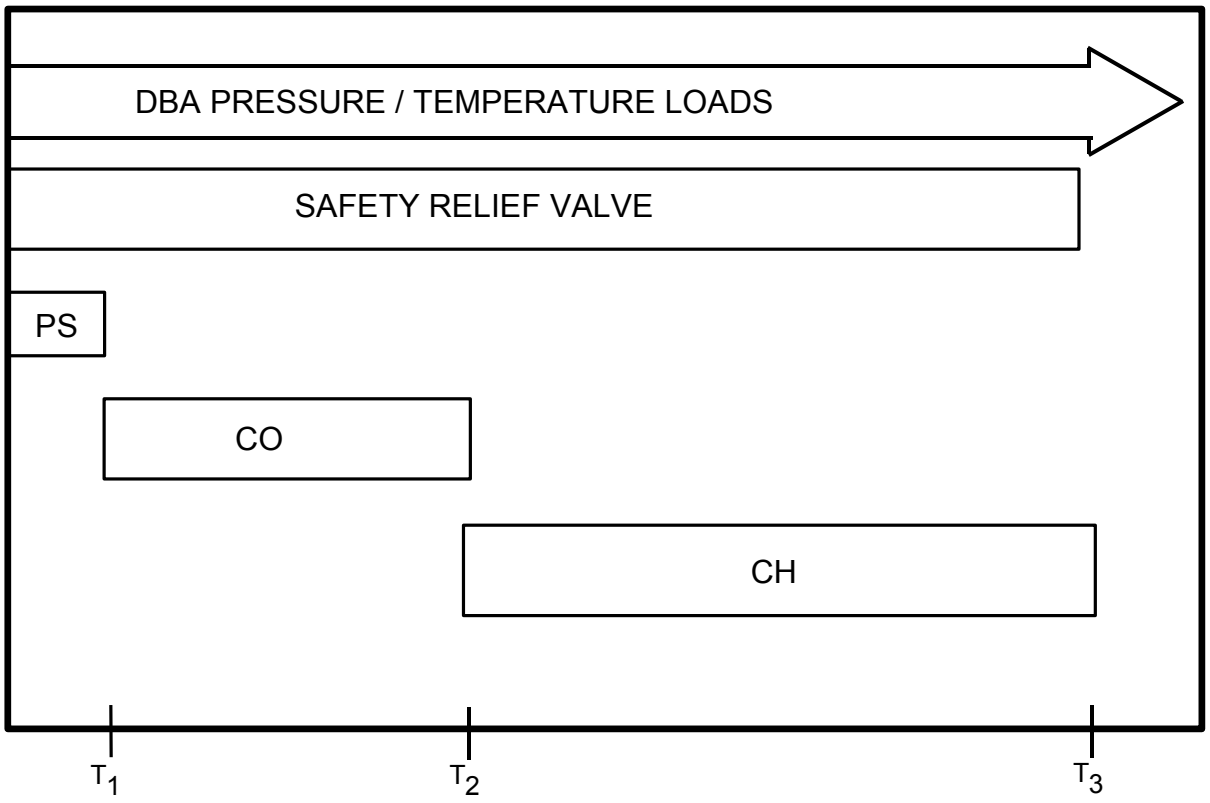

T_1 = 5 sec T_2 = 500 sec T_3 = 72 hr

PS = POOL SWELL

CO = CONDENSATION OSCILLATION

CH = CHUGGING

Figure 3B-3. Typical Event – Time Relationship for a DBA

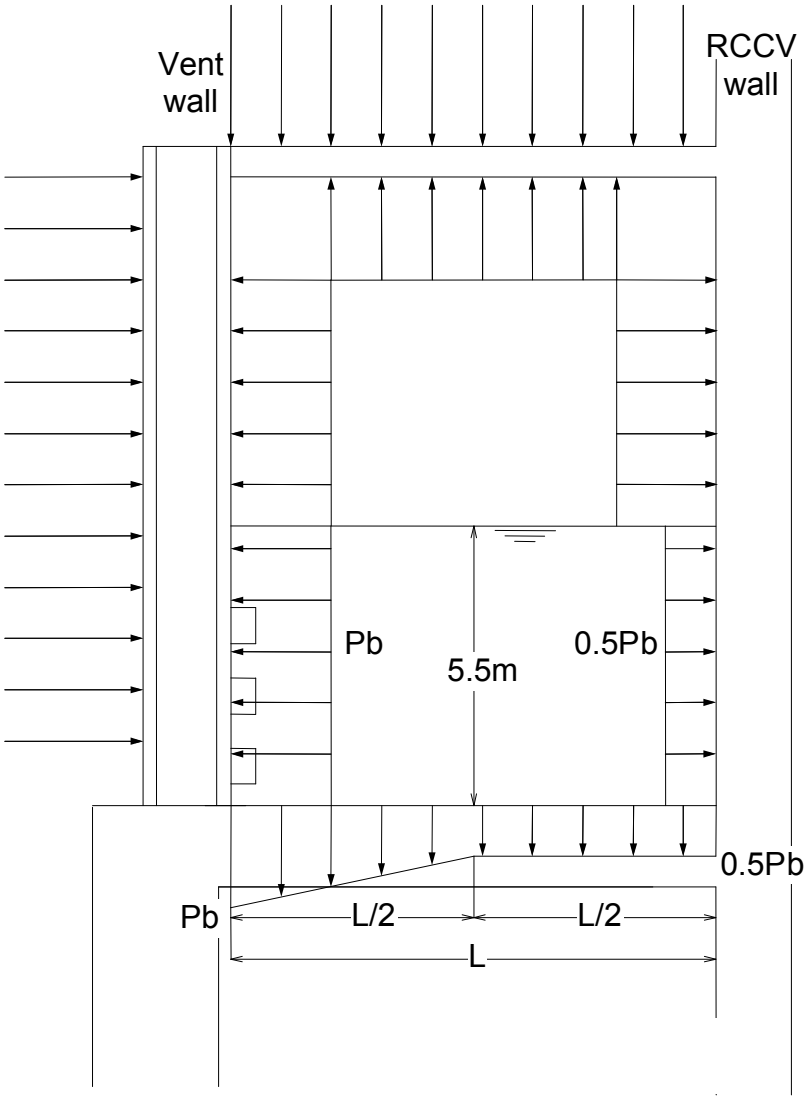

Note: Pb is the maximum pool swell boundary load. Pool swell height is 5.5 m. In addition to the gas space pressure, Pg, there is a linear variation pool swell boundary pressure above the Suppression Pool (S/P) water surface. This additional pressure is not used for RCCV design but for platforms and objects in the S/P air space (catwalks, pipes, etc.).

Figure 3B-4. Pool Swell (PS) Pressure Loads

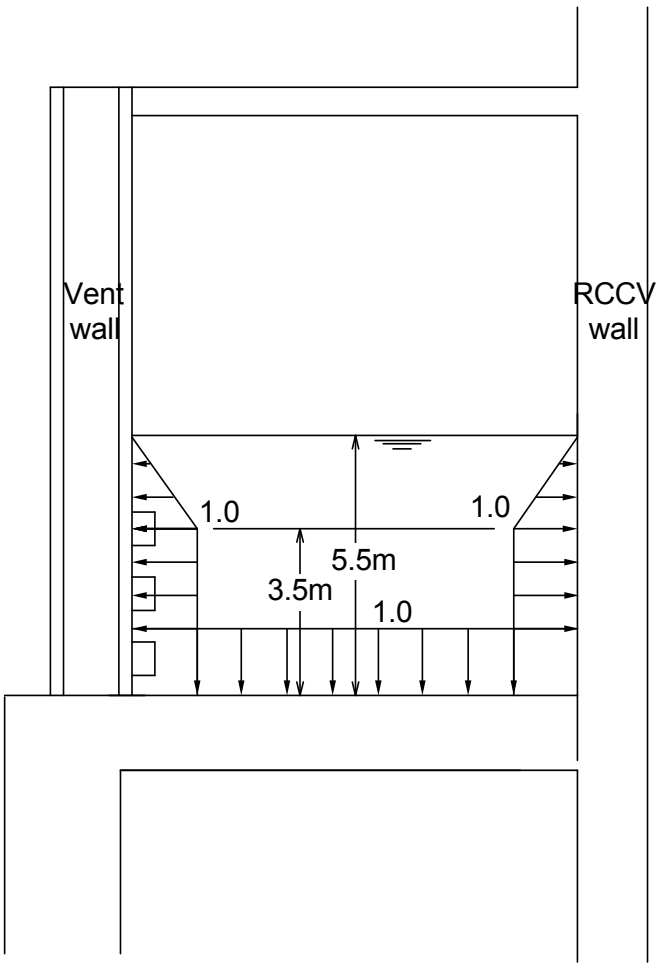

CO Peak Positive Pressure = 186 kPag
CO Peak Negative Pressure = -186 kPag
Dynamic Load Factor (DLF) = 2.0

Figure 3B-5. Condensation Oscillation (CO) Pressure Loads

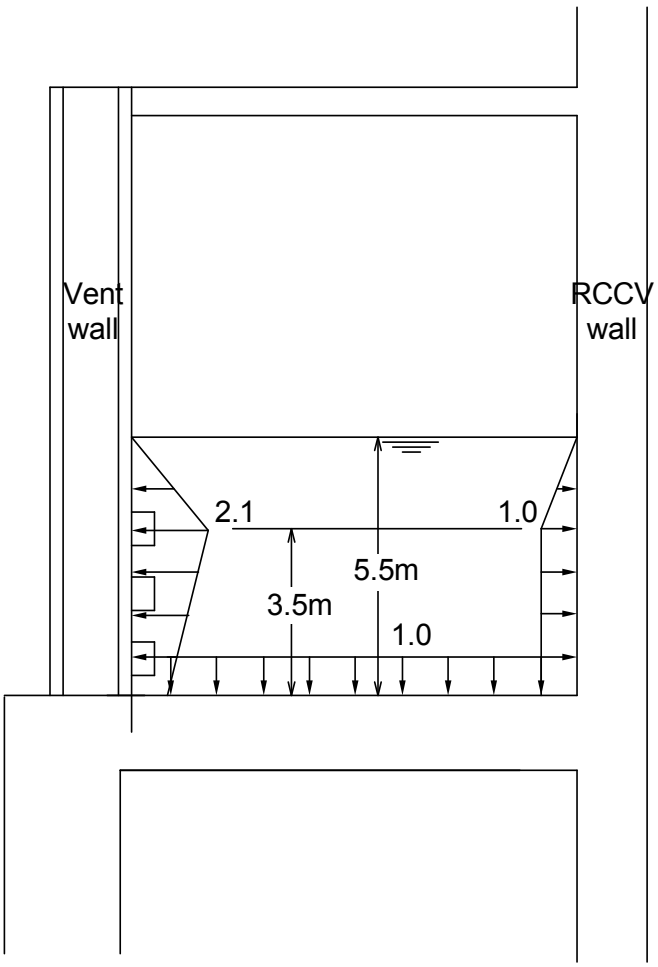

CHUG Peak Positive Pressure = 91 kPag
CHUG Peak Negative Pressure = -66 kPag
Dynamic Load Factor (DLF) = 2.0

Figure 3B-6. Chugging (CH) Load Spatial Distribution

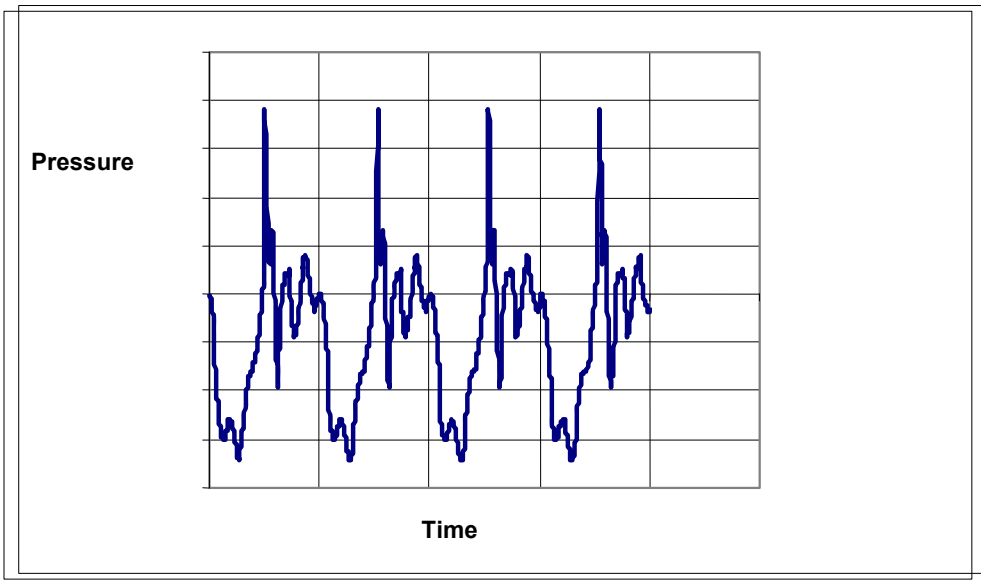

Figure 3B-7. A Typical Pressure Time History of CO

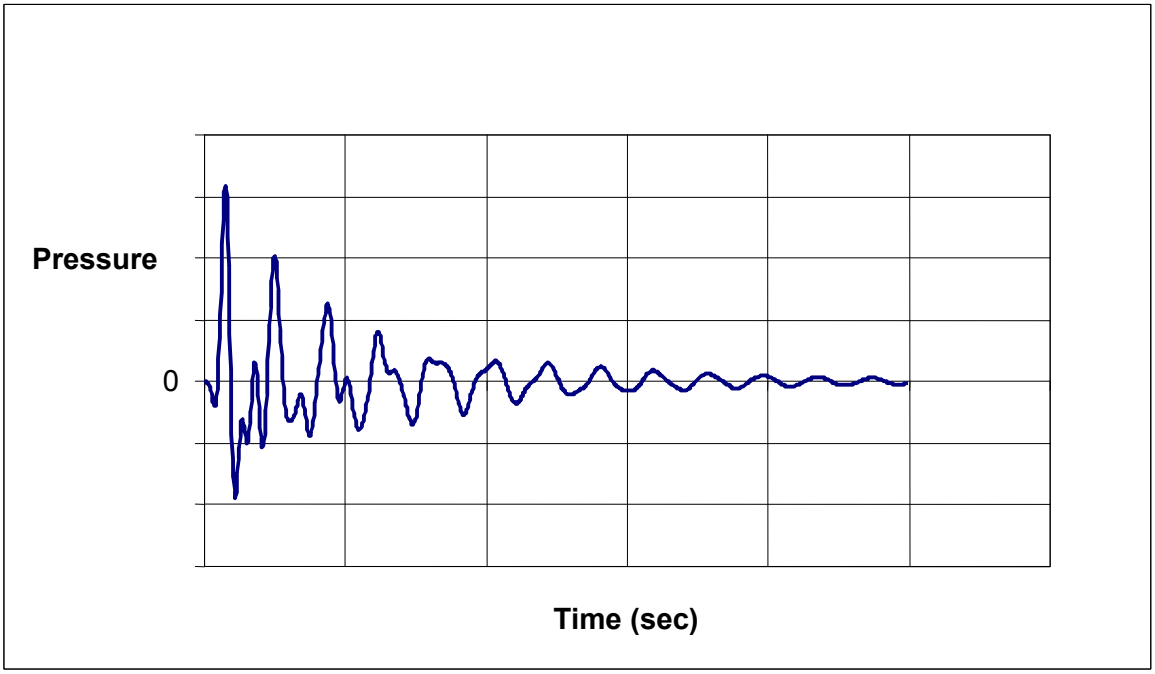

Figure 3B-8. A Typical Pressure Time History of CH

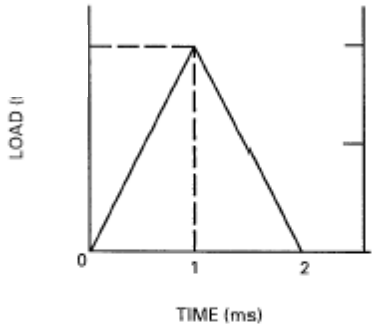

Figure 3B-9. Horizontal Vent Upward Loading for Structure Response Analysis

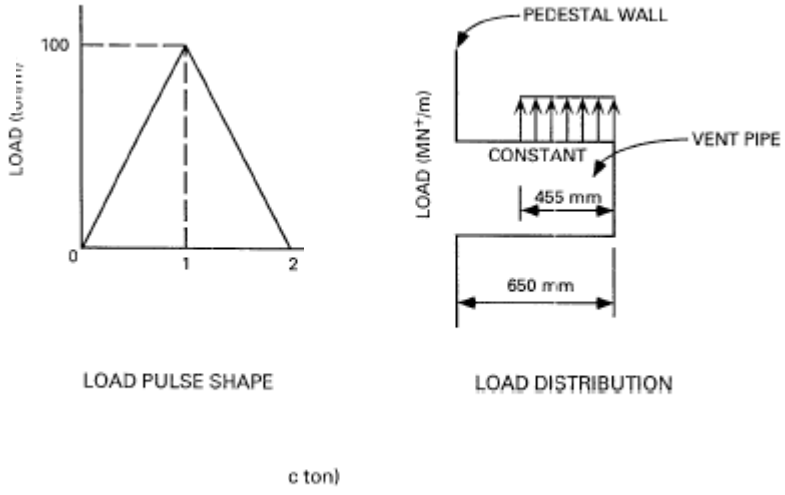

Figure 3B-10. Horizontal Vent Upward Loading for Vent Pipe and Pedestal

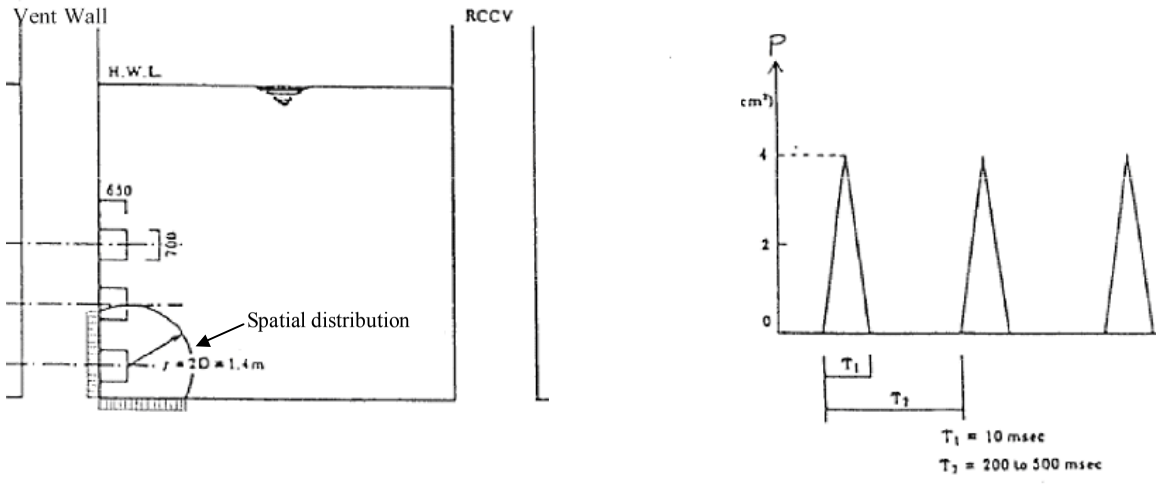

Figure 3B-11. Local CO Load

3C. COMPUTER PROGRAMS USED IN THE DESIGN AND ANALYSIS OF SEISMIC CATEGORY I STRUCTURES

3C.1 INTRODUCTION

The following Seismic Category I structures and their foundations of the Nuclear Island are analyzed and/or designed using the computer programs described in this appendix:

(1) Concrete Containment Structure

(2) Reactor Building (RB)

(3) Fuel Building (FB)

(4) Control Building (CB)

3C.2 STATIC AND DYNAMIC STRUCTURAL ANALYSIS PROGRAM (NASTRAN)

3C.2.1 Description

NASTRAN is a general purpose computer program for finite element analysis; its capabilities include: static response to concentrated and distributed loads; static response to thermal expansion; static response to enforced displacements; dynamic response to transient loads; dynamic response to steady-state sinusoidal loads;dynamic response to random excitation; and determination of eigenvalues for use in vibration analysis.

3C.2.2 Validation

The MSC_Software Corporation of Santa Ana, California developed NASTRAN. The program validation documentation is available at MSC Software Corporation.

3C.2.3 Extent of Application

This program is used for the static and eigenvalue analysis of the concrete containment, the RB, the FB and the CB. This program is also used for the static and dynamic analysis of the Drywell Head and containment internal structures.

3C.3 ABAQUS AND ANACAP-U

3C.3.1 Description

ABAQUS/Standard is a widely used, commercially available finite-element program with a broad range of analysis capabilities. Implicit formulations for steady state solutions, transient thermal solutions and static stress analyses are employed using 3-dimensional models of continuum concrete elements, truss-type reinforcement sub-elements, and plate and membrane elements for liners and other steel components. Classical von Mises plasticity models and strength degradation with elevated temperature for the steel material are used for the nonlinear analyses. The ANACAP-U software is an advanced concrete constitutive model coupled to the ABAQUS software as a user subroutine. The ANACAP-U concrete material model provides formulations for concrete cracking under tensile and shear loads, post-cracking shear stiffness and shear capacity as a function of crack width and shear deformations, with yielding and strain

softening (crushing) under large compressive loads. Modulus and strength degradation with increasing temperatures is also included for the concrete model.

3C.3.2 Validation

ABAQUS is written and maintained by ABAQUS, Inc. of Providence R.I., (formerly Hibbitt, Karlssen, and Sorensen, Inc.). The program has an extensive library of example problems that are used for verification and validation testing. Additional descriptions and information on the quality controls can be found on the ABAQUS web site, (www.abaqus.com). The ANACAP-U concrete material model for use with the ABAQUS program is written and maintained by ANATECH Corp, San Diego, CA. This software has been extensively verified with test problems and also validated against large-scale test results for the performance of reinforced concrete structures. ANACAP-U Program validation documentation is available at ANATECH Corp.

3C.3.3 Extent of Application

The ABAQUS/ANACAP-U software coupling is used in the nonlinear analyses for the structural performance of the reinforced concrete containment under LOCA thermal conditions.

3C.4 CONCRETE ELEMENT CRACKING ANALYSIS PROGRAM (SSDP-2D)

3C.4.1 Description

SSDP-2D computes stresses in a thick concrete element under thermal and/or non-thermal (such as dead load, service loads) loads, and considers the effect of concrete cracking. The element that represents a section of a concrete shell or slab may include two layers of orthogonal reinforcing. It does not include the effect of the liner.

SSDP-2D calculates the stresses considering two-dimensional equilibrium conditions of section forces with the existence of thermal loads and concrete cracking. It is assumed in the code that concrete has an anisotropic property and that cracked concrete does not carry tensile forces. Concrete is assumed to have no tensile strength.

3C.4.2 Validation

SSDP-2D is written and maintained by Shimizu Corporation of Tokyo, Japan. Program validation documentation is available at Shimizu Corporation.

3C.4.3 Extent of Application

This program is used for the analysis of the concrete containment, the RB, the FB and the CB.

3C.5 HEAT TRANSFER ANALYSIS PROGRAM (TEMCOM2)

3C.5.1 Description

TEMCOM2 solves a temperature distribution in a two-dimensional model based on a finite differential method. It performs analyses under the following conditions

- Element: triangle and quadrilateral elements
- Surface heat transfer: convection and radiation
- Temperature condition: steady-state and transient temperature conditions

3C.5.2 Validation

TEMCOM2 is written and maintained by Shimizu Corporation of Tokyo, Japan. Program validation documentation is available at Shimizu Corporation.

3C.5.3 Extent of Application

This program is used in the transient heat transfer analysis of the concrete containment and the RB.

3C.6 STATIC AND DYNAMIC STRUCTURAL ANALYSIS SYSTEMS: ANSYS

3C.6.1 Description

ANSYS is a large, finite element program for a broad range of analyses types. The structural analysis capabilities include material and geometric non-linear analysis, static analysis and a variety of dynamic analyses.

The element used in concrete cracking analysis allows for a full non-linear analysis of reinforced concrete with cracking and crushing of concrete.

3C.6.2 Validation

ANSYS is maintained by ANSYS INC., located at 275 Technology Drive, Canonsburg, PA, 15317.

3C.6.3 Extent of Application

This program is used for the containment dynamic analysis of containment loads, the containment ultimate capacity analyses and the containment seismic margin analysis.

3C.7 SOIL-STRUCTURE INTERACTION

3C.7.1 Dynamic Soil-Structure Interaction Analysis Program—DAC3N

3C.7.1.1 Description

DAC3N is a three-dimensional dynamic analysis program used for the seismic response analysis of a building structure considering soil-structure interaction. The response analysis is performed using the time history method solved by direct integration, Newmark's beta method. Eingenvalue analysis is performed using Subspace method.

In the DAC3N, soil-structure interaction system is modeled by the combination of soil spring and damping coefficient. Spring and damping coefficient are determined as frequency independent values, which fit the frequency dependent real and imaginary parts of soil spring obtained by the theoretical methods, such as vibration admittance theory based on three-dimensional wave propagation theory for uniform half space soil.

As mass elements, lumped masses and consistent masses are available. Structural elements, such as beams, trusses, dampers and direct input matrices are available in this program.

This program has nonlinear analytical capability.

3C.7.1.2 Validation

DAC3N is coded and maintained by Shimizu Corporation of Tokyo, Japan. Program validation documentation is available at Shimizu Corporation.

3C.7.1.3 Extent of Application

This program is used to perform the soil-structure interaction analysis required to obtain enveloped seismic design loads of the concrete containment, the RB, the FB and the CB.

3C.7.2 Dynamic Soil-Structure Interaction Analysis Program – SASSI2000

3C.7.2.1 Description

SASSI2000 is used to solve a wide range of dynamic soil-structure interaction (SSI) problems, including layered soil conditions and embedment conditions, in two or three dimensions. It was developed at the University of California, Berkeley in 1982 under the technical direction of John Lysmer. The program is based on the finite-element method formulated in the frequency domain using a substructuring technique.

3C.7.2.2 Validation

SASSI version 2000 was obtained from the University of California, Berkeley and implemented by Shimizu Corporation of Tokyo, Japan on the PC computer on Linux OS. Program validation documentation is available at UC Berkeley.

3C.7.2.3 Extent of Application

SASSI is used to obtain seismic design loads and in-structure floor response spectra for the Seismic Category I buildings accounting for the effects of SSI.

3C.7.3 Free-Field Site Response Analysis – SHAKE

3C.7.3.1 Description

SHAKE is a program, which can perform the free-field site response analysis. It was developed at the University of California, Berkeley by B. Schnabel, John Lysmer and H.B. Seed in 1972. The program is based on the theory of one-dimensional propagation of shear waves in the vertical direction in a horizontally-layered visco-elastic soils system overlying an elastic half-space medium.

SHAKE also has a function to account for non-linearities in soil shear modulus and hysteresis damping as functions of shear strain in soil by the use of equivalent-linear soil properties using an iterative equivalent linearization procedure to obtain constant values of shear modulus and hysteresis damping ratio compatible with the effective shear strain in each soil layer.

3C.7.3.2 Validation

SHAKE was developed at the University of California, Berkeley and implemented by Shimizu Corporation of Tokyo, Japan on the Hewlett Packard computer workstation. Program validation documentation is available at UC Berkeley.

3C.7.3.3 Extent of Application

SHAKE is used to generate the free-field site response motions required in the seismic SSI analysis.

3D. COMPUTER PROGRAMS USED IN THE DESIGN OF COMPONENTS, EQUIPMENT AND STRUCTURES

3D.1 INTRODUCTION

As discussed in Subsection 3.9.1.2, this appendix describes the major computer programs used in the analysis of the safety-related components, equipment and structures. The quality of the programs and the computed results is controlled. The programs are verified for their application by appropriate methods, such as hand calculations, or comparison with results from similar programs, experimental tests, or published literature, including analytical results or numerical results to the benchmark problems.

3D.2 FINE MOTION CONTROL ROD DRIVE

3D.2.1 (Deleted)

3D.2.2 ANSYS

3D.2.2.1 Description

See Subsection 3D.3.1.1.

3D.2.2.2 Validation

Hand calculations for theoretical equations published in literature.

3D.2.2.3 Extent of Application

This program is used for the elastic stress analysis and vibration analysis of the FMCRD. The program calculates elastic stresses for level D, faulted limits, but the ASME Code Section III Appendix F limits are not within the program. Evaluation for level D limits are performed by hand calculation.

3D.3 REACTOR PRESSURE VESSEL AND INTERNALS

Computer programs used in the analysis of the reactor pressure vessel, core support structures, and other safety class reactor internals are described below and in Subsection 4.1.4.1.

3D.3.1 ANSYS

3D.3.1.1 Description

The ANSYS computer program is a finite element large-scale general-purpose program for the solution of several classes of engineering analysis problems. Analysis capabilities include static and dynamic, plastic, creep and swelling, small and large deflections, and other applications like thermal analysis, material non-linearities, contact analysis, etc.

3D.3.1.2 Validation

ANSYS is maintained by ANSYS INC., located at 275 Technology Drive, Canonsburg, PA, 15317.

3D.3.1.3 Extent of Application

This program is used for the elastic stress analysis and vibration analysis of the reactor pressure vessel and internals. The program calculates elastic stresses for level D, faulted limits, but the ASME Code Section III Appendix F limits are not within the program. Evaluations for level D limits are performed by hand calculation.

3D.3.2 Dynamic Stress Analysis of Axisymmetric Structures Under Arbitrary Loading - ASHSD2

3D.3.2.1 Description

This FORTRAN program was created at the Earthquake Engineering Research Center, University of California, Berkeley. A finite element method is presented for the dynamic analysis of complex axisymmetric structures subjected to any arbitrary static or dynamic loading or base acceleration. The three-dimensional axisymmetric continuum is represented either as an axisymmetric thin shell or as a solid of revolution or as a combination of both. The axisymmetric shell is discretized as a series of frustrums of cones and the solid of revolution as triangular or quadrilateral "toroids" connected at their nodal point circles. Hamilton's variational principle is used to derive the equations of motion for this discrete structure. This leads to a mass matrix, stiffness matrix and load vectors that are all consistent with the assumed displacement field. But to minimize computer storage and execution time a diagonal mass matrix has been assumed in writing the computer program (with the input diagonalized accordingly by coordinate system transform). These equations of motion are solved numerically through the time domain either by direct integration or by modal superposition. In both cases, a step-by-step integration procedure was used.

3D.3.2.2 Validation

Hand calculations using theoretical equations published in literature are performed to demonstrate the program’s applicability and validity.

3D.3.2.3 Extent of Application

This program will be used to calculate elastic stresses in the reactor pressure vessel and shroud support using axisymmetric shell and solid elements for axisymmetric and non-axisymmetric

static loading. The program calculates stresses for level D, faulted limits, but only ASME Code Section III elastic analysis defined in F1321.3 requirements.

3D.3.3 EVAST

3D.3.3.1 Description

This FORTRAN program was created by Babcock-Hitachi K.K. to calculate stress intensities, perform fatigue evaluation and evaluate thermal ratcheting.

3D.3.3.2 Validation

Hand calculations are performed to demonstrate the program's applicability and validity.

3D.3.3.3 Extent of Application

This program will be used to evaluate the primary stress intensities, fatigue and thermal ratcheting of the shroud support. Where fatigue curves are used, environmental effects are not considered.

3D.3.4 TACF

3D.3.4.1 Description

This FORTRAN program was created by Babcock-Hitachi K.K. to evaluate temperature distribution.

3D.3.4.2 Validation

Hand calculations using theoretical equations published in literature are performed to demonstrate the program's applicability and validity.

3D.3.4.3 Extent of Application

This program will be used to evaluate the steady and non-steady state axisymmetric thermal conduction of the reactor pressure vessel and shroud support.

3D.3.5 ABAQUS

3D.3.5.1 Description

This PC based program was created by ABAQUS, Inc. ABAQUS solves traditional implicit finite element analyses, such as static, dynamics, thermal, all powered with a wide range of contact and nonlinear material options. ABAQUS also has optional add-on and interface products with address design sensitivity analysis. ABAQUS enables a wide range of linear and nonlinear engineering simulations.

3D.3.5.2 Validation

Hand calculations using theoretical equations published in literature are performed to demonstrate the program's applicability and validity.

3D.3.5.3 Extent of Application

This program will be used for elastic and plastic stress analysis in addition to temperature distribution analysis of the reactor pressure vessel. The program calculates stresses for level D, faulted limits, but only ASME Code Section III elastic analysis defined in F1321.3 requirements.

3D.3.6 FEMFL

3D.3.6.1 Description

This FORTRAN program was created by Babcock-Hitachi K.K. to evaluate elastic stresses.

3D.3.6.2 Validation

Hand calculations using theoretical equations published in literature are performed to demonstrate the program's applicability and validity.

3D.3.6.3 Extent of Application

This program will be used for elastic stress analysis using axisymmetric structural shell and solid elements. The static loading may be axisymmetric or non-axisymmetric. The program is used in the analysis of the reactor pressure vessel. The program calculates stresses for level D, faulted limits, but only ASME Code Section III elastic analysis defined in F1321.3 requirements.

3D.3.7 SEISM03

3D.3.7.1 Description

See Subsection 4.1.4.1.3.

3D.3.7.2 Validation

Test cases analyzed and compared with previous design problems are performed to demonstrate the program's applicability and validity.

3D.3.7.3 Extent of Application

In addition to those applications outlined in Chapter 4, this program will be used to evaluate non-linear fuel lift analysis with spring, stop and friction elements.

3D.4 PIPING

3D.4.1 Piping Analysis Program – PISYS

3D.4.1.1 Description

PISYS is a computer code for analyzing piping systems subjected to both static and dynamic piping loads. Finite element models of a piping system formed by assembling stiffness matrices represent standard piping components. The piping elements are connected to each other via nodes called pipe joints. It is through these joints that the model interacts with the environment, and loading of the piping system becomes possible. PISYS is based on the linear elastic analysis

in which the resultant deformations, forces, moments and accelerations at each joint are proportional to the loading and the superposition of loading is valid.

PISYS has a full range of static dynamic load analysis options. Static analysis includes dead weight, uniformly distributed weight, thermal expansion, externally applied forces, moments, imposed displacements and differential support movement (pseudo-static load case). Dynamic analysis includes mode shape extraction, response spectrum analysis, and time-history analysis by modal combination or direct integration. In the response spectrum analysis [i.e., uniform support motion response spectrum analysis (USMA) or independent support motion response spectrum analysis (ISMA)], the user may request modal response combination in accordance with Regulatory Guide 1.92. In the ground motion (uniform motion) or independent support time history analysis, the normal mode solution procedure is selected. In analysis involving time varying nodal loads, the step-by-step direct integration method is used.

3D.4.1.2 Validation

The PISYS program has been benchmarked against NRC piping models. The results are documented in Reference 3D-1 for mode shapes and USMA options. The ISMA option has been validated against NUREG/CR-1677 (Reference 3D-2).

Subsequently, the PISYS07 program, which is used for ESBWR piping analysis, has been benchmarked against NUREG/CR-6049.

3D.4.1.3 Extent of Application

This program will be used for elastic stress analysis of piping systems.

3D.4.2 Component Analysis - ANSI7

3D.4.2.1 Description

ANSI7 is a computer code for calculating stresses and cumulative usage factors and to calculate combined stresses for service levels A, B, C and D loads in accordance with ASME Section III article NB-3650. The program includes environmental fatigue effects on fatigue curves according to DG-1144 and NUREG/CR-6909.

3D.4.2.2 Validation

Hand calculations are performed to demonstrate the program's applicability and validity.

3D.4.2.3 Extent of Application

This program will be used for calculating stresses and cumulative usage factors for Class 1, 2 and 3 piping components in accordance with articles NB, NC and ND-3650 of ASME Code Section III. ANSI7 is also used to combine loads and calculate combined service levels A, B, C and D loads on piping supports and pipe-mounted equipment. The program calculates elastic stresses for level D, faulted limits, but the ASME Code Section III Appendix F requirements are not within the computer program.

3D.4.3 (Deleted)

3D.4.4 Dynamic Forcing Functions

3D.4.4.1 Relief Valve Discharge Pipe Forces Computer Program – RVFOR

3D.4.4.1.1 Description

The relief valve discharge pipe connects the pressure-relief valve to the suppression pool. When the valve is opened, the transient fluid flow causes time-dependent forces to develop on the pipe wall. This GE developed FORTRAN computer program computes the transient fluid mechanics and the resultant pipe forces using the method of characteristics.

3D.4.4.1.2 Validation

Hand calculations and experimental tests are used to demonstrate the program's applicability and validity.

3D.4.4.1.3 Extent of Application

This program will be used to calculate the time-dependent forces on the wall of the discharge pipe.

3D.4.4.2 Turbine Stop Valve Closure – TSFOR

3D.4.4.2.1 Description

This GE developed FORTRAN program utilizes the method of characteristics to compute fluid momentum and pressure loads at each change in pipe section or direction due to the fast closure of the turbine stop valve.

3D.4.4.2.2 Validation

Hand calculations are used to demonstrate the program's applicability and validity.

3D.4.4.2.3 Extent of Application

The TSFOR program computes the time-history forcing function in the main steam piping due to turbine stop valve closure.

3D.4.4.3 (Deleted)

3D.4.4.4 (Deleted)

3D.4.5 (Deleted)

3D.4.6 Response Spectra Generation

3D.4.6.1 ERSIN Computer Program

3D.4.6.1.1 Description

ERSIN is a computer code used to generate secondary response spectra for pipe-mounted and floor-mounted equipment. ERSIN provides direct generation of local or global acceleration response spectra.

3D.4.6.1.2 Validation

Hand calculations and test cases analyzed are used to demonstrate the program's applicability and validity.

3D.4.6.1.3 Extent of Application

Equipment Control Panels, Local Equipment Racks, Main Steam Isolation Valves (MSIVs), Safety Relief Valves (SRVs) and Hydraulic Control Units (HCUs) are some of the components that are analyzed using ERSIN computer code.

3D.4.6.2 RINEX Computer Program

3D.4.6.2.1 Description

RINEX is a computer code used to interpolate and extrapolate amplified response spectra used in the response spectrum method of dynamic analysis. RINEX is also used to generate response spectra with nonconstant model damping. The non-constant model damping analysis option can calculate spectral acceleration at the discrete eigenvalues of a dynamic system using either the strain energy weighted modal damping or the ASME Code Class N-411-1 damping values.

3D.4.6.2.2 Validation

Hand calculations and test cases analyzed are used to demonstrate the program's applicability and validity.

3D.4.6.2.3 Extent of Application

This program will be used to generate multiple damping spectra for piping.

3D.4.6.3 (Deleted)

3D.4.6.4 (Deleted)

3D.4.7 Piping Dynamic Analysis Program – PDA

3D.4.7.1 Description

PDA is a FORTRAN program used to determine the response of a pipe subjected to the thrust force occurring after a pipe break. It also is used to determine the pipe whip restraint design and capacity.

The program treats the situation in terms of generic pipe break configuration, which involves a straight, uniform pipe fixed (or pinned) at one end and subjected to a time-dependent thrust force at the other end. A typical restraint used to reduce the resulting deformation is also included at a location between the two ends. Nonlinear and time-independent stress-strain relations are used to model the pipe and the restraint. Using a plastic hinge concept, bending of the pipe is assumed to occur only at the fixed (or pinned) end and at the location supported by the restraint.

Effects of pipe shear deflection are considered negligible. The pipe-bending moment-deflection (or rotation) relation used for these locations is obtained from a static nonlinear cantilever beam analysis. Using moment angular rotation relations, nonlinear equations of motion are formulated using energy considerations, and the equations are numerically integrated in small time steps to yield the time-history of the pipe motion.

3D.4.7.2 Validation

PDA output pipe whip restraint force and displacement benchmarked with ANSYS nonlinear time history analysis results.

3D.4.7.3 Extent of Application

Pipe break analyses.

3D.4.8 Thermal Transient Program – LION

3D.4.8.1 Description

LION is a FORTRAN program used to compute radial and axial thermal gradients in piping. The program calculates a time-history of ΔT_1, ΔT_2, Ta, and Tb (defined in ASME Code Section III, Subsection NB) for uniform and tapered pipe wall thickness.

3D.4.8.2 Validation

LION was compared to analytical results published in literature.

3D.4.8.3 Extent of Application

Pipe thermal analyses.

3D.4.9 Engineering Analysis System - ANSYS05

3D.4.9.1 Description

See Subsection 3D.3.1.1.

3D.4.9.2 Validation

See Subsection 3D.3.1.2.

3D.4.9.3 Extent of Application

This program is used to perform non-linear analysis of piping systems for time varying displacements and forces due to postulated pipe breaks. Also, this program is used to perform finite element analysis of pressure retaining components and civil structures against the loads and events postulated in the design specifications.

3D.4.10 Piping Analysis Program – EZPYP

3D.4.10.1 Description

EZPYP is a GE FORTRAN program that links the ANSI7 and PISYS program together. The EZPYP program can be used to run several PISYS cases by making user-specified changes to a basic PISYS pipe model. By controlling files and PISYS runs, the EZPYP program gives the analyst the capability to perform a complete piping analysis in one computer run.

3D.4.10.2 Validation

No calculations are performed in the program.

3D.4.10.3 Extent of Application

Sorting of data output from PISYS and ANSI7.

3D.4.11 (Deleted)

3D.5 PUMPS AND MOTORS

Following are the computer programs used in the dynamic analysis to assure the structural and functional integrity of the ESBWR pump and motor assemblies.

3D.5.1 Structural Analysis Program - SAP4G07

3D.5.1.1 Description

This program is a general structural analysis program for static and dynamic analysis of linear elastic complex structures. The finite-element displacement method is used to solve the displacement and stresses of each element of the structure. The structure can be composed of unlimited number of three-dimensional truss, beam, plate, shell, solid, plane strain-plane stress and spring elements that are axisymmetric. The program can treat thermal and various forms of mechanical loading. The dynamic analysis includes mode superposition, time-history, and response spectrum analysis. Seismic loading and time-dependent pressure can be treated. The program is versatile and efficient in analyzing large and complex structural systems. The output contains displacement of each nodal point as well as stresses at the surface of each element.

3D.5.1.2 Validation

Hand calculations and test cases analyzed are used to demonstrate the program's applicability and validity.

3D.5.1.3 Extent of Application

SAP4G07 is used to analyze the structural and functional integrity of the pump/motor systems.

3D.5.2 (Deleted)

3D.6 (DELETED)

3D.7 REFERENCES

3D-1 General Electric Co., "PISYS Analysis of NRC Benchmark Problems," NEDO-24210, August 1979.

3D-2 USNRC, "Piping Benchmark Problems Dynamic Analysis Independent Support Motion Response Spectrum Method," NUREG/CR-1677, August 1985.

3E. (DELETED)

3F. RESPONSE OF STRUCTURES TO CONTAINMENT LOADS

3F.1 SCOPE

This appendix specifies the design inputs, methodologies and responses of applicable safety-related structures, systems and components that receive dynamic excitation from primary containment operational-transient events or a LOCA event. The input containment loads are described in Appendix 3B. The containment loads considered for structural dynamic response analysis are (1) Hydrodynamic Loads which are Condensation Oscillation (CO), Pool Chugging (CH), Horizontal Vent Chugging (HVL), Local Condensation Oscillation (LCO) and Safety Relief Valve discharge (SRV) in the Suppression Pool (SP), and (2) Pipe Break Loads which consist of Annulus Pressurization (AP) in the annulus between the Reactor Shield Wall (RSW) and Reactor Pressure Vessel (RPV), nozzle jet, jet impingement and pipe whip restraint loads.

3F.2 DYNAMIC RESPONSE

3F.2.1 Classification of Analytical Procedure

Analytical procedure of containment loads is classified into the following two groups:

(1) Hydrodynamic Loads in the SP: The loads included in this group are SRV loads and LOCA related loads such as CO, CH, HVL and LCO. Depending on the distribution of these loads in the pool, they can be further classified as:

- Symmetric loads in the suppression pool; or
- Asymmetric loads in the suppression pool

(2) Pipe break loads due to Main Steam (MS), Reactor Water Cleanup (RWCU) or Feedwater (FW) line break. The loads included in this group are pressure loads AP and concentrated loads, which are nozzle jet, jet impingement and pipe whip restraint loads.

3F.2.2 Analysis Models

(1) Analysis Model

The structural models used in the analyses represent a synthesis of the Reactor Building (RB) model and the RPV model. The beam model to be used for the pipe break load analysis is illustrated in Figure 3F-1. The hydrodynamic load analysis model of the building structure is illustrated in Figure 3F-2, which is coupled with the RPV model shown in Figure 3F-3. This coupled model is used for symmetric and asymmetric load cases.

The uncertainty associated with stiffness of the in-fill concrete in the Vent Wall and Diaphragm Floor is considered with two models in the same manner as the seismic analysis:

a. No concrete stiffness, where $E_c = 0$ MPa for the in-fill concrete.

b. 50% concrete stiffness, where $E_c = 13900$ MPa for the in-fill concrete.

(2) Structural Damping

Material damping values used for SRV and LOCA analyses are in accordance with Regulatory Guide 1.61.

3F.2.3 Load Application

(1) Pipe Break Nozzle Load

The AP pressures are converted to horizontal forces according to the following formula.

For RSW side:

$$Fj(t) = 2\sum_{i=1}^{8} Pij(t) \int_{\theta=ai}^{\theta=bi} R\cos(\theta)d\theta \qquad (3F\text{-}1)$$

For RPV side:

$$Fj(t) = -2\sum_{i=1}^{8} Pij(t) \int_{\theta=ai}^{\theta=bi} r\cos(\theta)d\theta \qquad (3F\text{-}2)$$

where :

Fj(t)	=	Force per unit height each level
Pij(t)	=	Pressure each level and angle
i	=	Cell No.
j	=	Level No.
R	=	RSW Inner Radius
r	=	RPV Outer Radius
θ	=	Angle (180°)
ai,bi	=	Extreme angles of the arc on which the load is applied

Jet reaction, jet impingement, and pipe whip reaction forces are considered as constant forces with a finite rise time of one millisecond. Pipe whip load is included as a transient load ending with a steady-state load.

(2) SRV Load

Symmetric SRV (all) response analysis is covered by n=0 harmonic. Asymmetric case of SRV (all) actuation is covered by n=1 harmonic that corresponds to overturning moment. The SRV air bubble frequencies are expected to be within a range of 5 to 12 Hz. Ways of selecting the minimum number of bubble frequencies for dynamic analysis are selected as follows.

Frequency range of SRV Loads: $f_1 \leq f \leq f_2$ (f_1 = 5 Hz, f_2 = 12 Hz)

For vertical structural frequencies $(f_s)_v$ (n=0):

a. If $(f_s)_v > f_2$ then use f_2

b. If $f_1 < (f_s)_v < f_2$ then use $(f_s)_v$

c. If $f_1 > (f_s)_v$ then use f_1

For horizontal structural frequencies $(f_s)_h$ (n=1):

a. If $(f_s)_h > f_2$ then use f_2

b. If $f_1 < (f_s)_h < f_2$ then use $(f_s)_h$

c. If $f_1 > (f_s)_h$ then use f_1

In the symmetric load case, three vertical frequencies of 5 Hz (SRV-V1), 6.06 Hz (SRV-V2) and 12 Hz (SRV-V3) are selected. In the asymmetric load case, 3 horizontal frequencies, 5 Hz (SRV-H1), 8.83 Hz (SRV-H2) and 12 Hz (SRV-H3), of the structure satisfying the above selection criteria are adopted as bubble frequencies.

(3) HVL Load

Both symmetric and non-symmetric upward loads are considered on the ventwall structure due to chugging in the top horizontal vents.

(4) Chugging, Condensation Oscillation Loads

Sixteen critical pressure time histories for CH and 5 CO are selected for dynamic analysis. Furthermore, one local spike load is added in CO response study.

3F.2.4 Analysis Method

(1) Pipe Break Load Analysis

For these analyses, multi-input excitation time history analyses are performed using a full transient analysis. The α mass matrix and β stiffness matrix multipliers are used for the damping matrix.

(2) Symmetric Load Analysis

For the dynamic response analyses of SRV and LOCA cases, the full harmonic analysis solution method is used. The input time history is first transformed into harmonic loads. Each harmonic loading is analyzed individually for Fourier n=0 spatial distribution in the frequency domain. Responses to each harmonic loading are transformed back to the time domain and then superimposed, on a time consistent basis, to obtain the total responses. The constant (frequency-independent) stiffness for each material is used. The damping matrix is obtained as follows:

$$[C] = \sum_{j=1}^{Nm} \frac{2}{\Omega} \beta_j [K_j] \qquad \text{(3F-3)}$$

where:

N_m = Number of materials

Ω = circular excitation frequency

$[K_j]$ = structural stiffness matrix

[C] = structural damping matrix

β_j = constant damping stiffness matrix coefficient

(3) Asymmetric Load Analysis

The same analysis approach as symmetric loads is used except that Fourier n=1 spatial distribution is considered.

3F.3 CONTAINMENT LOADS ANALYSIS RESULTS

The acceleration response spectra at selected locations for each loading event are presented in Figures 3F-4 through 3F-25. The maximum displacements and accelerations at selected locations for each loading event are presented Tables 3F-1 through 3F-4.

The input excitation of suppression pool boundary horizontal loads (SRV, CH, and HVL) is considered unidirectional which can be set at any direction in the horizontal plane, and the AP analysis is performed assuming that pipe break can be associated with any one of the vessel nozzles for each of the postulated line breaks.

The resulting response of structures considered in the analyses is thus unidirectional applicable to any azimuth angle for suppression pool loads and to the horizontal direction corresponding to the break direction for AP loads.

For subsystem analyses using floor response spectra and, if applicable, building displacement data, the input direction of the horizontal load is selected to result in the worst subsystem response.

As an alternate approach, the horizontal input to the subsystem may be taken to be the same in the two orthogonal horizontal directions.

The results shown in Tables 3F-1 through 3F-4 and Figures 3F-4 through 3F-25 are the envelope of the two models as described in 3F.2.2. Analysis Model, with no stiffness or 50% stiffness for the in-fill concrete in the Vent Wall and Diaphragm Floor.

Table 3F-1

Maximum Accelerations for AP Loadings (g)

Location	Direction	Node	MS	RWCU	FW
Top of Vent wall	Horizontal Vertical	701	0.0049 0.0019	0.0146 0.0036	0.0144 0.0419
Top of pedestal	Horizontal Vertical	706	0.0062 0.0114	0.0141 0.0214	0.0091 0.0146
Upper pool slab	Horizontal Vertical	208	0.0105 0.0265	0.0240 0.0603	0.0086 0.0026

Table 3F-2

Maximum Accelerations for Hydrodynamic Loads (g)

Location	Direction	Node	SRV	HVL	CH	CO	LCO
Top of vent wall	Horizontal Vertical	1104 1104	0.22 0.23	0.01 0.15	0.63 0.84	0.43 0.97	0.37 0.87
SP Floor	Horizontal Vertical	1254 1254	0.14 0.33	0.00 0.03	0.34 1.54	0.40 1.88	0.07 0.60
RCCV Top slab side	Horizontal Vertical	1119 1119	0.08 0.09	0.000 0.000	0.07 0.15	0.01 0.22	0.01 0.10
RCCV Top slab center	Horizontal Vertical	1159 1159	0.08 0.14	0.000 0.000	0.06 0.04	0.01 0.21	0.00 0.03

Table 3F-3

Maximum Displacements for AP Loadings (mm)

Location	Direction	Node	MS	RWCU	FW
Top of Vent Wall	Horizontal Vertical	701	0.0123 0.0162	0.0180 0.0425	0.0115 0.0302
Top of Pedestal	Horizontal Vertical	706	0.0063 0.0097	0.0144 0.0180	0.0098 0.0125
Upper pool slab	Horizontal Vertical	208	0.0109 0.0010	0.0170 0.0025	0.0114 0.0017

Table 3F-4

Maximum Displacements for Hydrodynamic Loads (mm)

Location	Direction	Node	SRV	HV	CH	CO	LCO
Top of Vent Wall	Horizontal Vertical	1104 1104	0.28 1.63	0.00 0.01	0.09 0.12	0.11 8.93	0.03 0.32
SP Floor	Horizontal Vertical	1254 1254	0.27 1.15	0.00 0.01	0.05 0.28	0.07 8.06	0.00 0.25
RCCV Top slab side	Horizontal Vertical	1119 1119	0.20 0.97	0.00 0.00	0.05 0.04	0.01 7.54	0.00 0.20
RCCV Top slab center	Horizontal Vertical	1159 1159	0.20 1.43	0.00 0.01	0.05 0.03	0.00 8.52	0.00 0.27

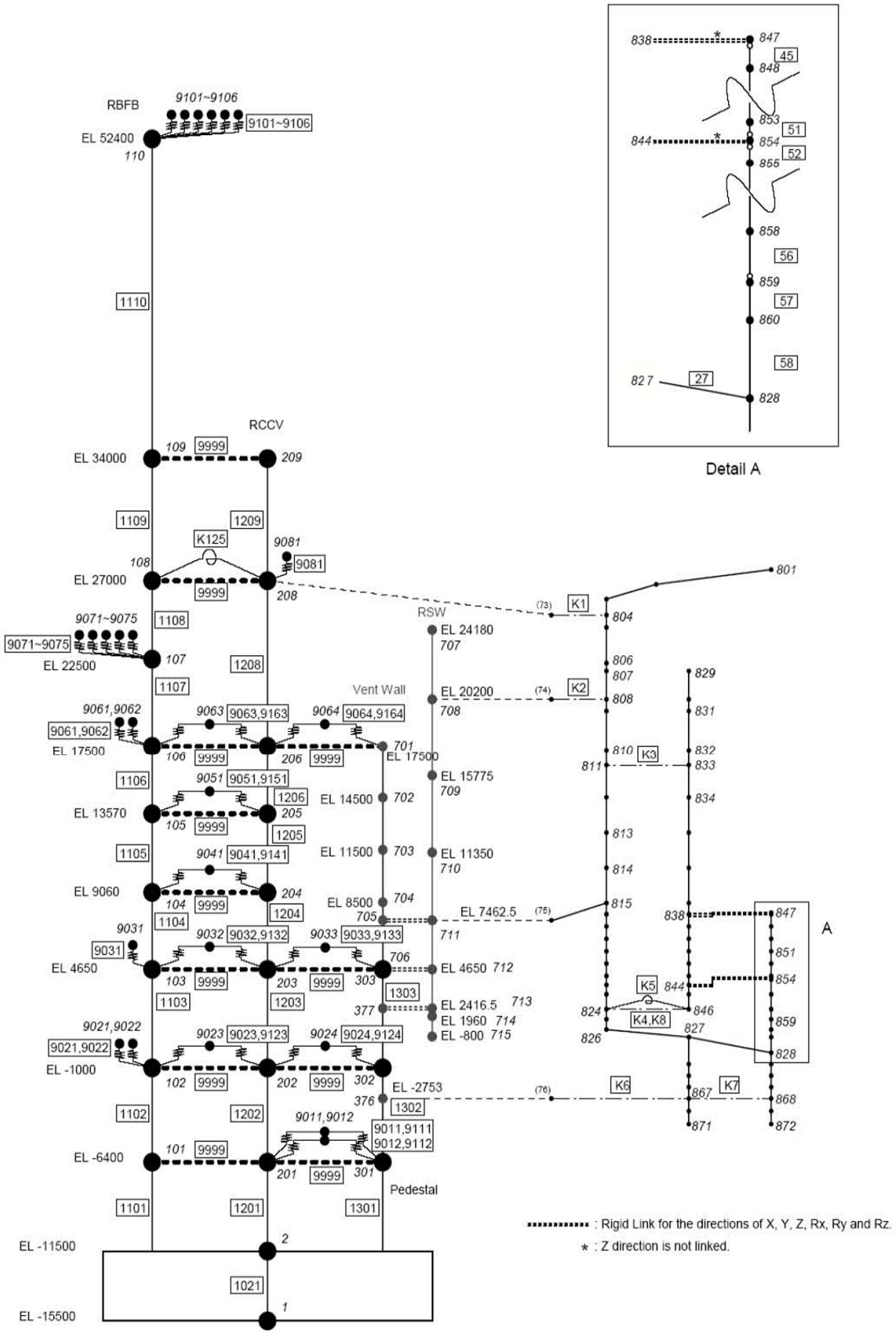

Figure 3F-1. Beam Model for AP Load

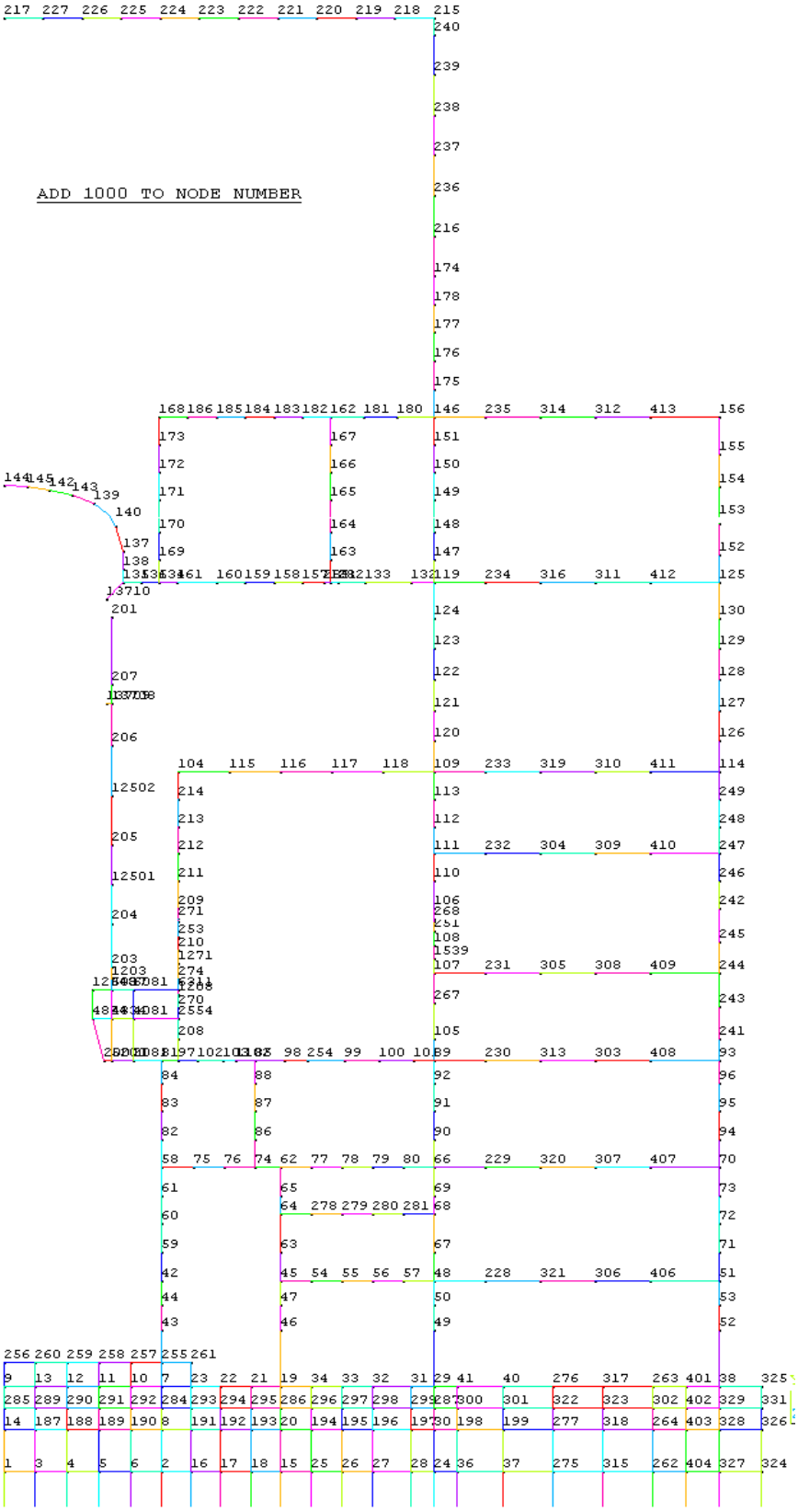

Figure 3F-2. Building Shell Model

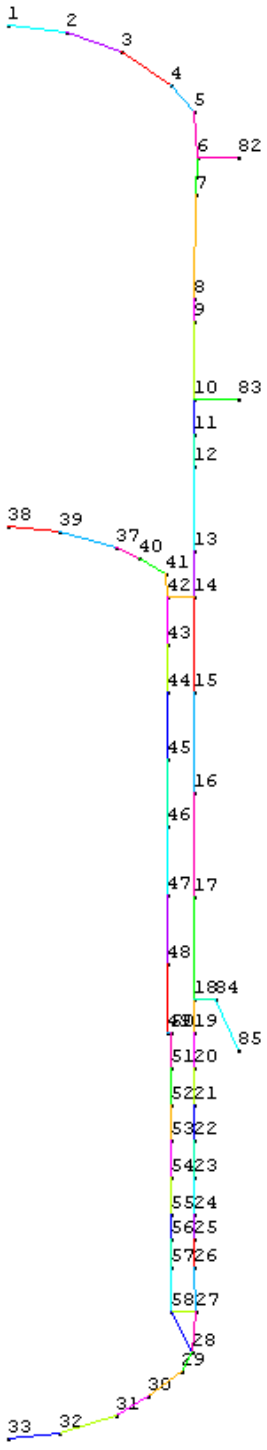

Figure 3F-3. RPV Shell Model

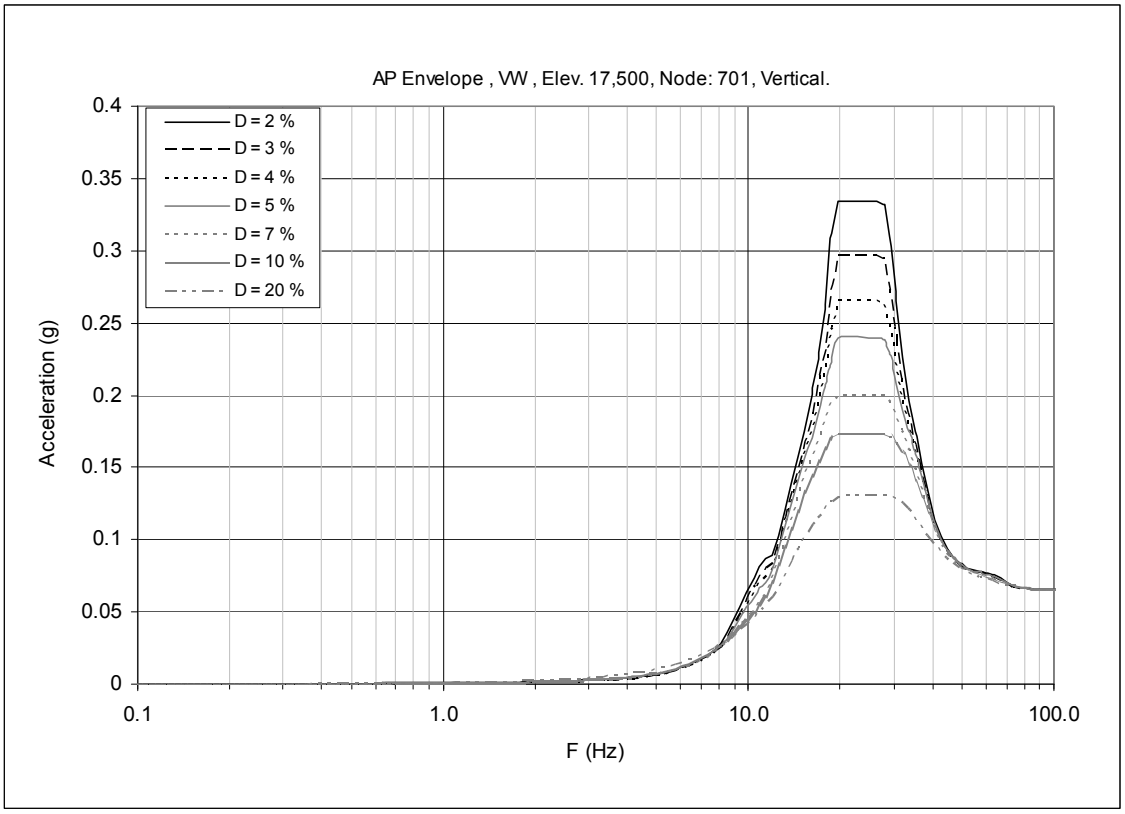

Figure 3F-4. Floor Response Spectrum—AP Envelope, Node: 701, Vertical

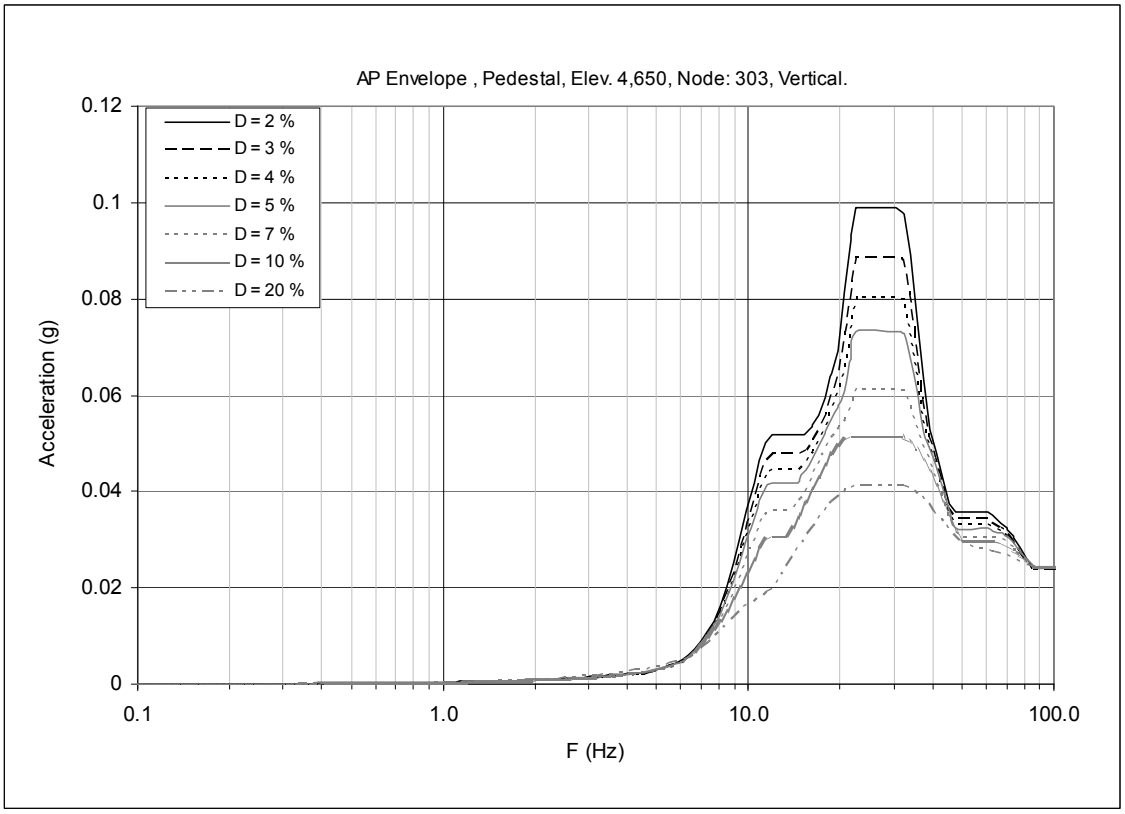

Figure 3F-5. Floor Response Spectrum-AP Envelope, Node: 706/303, Vertical

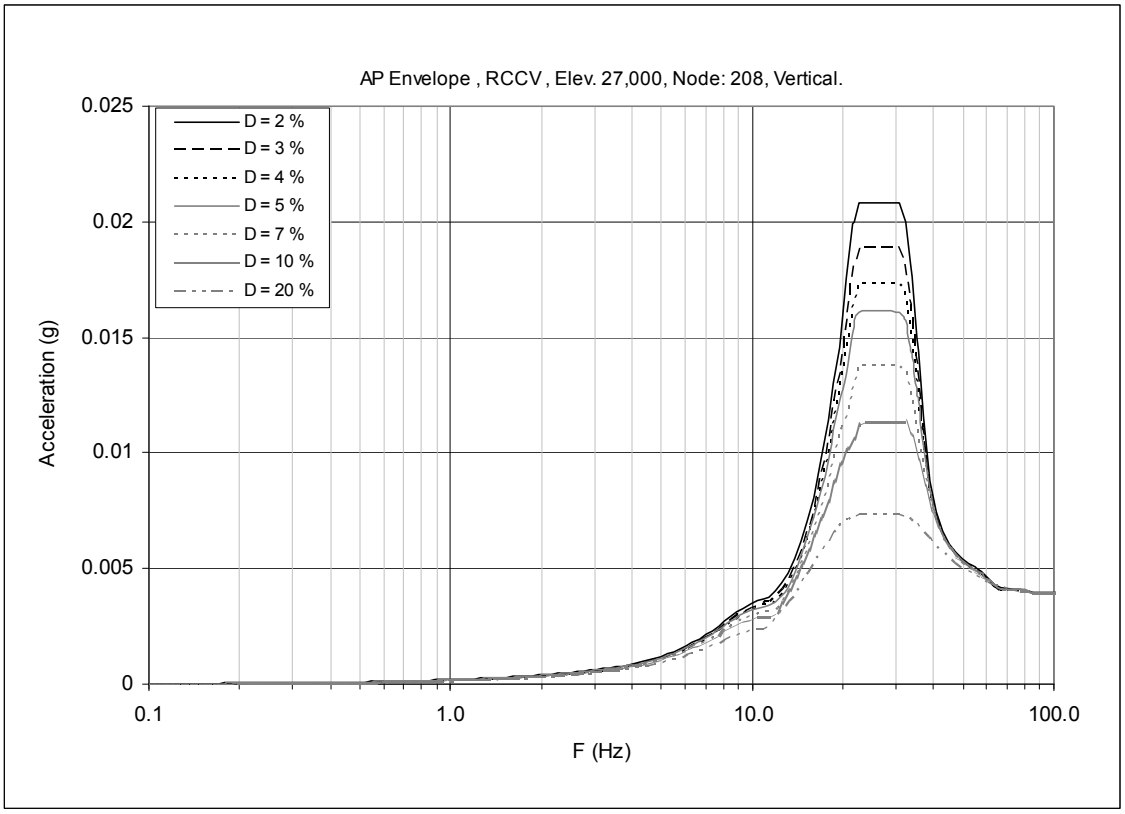

Figure 3F-6. Floor Response Spectrum-AP Envelope, Node: 208, Vertical

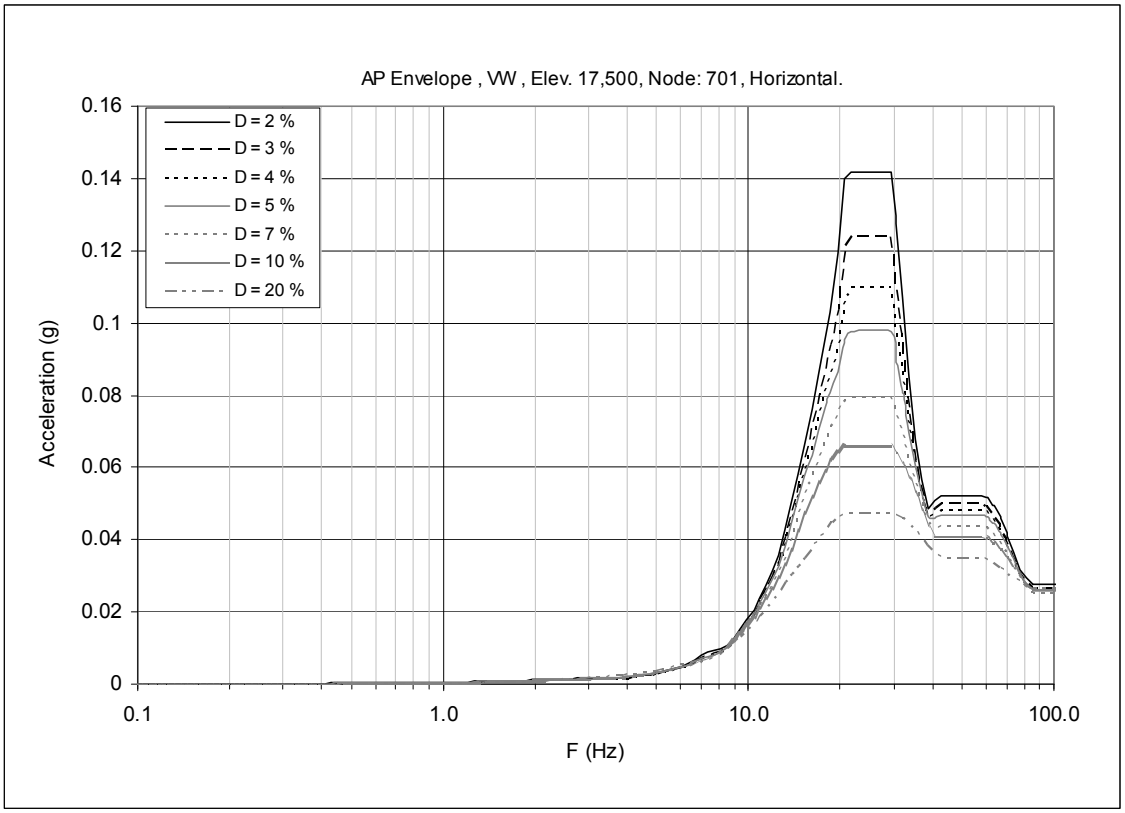

Figure 3F-7. Floor Response Spectrum—AP Envelope, Node: 701, Horizontal

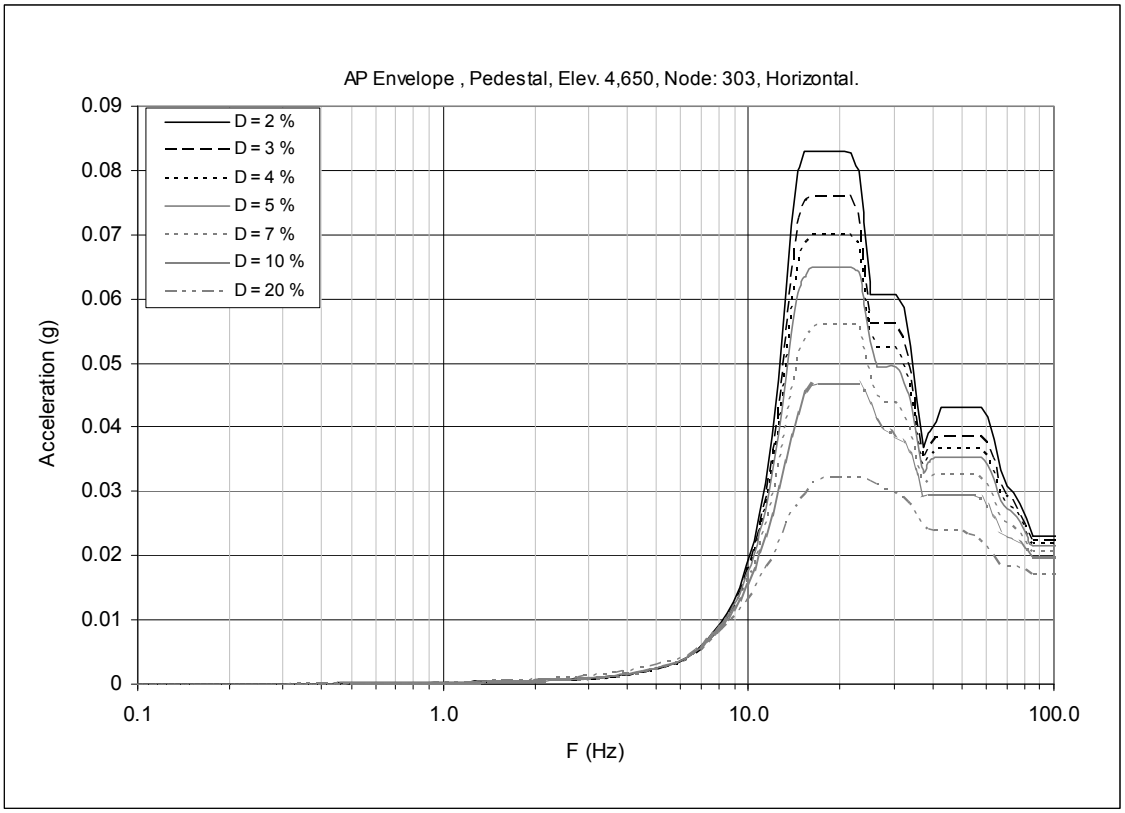

Figure 3F-8. Floor Response Spectrum—AP Envelope, Node: 706/303, Horizontal

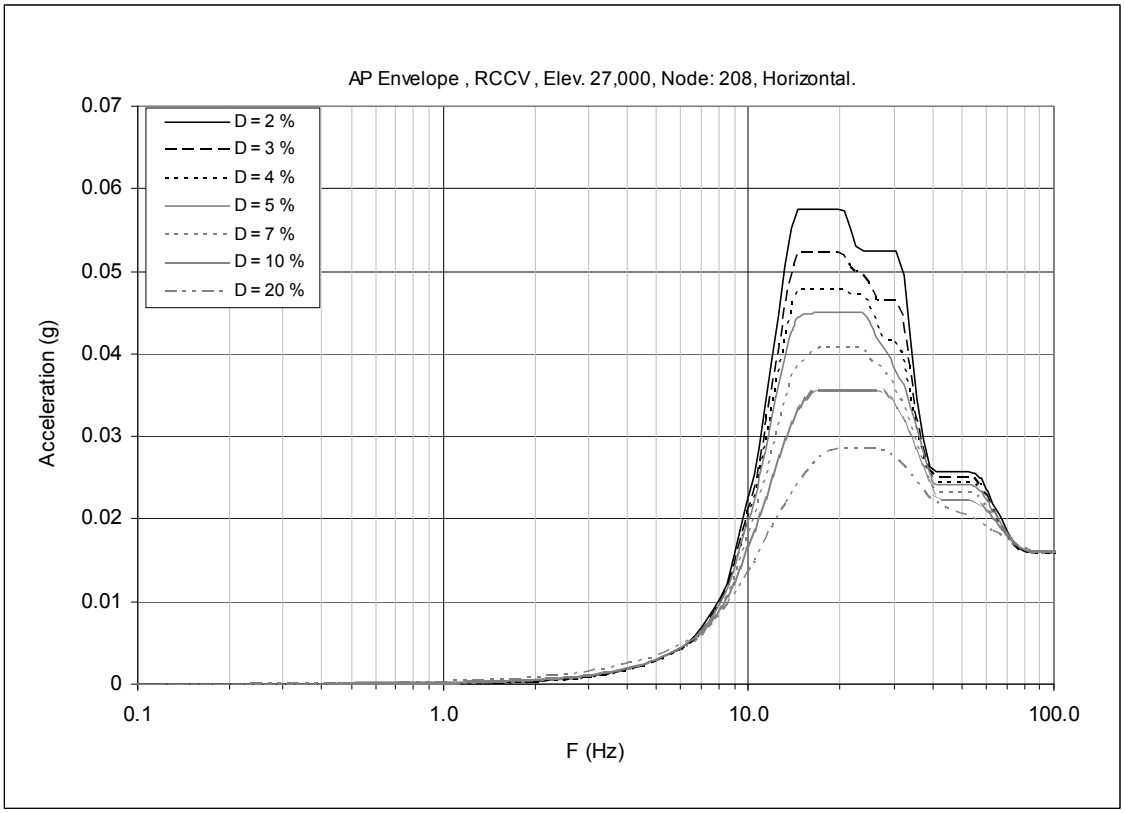

Figure 3F-9. Floor Response Spectrum—AP Envelope, Node: 208, Horizontal

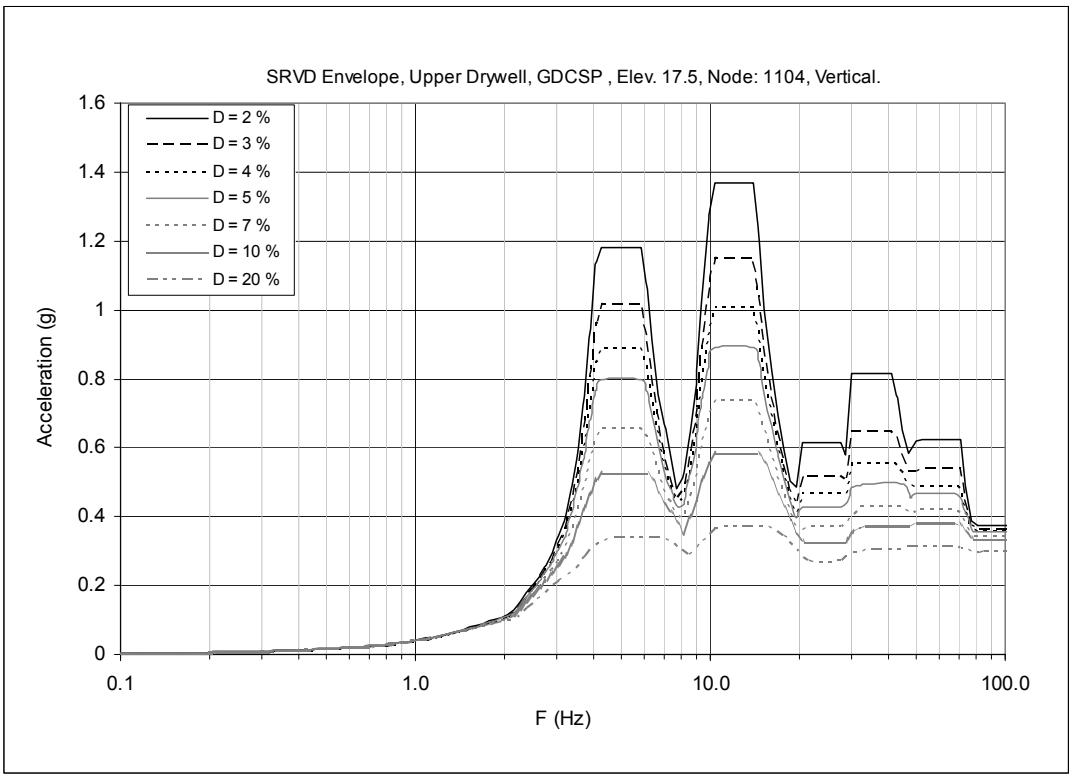

Figure 3F-10. Floor Response Spectrum—SRV Envelope, Node: 1104, Vertical

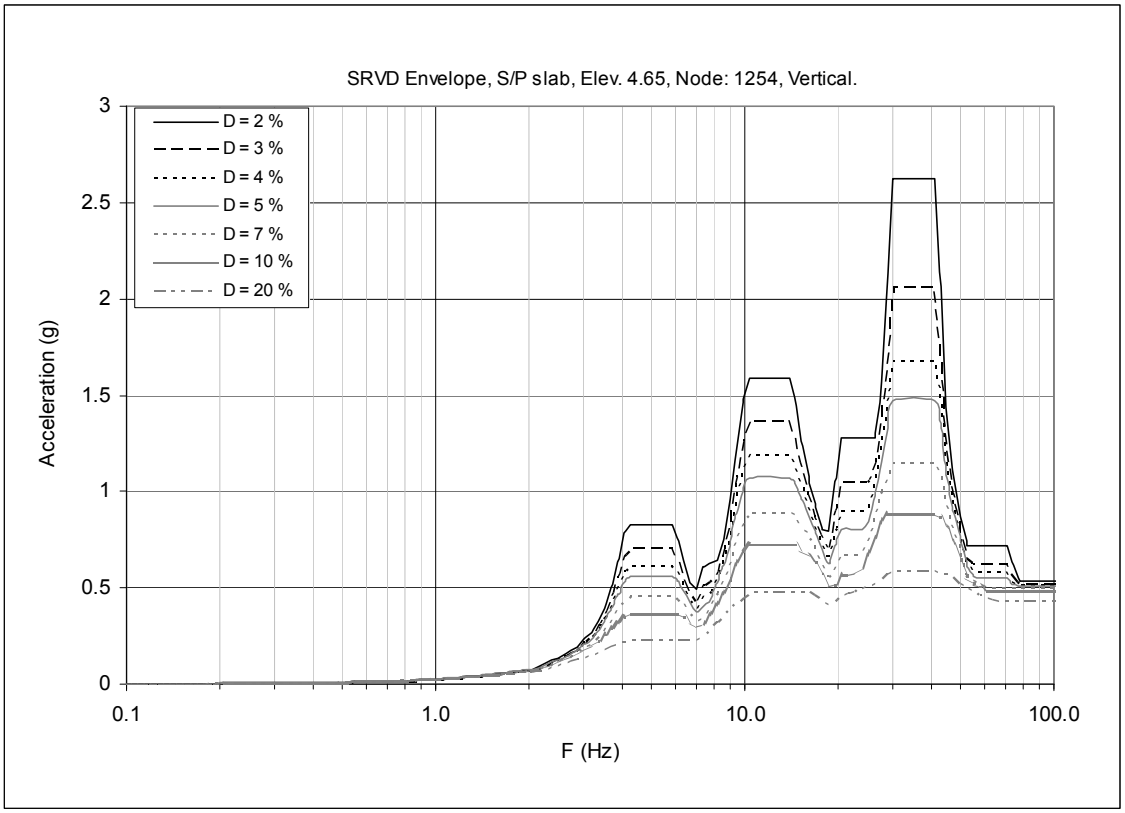

Figure 3F-11. Floor Response Spectrum—SRV Envelope, Node: 1254, Vertical

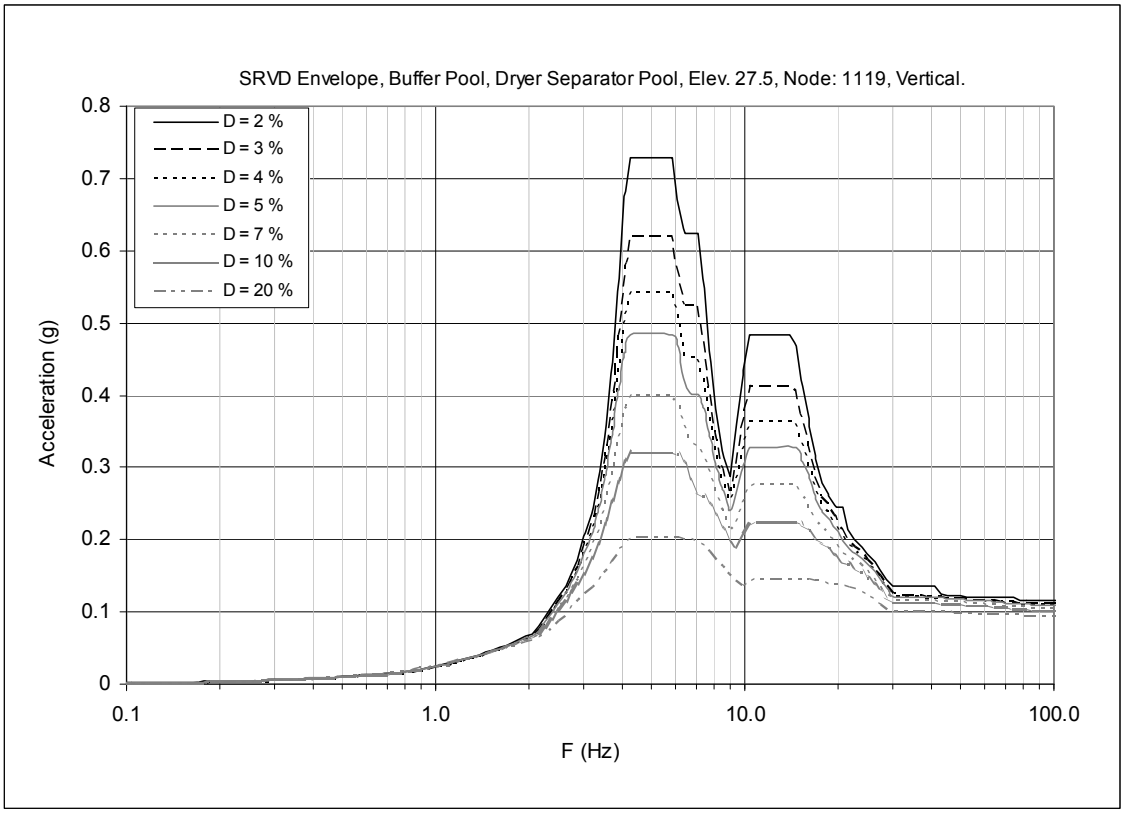

Figure 3F-12. Floor Response Spectrum—SRV Envelope, Node: 1119, Vertical

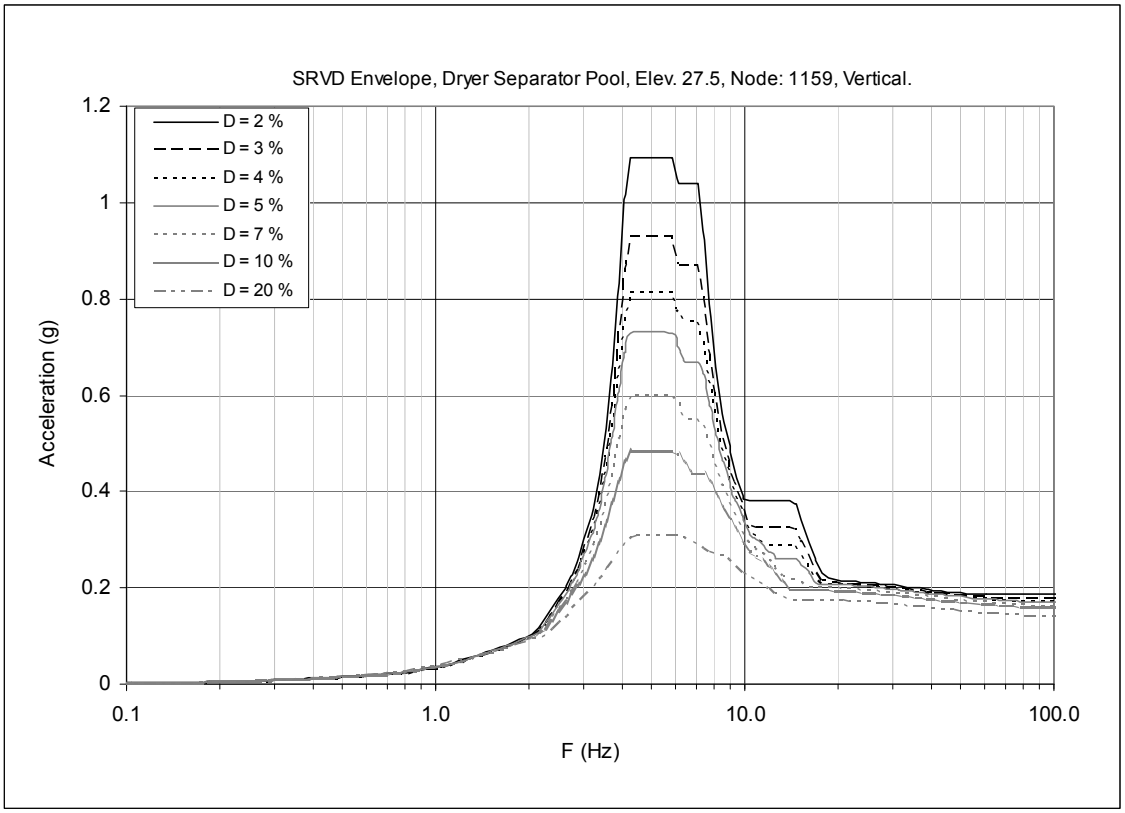

Figure 3F-13. Floor Response Spectrum—SRV Envelope, Node: 1159, Vertical

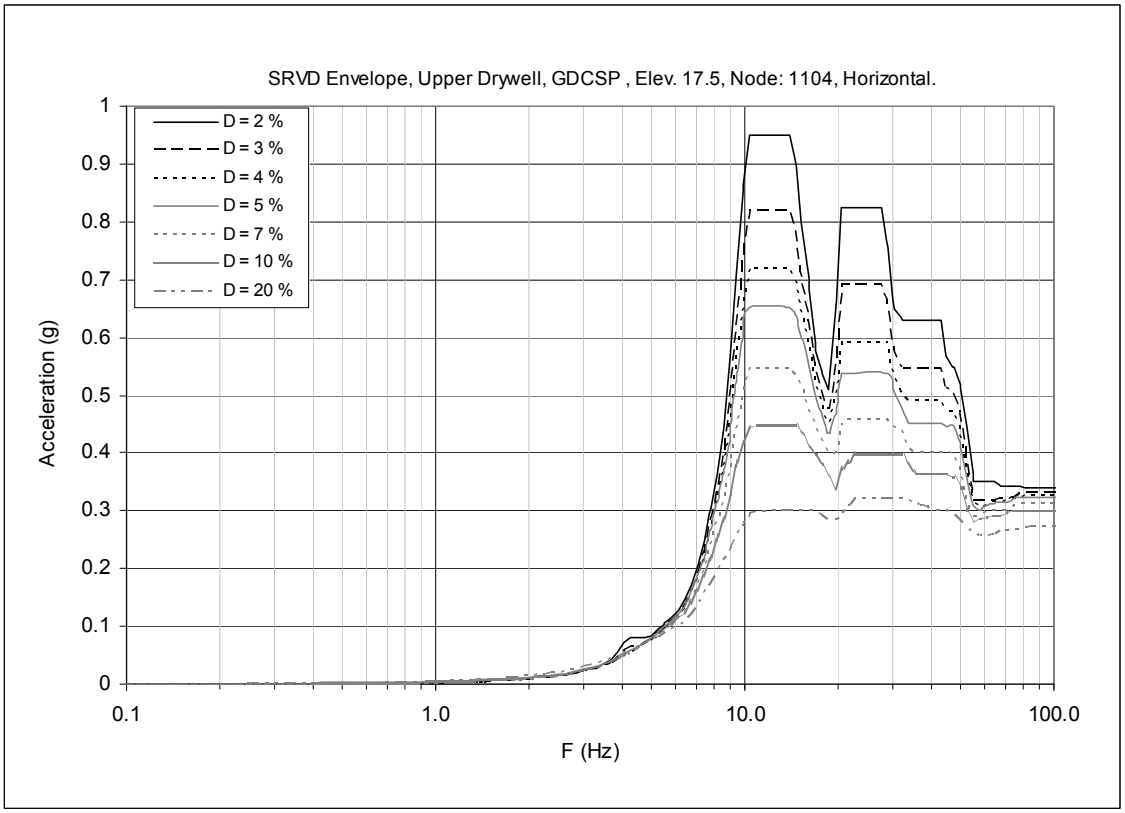

Figure 3F-14. Floor Response Spectrum—SRV Envelope, Node: 1104, Horizontal

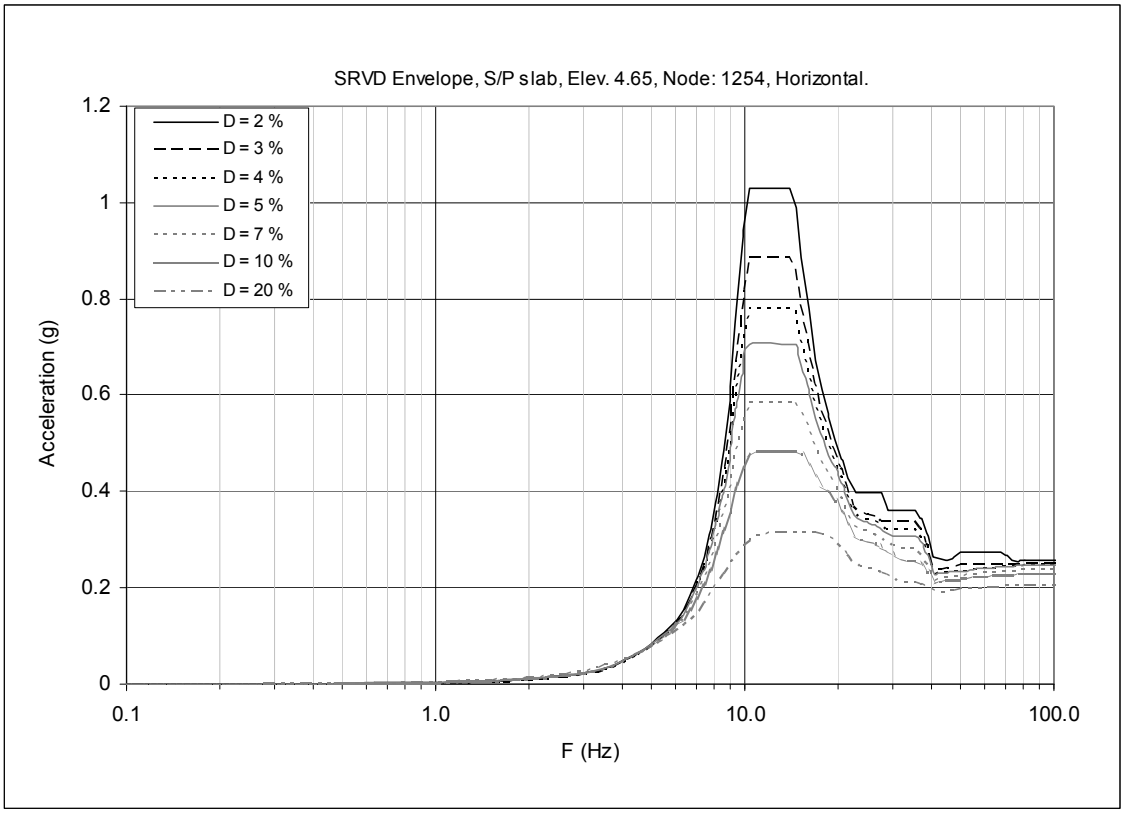

Figure 3F-15. Floor Response Spectrum—SRV Envelope, Node: 1254, Horizontal

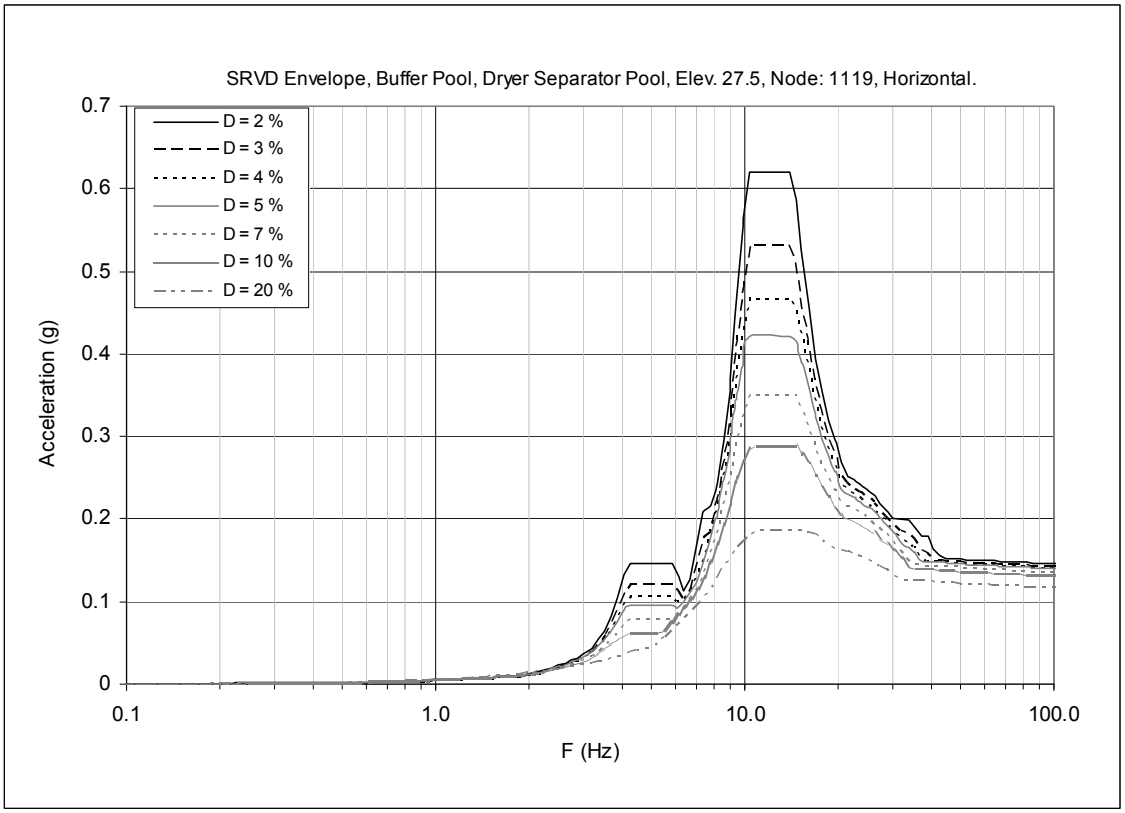

Figure 3F-16. Floor Response Spectrum—SRV Envelope, Node: 1119, Horizontal

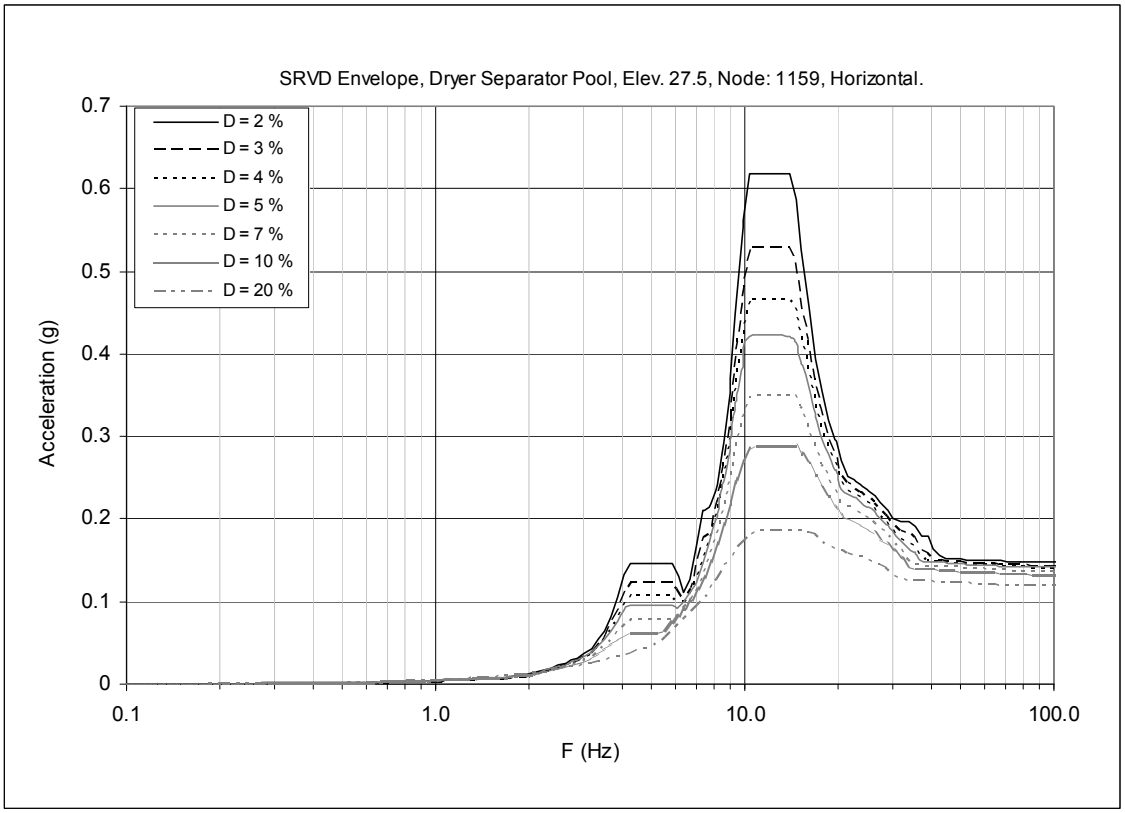

Figure 3F-17. Floor Response Spectrum—SRV Envelope, Node: 1159, Horizontal

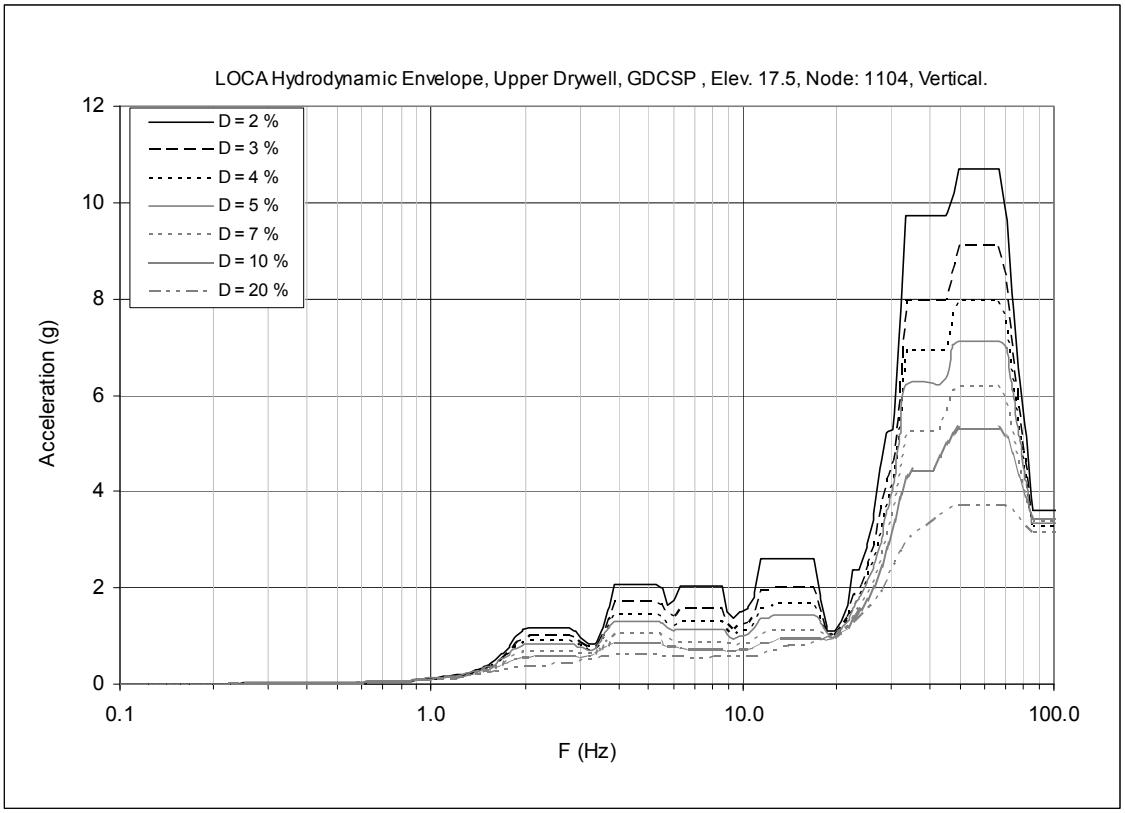

Figure 3F-18. Floor Response Spectrum—CH & CO Envelope, Node: 1104, Vertical

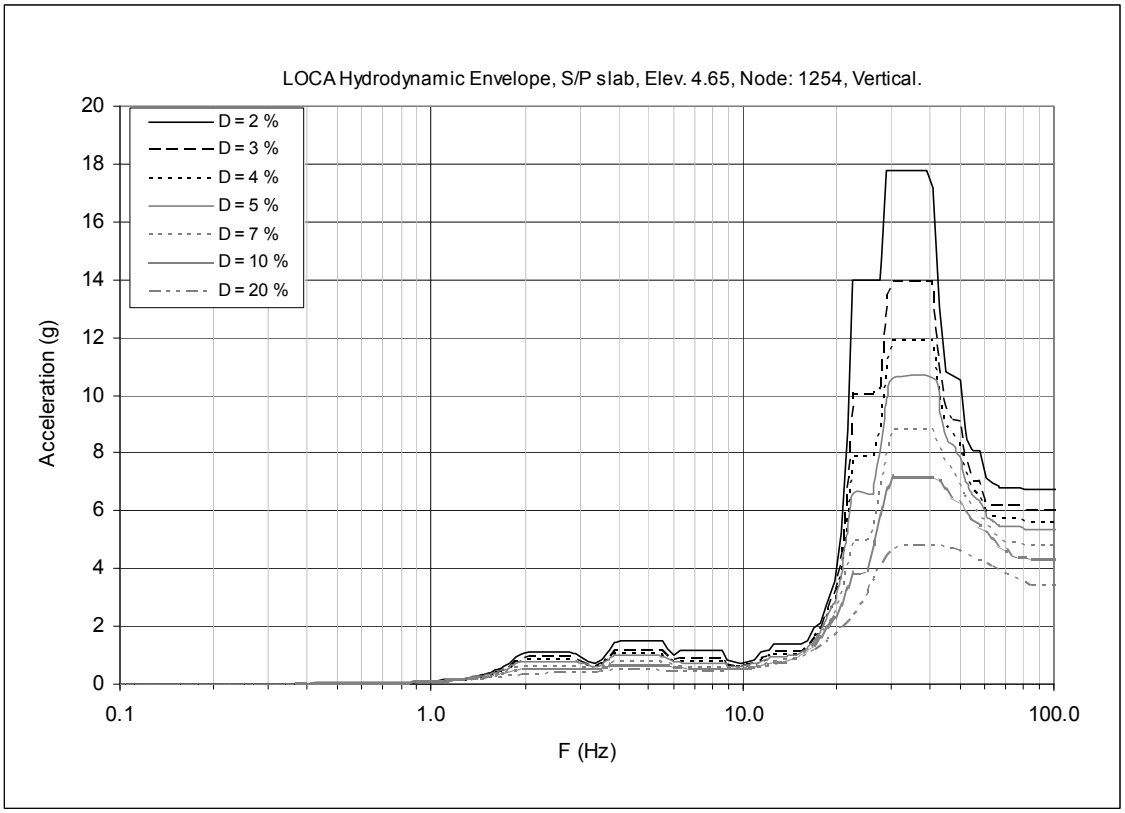

Figure 3F-19. Floor Response Spectrum—CH & CO Envelope, Node: 1254, Vertical

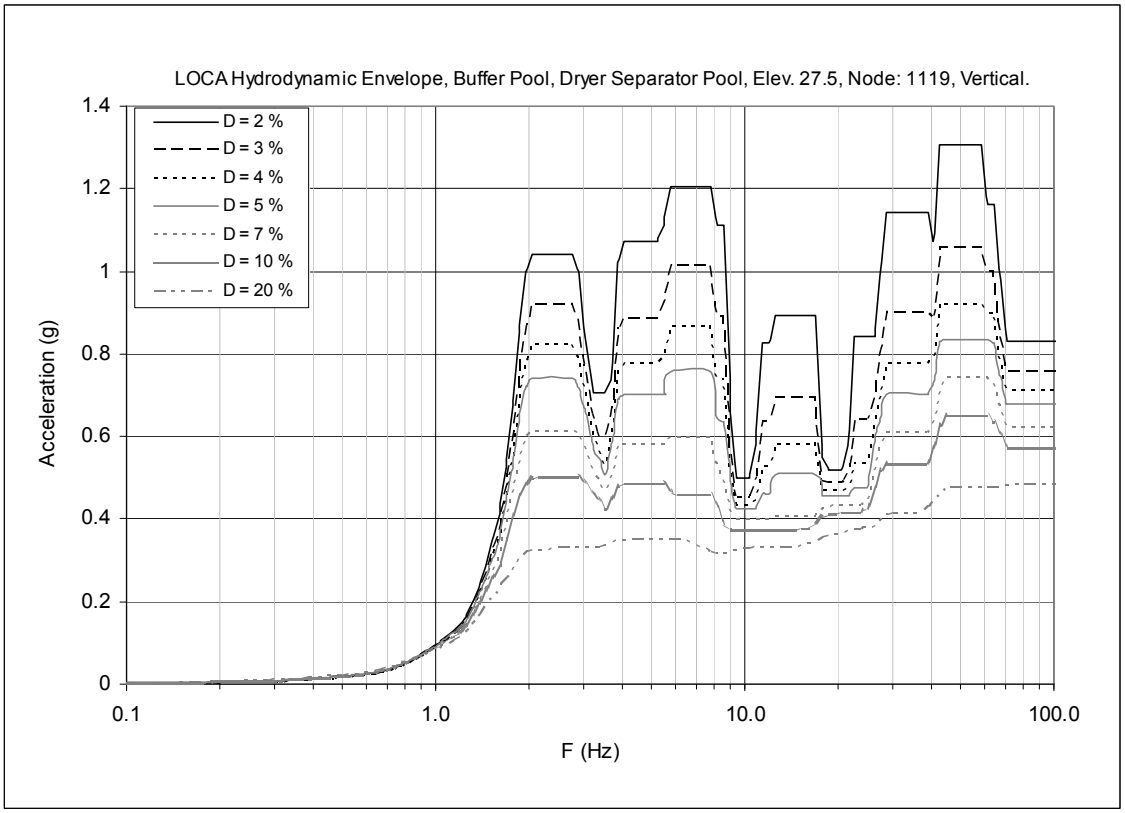

Figure 3F-20. Floor Response Spectrum—CH & CO Envelope, Node: 1119, Vertical

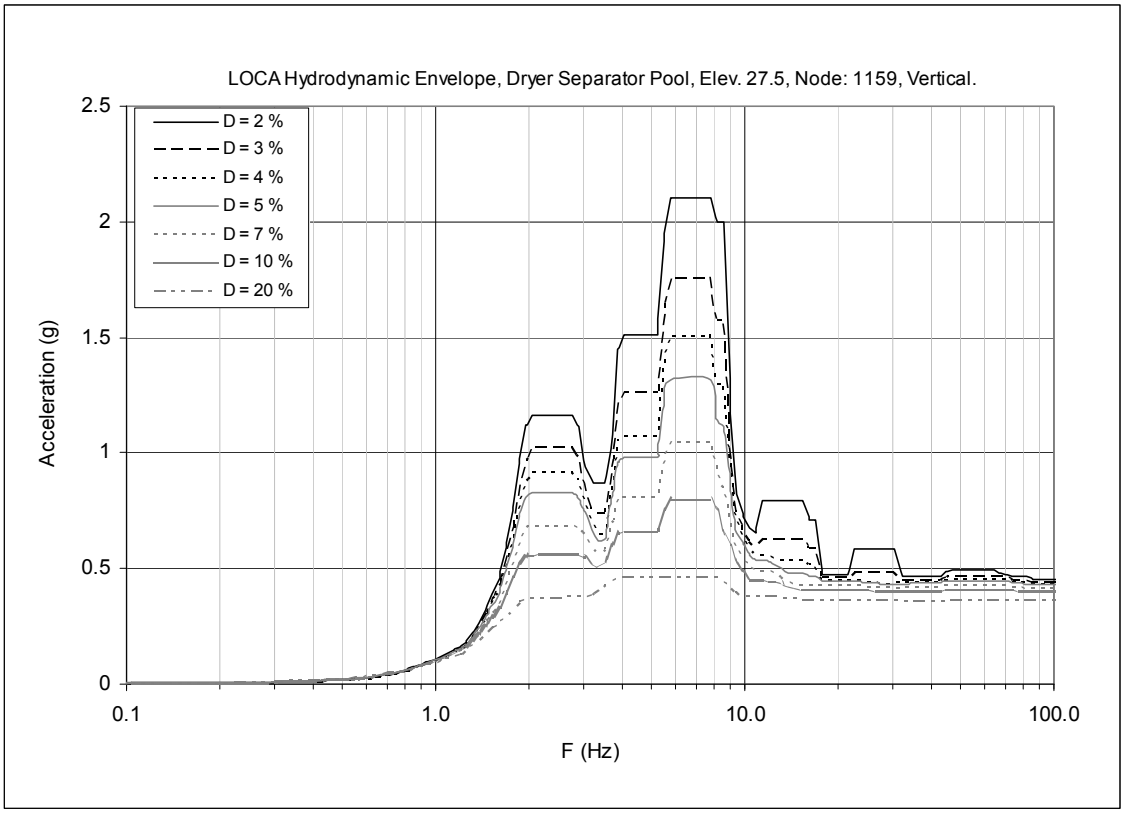

Figure 3F-21. Floor Response Spectrum—CH & CO Envelope, Node: 1159, Vertical

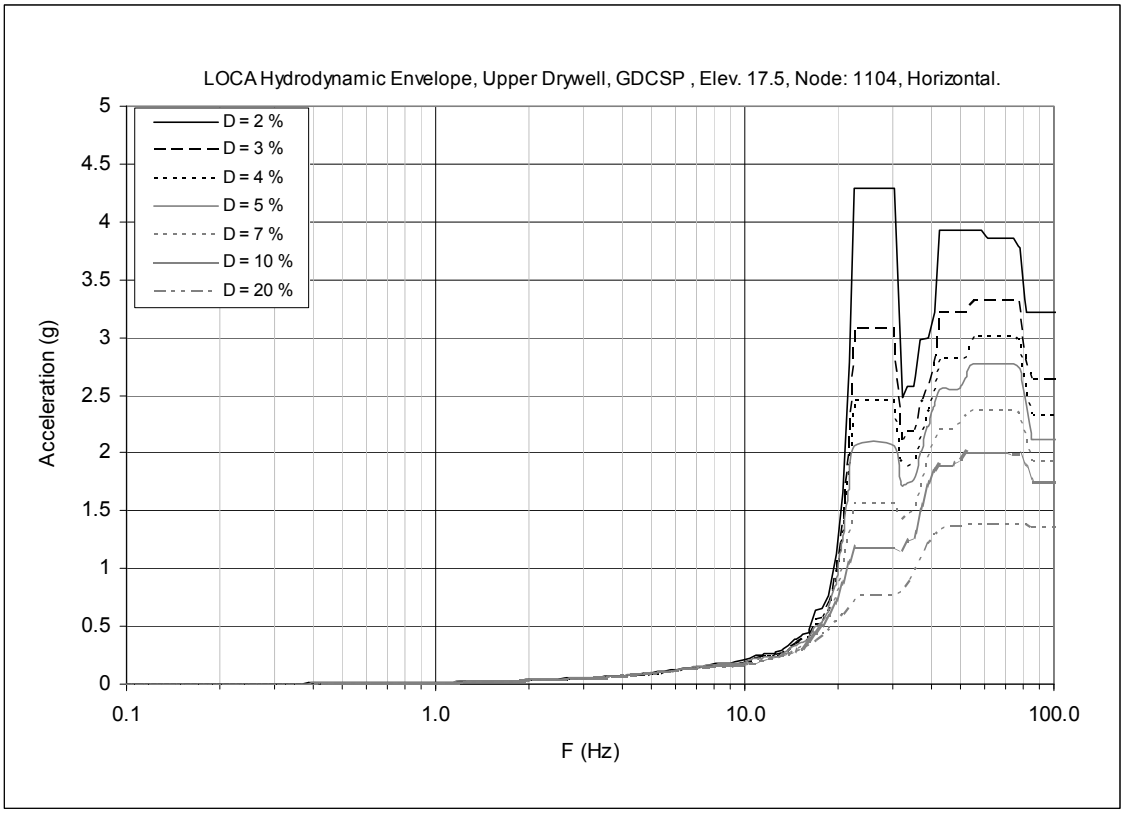

Figure 3F-22. Floor Response Spectrum—CH & CO Envelope, Node: 1104, Horizontal

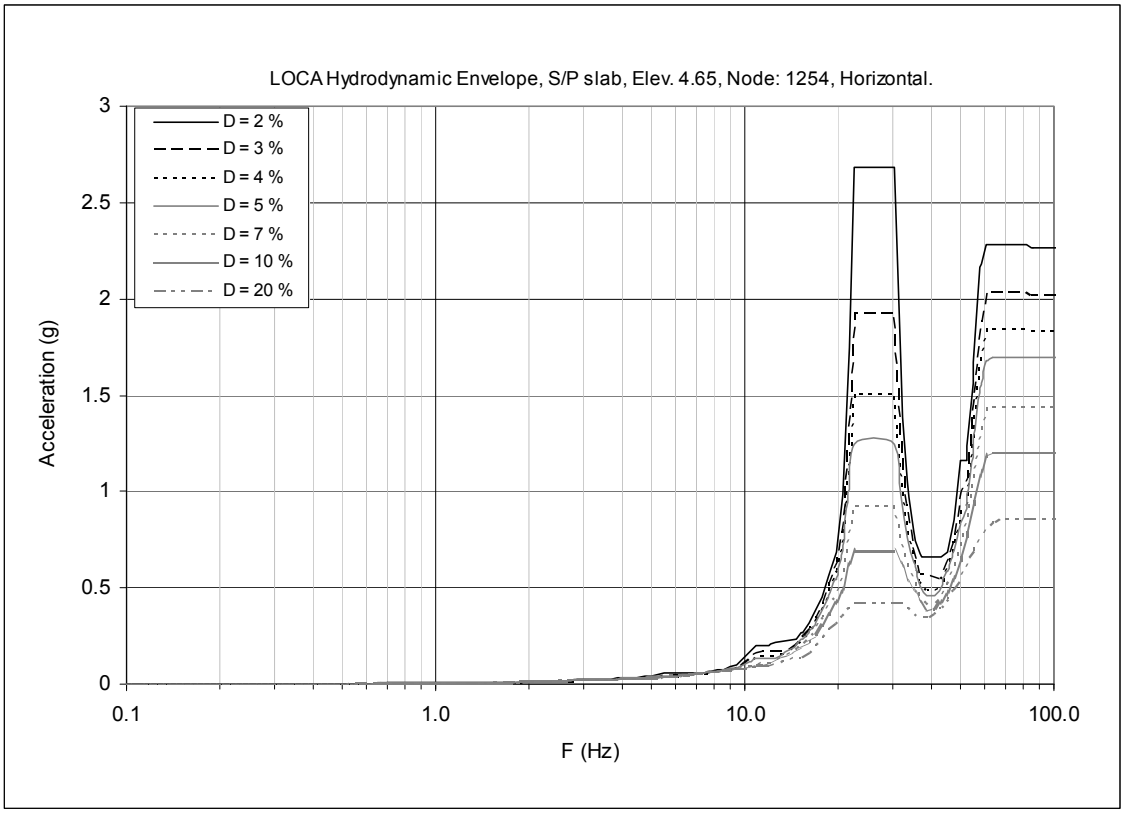

Figure 3F-23. Floor Response Spectrum—CH & CO Envelope, Node: 1254, Horizontal

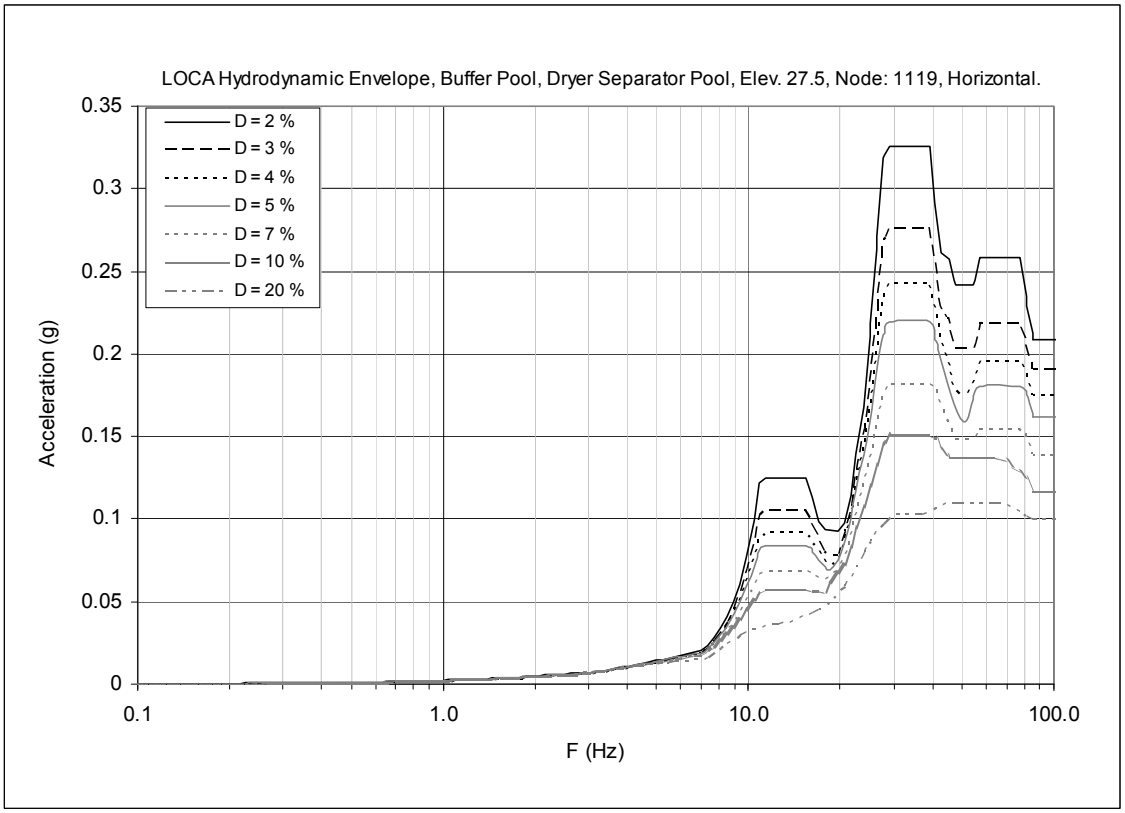

Figure 3F-24. Floor Response Spectrum—CH & CO Envelope, Node: 1119, Horizontal

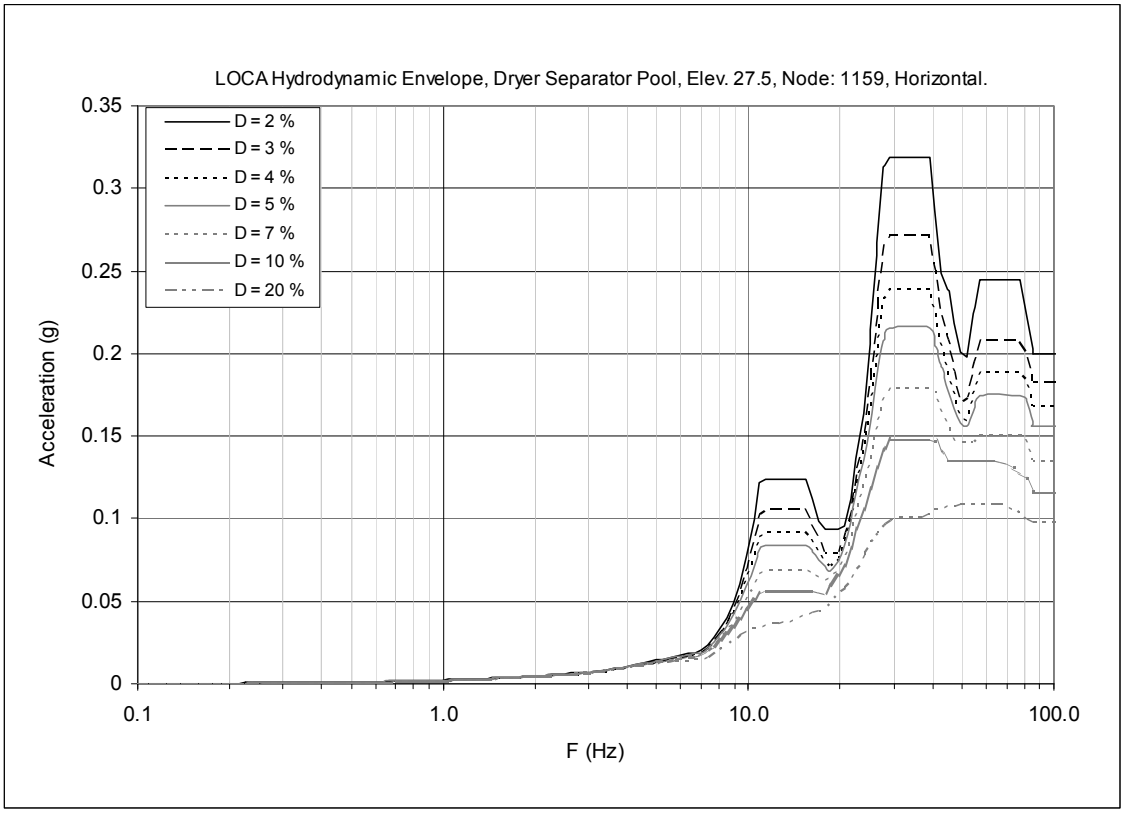

Figure 3F-25. Floor Response Spectrum—CH & CO Envelope, Node: 1159, Horizontal